UNIVERSITY OF CAPE COAST

AN APPLICATION OF OPTIMAL CONTROL TO THE SUSTAINABLE HARVESTING STRATEGIES OF GHANA'S SARDINELLA FISHERY

BY

MAHMUD IBRAHIM

Thesis submitted to the Department of Mathematics of the School of Physical Sciences, College of Agriculture and Natural Sciences, University of Cape Coast, in partial fulfilment of the requirements for the award of Doctor of Philosophy degree in Mathematics

CALL No.

ACCESSION No.

0096

CAT. CHECKED | FINAL CHECKED

JUNE 2018

SAM JONAH LIBRARY
UNIVERSITY OF CAPE COAST
CAPE COAST

DECLARATION

Candidate's Declaration

I hereby declare that this thesis is the result of my own original research and that no part of it has been presented for another degree in this university or elsewhere.

Candidate's Signature..... Date..29/8/19..

Name: Mahmud Ibrahim

Supervisors' Declaration

We hereby declare that the preparation and presentation of the thesis were supervised in accordance with the guidelines on supervision of thesis laid down by the University of Cape Coast.

Principal Supervisor's Signature..... Date..29/08/2019..

Name: Prof. Francis Benyah

Co-Supervisor's Signature..... Date..29/08/2019..

Name: Dr. Henry Amankwah

ABSTRACT

The main objective of this study was to apply optimal control techniques to determine the optimal harvesting strategies that would ensure the sustainability of the *Sardinella aurita* for future generations. In this vein, the Gordon-Schaefer bioeconomic model was employed to aid in the analyses. The model was initially analysed using three different rates of harvest: constant, proportional and periodic. Also reviewed were the Craven model, the Goh model, the optimal yield model and the model with effective utilisation factor. The models were subjected to bifurcation analyses to determine the stability properties; and the static reference points, maximum sustainable yield (MSY), maximum economic yield (MEY) and open access yield (OAY), computed. Also determined was the dynamic reference point, optimum sustainable yield (OSY). An original model incorporating the total allowable catch (TAC) showed that, for the binding constraints, the resource should be harvested if and only if the marginal net revenue of harvest as a result of applying the maximum effort exceeds the difference of the shadow price of fish stock and the shadow price of the TAC. The model developed to simulate the effects of illegal fishing practices on fish stocks revealed that the increased catchability induced by the illegal methods severely depletes the stocks, to as low less than half of the carrying capacity in finite time. Employing a dynamic effort, predator-prey model with reserve area and critical biomass level, the optimal fishing strategy indicates that the critical biomass level must be set at the MSY level in order to attain sustainability of the resource. In general, all the models indicate that the optimal fishing effort must be set at the OSY level: estimated at 351,328 trips annually at a discount rate of 15%, provided the initial fish stock size is at least 554,654 tonnes. Recommendations are offered to the Fisheries Commission.

KEY WORDS

Gordon-Schaefer bioeconomic model

Numerical simulation

Optimal control

Optimum sustainable yield

Pontryagin's maximum principle

Round sardinella (*Sardinella aurita*)

ACKNOWLEDGEMENTS

I would like to express my profound gratitude to the Almighty Allah for the strength and wisdom to successfully complete this study.

Thanks go to the principal supervisor, Professor Francis Benyah and the co-supervisor, Dr. Henry Amankwah for their guidance and assistance.

I would acknowledge the support rendered by the various Heads as well as the entire lecturers and staff of the Department of Mathematics for this research to be fruitful. Also acknowledged is the support granted by the University of Cape Coast.

Acknowledgements also go to Professor Ussif Rashid Sumaila, Director of the Fisheries Economics Research Unit at the University of British Columbia Institute for Oceans and Fisheries, for his insightful and encouraging comments on the thesis.

Finally, I wish to thank my family for the invaluable motivation and encouragement that made it possible for this work to see the light of day.

DEDICATION

To my parents

TABLE OF CONTENTS

	Page
DECLARATION	ii
ABSTRACT	iii
KEY WORDS	iv
ACKNOWLEDGEMENTS	v
DEDICATION	vi
LIST OF TABLES	x
LIST OF FIGURES	xi
LIST OF ACRONYMS	xviii
CHAPTER ONE: INTRODUCTION	
Background to the Study	1
Statement of the Problem	6
Objectives	7
Methods	7
Scope of the Study	8
Justification of the Study	9
Organisation of the Study	9
Chapter Summary	10
CHAPTER TWO: LITERATURE REVIEW	
Introduction	11
Modelling and Optimal Management of Resources	11
Chapter Summary	29
CHAPTER THREE: RESEARCH METHODS	
Introduction	31
Definitions and Concepts	31
Calculus of Variations	49
Optimal Control Theory	52

Chapter Summary 79

CHAPTER FOUR: PROPORTIONAL HARVESTING MODELS

Introduction 80

The Canonical Gordon-Schaefer Model 80

Optimal Yield Model 104

The Craven Model 115

A Model with Isoperimetric Constraint 131

A Model with Modified Catchability 144

Chapter Summary 179

CHAPTER FIVE: CONSTANT AND PERIODIC HARVESTING MODELS

Introduction 181

The Gordon-Schaefer Model 181

The Goh Model 192

A Model with Effective Utilisation Factor 199

Periodic Harvesting Model 209

Chapter Summary 228

CHAPTER SIX: A PREDATOR-PREY MODEL WITH RESERVE AREA

Introduction 230

Model Formulation 231

Stability Analysis 232

Optimality of the Model 237

Numerical Simulations 242

Chapter Summary 257

CHAPTER SEVEN: SUMMARY, CONCLUSIONS AND RECOMMENDATIONS

Overview 259

Summary 259

Conclusions 262

Recommendations 265

REFERENCES 268

APPENDIX 279

LIST OF TABLES

Table		Page
1	Parameter Values for Model	82
2	Annual Net Revenue at MEY, MSY and OAY Levels of Harvesting	87
3	Annual Net Revenue at OSY Levels of Harvesting	91
4	Sensitivity of x_δ to Economic Parameters	92
5	Annual Net Revenue at the Static Reference Points	120

LIST OF FIGURES

Figure		Page
1	The Static Gordon-Schaefer Model	73
2	Solution Curves for $E = 323.255$	82
3	Solution Curves for $E = 394.444$	83
4	Solution Curves for $E = 646.450$	84
5	Solution Curves for $E = 788.889$	85
6	Solution Curves for $E = 1.183.333$	86
7	Shadow Price and Net Revenue for $E_{max} = 351,328$, $x_0 = 750,000$ and $T = 1$	93
8	(a) Effort and (b) Biomass Levels for $E_{max} = 351,328$, $x_0 = 750,000$ and $T = 1$	94
9	Shadow Price and Net Revenue for $E_{max} = 351,328$, $x_0 = 750,000$ and $T = 20$	95
10	(a) Effort and (b) Biomass Levels for $E_{max} = 351,328$, $x_0 = 750,000$ and $T = 20$	96
11	(a) Effort and (b) Biomass Levels for $E_{max} = 351,328$, $x_0 = 550,000$ and $T = 1$	97
12	Shadow Price and Net Revenue for $E_{max} = 351,328$, $x_0 = 550,000$ and $T = 5$	98
13	(a) Effort and (b) Biomass Levels for $E_{max} = 351,328$, $x_0 = 550,000$ and $T = 5$	99
14	(a) Effort and (b) Biomass Levels for $E_{max} = 175,664$, $x_0 = 550,000$ and $T = 20$	100
15	Shadow Price and Net Revenue for $E_{max} = 800,000$, $x_0 = 200,000$ and $T = 1$	101
16	(a) Effort and (b) Biomass Levels for $E_{max} = 800,000$, $x_0 = 200,000$ and $T = 1$	102

17 (a) Effort and (b) Biomass Levels for $E_{max} = 394,444$, $x_0 = 750,000$ and $T = 1$ 107

18 (a) Effort and (b) Biomass Levels for $E_{max} = 394,444$, $x_0 = 750,000$ and $T = 20$ 108

19 (a) Effort and (b) Biomass Levels for $E_{max} = 394,444$, $x_0 = 550,000$; $750,000$ and $T = 1$ 109

20 (a) Effort and (b) Biomass Levels for $E_{max} = 394,444$, $x_0 = 550,000$; $750,000$ and $T = 20$ 110

21 (a) Effort and (b) Biomass Levels for $E_{max} = 500,000$, $x_0 = 750,000$ and $T = 3.5$ 111

22 (a) Effort and (b) Biomass Levels for $E_{max} = 500,000$, $x_0 = 550,000$ and $T = 2.5$ 112

23 Marginal Yield and Biomass Change for $E_{max} = 800,000$ and $T = 1$ 113

24 (a) Effort and (b) Biomass Levels for $E_{max} = 800,000$, $x_0 = 200,000$ and $T = 1$ 114

25 Solution Curves for $u = 0.71$ 117

26 Solution Curves for $u = 1.42$ 117

27 Solution Curves for $u = 2.13$ 118

28 Linear and Quadratic Revenues 119

29 (a) Harvest and (b) Biomass Levels for $x_0 = 550,000$; $750,000$, $u_{max} = 0.53$ and $T = 1$ 124

30 (a) Harvest and (b) Biomass Levels for $x_0 = 550,000$; $750,000$, $u_{max} = 0.53$ and $T = 20$ 125

31 (a) Harvest and (b) Biomass Levels for $x_0 = 550,000$; $750,000$, $u_{max} = 1.14$ and $T = 1$ 126

32 (a) Harvest and (b) Biomass Levels for $x_0 = 550,000$; $750,000$, $u_{max} = 1.14$ and $T = 20$ 127

33 (a) Harvest and (b) Biomass Levels for $x_0 = 550,000$, $u_{max} = 0.53$, 0.71 and $T = 1$ 128

34 (a) Harvest and (b) Biomass Levels for $x_0 = 550,000$, $u_{max} = 0.53, 0.71$ and $T = 20$ 129

35 (a) Effort, (b) Biomass and (c) Total Harvest Levels for $x_0 = 750,000$, $z(T) = 355,000$, $E_{max} = 800,000$ and $T = 1$ 137

36 Harvest Level for $x_0 = 750,000$, $z(T) = 355,000$, $E_{max} = 800,000$ and $T = 1$ 138

37 (a) Effort, (b) Biomass and (c) Harvest Levels for $x_0 = 550,000$, $z(T) = 355,000$, $E_{max} = 800,000$ and $T = 1$ 139

38 (a) Effort, (b) Biomass and (c) Harvest Levels for $x_0 = 1,000,000$, $z(T) = 400,000$, $E_{max} = 800,000$ and $T = 1$ 140

39 (a) Effort, (b) Biomass and (c) Harvest Levels for $x_0 = 750,000$, $z(T) = 400,000$, $E_{max} = 800,000$ and $T = 1$ 141

40 (a) Effort, (b) Biomass and (c) Harvest Levels for $x_0 = 500,000$, $z(T) = 250,000$, $E_{max} = 800,000$ and $T = 1$ 142

41 (a) Effort, (b) Biomass and (c) Harvest Levels for $x_0 = 500,000$, $z(T) = 350,000$, $E_{max} = 800,000$ and $T = 1$ 143

42 Solution Curves for $E = 394.444$ 147

43 Solution Curves for $E = 394.444$ with $\theta = 0.25$ 148

44 Solution Curves for $E = 394.444$ with $\theta = 0.5$ 149

45 Solution Curves for $E = 394.444$ with $\theta = 0.75$ 149

46 Solution Curves for $E = 394.444$ with $\theta = 1$ 150

47 Linear and Quadratic Costs 159

48 (a) Effort and (b) Biomass Levels for $E_{max} = 296,380$, $x_0 = 550,000$; $750,000$ and $T = 1$ 160

49 (a) Effort and (b) Biomass Levels for $E_{max} = 296,380$, $x_0 = 550,000$; $750,000$ and $T = 20$ 161

50 (a) Effort and (b) Biomass Levels for $E_{max} = 592,761$, $x_0 = 550,000$; $750,000$ and $T = 1$ 163

51 (a) Effort and (b) Biomass Levels for $E_{max} = 592,761$, $x_0 = 550,000$; $750,000$ and $T = 1.5$ 164

52 (a) Effort and (b) Biomass levels for $E_{max} = 296,380$; $315,000$, $x_0 = 750,000$ and $T = 1$ 165

53 (a) Effort and (b) Biomass Levels for $E_{max} = 296,380$; $315,000$, $x_0 = 750,000$ and $T = 20$ 166

54 (a) Effort and (b) Biomass Levels for $E_{max} = 296,380$; $315,000$, $x_0 = 550,000$ and $T = 1$ 167

55 (a) Effort and (b) Biomass Levels for $E_{max} = 296,380$; $315,000$, $x_0 = 550,000$ and $T = 20$ 168

56 (a) Effort and (b) Biomass Levels for $E_{max} = 200,000$, $\theta = 0$, 0.25 and $T = 1$ 169

57 (a) Effort and (b) Biomass Levels for $E_{max} = 200,000$, $\theta = 0$, 0.25 and $T = 20$ 170

58 (a) Effort and (b) Biomass Levels for $E_{max} = 200,000$, $\theta = 0$, 0.5 and $T = 1$ 171

59 (a) Effort and (b) Biomass Levels for $E_{max} = 200,000$, $\theta = 0$, 0.5 and $T = 20$ 172

60 (a) Effort and (b) Biomass Levels for $E_{max} = 200,000$, $\theta = 0$, 0.75 and $T = 1$ 173

61 (a) Effort and (b) Biomass Levels for $E_{max} = 200,000$, $\theta = 0$, 0.75 and $T = 20$ 174

62 (a) Effort and (b) Biomass Levels for $E_{max} = 200,000$, $\theta = 0$, 1 and $T = 1$ 175

63 (a) Effort and (b) Biomass Levels for $E_{max} = 200,000$, $\theta = 0$, 1 and $T = 9$ 176

64 Net Revenue against θ for $\delta = 0.15$ and $T = 20$ 177

65 Net Revenue against θ for $\delta = 0$, 0.15 and $T = 20$ 178

66 Solution Curves for $h = 200,000$ 183

67 Solution Curves for $h = 355,000$ 183

68 Solution Curves for $h = 400,000$ 184

69 (a) Harvest and (b) Biomass Levels for $h_{max} = 351,039$, $x_0 = 450,000$; $600,000$ and $T = 1$ 188

70 (a) Harvest and (b) Biomass Levels for $h_{max} = 351,039$, $x_0 = 450,000$; $600,000$ and $T = 100$ 189

71 (a) Harvest and (b) Biomass Levels for $h_{max} = 351,039$, $x_0 = 400,000$ and $T = 6$ 190

72 (a) Harvest and (b) Biomass Levels for $h_{max} = 400,000$, $x_0 = 750,000$ and $T = 8$ 191

73 (a) Harvest and (b) Biomass Levels for $h_{max} = 355,000$, $x_0 = 550,000$; $750,000$ and $T = 1$ 195

74 (a) Harvest and (b) Biomass Levels for $h_{max} = 355,000$, $x_0 = 550,000$; $750,000$ and $T = 500$ 196

75 (a) Harvest and (b) Biomass Levels for $h_{max} = 355,000$, $x_0 = 450,000$ and $T = 12$ 197

76 (a) Harvest and (b) Biomass Levels for $h_{max} = 380,000$, $x_0 = 750,000$ and $T = 12$ 198

77 Shadow Price and Net Revenue for $h_{max} = 200,000$ and $T = 1$ 203

78 (a) Harvest Strategy and (b) Biomass Level for $h_{max} = 200,000$ and $T = 1$ 204

79 Shadow Price and Net Revenue for $h_{max} = 250,000$ and $T = 1$ 205

80 (a) Harvest Strategy and (b) Biomass Level for $h_{max} = 250,000$ and $T = 1$ 206

81 Shadow Price and Net Revenue for $h_{max} = 300,000$ and $T = 1$ 207

82 (a) Harvest Strategy and (b) Biomass Level for $h_{max} = 300,000$ and $T = 1$ 208

83 Periodic Rate Harvesting 210

84 Periodic Cycles for $h = 200,000$ 212

85 Periodic Cycles for $h = 355,000$ 213

86 Periodic Cycles for $h = 400,000$ 213

87 Shadow Price and Net Revenue for $h_{max} = 351,039$, $x_0 = 750,000$, $a = 0.25$ and $T = 1$ 217

88 (a) Harvest and (b) Biomass Levels for $h_{max} = 351,039$, $x_0 = 500,000$; $750,000$, $a = 0.25$ and $T = 1$ 218

89 Shadow Price and Net Revenue for $h_{max} = 351,039$, $x_0 = 750,000$, $a = 0.25$ and $T = 50$ 219

90 (a) Harvest and (b) Biomass Levels for $h_{max} = 351,039$, $x_0 = 500,000$; $750,000$, $a = 0.25$ and $T = 50$ 220

91 (a) Harvest and (b) Biomass Levels for $h_{max} = 351,039$, $x_0 = 400,000$, $a = 0.25$ and $T = 5$ 221

92 (a) Harvest and (b) Biomass Levels for $h_{max} = 400,000$, $x_0 = 750,000$, $a = 0.25$ and $T = 8$ 222

93 (a) Harvest and (b) Biomass Levels for $h_{max} = 351,039$, $a = 0$, 0.5 and $T = 1$ 224

94 (a) Harvest and (b) Biomass Levels for $h_{max} = 351,039$, $a = 0$, 0.5 and $T = 50$ 225

95 (a) Harvest and (b) Biomass Levels for $h_{max} = 351,039$, $x_0 = 400,000$, $a = 0$, 0.5 and $T = 4$ 226

96 (a) Harvest and (b) Biomass Levels for $h_{max} = 400,000$, $x_0 = 750,000$, $a = 0$, 0.5 and $T = 8$ 227

97 Phase-Plane Portrait for $a = 200,000$ and $u = 0.5$ 235

98 Phase-Plane Portrait for $a = 500,000$ and $u = 0.5$ 236

99 Determination of Sign of $\alpha(x, E)$ 241

100 (a) Biomass Proportion, (b) Biomass, (c) Effort and (d) Harvest Levels for $a = 200,000$, $u_{max} = 0.5$ and $T = 1$ 243

101 Shadow Price and Price for $a = 200,000$, $u_{max} = 0.5$ and $T = 6$ 244

102 (a) Biomass Proportion, (b) Biomass, (c) Effort and (d) Harvest Levels for $a = 200,000$, $u_{max} = 0.5$ and $T = 6$ 246

103 (a) Biomass Proportion, (b) Biomass, (c) Effort and (d) Harvest Levels for $a = 500,000$, $u_{max} = 0.5$ and $T = 1$ 248

104 Shadow Price and Price for $a = 500.000$, $u_{max} = 0.5$ and $T = 20$ 249

105 (a) Biomass Proportion, (b) Biomass, (c) Effort and (d) Harvest Levels for $a = 500,000$, $u_{max} = 0.5$ and $T = 20$ 250

106 (a0 Biomass Proportion, (b) Biomass, (c) Effort and (d) Harvest Levels for $a = 200,000$, $u_{max} = 0.9$ and $T = 1$ 253

107 (a) Biomass Proportion, (b) Biomass, (c) Effort and (d) Harvest Levels for $a = 200,000$, $u_{max} = 0.9$ and $T = 3$ 254

108 (a) Biomass Proportion, (b) Biomass, (c) Effort and (d) Harvest Levels for $a = 500,000$, $u_{max} = 0.9$ and $T = 1$ 255

109 (a) Biomass Proportion, (b) Biomass, (c) Effort and (d) Harvest Levels for $a = 500,000$, $u_{max} = 0.9$ and $T = 20$ 256

LIST OF ACRONYMS

BE	Bionomic Equilibrium
CPI	Consumer Price Index
CPUE	Catch Per Unit Effort
DIMEY	Dynamic Immediate Maximum Economic Yield
EEZ	Exclusive Economic Zone
FAO	Food and Agriculture Organisation of the United Nations
FASDP	Fisheries and Aquaculture Sector Development Plan
GSS	Ghana Statistical Service
IEZ	Inshore Exclusion Zone
IMEY	Immediate Maximum Economic Yield
IUU	Illegal, Unreported and Unregulated
MEY	Maximum Economic Yield
MFRD	Marine Fisheries Research Division
MOFAD	Ministry of Fisheries and Aquaculture Development
MPAs	Marine Protected Areas
MSY	Maximum Sustainable Yield
MVP	Minimum Viable Population
OAY	Open Access Yield
OSY	Optimum Sustainable Yield
SFMP	Sustainable Fisheries Management Project
SVU	Standard Vessel Units
TAC	Total Allowable Catch
TC	Total Cost
TR	Total Revenue
UNCLOS	United Nations Convention on the Law of the Sea
USAID	United States Agency for International Development

CHAPTER ONE

INTRODUCTION

The fishing industry in Ghana is dominated by the artisanal sector, which accounts for over 80% of the fishing population and contributes up to 70% of the landed catch. Presently, the catches emanating from the sector have been dwindling and some fisheries experts have characterised the situation as approaching a crisis. Therefore, there is the need to equip the Fisheries Commission with the necessary technical tools to effectively manage the situation before it reaches a full-blown crisis.

The aim of the research is to employ Optimal Control Theory in conjunction with Systems Simulation Approach, as advocated by Manetsch and Park (1982) and Seijo, Defeo and Salas (1998). The approach involves: a clear definition of fishery information needs; fishery characterisation, in terms of resource and fishing effort dynamics, ecological and technological interdependencies and management instruments; mathematical modelling of the fishery components or subsystems; data to fit equations of the mathematical model; development of a computer model to solve numerically the mathematical model; stability and sensitivity analyses for the computer model; model validation; evaluation of the bioeconomic impacts of alternative management strategies.

Background to the Study

The study focuses on the optimal harvesting of a renewable resource, more specifically a fishery resource, in order to ensure its sustainability for future generations. 'Optimal' is a loaded word. It is important for one to realise that what strategy is deemed optimal entirely depends on the specification of a performance criterion (Clark, 2010).

Once upon a time, there existed a myth about the inexhaustibility of marine resources. Gordon (1954) has asserted that during the latter part of the 19th century,

Scottish fishery biologist W. C. MacIntosh, and the evolutionist, T. H. Huxley, argued strongly against all restrictive measures on the basis of the inexhaustible nature of the fishery resources of the sea. Huxley, in 1883, (as cited in Gordon, 1954) asserted that:

> The cod fishery, the herring fishery, the pilchard fishery, the mackerel fishery, and probably all the great fisheries, are inexhaustible: that is to say that nothing we do seriously affects the number of fish. And any attempt to regulate these fisheries seems consequently, from the nature of the case, to be useless (p. 126).

However, rapid human population growth coupled with technological advances has resulted in increasing demand for resources, thereby leading to heavy exploitation. As Clark (2010) acknowledges, in the particular case of marine fisheries, depletion of fish stocks has gradually extended from readily accessible near-shore to remote offshore populations. Large-sized, valuable species have been progressively overfished or eliminated (Myers & Worm, 2003), in a process that Pauly, Christensen, Dalgaard, Froese and Torres (1998) have called 'fishing down the food web'.

The 1992/93 collapse of the Atlantic cod fishery in Canada heralded the end of 500 years of plentiful cod harvests, which had provided European nations such as England, France and Spain with a major source of animal protein for over five centuries (Clark, 2010).

The Food and Agriculture Organisation of the United Nations (FAO) analysis of assessed fish stocks shows that the share of stocks within biologically sustainable levels has exhibited a downward trend, declining from 90% in 1974 to 68.6% in 2003. Thus, 31.4% of fish stocks were estimated as fished at a biologically unsustainable level and therefore overfished. Also, of all the fish stocks assessed in 2013, 58.1% were fully fished and only 10.5% underfished (FAO, 2016).

Mullon, Freon, and Curry (2005) underscore that the fear of rapid depletion of fish stocks due to overexploitation is increasing and genuine. Analysis of 1,519

main series of the FAO world fisheries catch database over the last 50 years reveals that 366 fisheries' collapses occurred, that is nearly one fishery out of every four.

According to the Ministry of Fisheries and Aquaculture Development (MOFAD) (2016), the Ghana fisheries sector comprises three areas—marine, inland and aquaculture. While aquaculture and inland fisheries are mainly small scale, the marine are a combination of small and large scale industrial fisheries. Fisheries resources are obtained from the capture and culture environments. Capture fisheries comprise fish from the wild, which includes the sea, lagoons, lakes, rivers, streams, dams and reservoirs, constituting 90% of total fish production; while the remaining 10% is made up of culture fisheries, which includes farming or growing fish in ponds, lakes and cages.

The sector plays an enormous role in the socioeconomic development of the country. It serves as a major source of employment, wealth creation and livelihood, among others, especially for coastal and inland communities. The sector has served and continue to serve as the economic backbone of many adjoining communities for centuries. Employment generated by the sector is over 2.7 million of the population (Ghana Statistical Service [GSS], 2014). This comprises fishers as well as boat owners, boat builders, processors of landed fish and other ancillary jobs. It essentially provides over 70% of the total fish requirements and, by extension, the bulk of the country's protein requirements (MOFAD, 2016).

Furthermore, the sector contributed positively to the nation's objective of promoting food security, improved foreign exchange earnings and sizable individual incomes. Production of fish domestically totalled 451,099.4 metric tonnes (or simply, tonnes), which include 320,221.4 tonnes of marine capture (71.0%), nearly 86,268.3 tonnes of inland capture (19.1%) and 45,610 tonnes of aquaculture (9.9%) in 2015. To supplement domestic production, 145,910.3 tonnes of fish valued at US$120,443,785 were imported into the country. In terms of foreign exchange earnings accruing to the country, an estimated 53,750 tonnes of fish and seafood were exported, generating US$309,790,723.90 (MOFAD, 2016).

The marine fishery sector in Ghana comprises three main sub-sectors; namely,

small scale (for artisanal or canoe), semi-industrial (for inshore) and industrial (Nunoo, Asiedu, Olauson & Intsiful, 2015). As already alluded to, the marine sector is the most important of all the fisheries sectors, accounting for 71% of domestic fish production. Also, among the sub-sectors in the marine sector, the artisanal fisheries are prominent. Out of the estimated 135,000 fishers in the marine sector, up to 124,000, constituting 92% are artisanal fishers (Republic of Ghana Fisheries & Aquaculture Sector Development Plan [FASDP], 2016).

The artisanal fisheries are characterised by the use of several fishing gears operating from dugout canoes carved out of a single log of wood species called 'wawa' (*Triplochiton scleroxylon*) and 'Onyina' (*Ceiba petendra*). The preferred gear of the fishermen are purse seine, beach seine, gill net, and lobster net, among others. There are more than 12,700 canoes operating in 315 landing beaches and 190 fishing villages producing between 75 and 80% of the total marine production (Akyempon, Bannerman, Amador & Nkrumah, 2013; Bannerman & Quartey, 2006; Nunoo *et al.*, 2015).

The artisanal fisheries are dominated by the small pelagic species, which include round sardinella (*Sardinella aurita*), flat sardinella (*Sardinella maderensis*), chub mackerel (*Scomber japonicus*) and anchovy (*Engraulis encrasicolus*). The round sardinella (hereafter referred to as sardinella) forms the bulk of the small pelagics and does well when the temperatures are below 26 °C (MOFAD, 2016). The sardinella fishery has a long history in Ghana and it is very important both socially and economically. Investigations have shown that sardinella is influenced by climatic and oceanographic conditions; and it is seasonal and most abundant during the period of the major coastal upwelling (July to September), although juveniles are fished throughout the year. The minor upwelling season, which usually lasts for only three weeks, normally begin in December or January and end, by the latest, in February. Therefore, there are two fishing seasons for the sardinella (Koranteng, 1991).

Presently, the sardinella fishery teeters on the verge of collapse. The annual catch has plummeted year after year while the number of artisanal fishing canoes

has risen year after year due to the open access nature of the fishery. Annual catch fell to just over 17,000 tonnes in 2012 from a high of 120,000 tonnes just a dozen years earlier. Therefore, from all indications, the sardinella fishery is in a state of crisis since this is the longest period of decline after the start of heavy exploitation of the resource (USAID/Ghana SFMP, 2015).

In light of the numerous challenges confronting the sardinella fishery in Ghana, it is imperative to develop a bioeconomic model to help address these challenges; and optimal control theory provides a tool in this direction.

Optimal control theory is a powerful mathematical tool that can be used to make decisions involving complicated biological scenarios. For example, what percentage of the population should be vaccinated as time evolves in a given epidemic model to minimise the number of infected and the cost of implementation of the vaccination strategy? The desired outcome or objective depends on the particular scenario. Most of the time, the problem will include trade-offs between two competing interests. For instance, consider minimising a certain harmful virus population while keeping the level of the toxic drug administered low. Such a case could be modelled as a system of ordinary differential equations involving both levels of virus and drug as functions of time (Lenhart & Workman, 2007).

The behaviour of the underlying dynamical system is described by a state variable(s). It is assumed that there is a way to steer the state by acting upon it with an appropriate control function(s). The control enters the system of ordinary differential equations and affects the dynamics governed by the state system. The goal is to maximise (or minimise) a given objective functional by adjusting the control. Often times this functional will delicately balance the desired goal with the required cost to reach it. The cost referred to here may not necessarily represent money but may include side effects or damages as a result of applying the control. Generally, the objective functional depends on one or more of the state and control variables; and most of the time, the objective functional is represented by an integral of the state and/or control variables (Lenhart & Workman, 2007).

Kirk (1998) summarises the requirements for the formulation of an optimal

control problem as:

1. A mathematical description of the process to be controlled.

2. A statement of the physical constraints.

3. Specification of a performance criterion.

Applications of optimal control are many and varied; not excluding resource management, economics, management sciences, chemical and electrical engineering, aircraft guidance and control systems, science of human locomotion and the control of epidemics. In the context of natural resource management of which fisheries form an integral part, the study considered optimal control models with three different harvesting strategies.

Statement of the Problem

Given the importance of the sardinella fishery to the socioeconomic development of the country vis-a-vis its current near collapse status, there is the need to develop a bioeconomic model to provide answers to all concerned stakeholders in the fishing industry. A bioeconomic model not only models the biological population dynamics of the resource but also provides an economic perspective through cost-benefit analysis of the model.

The goal of the research was to use optimal control techniques to assess the impact of three harvesting scenarios—constant rate harvesting, proportional rate (or constant effort) harvesting and periodic rate (or seasonal) harvesting—on the fishery. Additionally, the impact of technology on the harvesting process was analysed; as well as analysing a model incorporating diminishing returns due to inadequate storage facilities when there is a bumper harvest.

Furthermore, while the effects of climatic conditions induced by global warming on the decline of the sardinella fishery could not be discounted, excessive exploitation by fishermen through the use of fishing gear with unapproved mesh sizes and also the use of attractants (light fishing) exacerbate the problem. To

investigate this claim, sensitivity analysis was performed on the catchability parameter in the model. Finally, a predator-prey model of the sardinella fishery is analysed and discussed.

Objectives

The overall objective of this study was to determine the sustainable harvesting strategies that could be applied to the Ghana sardinella fishery through the application of optimal control techniques and procedures.

In order to achieve the desired goal of ensuring the sustainability of the resource, the following were the specific objectives:

1. To develop autonomous and non-autonomous mathematical models representing the sardinella growth and harvesting dynamics.
2. To perform a qualitative analysis of the models through bifurcation techniques.
3. To investigate the performance of linear and quadratic controls in an optimal control model.
4. To derive and analyse the necessary conditions for the models to be optimal.
5. To determine the sufficient optimality conditions for the models.
6. To determine the equilibrium points, local and global stability of the predator-prey model.
7. To perform numerical simulations for easy analysis and discussion of the models.

Methods

The exponential and logistic growth functions were employed for the state dynamics of the resource while the objective functional would, generally, be to

maximise the discounted present value of future net revenues or profits.

Direct computation as well as computer resources was applied in the analyses. The software employed included Matlab, Maple, Matlab-interface software dfield8 and pplane8 (created by John Polking) and LaTeX.

Simulations were carried out on Matlab using the Forward-Backward Sweep method outlined in Lenhart and Workman (2007). The method uses a Runge-Kutta fourth order routine in which the state equation is solved forward in time and the adjoint equation backward in time using an initial guess. At the end of each iteration, the control is updated using the derived formula for the optimal control; and the iterations continue until convergence is achieved. This is for one state variable and one control function, but it is easily extended to cover situations of multiple states and controls as well as states with both initial and terminal levels fixed, and also for bounded controls.

The actual computer codes used in the simulations were originally developed by Lenhart and Workman (2007), and diligently modified to suit the particular models investigated in this study. In all the simulations, the performance criterion—the value of the objective functional—is computed using the trapz function in Matlab.

Scope of the Study

The area of study encompasses the entire coastline of Ghana, estimated at 528 km long with an Exclusive Economic Zone (EEZ) of 218 km^2 and a continental shelf of $23,700km^2$ (Minta, 2003). However, the artisanal fishermen who largely exploit the sardinella stocks operate within the Inshore Exclusion Zone (IEZ), which covers the coastal waters between the coastline and the 30-meter depth contour or six nautical miles offshore limit, whichever is farthest (Nunoo, Asiedu, Amador, Belhabib & Pauly, 2014).

Regarding the mathematical modelling employed in the study, only deterministic continuous-time, ordinary differential equations were considered. This

included both autonomous and non-autonomous models. Most of the models are one-dimensional, except the catch-quota model and the predator-prey model, which are two-dimensional systems of ordinary differential equations.

Justification of the Study

The study is intended to provide stakeholders in the fishing industry, namely government, fishers, conservationists and academics, with a science-based tool for sound decision making regarding the current unenviable situation of the sardinella fishery.

Most of the models reviewed in connection with the sardinella fishery use of discrete-time, difference equations. However, sardinella stocks and all associated activities like growth and harvesting do not only occur at discrete points in time but can be monitored at any point in time. Hence, the preference for continuous-time, differential equations to model the fishery in order to bring out new and interesting perspectives regarding the fishery.

This study will spur on other academics and researchers to undertake similar activities to help arrest the decline and near-extinction of the all-important sardinella fishery, not only in Ghana but also across the entire coast of West Africa, since the sardinella is highly migratory and is a shared resource among countries in the subregion.

Organisation of the Study

This piece of research work consists of nine chapters. Chapter One deals with the background to the study, where a brief description of the marine fishery sector in general and the artisanal fishery sub-sector in particular is presented. Also mentioned is the sardinella fishery, the focus of the study, as well as the main mathematical tool used in the analysis—optimal control theory. The chapter also includes the statement of the problem, the research objectives, the methodology employed, the scope and limitation of the study and the organisation of thesis.

In Chapter Two, the relevant literature on modelling and optimal management of fishery resources is presented. This gives an insight into how various authors and researchers confronted the problem of not only harvesting a renewable resource but also ensuring its sustainability for posterity. Some concepts on mathematical modelling and theory underlying the optimal control of resources are explored in Chapter Three.

Chapter Four looks at determining the optimal scheme with proportional rate (or constant effort) as the harvesting strategy. Also explored are the effects of illegal, unreported and unregulated (IUU) fishing on the sardinella stock; especially, the use of unapproved mesh sizes as well as attractants in fishing.

Regarding Chapter Five, the analysis of the fishery to determine the optimal harvesting strategy using constant harvesting is outlined. Periodic rate (or seasonal) harvesting of the resource is also investigated in this chapter. A predator-prey model is presented is Chapter Six. This models the sardinella as prey undergoing predation by man. Finally, Chapter Seven presents the summary, conclusions, and recommendations for the Fisheries Commission borne out of the research.

Chapter Summary

The introductory chapter has laid out the background to the study by providing the current unenviable situation of the artisanal fisheries. However, given the importance of the artisanal fishermen to the socioeconomic development of the country, the goal of the research is to use optimal control techniques to assess the impact of harvesting on the sustainability of the sardinella fishery.

The chapter has given the background to the study, as well as providing the statement of the problem and the objectives of the research. Also covered in this chapter are the methods, scope and justification of the study. Finally, the organisation of the study, which gives an overview of all the seven chapters, is provided.

CHAPTER TWO

LITERATURE REVIEW

Introduction

This chapter deals with the review of the relevant literature pertaining to the field of study. Mathematical models of fishery resources as well as models presented in the form of optimal control problems will be reviewed and discussed.

Modelling and Optimal Management of Resources

According to Clark (2010), models come in every size and form, from verbal descriptions and mathematical equations to large-scale computer models. However, one feature shared by all models in the life and social sciences is that they constitute abstractions and simplification of the real world. As a matter of fact, any model that merely duplicated reality (if such were possible) would be all but useless, at least in terms of providing insights.

Even though desirable and inevitable, model simplicity comes with a cost—the model may turn out to be seriously flawed in some respects. A well-chosen model may provide insightful or convincing explanations of some phenomenon, but nevertheless be completely misleading in other ways. The inherent danger is that such a model will become uncritically accepted in applications for which it is not intended (Daly & Cobb, 1989). Therefore, every modeller has a moral obligation to think about and publicise the underlying assumptions and limitations of his or her model (Clark, 2010).

An optimal control problem is an extension of a mathematical model in the sense that a performance criterion is specified for a given model, as pointed out by Kirk (1998) in the first section of Chapter One. Lenhart and Workman (2007) further explained that the performance criterion is called an objective functional, which is usually an integral of the state and/or control variables. The goal is seek

an optimal control(s) that will maximise or minimise the objective functional subject to the state dynamics of the formulated model. In general, the maximisation is sought for net revenues or profits and the minimisation for costs.

Modern applications of optimal control theory have roots in the classical model proposed by Gordon (1954) and Schaefer (1954), known as the Gordon-Schaefer bioeconomic model. As the name of the model suggests, it combines both economic and biological parameters in the model. The economics aspect of the model is due to Gordon while the biological aspect is credited to Schaefer. This pioneering model was static in nature; that is, it was time-invariant or time-independent. To further elucidate, the model only looked at the steady-state conditions (also known as equilibrium conditions) of a resource under harvesting and not the evolution over time.

Schaefer (1954) notes that the population of marine fish under exploitation by a fisher may be influenced by a great number of factors in the complex biological system of which it is a part. Of these, however, only one, predation by man is capable of being controlled or modified to a significant degree by regulating the activities of man. Any management or control of the fishery, to the extent that this may even be possible, must, therefore, be effected through the activity of the fisherman.

Management of a fishery has at its cornerstone the modification or limitation of the activities of the fisherman in order to realise a change in fish population, or the catch, or both, which in some way is preferable to which would obtain if the fishermen were allowed to operate unregulated (Schaefer, 1954).

In the pioneering work by Gordon (1954), the author acknowledged that the major goal of the study was to examine the economic theory of natural resource utilisation as it related to the fishing industry. The argument advanced was that it appeared most of the problems associated with the words 'conservation', 'depletion' or 'overexploitation' in the fishery were, in reality, manifestations of the fact that the natural resources of the sea yielded no economic rent. The term economic rent may be viewed as the regular income derived from an endurable resource; it

also refers to the net income (also known as net revenue) or profit (Clark,1973).

Fishery resources, by and large, are treated as common-property, thereby creating lots of problems for all stakeholders involved with the industry. Clark and Munro (1975) demonstrated that, with the aid of optimal control theory, fisheries economics can without difficulty be cast in the framework of capital theory, and yielding results that are both general and readily comprehensible.

Having found inadequacies in the static Gordon-Schaefer model, they developed a dynamic linear autonomous model; where the static version of the fisheries economics model was seen to be the equivalent of the special case of the dynamic autonomous model. The model was then extended, first by making it non-autonomous in the price and cost parameters and second, non-linear, in the sense that the objective functional was made a non-linear function of the control variable—rate of harvest.

Explaining further, Clark and Munro (1975) stated that there was a recognition, virtually from the time of its inception, that fisheries economics like other aspects of resource economics, should ideally be cast in terms of capital theory. The fish population, or biomass, can be viewed as a capital stock in that, like 'conventional' or man-made capital, it has the capacity for yielding sustainable consumption flow through time. As with conventional capital, today's consumption decision by its impact upon stock level, will surely have implications for future consumption options. Thus, the resource management problem becomes one of selecting an optimal consumption flow through time, which in turn implies selecting an optimal stock level as a function of time.

In their study of the linear autonomous model, they found the existence of an optimal stationary equilibrium, determined by a generalised 'modified Golden Rule'. The golden rule of capital investment (investment is simply increasing the stock of capital) says that the stock of capital should be increased (or if necessary, decreased) until marginal productivity equals the rate of discount, or rate of interest. The general bioeconomic rule could thus be referred to as a modified Golden Rule in the sense that the modification (marginal stock effect) reflects the fact that

the unit harvest costs are a decreasing function of stock size. The optimal management policy that emerged out of the study was that of following the bang-bang feedback control law: adjust the stock toward the stationary equilibrium as rapidly as possible. The bang-bang control is so-called because the optimal values of the control variable lie at its extremals. Therefore, the control variable switches (or bangs) from the lower value (usually zero) to an upper value denoting the allowable maximum for the control. Also, a harvest strategy in which the rate of harvest is a function of the current size of the resource is known as a feedback strategy (Clark, 2010).

Goh (1969) was among the first to apply optimal control theory to the management of a fishery resource. However, the model formulated was not a bioeconomic model per se, as the objective functional was an integral of only the control variable, the catch (also referred to as the yield or the harvest). Thus the performance criterion was to maximise the total catch over a period of time subject to the resource dynamics, which were modelled by a logistic growth function. The constant rate harvesting optimal control model yielded both singular and bang-bang approaches as the probable optimal rate of harvest since the problem was linear in the control variable.

Among the pioneering articles on fishery regulation was one authored by Palm (1975). The paper attempted to show how optimal control theory could be used to formulate a regulatory scheme for fisheries. The regulatory mechanism identified in the study was a limit imposed on fishing effort. The study also showed that static optimisation methods, such as maximum equilibrium yield analysis, need to be supplemented by dynamic methods such as optimal control theory, which takes into account the variable nature of a fishery. The dynamic analysis is used to show that the quantum of a limit on effort should be a feedback function of the state variables of the fishery. The concept of the Linear-Quadratic Optimal Control Problem was also introduced as a mechanism for devising such a feedback control scheme for fishery regulation. The paper started with a single-variable logistic model, and the analysis was later extended to a model containing three variables

to show how the techniques employed in the single-variable case could easily be applied to the general multivariate case.

Palm (1975) maintains that the need for fishery regulation is apparent and will become even more so with the establishment of resource management zones off the coasts. Regulatory mechanisms include catch quotas and limits on fishing effort (number of boats permitted entry into the fishery, number of fishing days, reserve areas, mesh size of fishing gear used, and so on). Therefore, a mathematical model of a fishery that includes both biological and economics factors is useful for determining the best regulatory strategy.

Elaborating further, Palm (1975) stressed that much of the analysis of fisheries was based on the concept of equilibrium. However, equilibrium is an idealisation and is never actually encountered in reality because continually changing environmental influences act as disturbances which displace the system from its equilibrium condition. For systems that are unstable, this is disastrous as equilibrium is never regained; and for systems that are stable with large time constants, the return to equilibrium might take so long as to negate the assumptions and usefulness of the equilibrium analysis. Therefore, as already alluded to, static or equilibrium-based analysis should be supplemented with dynamic methods which take into account the complex nature of the fishery.

Dubey and Patra (2013a) proposed a two-dimensional resource model to study and analyse the effects of crowding. The renewable resource was being utilised by the human population for its growth and development while taking into account the consequences of crowding. Variables representing the resource and population were modelled using the logistic equation. The intrinsic growth rate and carrying capacity of the resource stock were modelled as decreasing functions of the population, while the intrinsic growth rate and carrying capacity of the population were modelled as increasing functions of the resource stock. In other words, the interaction between the resource and the population effected a decrease in the resource stock and an increase in the size of the population. Furthermore, the resource stock was assumed to be harvested at a rate proportional to the size of the stock

and of the effort expended in harvesting. The biological and bioeconomic equilibria of the system were analysed and discussed. Global stability behaviour of the positive equilibrium point was also analysed and discussed through output feedback control. The objective functional employed in the study was the discounted present value of future net revenues, which was to be maximised. Pontryagin's maximum principle was used for the analysis and afterwards numerical simulations were carried out to validate theoretical results.

In yet another study, Dubey and Patra (2013b) proposed a three-dimensional optimal control model of a renewable resource utilised by a population with taxation as the control instrument. The model is similar to the earlier one (Dubey & Patra, 2013a) discussed. However, in this model, the additional third variable representing harvesting effort is assumed to be dynamic and not static as in the earlier version. Also, the harvesting effort (or fishing effort) served as the control for the earlier model but in this current paper, the control variable is the taxation imposed on the harvested stock of the fishermen by the regulatory agency. As in the previous model, the equilibria and stability dynamics of the model were analysed and discussed. The objective for the regulatory agency imposing the tax is to maximise the discounted net revenues accruing to society from the fishery subject to, of course, the state dynamics as well as the bounds placed on the taxation control. It is of interest to note that the control does not explicitly appear in the objective functional as the effect of the taxation on the fishermen by the agency is cancelled out for the mutual benefit of the larger society. The control only manifests itself in the dynamic harvesting effort. The necessary conditions for optimality of the model were derived using Pontryagin's maximum principle. Numerical simulations were again performed to give meaning to theoretical results. The simulation process yielded the optimal tax policy for the model. It was shown that if the resource stock, population and harvesting effort were kept along the optimal path, the resource and population can be maintained at an appropriate level.

A bioeconomic model of a fishery with variable price was studied by Mansal,

Nguyen-Huu, Auger and Balde (2014). The model described the time evolution of the resource, with fishing effort and price assumed to vary with respect to demand and supply. The supply is the instantaneous catch while the demand function is assumed to be a monotonic decreasing function of the price. It was shown that the generic market price equation can be derived and solved to provide the nontrivial equilibria of the model. Further, the market price equation was also shown to have one, two or three equilibria; and their local and global stability investigated. Also, the market price equation was then extended to two cases: an age-structured fish population and a fishery with storage of the resource.

Kar and Misra (2010) proposed a resource-based stage-structured model with selective harvesting of mature or adult species. The model involved three variables, the plankton, juveniles and adults. The fish population was stage-structured such that the juveniles lived off the adults who in turn fed on the plankton, which was assumed to follow a logistic law of growth. Another key and novel feature of the model was the inclusion of the universally prevalent intraspecific interference competition in the consumer growth dynamic (Kuang, Fagan & Loladze, 2003). This competition is assumed to induce additional deaths only to the adult subpopulation, and the increased death rate is proportional to the square of the adult subpopulation. The terms describing the competition refer to either self-limitation of consumers or the influence of predation. Self-limitation is known to occur if there is some other factor (other than food) which becomes limiting at high population densities. It was also assumed that only the adults were subjected to harvesting, which was proportional to the harvesting effort and size of the adult subpopulation. Stability and permanence of the system were analysed and discussed. The goal was to maximise the discounted net revenues from the harvested adults. Furthermore, the maximum sustainable yield, maximum economic yield and optimal sustainable yield for the model were obtained. Different tax policies were then discussed that led to the attainment of the aforementioned reference points. The results were portrayed in the form of plotted figures.

The issue of a reserve area or a marine protected zone in fishery, where fish-

ing is completely prohibited or closely monitored, is controversial and has been studied by many authors (Bonocoeur, Alban, Guyader & Thebaud, 2002; Hilborn, Micheli & De Leo, 2006; Holland & Brazee, 1996; Kar & Matsuda, 2008; Lauck, Clark, Mangel & Munro, 1998; Neubert, 2003; Pollacheck, 1990; Rodwell, Barbier, Roberts & McClanahen, 2002; Sanchirico & Wilen, 1999, 2001, 2005).

Dubey, Chandra and Sinha (2003) have investigated an optimal control model involving a fishery with reserve area. The two-dimensional model represented the two zones of the fishery: a free fishing zone and a reserve zone were fishing was strictly prohibited. The variables in the model therefore represented the subpopulation densities of the same fish population inside the unreserved and reserved areas. Migration of fish from either zone was made permissible in the model. The growth of fish in each zone was assumed to obey the logistic growth function. Fishing was only allowed in the unreserved area, harvested at a constant fishing effort. Thus the catch per unit effort (CPUE) in the fishery was proportional to the unreserved area's population density. Biological and bioeconomic equilibria of the system were obtained, and criteria for the local and global stability of the system derived. The objective was to maximise the discounted net revenue from harvesting the fish from the unreserved area. The optimal harvesting policy was also discussed using Pontryagin's maximum principle. The study showed that even if fishery is exploited continuously in the unreserved zone, the fish subpopulations of the zones can be maintained at an appropriate equilibrium level in the habitat.

Freedman (1984) studied persistence on three interacting predator-prey populations. In the paper, the author considers a class of deterministic models of three interacting populations with a view towards determining when all of the populations persist. In analytical terms, persistence refers to the scenario where $\liminf_{t\to\infty} x(t) > 0$ for each population $x(t)$; in geometric terms, this means each trajectory of the modelling system of differential equations is eventually bounded away from the coordinate planes. The class of systems considered in the study allowed three level food webs: two competing predators feeding on a single prey,

or a single predator feeding on two competing prey populations. As a corollary to the last case, the study shows that the addition of a predator can lead to persistence of a three population system; where without a predator, the two competing populations on the lower trophic level would have only one survivor. Kolmogorov-type basic models are used in the study, and the results obtained improved on several previous theorems on persistence.

In a study on fish management and harvesting strategies using the logistic growth model, Laham, Krishnarajah and Shariff (2012) considered two harvesting strategies, constant harvesting and periodic harvesting. According to Idels and Wang (2008), constant harvesting refers to the situation where a fixed number of fish is removed each year, while periodic harvesting (also referred to as seasonal or oscillatory harvesting) depicts the scenario where the harvest varies from season to season; and if in some season fishing is stopped, the amount of fish might be able to increase again. Laham *et al.* applied the single-variable model to tilapia fish farming in Malaysia. The periodic harvesting function considered in the study was piece-wise constant having a period of 12 months; and the harvesting and no harvesting duration was six months apiece. The maximum sustainable yield for the model was obtained and discussed with the aid of plotted figures. The findings of the research showed that, comparatively, the better strategy was periodic harvesting as it allows for the growth of the fish to be unhindered during the no harvesting period.

According to a study by Kar and Chakraborty (2010) on effort dynamics in a predator-prey model with harvesting, setting up the correct marine reserve is qualitatively similar to setting the correct total allowable catch, or of fisheries tax rate. However, the main difference is that the knowledge base for setting the reserve is probably substantially weaker than the more traditional controls.

In the study, they have considered a fully dynamic model of an open access fishery where the level of fishing effort expand or contract according as the discounted net revenue to the fisheries is positive or negative. This type of model, reflecting the dynamic interaction between the net revenue and effort in a fishery,

is called a dynamic reaction model. The model has three state variables: prey, predator and fishing effort. The growth dynamics of the prey are modelled by a logistic equation; and the predator-prey interaction is not the traditional direct product term, but a Holling-type response function—a limited growth function—called the Michaelis-Menton kinetics (or Monod). The intraspecific interference competition is also introduced among the prey species. This predator-prey type optimal control fishery model incorporated a partial closure of prey species. The steady states, local and global stability of the system were determined, as well as examining the dynamic behaviour of both species. The optimal harvesting policy was formulated and solved with the aid of Pontryagin's maximum principle. With numerical examples, simulations were performed to illustrate the results.

Hanson and Ryan (1998) studied an optimal harvesting model with both population and price dynamics. They considered the effects of large price fluctuations on the computed harvest strategy for a randomised Schaefer model. Both prices and population size were assumed random with both background (Wiener) and jump (Poisson) components. Population fluctuations were assumed to be density independent; in other words, relative changes were not functions of population size. The model assumed quadratic cost with no inflationary effects. Stochastic dynamic programming was employed to find the optimal harvesting effort and discounted net revenue for a realistic set of bioeconomic data for Pacific halibut fishery. It was found that inflationary effects had a pronounced influence on the optimal net revenue, even in a hazardous or disastrous environment. However, optimal harvesting effort levels were much less sensitive to inflationary effects.

In their research on harvesting fisheries management strategies with modified effort function, Idels and Wang (2008) identified five standard fishery harvesting strategies: constant harvesting, proportional harvesting, proportional threshold harvesting, seasonal harvesting and rotational harvesting. In traditional fishery models, fishing effort is simply expressed as a function of time. However, this does not address the effect of fish abundance on fishing effort (Murray, 2003). That is, for higher densities of fish, there is the expectation that less effort will

be expended per unit of harvest. Therefore in their paper, based on a canonical differential equation model (Schaefer model), they developed a new fishing effort that relied on the density of fish population. In other words, the fishing effort is assumed to be a function of the population dynamics of the fishery. The study showed that a control parameter—the magnitude of the effect of the fish population size on the fishing effort—changes not only the rate at which the population approaches equilibrium but the equilibrium values themselves. To investigate the consequences of the different harvesting strategies aforementioned, qualitative analyses and numerical simulations were employed.

A bioeconomic model of a single-species fishery was the subject of study by Kar and Matsuda (2008). The research work examined the impact of the creation of marine protected areas from both economic and biological perspectives. In particular, they examined the effects of protected patches and harvesting on resource populations. The two-dimensional model had variables representing the nature reserve and harvesting reserve sub-areas of the population's habitat area. A logistic growth model was employed with each subpopulation possessing its own carrying capacity, which is proportional to its distribution area. It was assumed that the fish are free to migrate between the two patches of the fishery, as well as within each of them. The objective was to maximise the discounted net revenue from the harvest of the fish in the harvesting reserve sub-area subject to the population dynamics of the system and the bounds placed on fishing effort. The steady states, local and global equilibria were obtained and analysed. They concluded that the protected patches are an effective means of conserving resource population, even though extinction cannot be ruled out in all cases. The optimal equilibrium harvest policy was discussed, and explanations proffered for the economic and biological interpretations of the results.

In their paper, Fan and Wang (1998) examined the exploitation of a single population modelled by time-dependent logistic equation with periodic coefficients. Almost all known models assume that the intrinsic growth rate and carrying capacity of the population are independent of time, but in the real world the natural

growth rates of many populations vary with time; for example, due to seasonality. Thus the proposed model is non-autonomous in the intrinsic growth rate and carrying capacity parameters. They showed that the time-dependent logistic equation has a unique positive periodic solution, which is globally asymptotically stable for positive solutions, and also obtained its explicit representation. Furthermore, they chose the maximum sustainable yield as the management objective and investigated the optimal harvesting policies for constant effort harvest and periodic effort harvest. The optimal harvesting effort that maximised the annual sustainable yield, the corresponding optimal population level, the corresponding harvesting time-spectrum and the maximum sustainable yield were determined. Also, explicit expressions were obtained in terms of the intrinsic growth rate and carrying capacity of the given population. The interesting and brief results obtained in the study generalise the classical results of Clark (2010) for a population described by an autonomous logistic equation in a renewable resource management.

Keesom, Macrae, Uhlig and Wang (2010) investigated sustainable harvesting rates in a model, which was compiled as a technical report. The report was to determine and propose a model by which an optimal harvesting frequency could lead to the maintenance of a steady population of Alaskan salmon. In order to do so, they looked at the growth rates of the salmon population as well as death rates due to harvesting and other factors. Some mortality factors are known to be age-dependent (for instance, only adult fish have been found to cannibalise young fish), so they considered the overall Alaskan salmon as two subpopulations of adults and juveniles. A differential equation to model the population dynamics of the adult and juvenile fish was obtained. They also considered the periodic nature of harvesting in the salmon fishery. Every year, the harvest target is the adult fish that return to reproduce; for the spawning salmon is considered by human consumers as a delicacy. Because the mating season occurs annually and around the same time, harvesting can be represented by a constant trigonometric function whose amplitude and frequency represent the harvesting rate limit and the frequency per unit time, respectively. Thus a non-linear differential equation

with an oscillatory harvesting component of the salmon population was obtained. The model was solved numerically using Euler's method of approximation, and the results analysed and discussed.

In a research article by Hasanbulli, Rogovchenko and Rogovchenko (2013), they studied the dynamics of a single-species population in a fluctuating environment under periodic yield harvesting. The underlying model was logistic with the growth rate, carrying capacity and harvesting rate all periodic. They obtained positive estimates for positive attracting and repelling periodic solutions and described behaviour of other solutions. Extinction and blow-up times are evaluated for solutions with small and large initial data; dependence of the number of periodic solutions on a parameter associated with the intensity of harvesting is explored. As the parameter grows, the number of periodic solutions changes from two to zero. They also found bounds for the bifurcation parameter whose value in practice can be efficiently approximated using numerical techniques.

Akpalu and Vondolia (2011) explored a model of spatial fishery management in developing countries. The understanding is that fishers in developing countries do not have the resources to acquire advanced technologies to exploit offshore stocks. As a result, the United Nations Convention on the Law of the Sea (UNCLOS) requires countries to sign partnership agreements with distant water fishing nations to exploit offshore stocks. However, for migratory stocks, the offshore may serve as a natural marine reserve (or a source) to the inshore (or a sink); hence the partnership agreements generate spatial externality. According to Clark (2010), an external cost or externality is a cost imposed on society or a subset of society by the action of an individual or firm. For example, the Black Sea, once a major food source for Middle Eastern civilisations, is now virtually devoid of fish (besides being shunned by tourists), as a result of industrial pollution from the rivers Danube, Dniester, Dnieper and others (Woodward, 2000).

Furthermore, Akpalu and Vondolia (2011) emphasise that the differences in abundance of fish stocks in habitats are important for ecosystem resilience since a biomass collapse in one habitat could be revived by the inflow of biomass from the

adjacent habitat. According to Elmqvist *et al.* (2003), response diversity among species in an environment is a crucial requirement for ecosystem resilience, and it is required to overcome the temporal and spatial variations in disturbances for continuous provision of ecosystem services and for reorganisation. Therefore, any management strategy that fails to recognise the sub-stock diversity may as a consequence lead to overestimates of stock levels, harvest potential, and subsequently the collapse of fisheries resources (Sterner, 2007).

Bioeconomics of commercial marine fisheries of Bay of Bengal was the focus of study by Habib, Ullah and Duy (2014). The paper aimed to assess the sustainability of current level of fishing effort as well as possible changes driven by anthropogenic and climatic factors. Therefore, the commercial marine fisheries of the Bay for the period spanning 1985 to 2007 was analysed with the help of the static Gordon-Schaefer bioeconomic model. Static reference points such as open access equilibrium (also referred to as bionomic equilibrium), maximum sustainable yield and maximum economic yield are established from parameter values obtained from the study of the fishery. Sensitivity analysis simulating the effects of potential anthropogenic and climatic factors is performed on the intrinsic growth rate and carrying capacity of the Bay fishery under the aforementioned reference points. The results from the study showed that the fishery is not biologically overexploited; however, it is predicted to be passing through a critical situation in terms of achieving the desirable reference points in the near future. Higher fishing effort and inadequate institutional and legal framework have been the major bottlenecks for the proper management of the Bay fisheries, and these may lead to the fishery becoming more vulnerable to the changing marine realm as a result of the anthropogenic and climatic factors. The study therefore calls for policy intervention to restore the stock from the current high fishing pressure that would eventually lead to the depletion of the resource.

A bioeconomic model with logistic growth in which a social planner uses landing tax (ad valorem tax) to internalise the spatial externality was studied by Akpalu and Vondolia (2011). The goal of the landing tax is to maintain the off-

shore stock at a reserve level or maximise the fishery manager's net benefit. The results of the study indicated that the tax must reflect the biological connectivity between the two patches, intrinsic growth rate, the price of fish, cost per unit effort and social discount rate. The findings are empirically illustrated using data on Ghana.

Kaplan and Smith (2000) considered a model relating to optimal fisheries management in the presence of an endangered predator and harvestable prey. The paper analyses the presence of an endangered predator that competes with humans for a commercially viable prey. Because traditional predator controls are not possible when the predator is endangered, the study rather focuses on harvest effort controls over the prey's habitat as a means to sustain the predator-prey relationship and sustain the economic viability of the fishery. The management model employed is based on optimising fishery rents subject to maintaining a growing predator population. The authors explored optimal management decisions along a singular path, with and without a predator constraint, and demonstrated the need to consider the predator-prey relationship explicitly. In addition, they derived an expression for the shadow price of the endangered predator along the singular path in terms of the opportunity cost of fishery rents. To illustrate the results, the model was applied to the contentious California sea otter-urchin system and the related urchin fishery.

Optimal impulsive harvesting policy for a single population was the subject of study by Zhang, Shuai and Wang (2003). In the paper, they considered the exploitation of a single population with dynamics modelled by the autonomous logistic equation under impulsive harvesting. By some innovative methods, they analysed the impulsive harvesting population model and obtained the explicit expression for the existence and global attractiveness of impulsive periodic solutions for both constant yield and proportional harvesting. The management objective was the maximum sustainable yield, and the two harvesting policies were investigated under the reference point. The optimal harvesting effort that maximises the sustainable yield per unit time as well as the corresponding optimal population

levels was determined. The findings from the study indicate that the continuous harvesting policy is superior to the impulsive harvesting policy; however, the latter is more beneficial in the sense that it is easier to implement in practice.

Lleonart and Merino (2009) proposed the concept of immediate maximum economic yield (IMEY) as a realistic fisheries economic reference point. They contend that unregulated or poorly managed fisheries tend towards overexploitation, but fisheries rent does not completely dissipate when immediate rent maximisation is sought. The principle of immediate rent maximisation is the basis of the derivation of a classical model, and has led to the definition of a relationship in a catch-and-effort diagram referred to as the dynamic immediate maximum economic yield (DIMEY) curve. For any initial biomass, if the economic rent in the immediate harvesting season is maximised, then the harvesting effort and catch strategy follow will be located on the DIMEY curve. The DIMEY curve is not only used for dynamic simulation but also used to identify the new reference point, IMEY, which is proposed as a more realistic reference point than the classical open access solution often advocated for in unregulated fisheries. IMEY properties are described and compared in the yield-and-effort diagram with traditional reference points—maximum sustainable yield, maximum economic yield and open access yield. Theoretical conclusions are compared with empirical evidence provided by the red shrimp fishery off Blanes, Spain (NW Mediterranean). Observed catch-and-effort records are plotted and the results show that they are positively correlated with the DIMEY and the IMEY.

In a study, Udumyan, Ami and Cartigny (2010) integrated habitat concerns into the classical Gordon-Schaefer model. The traditional Gordon-Schaefer model only considers the resource stock dynamics of the fishery while assuming a constant carrying capacity. They proposed an extension to the model that incorporates the dynamics of the carrying capacity as an indicator of the changes to the marine habitat. Recent studies by several authors support this notion (Pikitch *et al.*, 1998; Powers & Monk, 1988; Worm *et al.*, 2006). According to these authors, ecosystem attributes must be integrated into management, and successful management

cannot be achieved without a clear understanding of the biological processes at an ecosystem level.

The research work by Udumyan *et al.* (2010) yielded two major findings. First, they demonstrated that habitats matter, by showing that the main outcomes of the Gordon-Schaefer model are dramatically altered if habitat concerns are included in the analysis. Second, through a heuristic model and simulations, they showed that the extended model provides an appropriate framework to analyse the putative contributions of marine protected areas and artificial reefs.

According to Koranteng (1994), sardinellas were caught mainly with beach seines and various types of gill nets, the most important of which was the 'ali' net. This net has been used in Ghana since about 1850, and was the most important of all fishing gears used in the sardinella fishery (Lawson & Kwei, 1974).

It is of interest to note that when the ali net was first introduced, the local chiefs in the fishing communities foresaw its long-term destructive tendencies and therefore enacted bye-laws to prohibit its use. However, they were firmly opposed, paradoxically, by then Colonial Government which saw no adverse effects in the use of the net. In fact, according to Walker, (as cited in Akpalu, 2002), the Colonial Secretary of Agriculture in 1934 sent a memo to the Provincial Commissioner of Winneba seeking to bar the chiefs from enforcing the bye-laws on the use of the ali net with the key statement, "the best fishing net is the one that catches the most fish" (p.12).

The Secretary of Agriculture's memo drew inspiration from an earlier ruling in a case Colony vs Local chiefs delivered by the Colonial Chief Justice. Walker (as cited in Akpalu, 2002) stated that Justice Griffith remarked that:

> ...if [I] thought for a moment that the use of the Ali nets did tend to injure a fishing industry [I] would advise the defendants to apply to the government to legislate, but with the experience of practically the whole civilized world against that view, [I] did not hesitate to say that the Government should rather encourage than discourage the use of the Ali net (p. 11).

Furthermore, it became necessary to develop a more effective and efficient fishing net within the sardinella fishery since the ali net, a gill net, was found to be inadequate for harvesting schooling fish like sardinellas.

Koranteng (1994) further emphasised that the introduction of synthetic materials in the manufacture of netting contributed to a large extent in the quest for better fishing gears. Bigger and more durable nets were constructed that required less frequent mending. A surrounding net known locally as 'watsa' was developed. The watsa was modified into a purse seine net (Doyi, 1984). This was further developed into a new seine net called 'poli' which contains small-sized meshes made up of thinner twine. Doyi states that, whereas the watsa was constructed with only 50 – 60 mm mesh netting made of twine of 0.50 mm diameter, the poli net had mesh and twine sizes of 10 – 13 mm and 0.33 mm, respectively.

As previously mentioned, the artisanal fishery sector is open access with minimal regulatory framework. This open access nature of the fishery breeds unhealthy competition among the fishermen, with the mentality of each fisherman being, "If I don't catch the fish, someone else will or might!" (Stavins, 2012). It is therefore not surprising that faced with dwindling fish stocks, individual fishermen would go to extremes to outperform the competition. These extreme measures include use of under-sized mesh gears, light fishing, explosives like dynamites and chemicals.

To buttress this fact, Koranteng (1998) says it is common practice for fishers operating in an over-exploited and usually unmanaged or poorly managed fishery to use smaller-sized meshes as a means to increase their catch. Pauly, Silvetre and Smith (1989) and Pauly (1994) describe such a scenario as Malthusian overfishing, which is a situation where poor fishers, faced with declining catches and lacking any other alternative, initiate wholesale resource destruction in their effort to maintain their meagre incomes. Pauly *et al.* give the symptoms of Malthusian overfishing (in order of seriousness) as:

1. use of gears and mesh sizes that are not sanctioned by government;

2. use of gears not sanctioned within the fisherfolk communities;

3. use of gears that destroy the resource base; and

4. use of 'gears' such as dynamite or sodium cyanide that do all of the above and even endanger the fisherfolks themselves.

The practice of such unapproved and illegal fishing methods by artisanal fishers in Ghana results in the gear catching substantial quantities of young fish of all species, as well as destroying the fish habitats. This situation is aggravated by the fact that there is market for all sizes of fish in Ghana; therefore, there appears to be some benefit, even if marginal, in catching juvenile fish (Koranteng, 1998).

The few Government regulations on the artisanal fishery sector include adherence to a minimum mesh size of 25 mm, approximately one inch, in stretched diagonal length (Akpalu, 2002). This regulation has been wantonly disregarded by the fishermen, rendering it ineffective. The main argument advanced by the fishermen is that the minimum size of 25 mm in stretched diagonal length cannot catch some of the targeted species like anchovies. Thus, they continue to use the ali/poli/watsa net of mesh size 10 mm to disastrous consequences for the artisanal fishery sector (Akpalu, 2002).

Chapter Summary

The literature that has been reviewed for the study ranged from one-dimensional to multi-dimensional models. Most of the models were subjected to stability analysis and the equilibrium points determined.

The classical Gordon-Schaefer bioeconomic model was studied in depth, as well as the current modifications to the model. Pontryagin's maximum principle was employed in determining the optimality of the models. The optimal control in most instances was singular, with a few cases being bang-bang. Simulations were carried out on the models that yielded interesting results.

However, there were hardly any models on the artisanal fishery in Ghana. This

research therefore fills the gap by reviewing the existing models as they apply to the sardinella fishery, and also coming up with original models to study the fishery.

CHAPTER THREE

RESEARCH METHODS

Introduction

In the application of optimal control theory, there is the need to review some of the concepts and background theory that underpin the optimisation process. Therefore, a review of some definitions and concepts in dynamic optimisation was carried out in the first section of this chapter. The classical approach to dynamic optimisation problems is the calculus of variations. A review of this optimisation technique, the forerunner to modern optimisation tools, was performed in order to better appreciate the concept of optimal control theory. The concluding part of the chapter was devoted to techniques that ensure the successful application of optimal control theory.

Definitions and Concepts

The definitions and concepts necessary for the implementation of optimal control theory are presented in this section.

Definition 3.1. *Consider the following first order autonomous differential equation* $dx/dt = g(x,\mu)$:

(i) *If* $g(x^*,\mu) = 0$, *then* $x = x^*$ *is an equilibrium solution to the differential equation. Therefore,* x^* *is an equilibrium point.*

(ii) *If* $g_x(x^*,\mu) \neq 0$, *then* $x = x^*$ *is a hyperbolic equilibrium point.*

(iii) *If* $g_x(x^*,\mu^*) = 0$, *then* $x = x^*$ *is a nonhyperbolic equilibrium point, where* $\mu = \mu^*$ *is the bifurcation point.*

(King, Billingham & Otto, 2003)

Definition 3.2. *A dynamical system that contains one or more nonhyperbolic equilibrium points is said to be structurally unstable.*
(King *et al.*, 2003)

This means that a small perturbation, not to the solution but to the model itself in the form an addition of a small extra term to $g(x,\mu)$, can lead to a qualitative difference in the structure of the set of solutions; for instance, a change in the number of equilibrium points or their stability.

Definition 3.3. *A differential equation $dx/dt = f(t,x)$ has period P if for all t and x,*

$$f(t+P,x) = f(t,x).$$

A solution $x(t)$ of such a differential equation is periodic, or has a periodic cycle, if for all t,

$$x(t+P) = x(t).$$

(Benardete, Noonburg & Pollina, 2008)

The existence of periodic cycles for sufficiently small perturbations can be rigorously justified by the following theorem, which can be applied more widely to other cases where the parameters of an autonomous equation are allowed to vary periodically in time.

Theorem 3.1. *Let $dx/dt = g(x)$ be an autonomous differential equation with $g(x^*) = 0$, $g'(x^*) \neq 0$, and $x_1(t) = x^*$ the resulting hyperbolic equilibrium solution. Consider $dx/dt = f(t,x)$ where $f(t,x)$ is periodic in t with period P. If for all (t,x), $|f(t,x) - g(x)|$, $|f_x(t,x) - g'(x)|$ and $|f_t(t,x)|$ are sufficiently small, then there exists a periodic solution $x_2(t)$ of the non-autonomous equation that stays arbitrarily close to the solution $x_1(t)$ of the autonomous equation.*
(Benardete *et al.*, 2008)

In the language of dynamical systems, the theorem states that a hyperbolic equilibrium solution of an autonomous differential equation is structurally stable; that is, it persists as a periodic cycle under small perturbations of the parameters.

Hyperbolicity and structural stability remain important themes in pure and applied treatments of more complex higher dimensional systems (Benardete *et al.*, 2008).

Bifurcation theory

Consider the following first order differential equation $x' = f(x,\mu)$. It is of interest to look at this equation with respect to the change in parameter μ. There is the realization that, very small changes in the parameter can produce large changes in the qualitative behaviour of the solutions. The systematic study of these phenomena is referred to as bifurcation theory.

In particular, we see that there are certain values of μ where there is a qualitative change in the dynamics of a dynamical system. Such a point is known as a bifurcation point (or a bifurcation value) of the system.

Observe that by the implicit function theorem, the number of equilibrium points can only change at a point (x^*, μ^*) if $f(x^*, \mu^*) = 0$ and $f_x(x^*, \mu^*) = 0$. In other words, x^* must be a nonhyperbolic equilibrium point and μ^* becomes the bifurcation value, so that (x^*, μ^*) becomes the bifurcation point (Teschl, 2012).

We shall study the three most common types of bifurcation. These are the saddle-node, transcritical and pitchfork bifurcations. The following theorems on bifurcation can be found in King *et al.* (2003). For proof and other details, see the referenced text.

Theorem 3.2 (Saddle-node Bifurcation). *Consider the first order differential equation*

$$x' = f(x,\mu)$$

with $f(0,0) = f_x(0,0) = 0$. *Provided that* $f_\mu(0,0) \neq 0$ *and* $f_{xx}(0,0) \neq 0$, *there exists a continuous curve of equilibrium points in the neighbourhood of* $(0,0)$, *which is tangent to the line* $\mu = 0$ *there. In addition,*

(i) *if* $f_\mu(0,0)f_{xx}(0,0) < 0$, *then there are no equilibrium points in the neighbourhood of* $(0,0)$ *for* $\mu < 0$, *while for* $\mu > 0$, *in a sufficiently small neighbourhood of* $(0,0)$ *there are two hyperbolic equilibrium points.*

(ii) *if* $f_\mu(0,0)f_{xx}(0,0) > 0$, *then there are no equilibrium points in the neighbourhood of* $(0,0)$ *for* $\mu > 0$, *while for* $\mu < 0$, *in a sufficiently small neighbourhood of* $(0,0)$ *there are two hyperbolic equilibrium points.*

If $f_{xx}(0,0) < 0$, the equilibrium point with the larger value of x is stable while the other is unstable, and vice versa for $f_{xx}(0,0) > 0$.

Any first order system that undergoes a saddle-node bifurcation, in other words one that contains a bifurcation point where two equilibrium solutions meet and then disappear, can be written in the form

$$x' = \mu - x^2$$

in the neighbourhood of the bifurcation point. The equation $x' = \mu - x^2$ is known as the normal form for the saddle-node bifurcation. For $\mu > 0$, there are two hyperbolic equilibrium points at $x = \pm\sqrt{\mu}$, while for $\mu < 0$ there are no equilibrium points. When $\mu = 0$, $x' = -x^2$ and $x = 0$ is a nonhyperbolic equilibrium point. The point $\mu = 0$, $x = 0$ is the bifurcation point because the qualitative nature of the solution changes there.

Theorem 3.3 (Transcritical Bifurcation). *Consider the first order differential equation*

$$x' = f(x,\mu)$$

with $f(0,0) = f_x(0,0) = f_\mu(0,0) = 0$. *Provided that* $f_{xx}(0,0) \neq 0$ *and* $f_{\mu x}^2(0,0) - f_{xx}(0,0)f_{\mu\mu}(0,0) > 0$, *there exists two continuous curves of equilibrium points in the neighbourhood of* $(0,0)$. *For each* $\mu \neq 0$ *there are two hyperbolic points in the neighbourhood of* $x = 0$. *If* $f_{xx}(0,0) < 0$, *the equilibrium point with the larger value of* x *is stable, while the other is unstable, and vice versa for* $f_{xx}(0,0) > 0$.

Consider the normal form of a system that undergoes transcritical bifurcation,

$$x' = \mu x - x^2 .$$

This system has two equilibrium points at $x = 0$ and $x = \mu$. When $\mu = 0$ we again have the nonhyperbolic equilibrium point given by $x' = -x^2$, while when

$\mu \neq 0$ there are always two equilibrium points. In this case,

$$\frac{dx'}{dx} = \mu - 2x = \begin{cases} -\mu & \text{at} \quad x = \mu, \\ \mu & \text{at} \quad x = 0, \end{cases}$$

and hence,

$$x = \mu \quad \text{is} \quad \begin{cases} \text{stable for } \mu > 0, \\ \text{unstable for } \mu < 0; \end{cases}$$

$$x = -\mu \quad \text{is} \quad \begin{cases} \text{unstable for } \mu > 0, \\ \text{stable for } \mu < 0. \end{cases}$$

At the bifurcation point, these two equilibrium solutions pass through each other and exchange stabilities, so this type of bifurcation is often called exchange of stabilities. That is, when $\mu = 0$, the two equilibrium points of x coalesce into a single semi-stable equilibrium point at $x = 0$.

Theorem 3.4 (Pitchfork Bifurcation). *Consider the first order differential equation*

$$x' = f(x, \mu)$$

with $f(0,0) = f_x(0,0) = f_\mu(0,0) = f_{xx}(0,0) = 0$. *Provided that* $f_{\mu x}(0,0) \neq 0$ *and* $f_{xxx}(0,0) \neq 0$, *there exists two continuous curves of equilibrium points in the neighbourhood of* $(0,0)$. *One curve passes through* $(0,0)$ *transverse to the line* $\mu = 0$, *while the other is tangent to* $\mu = 0$ *at* $x = 0$. *In addition,*

(i) *if* $f_{\mu x}(0,0) f_{xxx}(0,0) < 0$, *then, close to* $(0,0)$, *there is a single equilibrium point for* $\mu < 0$ *and three equilibrium points for* $\mu > 0$.

(ii) *if* $f_{\mu x}(0,0) f_{xxx}(0,0) > 0$, *then, close to* $(0,0)$, *there is a single equilibrium point for* $\mu > 0$ *and three equilibrium points for* $\mu < 0$.

If $f_{xxx}(0,0) < 0$, the single equilibrium point and the outer two of the three equilibrium points are stable, while the middle of the three equilibrium points is unstable, and vice versa for $f_{xxx}(0,0) > 0$.

Consider the normal form of pitchfork bifurcation,

$$x' = \mu x - x^3.$$

This has a single equilibrium point at $x = 0$ for $\mu < 0$, and three equilibrium points at $x = 0$ and $x = \pm\sqrt{\mu}$ for $\mu > 0$. The bifurcation at $x = 0$, $\mu = 0$ is called a supercritical pitchfork bifurcation. A similar bifurcation, in which the two new equilibrium points created at the bifurcation point are unstable, is the subcritical pitchfork bifurcation, with normal form

$$x' = \mu x + x^3 .$$

Comparison theory of differential equations

Since a whole class of differential equations cannot be solved explicitly, it is essential to have a method of placing bounds on the solution of a given equation by comparing it with solutions of a related equation of much simpler solvability.

For example, we want to solve the initial value problem

$$x' = e^{-xt}, \quad x(0) = 1 .$$

This is a rather difficult non-linear differential equation, and the properties of its solution are not immediately obvious. However, since $0 \leq e^{-xt} \leq 1$ for $0 \leq t < \infty$ and $0 \leq x < \infty$, it would seem reasonable that $0 \leq x' \leq 1$. Integrating, we have the solution of the initial value problem trapped in the range $1 \leq x \leq 1 + t$ (King *et al.*, 2003).

Definition 3.4. *A function $f(t,x)$ satisfies a one-sided Lipschitz condition in a domain D if, for some constant k,*

$$x_2 > x_1 \Rightarrow f(t,x_2) - f(t,x_1) \leq k(x_2 - x_1)$$

for some (t,x_1), $(t,x_2) \in D$.

(King *et al.*, 2003)

If $\sigma(t)$ is differentiable for $t > a$, then $\sigma'(t) \leq k$ is referred to as a differential inequality. Note that if $\sigma'(t) \leq 0$ for $t \geq a$, then $\sigma'(t) \leq \sigma(a)$.

Lemma 3.1. *If $\sigma(t)$ is a differentiable function that satisfies the differential inequality $\sigma'(t) \leq k\sigma(t)$ for some $t \in [a,b]$ and some constant k, then it follows that*

$\sigma(t) \leq \sigma(a)e^{k(t-a)}$ *for* $t \in [a,b]$.

(King *et al.*, 2003)

For example, if x is a positive function and $x' \leq -x$, we want to show that $x(t) \leq x(0)e^{-t}$ for $t \geq 0$. Furthermore, $x(t) \leq x(0)$.

Invoking Lemma 3.1, let $x(t) = \sigma(t)$ for $t \in [0,\infty)$. Then $x' \leq -x$ implies $k = -1$. Hence $x(t) \leq x(0)e^{-t}$. Furthermore, since $x' \leq 0$, $x(t) \leq x(0)$.

Theorem 3.5 (Picard-Lindelof). *Assume that $f : D \to R_n$ is continuous on D, where $(t_0, x_0) \in D$, with D a non-empty open subset of $R \times R_n$, and satisfies the Lipschitz condition*

$$|f(t,x) - f(t,y)| \leq k_\Omega |x - y|$$

on each rectangle $\Omega \subset D$. Then there exists a unique solution to the initial value problem

$$\frac{dx}{dt} = f(t,x), \quad x(t_0) = x_0$$

on $I = (t_0 - \alpha, t_0 + \alpha)$, where a, b are chosen arbitrarily small so that for the rectangle centred at (t_0, x_0), $\Omega_{a,b} \subset D$

$$(\text{where} \quad \Omega_{a,b} = \{(t,x) : |t - t_0| \leq a, |x - x_0| \leq b\}, \quad a, b > 0)$$

and

$$\alpha = \min\left(a, \frac{b}{B}\right), \quad \text{where} \quad B = \max|f(t,x)|$$

the maximum over $(t,x) \in \Omega_{a,b}$.

(Lukes, 1982)

Well-posed problems and mathematical models

We shall consider the particular case of a one-dimensional differential equation. In addition to uniqueness, another fact worth considering is that solutions of the differential equation

$$\frac{dx}{dt} = f(t,x) \tag{3.1}$$

depend continuously on the initial value $x(a)$; that is, if $x_1(t)$ and $x_2(t)$ are two solutions of Equation (3.1) on the interval $0 \leq t \leq T$ such that the initial values $x_1(a)$ and $x_2(a)$ are sufficiently close to one another, then the values of $x_1(t)$ and $x_2(t)$ remain close to one another. In particular, if $|x_1(a) - x_2(a)| \leq \delta$, then from the uniqueness result (where k is the Lipschitz constant),

$$0 \leq |x_1(t) - x_2(t)| \leq |x_1(a) - x_2(a)|e^{k(t-a)} \tag{3.2}$$

implies that

$$|x_1(t) - x_2(t)| \leq \delta e^{k(T-a)} = \varepsilon$$

for all t with $a \leq t \leq T$. Obviously, we can make ε as small as we wish by choosing δ sufficiently close to zero. The continuity of solutions of Equation (3.1) with respect to initial values is important in practical applications where we are unlikely to know the initial value $x_0 = x(a)$ with certainty. For example, suppose that the initial value problem

$$\frac{dx}{dt} = f(t,x), \quad x(a) = x_0 \tag{3.3}$$

models a population for which we only know that the initial population is within $\delta > 0$ of the assumed value x_0. Then even if the function $f(t,x)$ is accurate, the solution $x(t)$ of Equation (3.3) will only be an approximation to the actual population. But Equation (3.2) implies that the actual population at time t will be within $\delta e^{k(T-a)}$ of the approximate population $x(t)$. Thus, on a given closed interval $[a,T]$, $x(t)$ will be a close approximation to the actual population provided that $\delta > 0$ is sufficiently small. An initial value problem is usually considered well-posed as a mathematical model for a real-world situation only if the differential equation has unique solutions that are continuous with respect to the initial values. Otherwise, it is unlikely that the initial value problem adequately mirrors the real-world situation (Edwards & Penney, 2004).

Stability in the phase plane

A large plethora of natural phenomena can be modelled by two-dimensional first order autonomous systems of the form

$$\begin{aligned} \frac{dx_1}{dt} &= f_1(x_1, x_2), \\ \frac{dx_2}{dt} &= f_2(x_1, x_2). \end{aligned} \tag{3.4}$$

Definition 3.5. *An equilibrium point (also known as a critical point, a fixed point, a stationary point, or a steady state) of the system* (3.4) *is a point* (x_1^*, x_2^*) *such that*

$$f_1(x_1^*, x_2^*) = f_2(x_1^*, x_2^*) = 0.$$

(Edwards & Penney, 2004)

If (x_1^*, x_2^*) is an equilibrium point of the system, then the constant-valued functions $x_1(t) = x_1^*$, $x_2(t) = x_2^*$ satisfy the equations in the system (3.4). Such a constant-valued solution is called an equilibrium solution.

Definition 3.6. *An equilibrium point of the autonomous system* (3.4) *is said to be stable provided that, if the initial point* (x_{10}, x_{20}) *is sufficiently close to* (x_1^*, x_2^*) *then* $(x_1(t), x_2(t))$ *remains close to* (x_1^*, x_2^*) *for all* $t > 0$.

Thus for an initial point $x_0 = (x_{10}, x_{20})$ *and a solution* $x(t) = (x_1(t), x_2(t))$, *the equilibrium point* $x^* = (x_1^*, x_2^*)$ *is stable provided that, for each* ε, *there exists* $\delta > 0$ *such that*

$$|x_0 - x^*| < \delta \quad \text{implies} \quad |x(t) - x^*| < \varepsilon \quad \text{for all } t > 0.$$

(Edwards & Penney, 2004)

An equilibrium point x^* is called unstable if it is not stable.

Definition 3.7. *The equilibrium point* x^* *is called asymptotically stable if it is stable and, moreover, every trajectory that begins sufficiently close to* x^* *also approaches* x^* *as* $t \to \infty$.

That is, there exists $\delta > 0$ *such that*

$$|x_0 - x^*| < \delta \quad \text{implies} \quad \lim_{t\to\infty} x(t) = x^* .$$

provided $x(t)$ *is a solution with* $x(0) = x_0$.

(Edwards & Penney, 2004)

Linear and almost linear systems

We shall discuss the behaviour of solutions of the autonomous system of equations (not necessarily linear)

$$\begin{aligned} \frac{dx}{dt} &= f(x,y), \\ \frac{dy}{dt} &= g(x,y), \end{aligned} \tag{3.5}$$

near an isolated equilibrium point (x^*, y^*) at which $f(x^*, y^*) = g(x^*, y^*) = 0$. An equilibrium point is called isolated if some neighbourhood of it contains no other equilibrium point (Edwards & Penney, 2004). In the discussions that follow, we assume that f and g are continuously differentiable in a neighbourhood of (x^*, y^*).

In general, we assume that $x^* = y^* = 0$; otherwise, we make the substitution

$$u = x - x^*, \qquad v = y - y^* .$$

Then

$$\frac{dx}{dt} = \frac{du}{dt} \quad \text{and} \quad \frac{dy}{dt} = \frac{dv}{dt},$$

and so System (3.5) is equivalent to the system

$$\begin{aligned} \frac{du}{dt} &= f(u+x^*, v+y^*) = f(u,v), \\ \frac{dv}{dt} &= g(u+x^*, v+y^*) = g(u,v), \end{aligned} \tag{3.6}$$

that has (0,0) as an isolated equilibrium point.

Linearisation near an equilibrium point

Taylor's formula for a function of two variables implies that, given $f(x,y)$ is continuously differentiable near the equilibrium point (x^*, y^*), then

$$f(u+x^*, v+y^*) = f(x^*, y^*) + f_x(x^*, y^*)u + f_y(x^*, y^*)v + R(u,v),$$

where the remainder term $R(u,v)$ satisfies the condition

$$\lim_{(u,v)\to(0,0)} \frac{R(u,v)}{\sqrt{u^2+v^2}} = 0.$$

If we apply Taylor's formula to both f anf g in System (3.6) and assume that (x^*, y^*) is an isolated equilibrium point so that $f(x^*, y^*) = g(x^*, y^*) = 0$, then the result is

$$\begin{aligned} \frac{du}{dt} &= f_x(x^*, y^*)u + f_y(x^*, y^*)v + R(u,v), \\ \frac{dv}{dt} &= g_x(x^*, y^*)u + g_y(x^*, y^*)v + S(u,v), \end{aligned} \tag{3.7}$$

where $R(u,v)$ and the analogous remainder term for g, $S(u,v)$ satisfy the condition

$$\lim_{(u,v)\to(0.0)} \frac{R(u,v)}{\sqrt{u^2+v^2}} = \lim_{(u,v)\to(0,0)} \frac{S(u,v)}{\sqrt{u^2+v^2}} = 0. \tag{3.8}$$

Then, when the values u and v are small, the remainder terms $R(u,v)$ and $S(u,v)$ are very small (being small even in comparison with u and v).

Consequently, when (u,v) is near (0,0), the (generally) non-linear system $u' = f(u+x^*, v+y^*)$, $v' = g(u+x^*, v+y^*)$ in System (3.7) is closely approximated by the linearised system

$$\begin{aligned} \frac{du}{dt} &= f_x(x^*, y^*)u + f_y(x^*, y^*)v, \\ \frac{dv}{dt} &= g_x(x^*, y^*)u + g_y(x^*, y^*)v, \end{aligned} \tag{3.9}$$

whose constant coefficients are the values $f_x(x^*, y^*)$, $f_y(x^*, y^*)$ and $g_x(x^*, y^*)$, $g_y(x^*, y^*)$ of the partial derivatives of the functions f and g at the equilibrium point (x^*, y^*). Assuming that (0,0) is also an isolated equilibrium point of this linear system, and that the remainder terms in System (3.7) satisfy the condition in Equation (3.8), the original system $x' = f(x,y)$, $y' = g(x,y)$ is said to be almost linear at the isolated equilibrium point (x^*,y^*). In this case, its linearisation at (x^*, y^*) is the linear system (3.9). In short, the linear system $U' = JU$ (where $U = (u,v)^T$) whose coefficient matrix is the so-called Jacobian matrix

$$\mathrm{J}(x^*, y^*) = \begin{bmatrix} f_x(x^*, y^*) & f_y(x^*, y^*) \\ g_x(x^*, y^*) & g_y(x^*, y^*) \end{bmatrix}$$

of the functions f and g is evaluated at the point (x^*, y^*) (Edwards & Penney, 2004).

Linear nth order differential equations

An nth order linear differential equation can be expressed as

$$\frac{d^n x}{dt^n} = a_1(t)\frac{d^{n-1}x}{dt^{n-1}} + \ldots + a_{n-1}(t)\frac{dx}{dt} + a_n(t)x = g(t). \tag{3.10}$$

The linear differential equation (3.10) is said to be homogeneous if $g(t) = 0$ and non-homogeneous otherwise.

Additionally, if the coefficients $a_i(t)$, $i = 1, \ldots, n$, of a homogeneous differential equation are constants, then the differential equation (3.10) has the form

$$\frac{d^n x}{dt^n} = a_1\frac{d^{n-1}x}{dt^{n-1}} + \ldots + a_{n-1}\frac{dx}{dt} + a_n x = 0. \tag{3.11}$$

Theorem 3.6. *If all of the roots of the characteristic polynomial $P(\lambda)$ are negative or have negative real part, then given any solution $x(t)$ of the homogeneous differential equation (3.10), there exist positive constants M and b such that*

$$|x(t)| \leq Me^{-bt} \quad \text{for} \quad t > 0 \quad \text{and} \quad \lim_{t\to\infty} |x(t)| = 0.$$

(Allen, 2006)

Routh-Hurwitz criteria

Important criteria that give necessary and sufficient conditions for all of the roots of the characteristic polynomial (with real coefficients) to lie in the left half of the complex plane are known as the Routh-Hurwitz criteria. The criteria are used to determine local asymptotic stability of an equilibrium point for non-linear systems of differential equations.

Theorem 3.7 (Routh-Hurwitz criteria). *Given the polynomial*

$$P(\lambda) = \lambda^n + a_1\lambda^{n-1} + \cdots + a_{n-1}\lambda + a_n,$$

where the coefficients a_i, $i = 1, \ldots, n$, are real constants, define the n Hurwitz matrices using the coefficients a_i of the characteristic polynomial:

$$H_1 = (a_1), \quad H_2 = \begin{bmatrix} a_1 & 1 \\ a_3 & a_2 \end{bmatrix}, \quad H_3 = \begin{bmatrix} a_1 & 1 & 0 \\ a_3 & a_2 & a_1 \\ a_5 & a_4 & a_3 \end{bmatrix} \quad \text{and}$$

$$H_n = \begin{bmatrix} a_1 & 1 & 0 & \ldots & 0 \\ a_3 & a_2 & a_1 & \ldots & 0 \\ a_5 & a_4 & a_3 & \ldots & 0 \\ \vdots & \vdots & \vdots & \ddots & \vdots \\ 0 & 0 & 0 & \ldots & a_n \end{bmatrix},$$

where $a_j = 0$ if $j > n$. All of the roots of the polynomial $P(\lambda)$ are negative or have negative real part if and only if the determinants of all Hurwitz matrices are positive:

$$\det H_j > 0, \qquad j = 1, 2, \ldots, n.$$

(Allen, 2006)

Corollary 1. *Suppose the coefficients of the characteristic polynomial are real. If all the roots for the characteristic polynomial*

$$P(\lambda) = \lambda^n + a_1\lambda^{n-1} + \cdots + a_{n-1}\lambda + a_n$$

are negative or have negative real part, then the coefficients $a_i > 0$ for $i = 1, 2, \ldots, n$.

Eigenvalue analysis in the phase plane

The solution behaviour of two-dimensional linear system is studied in the phase plane; that is, the $x - y$ plane. Let $X = (x, y)^T$ and $A = (a_{ij})$ so that

$$\frac{dX}{dt} = AX$$

can be expressed as

$$\frac{dx}{dt} = a_{11}x + a_{12}y, \qquad (3.12)$$
$$\frac{dy}{dt} = a_{21}x + a_{22}y.$$

Then, as already observed, the origin $x = 0$ and $y = 0$ is an equilibrium solution of the system (3.12). Assuming that $\det(A) \neq 0$, then the origin is the unique equilibrium solution—an isolated equilibrium.

Solutions to the linear system (3.12) are characterised by the eigenvalues of matrix A, which in turn depend on the trace and determinant of A. The eigenvalues are the solutions to the characteristic equation $\det(A - \lambda I) = 0$. Thus, the characteristic polynomial is of the following form:

$$\lambda^2 - (a_{11} + a_{22})\lambda + a_{11}a_{22} - a_{12}a_{21},$$

where the coefficients of the polynomial are the negative of the trace and determinant of the matrix A. Therefore, it can be written as

$$\lambda^2 - \mathrm{Tr}(A)\lambda + \det(A).$$

The origin will be classified as a node, saddle, spiral and centre. The origin is further classified as stable and unstable. The origin is asymptotically stable if the eigenvalues of A are negative or have negative real part. The origin is unstable if the eigenvalues of A are positive or have positive real part. Therefore, it is easy to determine the stability of the origin once the eigenvalues are known.

In addition, even without computing the eigenvalues, the stability can be determined by applying the Routh-Hurwitz criteria to the characteristic polynomial of A (Allen, 2006).

Corollary 2. *Suppose $dX/dt = AX$, where A is a 2×2 matrix with* $\det(A) \neq 0$. *The origin is asymptotically stable if and only if*

$$\mathrm{Tr}(A) < 0 \qquad \text{and} \qquad \det(A) > 0.$$

The origin is stable if and only if

$$\mathrm{Tr}(A) \leq 0 \qquad \text{and} \qquad \det(A) > 0.$$

The origin is unstable if and only if

$$\mathrm{Tr}(A) > 0 \qquad \text{or} \qquad \det(A) < 0.$$

We present specific criteria for the origin of a general linear differential system to be classified into one of four types: node, saddle, spiral or centre. The classification scheme depends on whether the eigenvalues are real or complex, whether the real eigenvalues are negative or positive, and whether the complex eigenvalues have negative real part.

Real eigenvalues

In the case of real eigenvalues λ_1 and λ_2, the origin is classified as either a node or saddle.

1. Node implies both eigenvalues have the same sign and may be distinct or equal, $\lambda_1 \leq \lambda_2 < 0$ or $0 < \lambda_1 \leq \lambda_2$.

2. Saddle implies eigenvalues λ_1 and λ_2 have opposite signs, $\lambda_1 \cdot \lambda_2 < 0$; for example, $\lambda_1 < 0 < \lambda_2$.

Complex eigenvalues

In the case of complex eigenvalues $\lambda_{1,2} = a \pm bi,\ b \neq 0$. The origin is classified as a spiral (or focus) if $a \neq 0$ and a centre if $a = 0$.

1. Spiral or focus implies eigenvalues have non-zero real part ($a \neq 0$).

2. Centre implies eigenvalues are purely imaginary ($a = 0$), $\lambda_{1,2} = \pm bi$.

A node or spiral can be classified as either asymptotically stable or unstable depending on whether the real part of the eigenvalue is negative or positive, respectively. A saddle point is always unstable and a centre is neither asymptotically

stable nor unstable. A centre is sometimes called neutrally stable (it is stable, but not asymptotically stable).

The classification scheme can be related to the signs of the trace and determinant of A and the discriminant of the characteristic polynomial. Let $\tau = \mathrm{Tr}(A)$ and $\delta = \det(A)$. Recall that the eigenvalues, the zeros of the characteristic polynomial

$$\lambda^2 - \mathrm{Tr}(A)\lambda + \det(A) = \lambda^2 - \tau\lambda + \delta,$$

satisfy

$$\lambda_{1,2} = \frac{\tau \pm \sqrt{\tau^2 - 4\delta}}{2}.$$

The discriminant is denoted as γ and defined as follows:

$$\gamma = \tau^2 - 4\delta.$$

The following classification scheme summarises the dynamics according to whether the eigenvalues are real or complex conjugates.

Eigenvalues are real $(\gamma \geq 0)$:

Unstable node if $\tau > 0$ and $\delta > 0$ $(\lambda_{1,2} > 0)$

Saddle point if $\delta < 0$ $(\lambda_1 < 0 < \lambda_2)$

Stable node if $\tau < 0$ and $\delta > 0$ $(\lambda_{1,2} < 0)$.

Eigenvalues are complex conjugates, $a \pm bi$ $(\gamma < 0)$:

Unstable spiral if $\tau > 0$ $(a > 0)$

Neutral centre if $\tau = 0$ $(a = 0)$

Stable spiral if $\tau < 0$ $(a < 0)$.

It is to be noted that if an equilibrium point is asymptotically stable, then it is stable (and not vice versa). Also, $\mathrm{Tr}(A) = \lambda_1 + \lambda_2$ and $\det(A) = \lambda_1 \cdot \lambda_2$.

Theorem 3.8 (Stability of Almost Linear Systems). *Let λ_1 and λ_2 be the eigenvalues of the coefficient matrix A of the linear system* (3.12) *associated with the almost linear system. Then*

1. *If* $\lambda_1 = \lambda_2$ *are equal real eigenvalues, then the equilibrium point* $(0,0)$ *of the almost linear system is either a node or spiral, and is asymptotically stable if* $\lambda_1 = \lambda_2 < 0$, *unstable if* $\lambda_1 = \lambda_2 > 0$.

2. *If* λ_1 *and* λ_2 *are pure imaginary, then* $(0,0)$ *is either a centre or a spiral, and may be either asymptotically stable, stable or unstable.*

3. *Otherwise—that is, unless* λ_1 *and* λ_2 *are either real equal or pure imaginary—the equilibrium point* $(0,0)$ *of the almost linear system is of the same type and stability as the equilibrium point* $(0,0)$ *of the associated linear system.*

(Edwards & Penney, 2004)

Definition 3.8. *A function* $V : R_n \to R$ *is said to be positive definite if*

(i) $V(x) > 0$ for all $x \neq 0$;

(ii) $V(0) = 0$.

Definition 3.9. *A function* $V : R_n \to R$ *is said to be positive semi-definite if*

(i) $V(x) \geq 0$ for all $x \neq 0$;

(ii) $V(0) = 0$.

Definition 3.10. *A function* $V : R_n \to R$ *is said to be negative definite if*

(i) $V(x) < 0$ for all $x \neq 0$;

(ii) $V(0) = 0$.

Definition 3.11. *A function* $V : R_n \to R$ *is said to be negative semi-definite if*

(i) $V(x) \leq 0$ for all $x \neq 0$;

(ii) $V(0) = 0$.

Definition 3.12 (Lyapunov Function). *Consider an autonomous system $x' = f(x)$, where we assume $f : R_n \to R_n$ is continuous in an open set containing the origin, 0 and $f(0) = 0$ (so that x(t)=0 is a solution and the origin is an isolated equilibrium point). A function $V(x)$, defined in the neighbourhood of $x = 0$ is called a Lyapunov function for the above problem if*

(i) $V(x)$ has partial derivatives;

(ii) $V(x) > 0$, if $x \neq 0$ (positive definite);

(iii) $V'(x) \leq 0$ (negative semi-definite).

In this context, V', the derivative of V along the trajectories, is given by

$$V'(x) = \sum_{i=1}^{n} \frac{\partial V(x)}{\partial x_i} x_i' = \sum_{i=1}^{n} \frac{\partial V(x)}{\partial x_i} f_i(x) = \nabla V(x) f(x).$$

It is also referred to as the Lie derivative of the function V along the vector field f. Existence of Lyapunov functions implies stability of the solution $x(t) = 0$ (Clark, 2000). Furthermore, V is radially unbounded if

$$V(x) \to \infty, \quad as \quad |x| \to \infty.$$

Additionally, by LaSalle's invariance principle, if V' is negative semi-definite, the set of accumulation points of any trajectory is contained in D, where D is the union of complete trajectories contained entirely in the set $\{x : V'(x) = 0\}$. That is, the largest invariant set around the equilibrium point—the origin—is a singleton (set containing only the origin).

Specifically, if $V'(x) < 0$ (negative definite) and V is radially unbounded, then by Lyapunov's theorem, $x(t) = 0$ is globally asymptotically stable. If $V'(x) > 0$ (positive definite), then $x(t) = 0$ is unstable. If $V'(x) \leq 0$ (negative semi-definite), then by La Salle's invariance principle, $x(t) = 0$ is locally asymptotically stable and globally stable.

Definition 3.13 (Invariant Set). *Consider the n-dimensional autonomous system*

$$x' = f(x), \qquad x(a) = x_0.$$

If for each $x_0 \in S \subseteq R_n$, $x(t) \in S$ for all $t \in R$, then S is called an invariant set of the given system. If for each $x_0 \in S \subseteq R_n$, $x(t) \in S$ for $t \geq 0$, then S is called a positively invariant set of the given system.

In other words, all solutions of the system $x(t)$ starting in S remain in S for all time.

Theorem 3.9 (Bendixson-Dulac Theorem). *Consider the dynamical system:*

$$\frac{dx}{dt} = f(x,y),$$
$$\frac{dy}{dt} = g(x,y),$$

in which the functions f and g are assumed to be smooth in a simply-connected region D. Let $\phi(x,y)$ (called the Dulac multiplier) be a smooth function in D such that for the equation

$$\Delta(x,y) = \frac{\partial(\phi f)}{dx} + \frac{\partial(\phi g)}{dy},$$

$\Delta(x,y)$ does not change sign in D. Then the given system has no closed trajectories (or limit cycles) in D. Hence, there exists no periodic solutions in D.

(Patra, 2013)

Calculus of Variations

According to Kamien and Schwartz (1991), the origin of the calculus of variation is commonly traced to the posing of the brachistochrone problem by John Bernoulli in 1696 and its solution by him and independently by his brother James in 1697. The problem states that: If a small object moves under the influence of gravity, which path between two fixed points enables it to make the trip in the shortest time?

Variational calculus was extended to other specific problems, which were also solved, and a general mathematical theory was developed by Euler and Lagrange. The most fruitful applications of the calculus of variations have been to theoretical physics, especially in connection with Hamilton's principle or the Principle of Least Action. Early applications in other fields such as economics appeared in the

late 1920s and early 1930s by Roos, Evans, Hotelling and Ramsey, with further applications published occasionally thereafter (Kamien & Schwartz, 1991).

The calculus of variations shows how to solve the fundamental problem of maximising (or minimising) the objective functional of the following:

$$\int_0^T f(t, x(t), x'(t))\, dt$$

$$\text{subject to} \quad x(0) = x_0$$

$$x(T) = x_T\,.$$

The function f is assumed to be continuous in all three arguments t, x, x', and have continuous partial derivatives with respect to the second and third, x and x'. It is worth noting that while the third argument of f is a time derivative of the second, f is to be viewed as a function of three independent arguments. The independent variable, time $t \in [0, T]$, where T is represents the terminal time.

Therefore, the task of variational calculus is to select from a set of admissible x paths (or trajectories) the one that yields an extremal of the objective functional. For further details, see Kamien and Schwartz (1991) and Chiang (1992).

In an attempt to solve the calculus of variation problem, we seek an optimal path x_δ that satisfies the Euler equation

$$\frac{\partial f(t, x_\delta(t), x_\delta{}'(t))}{\partial x(t)} = \frac{d}{dt}\left(\frac{\partial f(t, x_\delta(t), x_\delta{}'(t))}{\partial x'(t)}\right).$$

The Euler equation may be viewed as a generalisation of the standard calculus first order necessary conditions $f'(x_\delta) = 0$ for a number x_δ to maximise (or minimise) the function $f(x)$. Indeed, if

$$\frac{d}{dt}\left(\frac{\partial f}{\partial x'}\right) = 0,$$

then the Euler equation reduces to the standard calculus condition (Kamien & Schwartz, 1991).

As an example, consider the problem of finding the optimal path that will

SAM JONAH LIBRARY
UNIVERSITY OF CAPE COAST
CAPE COAST

minimise

$$\int_0^{10} \sqrt{1+x'(t)^2}\,dt$$

$$\text{subject to} \quad x(0) = 4$$

$$x(10) = 24.$$

We start the solution by letting

$$f(t.x(t),x'(t)) = \sqrt{1+x'(t)^2}.$$

Then applying the Euler equation

$$\frac{\partial f}{\partial x} = \frac{d}{dt}\left(\frac{\partial f}{\partial x'}\right)$$

to the problem yields

$$0 = \frac{d}{dt}\left(\frac{x'(t)}{\sqrt{1+x'(t)^2}}\right).$$

This implies

$$\frac{x'(t)}{\sqrt{1+x'(t)^2}} = c \qquad (c \text{ is a constant}).$$

Thus,

$$\frac{x'(t)^2}{1+x'(t)^2} = k, \qquad k = c^2$$

and

$$x'(t)^2(1-k) = k.$$

So

$$x'(t)^2 = \frac{k}{1-k}$$

and

$$x'(t) = k_1, \qquad k_1 = \sqrt{\frac{k}{1-k}}.$$

Therefore,

$$x(t) = k_1 t + k_0.$$

Using the initial and terminal conditions $x(0) = 4$ and $x(10) = 24$, respectively, we have $k_0 = 4$ and $k_1 = 2$. Hence the optimal path is

$$x_\delta(t) = 2t + 4.$$

The preceding example has the geometric interpretation of finding the minimum distance between two points $(0,4)$ and $(10,24)$ in a graph of the function $x(t)$. Of course, the minimum distance is the straight line joining the two points; and the function that achieves that is $x(t) = 2t + 4$ (Klein, 2001).

Optimal Control Theory

According to Chiang (1992), the calculus of variations, the classical method for tackling problems of dynamic optimisation, like the ordinary calculus, requires for its applicability the differentiability of the functions inherent in the problem. More importantly, in calculus of variations, only interior solutions can be handled. A more modern development that can deal with non-classical features such as corner or boundary solutions, is found in optimal control theory. As the name implies, the optimal-control formulation of a dynamic optimisation problem focuses upon one or more control variables that serve as the instrument of optimisation. Unlike the calculus of variations, therefore, where the goal is to find the optimal time path for a state variable x, optimal control theory has as its foremost objective the determination of the optimal path for a control variable, u. Of course, once the optimal control path, $u_\delta(t)$ has been found, we can also determine the optimal state path, $x_\delta(t)$, that corresponds to it. As a matter of fact, the optimal $u_\delta(t)$ and $x_\delta(t)$ paths are usually found in the same process. Therefore, the presence of a control variable at centre stage in optimal control theory does alter the basic orientation of the dynamic optimisation problem.

Consider an optimal control problem with n state variables and m control variables and a payoff term ϕ :

$$\max_{u_1,\ldots u_m} \int_0^T f(t,x_1(t),\ldots,x_n(t),u_1(t),\ldots,u_m(t))\,dt + \phi(x_1(T),\ldots x_n(T))$$

$$\text{subject to} \quad x_1'(t) = g_1(t,x_1(t),\ldots,x_n(t),u_1(t),\ldots,u_n(t))$$

$$\vdots$$

$$x_n'(t) = g_n(t,x_1(t),\ldots,x_n(t),u_1(t),\ldots,u_m(t))$$

$$x_1(0) = x_{10},\ldots,x_n(0) = x_{n0},$$

where the functions f and g are continuously differentiable in all variables. We place no restriction on the relative magnitude of m and n. In fact, $m < n$, $m = n$ and $m > n$ are all acceptable.

To have a more compact statement of the posed optimal control problem, we employ vector notation; and define the following:

$$x = \begin{bmatrix} x_1 \\ \vdots \\ x_n \end{bmatrix}, \quad u = \begin{bmatrix} u_1 \\ \vdots \\ u_m \end{bmatrix}, \quad \text{and} \quad g = \begin{bmatrix} g_1 \\ \vdots \\ g_n \end{bmatrix}.$$

Then the statement of the optimal control problem is simply

$$\max_u Z(u) = \int_0^T f(t,x(t),u(t))\,dt + \phi(x(T))$$

$$\text{subject to} \quad x'(t) = g(t,x(t),u(t)) \tag{3.13}$$

$$x(0) = x_0.$$

The control variable $u \in R_m$ is assumed to be piecewise continuous and also Lebesgue integrable, and the state variable $x \in R_n$ is assumed to be piecewise differentiable. Additionally, the time variable $t \in [0,T]$, where 0 is the initial time and T is the terminal time. The time horizon may be finite or infinite ($T \to \infty$).

It is also assumed that $u \in U_t$ for $0 \le t \le T$ where U_t is a specified control set, which may vary with time t. Such controls are called admissible controls.

The goal of the optimal control problem is to seek an optimal control $u_\delta(t)$ as well as the corresponding optimal path $x_\delta(t)$ that maximises the objective functional subject to all the constraints, which include the state equation x' with its initial condition x_0.

The principal technique used for such an optimal control problem is to solve a set of 'necessary conditions' that an optimal control and corresponding state must satisfy. It is important to logically distinguish between necessary conditions and sufficient conditions of solution sets.

Necessary Conditions: If $u_\delta(t)$, $x_\delta(t)$ are optimal, then the following conditions hold ...

Sufficient Conditions: If $u_\delta(t)$, $x_\delta(t)$ satisfy the following conditions ... , then $u_\delta(t)$, $x_\delta(t)$ are optimal.

The necessary conditions are normally obtained through an optimisation technique called Pontryagin's maximum principle; proposed by Pontryagin, Boltyanskii, Gamkrelize and Mishchenko (1962).

Theorem 3.10 (Pontryagin's Maximum Principle). *If $u_\delta(t)$ and $x_\delta(t)$ are optimal for problem* (3.13), *then there exists a piecewise differential adjoint function $\lambda \in R_n$ such that*

$$H(t, x_\delta(t), u(t), \lambda(t)) \leq H(t, x_\delta(t), u_\delta(t), \lambda(t))$$

for all controls u at each time t, where the Hamiltonian H is

$$H = f(t, x(t), u(t)) + \lambda^T(t) g(t, x(t), u(t))$$

and

$$\lambda'(t) = -\left[\frac{\partial H(t, x_\delta(t), u_\delta(t), \lambda(t))}{\partial x(t)}\right]^T,$$

$$\lambda(T) = \left[\frac{\partial \phi(x_\delta(T))}{\partial x(T)}\right]^T.$$

(Lenhart & Workman, 2007)

We also have the dynamics of the optimal state system as

$$x'(t) = \left[\frac{\partial H(t, x_\delta(t), u_\delta(t), \lambda(t))}{\partial \lambda(t)}\right]^T, \qquad x(0) = x_0.$$

The equation for $\lambda(T)$ is known as a transversality condition. In addition, if $u_\delta(t)$ is in the interior (rather than at a boundary) of the admissible region for

the control and if the Hamiltonian is differentiable in $u(t)$, then the optimality condition becomes

$$\frac{\partial H(t, x_\delta(t), u_\delta(t), \lambda(t))}{\partial u(t)} = 0 \qquad \text{(zero row vector, } 0 \in R_n\text{)}.$$

It should be noted that when the payoff term $\phi(x(T)) = 0$, the transversality condition reduces to $\lambda(T) = 0$. Also, when we are dealing with an infinite horizon problem, the transversality condition becomes $\lim_{T\to\infty} \lambda(T) = 0$.

It is also worth pointing out that there is a mathematical rule that says that the derivative of a scalar with respect to a row (column) vector is a column (row) vector (Chiang, 1992).

States with fixed endpoints

For ease of analysis, consider a one-dimensional optimal control problem, where the state is fixed at both the beginning and end of the time interval.

$$\begin{aligned} &\max_u \int_0^T f(t, x(t), u(t))\, dt \\ &\text{subject to} \quad x'(t) = g(t, x(t), u(t)) \\ &x(0) = x_0, \qquad x(T) = x_T. \end{aligned} \tag{3.14}$$

A slight modification of the necessary conditions is needed to solve such a problem. We present the following theorem.

Theorem 3.11. *If $u_\delta(t)$ and $x_\delta(t)$ are optimal for problem* (3.14), *then there exists a piecewise differential adjoint variable λ and a constant λ_0 equal to either* 0 *or* 1 *such that*

$$H(t, x_\delta(t), u(t), \lambda(t)) \leq H(t, x_\delta(t), u_\delta(t), \lambda(t))$$

for all admissible controls u at each time t, where the Hamiltonian H is

$$H = \lambda_0 f(t, x(t), u(t)) + \lambda(t) g(t, x(t), u(t))$$

and

$$\lambda'(t) = -\frac{\partial H(t, x_\delta(t), u_\delta(t), \lambda(t))}{\partial x(t)}.$$

(Lenhart & Workman, 2007)

The constant λ_0 arises in this situation to adjust for degenerate problems, or problems where the objective functional is immaterial. That is, in cases where all admissible controls yield the same objective functional value.

For non-degenerate problems ($\lambda_0 = 1$), the necessary conditions are similar to the free terminal state problems. The only exception is that there are no transversality conditions for any state with a fixed terminal state value.

Bounded controls

In order to solve problems with bounds on the control, we need to develop alternative necessary conditions. Consider the following problem:

$$\max_u \int_0^T f(t,x(t),u(t))\,dt$$

$$\text{subject to} \quad x'(t) = g(t,x(t),u(t)), \quad x(0) = x_0$$

$$a \leq u \leq b,$$

where a and b are fixed, real constants and $a < b$.

The necessary conditions for this type of problem are outlined. Forming the Hamiltonian

$$H(t,x,u,\lambda) = f(t,x,u) + \lambda(t)g(t,x,u),$$

the necessary conditions for x_δ and λ remain unchanged, namely

$$x'(t) = \frac{\partial H}{\partial \lambda}, \qquad x(0) = x_0,$$

$$\lambda'(t) = -\frac{\partial H}{\partial x}, \qquad \lambda(T) = 0.$$

However, assuming a non-linear control, the optimality condition

$$\frac{\partial H}{\partial u} = f_u(t,x,u) + \lambda(t)g_u(t,x,u)$$

leads to the characterisation of the optimal control u_δ as

$$\begin{cases} u_\delta = a & \text{if} \quad \frac{\partial H}{\partial u} < 0, \\ a \leq u_\delta \leq b & \text{if} \quad \frac{\partial H}{\partial u} = 0, \\ u_\delta = b & \text{if} \quad \frac{\partial H}{\partial u} > 0. \end{cases} \tag{3.15a}$$

An alternative characterisation of the optimal control u_δ is

$$\begin{cases} u_\delta = a & \text{if} \quad \frac{\partial H}{\partial u} \leq 0, \\ a < u_\delta < b & \text{if} \quad \frac{\partial H}{\partial u} = 0, \\ u_\delta = b & \text{if} \quad \frac{\partial H}{\partial u} \geq 0. \end{cases} \tag{3.15b}$$

It should be taken into account that if we have a minimisation problem, then u_δ is instead chosen to minimise H pointwise. This has the effect of reversing $<, \leq$; $\leq, <$; and $>, \geq$ in the first, second and third lines of Conditions (3.15a) and (3.15b), respectively. For further details, see Kamien and Schwartz (1991).

Isoperimetric constraints

Let $f(t,x(t),u(t))$, $g(t,x(t),u(t))$ and $h(t,x(t),u(t))$ be continuously differentiable functions in all three variables. Consider the optimal control problem:

$$\begin{aligned} & \max_u \int_0^T f(t,x(t),u(t))\,dt \\ \text{subject to} \quad & x'(t) = g(t,x(t),u(t)), \quad x(0) = x_0 \\ & \int_0^T h(t,x(t),u(t))\,dt = B \\ & a \leq u \leq b. \end{aligned} \tag{3.16}$$

The integral constraint is referred to as an isoperimetric constraint, and Pontryagin's maximum principle cannot be used to solve such a problem as it stands. However, there is a simple trick to convert the problem to a more familiar form. Introduce a second variable $z(t)$ and let

$$z(t) = \int_0^t h(s,x(s),u(s))\,ds.$$

Then, it follows from the fundamental theorem of calculus that

$$z'(t) = h(t,x(t),u(t)),$$

$$z(0) = 0,$$

$$z(T) = B.$$

Thus, Problem (3.16) is transformed into

$$\max_u \int_0^T f(t,x(t),u(t))\,dt$$

$$\text{subject to} \quad x'(t) = g(t,x(t),u(t)), \quad x(0) = x_0$$

$$z'(t) = h(t,x(t),u(t)), \quad z(0) = 0, \quad z(T) = B$$

$$a \le u \le b.$$

The problem can now be solved using the already developed methods; particularly those related to optimal control problems with fixed endpoints.

Linear controls

Optimal control problems in which there is a linear dependence on the control present themselves mainly in two forms, namely bang-bang controls and singular controls.

Consider the following optimal control problem:

$$\max_u \int_0^T f_1(t,x) + u(t)f_2(t,x)\,dt$$

$$\text{subject to} \quad x'(t) = g_1(t,x) + u(t)g_2(t,x), \quad x(0) = x_0 \tag{3.17}$$

$$a \le u \le b.$$

Notice the integrand function f and the right hand side of the state equation in Problem (3.17) are both linear functions of the control variable u. Therefore, the Hamiltonian is also linear in u and can be written as

$$H = [f_1(t,x) + \lambda(t)g_1(t,x)] + u(t)[f_2(t,x) + \lambda(t)g_2(t,x)].$$

As usual, the necessary condition $\lambda'(t) = -\dfrac{\partial H}{\partial x}$ is applicable. However, the optimality condition

$$\frac{\partial H}{\partial u} = f_2(t,x) + \lambda(t)g_2(t,x)$$

provides no information on the control. To find a characterisation for the optimal control u_δ, we define a switching function

$$\psi(t) = f_2(t,x) + \lambda(t)g_2(t,x).$$

Assuming an interior solution exists (for a non-binding control constraint), then the characterisation of u_δ is

$$\begin{cases} u_\delta = a & \text{if} \quad \psi(t) < 0, \\ a < u_\delta < b & \text{if} \quad \psi(t) = 0, \\ u_\delta = b & \text{if} \quad \psi(t) > 0. \end{cases} \tag{3.18}$$

Bang-bang controls

If $\psi(t) = 0$ cannot be sustained over an interval of time, but only occurs at finitely many points in the given time interval, then the control is called bang-bang. In this situation, the control is a piecewise constant function switching between only the upper and lower bounds. The switches coincide with the places where ψ changes signs (so that $\psi = 0$), hence the name switching function. The actual points where this occurs are called switching times. Therefore, the expressions in Condition (3.18) reduce to

$$u_\delta(t) = \begin{cases} a & \text{if} \quad \psi(t) < 0, \\ b & \text{if} \quad \psi(t) > 0. \end{cases}$$

To solve a bang-bang problem numerically, the forward-backward sweep method can be used. However, one must prove analytically that the problem is in fact bang-bang; that is, $\psi = 0$ over an interval is impossible.

Singular controls

If $\psi(t)$ is identically zero in some interval of time, $I \subseteq [0,T]$ ($\psi(t) = 0$ for all $t \in I$), we say u_δ is singular on that interval. A characterisation of u_δ on this interval must be obtained using other information. The endpoints of this interval are also called switching times.

It must be noted that if the problem is singular or a combination of singular and bang-bang controls the interior solution, the second line of the expressions in Condition (3.18), cannot be ruled out.

Evaluating the Hamiltonian along the optimal path

The application of Pontryagin's maximum principle enables us to determine a simple expression for the Hamiltonian over time along the optimal path. The total derivative of the Hamiltonian along the optimal path is given by

$$\frac{dH(t,x_\delta(t),u_\delta(t),\lambda(t))}{dt} = \frac{\partial H_\delta}{\partial u(t)}u'(t) + \frac{\partial H_\delta}{\partial x(t)}x'(t) + \frac{\partial H_\delta}{\partial \lambda(t)}\lambda'(t) + \frac{\partial H_\delta}{\partial t}.$$

Pontryagin's maximum principle requires that

$$\frac{\partial H_\delta}{\partial u(t)} = 0, \quad \lambda'(t) = -\frac{\partial H_\delta}{\partial x(t)} \quad \text{and} \quad x'(t) = \frac{\partial H_\delta}{\partial \lambda(t)}.$$

Therefore,

$$\begin{aligned}\frac{dH(t,x_\delta(t),u_\delta(t),\lambda(t))}{dt} &= 0 \cdot u'(t) + \frac{\partial H_\delta}{\partial x(t)}\frac{\partial H_\delta}{\partial \lambda(t)} - \frac{\partial H_\delta}{\partial \lambda(t)}\frac{\partial H_\delta}{\partial x(t)} + \frac{\partial H_\delta}{\partial t} \\ &= \frac{\partial H_\delta}{\partial t}.\end{aligned}$$

This result is only applicable to non-autonomous optimal control problems. However, for autonomous cases where the Hamiltonian does not include time as an explicit variable (even though it may include the discount term $e^{-\delta t}$), $\frac{\partial H_\delta}{\partial t}$ is zero and hence the Hamiltonian is constant along the optimal path.

Optimal time

For free terminal time optimal control problems, a version of Pontryagin's maximum principle can be employed. In problems were the terminal value of the state $x(T)$ is specified, but the terminal time, T, must be determined, the Hamiltonian evaluated along the optimal path must satisfy

$$H(T,x_\delta(T),u_\delta(T),\lambda(T)) = 0.$$

Relationship between calculus of variations and optimal control theory

Consider the calculus of variations problem:

$$\max_x \int_0^T f(t,x,x')\,dt$$

$$\text{subject to} \quad x(0) = x_0$$

$$x(T) = x_T\,.$$

Our intention is to determine the Euler equation from the Hamiltonian employing Pontryagin's maximum principle. We start by writing

$$x' = u\,,$$

which now represents the state equation. Then the Hamiltonian becomes

$$H = f(t,x,u) + \lambda u\,.$$

The adjoint equation is

$$\lambda' = -\frac{\partial H}{\partial x} = -f_x\,, \qquad \lambda(T) = 0\,.$$

The optimality condition implies

$$\frac{\partial H}{\partial u} = f_u + \lambda = 0\,.$$

Therefore,

$$\lambda' = -\frac{d}{dt} f_u\,.$$

Equating the two λ' equations, we have

$$f_x = \frac{d}{dt} f_u\,.$$

This is precisely Euler's equation.

Current value Hamiltonian

A lot of dynamic optimisation problems encountered in economics and biology involves the discounted present value of a functional. As the functional usually

represents net revenues, the objective used in such investment analysis and cost-benefit analysis is the discounted present value of future net revenues.

Consider the following infinite time horizon optimal control problem:

$$\max_u Z(u) = \int_0^\infty e^{-\delta t} f(t, x(t), u(t))\, dt$$

$$\text{subject to} \quad x'(t) = g(t, x(t), u(t)), \quad x(0) = x_0$$

$$a \le u \le b,$$

where δ denotes the instantaneous discount rate in the exponential term, $e^{-\delta t}$, referred to as discount factor. For more details on the discount factor as it relates to the current value Hamiltonian, see Chiang (1992), Clark (2010), Kamien and Schwartz (1991) and Klein (2001).

The present value Hamiltonian is given by

$$H = e^{-\delta t} f(t, x, u) + \lambda g(t, x, u).$$

Define the current value shadow price as $\mu(t) = e^{\delta t}\lambda(t)$. Then the current value Hamiltonian is constructed as

$$\begin{aligned} \bar{H} &= f(t, x, u) + \mu g(t, x, u) \\ &= e^{\delta t} H. \end{aligned}$$

Since $\mu = e^{\delta t}\lambda$, then $\lambda = e^{-\delta t}\mu$. Thus

$$\lambda' = \frac{d}{dt}(e^{-\delta t}\mu) = e^{-\delta t}(\mu' - \delta\mu).$$

Similarly, $\bar{H} = e^{\delta t} H$ implies $H = e^{-\delta t}\bar{H}$. Therefore

$$\frac{\partial H}{\partial x} = e^{-\delta t}\frac{\partial \bar{H}}{\partial x}.$$

Hence, the adjoint equation $\lambda' = -\dfrac{\partial H}{\partial x}$ becomes

$$e^{-\delta t}(\mu' - \delta\mu) = -e^{-\delta t}\frac{\partial \bar{H}}{\partial x}$$

or

$$\mu' = \delta\mu - \frac{\partial \bar{H}}{\partial x}.$$

This is the form often encountered in economics books, and preferred by most economists because of the ease in computation and analysis.

Convergence of objective functional

An improper integral, by definition, is said to converge, if, for $t \geq 0$, the value of the integral is finite ($< \infty$). Otherwise, the integral is said to diverge.

The optimal control problem with infinite time horizon has as its objective functional an improper integral, $\int_0^\infty e^{-\delta t} f(t,x,u)\,dt$. The integrand, as a whole, contains the discount factor $e^{-\delta t}$ which, in general, provides a dynamic driving force to send the integrand quickly down to zero over time. In most resource management applications, the $f(t,x,u)$ component of the integrand is positive; and suppose it has an upper bound $\hat{F}$ (this implies, $\sup_u f(t,x,u) = \hat{F}$). Then the downward force of $e^{-\delta t}$ is sufficient to make the integral converge. Therefore, we can write

$$\int_0^\infty e^{-\delta t} f(t,x,u)\,dt \leq \int_0^\infty e^{-\delta t} \hat{F}\,dt = \frac{\hat{F}}{\delta}.$$

Using comparison test, we can also determine the convergence of the finite horizon scenario. That is,

$$\int_0^T e^{-\delta t} f(t,x,u)\,dt \leq \int_0^\infty e^{-\delta t} f(t,x,u)\,dt = \frac{\hat{F}}{\delta}.$$

Hence,

$$\int_0^T e^{-\delta t} f(t,x,u)\,dt \leq \frac{\hat{F}}{\delta}.$$

Sufficiency conditions

As already stated, the first task in solving an optimal control problem is to develop the necessary conditions. There are, however, some difficulties arising from the application of this method. It is possible that, multiple solution sets, only some of which are optimal controls could be provided by the necessary conditions. Additionally, the development of the necessary conditions assumes the existence of an optimal control. However, the necessary conditions could be obtained when, in fact, the original optimal control problem has no solution. Again, there is the expectation that the objective functional value evaluated at the optimal state and control would yield a finite value. This may not necessarily be the case in all

situations. The optimal control problem is deemed not to have a solution if the objective functional value turns out to be ∞ or $-\infty$.

The idea of uniqueness of solutions is also very important. Suppose an optimal control exists; that is, there is a u_δ such that $Z(u) \leq Z(u_\delta) < \infty$ for all controls u in the control set (for the case of maximisation). Then u_δ is unique whenever $Z(u_\delta) = Z(u)$ implies $u_\delta = u$ at all but finitely many points. In such a situation, the associated states will be identical. This state, x_δ, is referred to a the unique optimal state.

Therefore, uniqueness of solutions of the optimality system—state equation and the adjoint equation coupled with the characterisation of the optimal control and the boundary conditions—ensures the uniqueness of the optimal control, if it exists. Frequently, the uniqueness of the solutions of the optimality system can be proven, but only for a small time interval. This small time interval condition is as a result of the opposite time orientations of the state and adjoint equations, in the sense that the state equation possesses an initial time condition and the adjoint equation possesses a final time condition.

A true existence and uniqueness result guarantees an optimal control with a finite objective functional value. The following is such a result from Fleming and Rishel (1975).

Theorem 3.12. *Consider the optimal control problem (3.13). There exists an optimal control u_δ that maximises the objective functional $Z(u)$ over the control set U.*

To prove the theorem, the following conditions must be satisfied:

(i) The class of all initial conditions with a control u in the admissible control set together with the state system is non-empty.

(ii) The admissible control set U is closed and convex.

(iii) The right hand side of the state system is continuous and bounded above by a sum of the bounded control and the state, and can be written as a

linear function of u with coefficients depending on time and state.

(iv) The integrand of the objective functional is concave in U.

(v) There exists constants w_1, $w_2 > 0$ and $\eta > 1$ such that the integrand $f(t,x,u)$ of the objective functional satisfies

$$f(t,x,u) \leq w_1 - w_2|u|^{\eta}.$$

(Fister & Panetta, 2000)

Notice that this holds true for a maximisation problem. For a minimisation problem, the fourth condition must have the objective functional convex in U; and on the last condition, the bound on the integrand must be from below. That is,

$$f(t,x,u) \geq w_1|u|^{\eta} - w_2.$$

Exponential growth model

One of the most popular population growth models as well as the simplest is the Malthusian growth model. The model assumes that the rate of growth is proportional to the size of the population. Therefore, if $x(t)$ represents the size of the population, then

$$x' = rx, \qquad x(0) = x_0 > 0,$$

where $r > 0$ is known as the per capita growth rate or intrinsic growth rate. This differential equation serves as a mathematical model for a remarkably wide variety of natural phenomena.

The solution of the differential equation is obtained by separating variables,

$$\int_0^x \frac{dy}{y} = \int_0^t r\,ds.$$

This implies,

$$\ln x - \ln x_0 = rt,$$

so that

$$x(t) = x_0 e^{rt}$$

becomes the unique solution of the given initial value problem.

Logistic growth model

Due to the problems associated with the exponential growth model, one of which being the fact that the population growth is unbounded, there was the need to establish a more realistic differential equation to model population growth. For instance, it was observed that in situations as diverse as the human population in a given country and a fruit fly population in an enclosure, the birth rate decreases as the population itself increases. This may be attributable to a wide range of factors, from increased scientific and cultural sophistication to a limited food supply and space. The model that addresses this issue of crowding in the population is called the Pearl-Verhurlst logistic growth model.

Let $x(t)$ represent the size of the population at time $t \geq 0$, which evolves according to

$$x' = rx\left(1 - \frac{x}{K}\right), \qquad x(0) = x_0 > 0,$$

where $r > 0$ is the intrinsic growth rate and $K > x_0$ is the carrying capacity of the environment which serves as an upper bound for $x(t)$. The first term on the right hand side, rx denotes exponential growth while the second term, $-\frac{r}{K}x^2$ represents the crowding effect. Such an effect is referred to as negative density dependence. The solution of this differential equation can also be found by separating variables,

$$\int_0^x \frac{dy}{y(K-y)} = \frac{r}{K}\int_0^t ds.$$

This implies

$$\frac{1}{K}\left[\ln\left(\frac{x}{K-x}\right) - \ln\left(\frac{x_0}{K-x_0}\right)\right] = \frac{r}{K}t,$$

so that

$$\frac{x(t)}{K-x(t)} = \frac{x_0}{K-x_0}e^{rt}.$$

Hence,

$$x(t) = \frac{x_0 K}{x_0 + (K-x_0)e^{-rt}}.$$

(Weber, 2009)

Lokta-Volterra model

Some of the most interesting and important applications in stability theory involve the interactions between two or more biological species inhabiting the same environment. We focus on a predator-prey scenario involving two species. One species—the predators—feeds on the other species—the prey—which in turn feeds on some food item readily accessible within the environment. A standard example involves a population of foxes and rabbits inhabiting a woodland; the foxes (predators) consume the rabbits (prey), while the rabbits consume certain vegetation in the woodland. Other examples include whales (predators) and krill (prey), bass (predators) and sunfish (prey), and salmon (predators) and herring (prey).

The Lokta-Volterra model constitutes the basic predator-prey model

$$\begin{aligned} \frac{dx}{dt} &= rx - \alpha xy, \\ \frac{dy}{dt} &= -sy + \beta xy, \end{aligned}$$

where $x(t)$ denotes the size of prey population and $y(t)$ denotes the size of predator population. The main assumption of the model is that the prey population grows exponentially in the absence of predators, and the predator population declines exponentially in the absence of prey. The rate of decrease in prey population caused by predation equals αxy, while the rate of increase of predator population is βxy. The ratio β/α measures the biological efficiency of predation.

Gordon-Schaefer bioeconomic model

As stated earlier, the pioneering model in renewable resource management was proposed by Gordon (1954) and Schaefer (1954). The model possesses both biological and economic features, hence the name Gordon-Schaefer bioeconomic model.

We shall look at the first model proposed, which was static in nature, and then progress to the current dynamic version. The biological component of the model

makes use of the following basic differential equation:

$$\frac{dx}{dt} = g(x) - h(t), \qquad x(0) = x_0,$$

where $x(t)$ represents the population size, or biomass (in tonnes) of fish stock at time t, x_0 is the initial population size at time $t = 0$, $g(x)$ denotes the net natural growth rate of the population biomass, (in tonnes per year) depending on the current size $x(t)$, and $h(t)$ represents the rate of removals, or harvest, of the resource stock at time t.

The assumption is that the function g is differentiable and concave, and it satisfies, for $0 < x < K$,

$$g(0) = g(K) = 0, \quad g(x) > 0, \quad g''(x) < 0,$$

where K denotes the carrying capacity of the given population. This term reflects the fact that if $h(t) = 0$, then

$$\lim_{t \to \infty} x(t) = K.$$

The most common growth function g favoured by most researchers is the logistic function. See, for, example, Clark (2010), Craven (1995), Dubey and Patra (2013a), Dubey *et al.* (2003) and Kar and Chakraborty (2010). On the other hand, the rate of harvest, $h(t)$ may be represented by h, where h denotes a constant harvesting rate (also known as stock-independent harvesting); $h(t)$ may be represented by a periodic function, denoting a time-dependent periodic harvesting rate; or $h(t)$ may be represented by $h(t,x)$, denoting proportional harvesting rate (also referred to as stock-dependent harvesting).

Proportional harvesting model

We shall start by doing a detailed investigation of the last scenario—proportional harvesting. The model is also known as a constant effort harvesting model. Consider the following basic biological model (also referred to as the Schaefer model):

$$\frac{dx}{dt} = rx\left(1 - \frac{x}{K}\right) - qEx, \qquad x(0) = x_0. \tag{3.19}$$

where the harvesting rate,

$$h(t) = qEx \tag{3.20}$$

(a bilinear function of E and x) is known as the catch-effort relation. The parameter $E(t)$ represents the harvesting effort at time t. In the context of fisheries, $E(t)$ is typically specified as the number of (standard) vessels actively fishing at time t. Units of effort would be Standard Vessel Units (SVU).

The constant q is known as the catchability coefficient, with units $\text{SVU}^{-1} \times (\text{time unit})^{-1}$. Therefore, q represents the proportion of the current stock x caught by one standard vessel in one time unit.

There are two equilibrium points associated with Equation (3.19); namely, 0 and a positive equilibrium point

$$x^* = K\left(1 - \frac{qE}{r}\right), \tag{3.21}$$

provided $E < \frac{r}{q}$. The equilibrium points 0 and x^* are hyperbolic, with 0 being unstable and x^* being stable; and therefore the system is structurally stable. Invoking Theorem 3.3, the model undergoes transcritical bifurcation at the point $E = \frac{r}{q}$. That is, there is a single nonhyperbolic equilibrium point, 0, which is semi-stable; hence making the system structurally unstable. In other words, for any initial population x_0, the resource will eventually go into extinction (as time approaches infinity). When $E > \frac{r}{q}$, there are two hyperbolic equilibrium points, 0 and a negative equilibrium point. Of course, the non-negative equilibrium point, 0 is stable (and for sake of completeness, the negative equilibrium point is unstable); and for any initial population, the resource will die out in finite time.

Maximum sustainable yield

The level of harvesting that maximises the sustainable yield is called the maximum sustainable yield (MSY). That is, the maximum harvest which can be maintained indefinitely.

Substituting Equation (3.21) into Equation (3.20), with $x = x^*$, gives the sus-

tainable yield

$$h_S = qEK\left(1 - \frac{qE}{r}\right). \tag{3.22}$$

The effort that maximises the sustainable yield h_S is found as

$$E_{MSY} = \frac{r}{2q}. \tag{3.23}$$

The value of MSY, denoted h_{MSY}, is found by plugging Equation (3.23), with $E = E_{MSY}$, into Equation (3.22). Hence,

$$h_{MSY} = \frac{rK}{4}, \tag{3.24}$$

and the biomass level at the MSY is

$$x_{MSY} = \frac{K}{2}. \tag{3.25}$$

Incorporating economic parameters into the afore-mentioned biological model gives the bioeconomic model. This is also known as the (static) Gordon-Schaefer model.

Open access yield

Operating under an open access regime where there is little or no regulation of the resource, effort E tends to a level where the sustainable economic rent or net revenue is zero. This phenomenon is known as open access yield (OAY). That is, the harvesting level which can be maintained indefinitely when the net revenue is zero. This scenario often leads to what is referred to as economic overfishing.

The sustainable net revenue is the difference of total sustainable revenue TR_S and total cost TC, and it is given by

$$\begin{aligned} \textit{Sustainable net revenue} &= ph_S - cE \\ &= pqEK\left(1 - \frac{qE}{r}\right) - cE, \end{aligned} \tag{3.26}$$

where p is the price per unit harvest or the ex-vessel price of fish, with units \$ tonne^{-1} and c is the cost per unit effort (the costs may include cost of fuel powering the fishing vessels), having units \$ SVU^{-1} $\times$ (time unit)$^{-1}$.

Letting Equation (3.26) go to zero gives

$$E_{OAY} = \frac{r}{q}\left(1 - \frac{c}{pqK}\right), \tag{3.27}$$

where $pqK > c$.

To get the biomass level x_{OAY} associated with E_{OAY}, substitute Equation (3.27), with $E = E_{OAY}$, into Equation (3.21) to get

$$x_{OAY} = \frac{c}{pq}. \tag{3.28}$$

The associated harvest level is

$$h_{OAY} = \frac{rc}{pq}\left(1 - \frac{c}{pqK}\right). \tag{3.29}$$

It is worth noting that when $E_{OAY} > E_{MSY}$, the rate of harvest exceeds h_{MSY} resulting in $x_{OAY} < x_{MSY}$. This situation is known as biological overfishing and eventually leads to the depletion of the resource. Thus OAY can lead to both biological and economic overfishing. The OAY is also known as bionomic equilibrium (BE) because it simultaneously gives equilibrium in both biological and economic sense (Suri, 2008).

Alternatively, we can write the fishermen's combined net revenue flow at time t as,

$$\begin{aligned}\pi &= (p - c(x))h \\ &= (p - \frac{c}{qx})qEx \\ &= (pqx - c)E.\end{aligned}$$

Then, in the absence of any regulatory control over fishing (open access), the fish population will be fished down to a level where the net revenue, π equals zero. That is,

$$(pqx - c)E = 0,$$

implying

$$x_{OAY} = \frac{c}{pq}.$$

Thus, an important prediction of the model is that fishing is only profitable if and only if $x(t) > x_{OAY}$. In other words, whenever $x(t) > x_{OAY}$, $\pi > 0$ (fishing is profitable). Therefore, the effort E will tend to be large, so that $dx/dt < 0$ (fish population decreases). However, once $x(t)$ falls to (or below) x_{OAY}, we have $\pi \leq 0$ (fishing is no longer profitable), so fishing ceases.

From Equation (3.28), it is instructive to note that x_{OAY} is proportional to cost c, and inversely proportional to price p. Therefore, lower costs or higher prices induce intensive overexploitation of resource. This implies more intensive overfishing, resulting in $x_{OAY} < x_{MSY}$.

However, the scenario just depicted is the exact opposite of what one should expect in a free economy—higher prices or lower costs should lead to an increase in productive capacity, $x(t)$, not a decrease. Gordon (1954) explains this unusual 'upside down' behaviour of natural resource economics down to the fact that the fishery (in the model employed) is assumed to be common property. No one owns the fish, so no one has the incentive to protect it. This leads to a situation that Hardin (1968) calls 'the tragedy of the commons'.

The unregulated fishery model further gives the following two predictions:

- There is no limit to how low x_{OAY} can be. That is, the population will persist indefinitely at any level of x_{OAY}, no matter how low.
- Population will always recover if fishing ceases.

In reality, many fish populations fail to recover from severe overfishing. The reasons why this is so are seldom fully understood. First, the reproductive success may fall below sustainable levels when the stock is sufficiently low; and second, a depleted population may be replaced by a competing species (Clark, 2010).

Maximum economic yield

The rate of harvesting that maximises the sustainable net revenues is called the maximum economic yield (MEY). That is, the maximum net revenues which can be maintained indefinitely at that level of harvest.

The effort level that maximises the net revenues is found from Equation (3.26) as

$$E_{MEY} = \frac{r}{2q}\left(1 - \frac{c}{pqK}\right). \tag{3.30}$$

Using Equation (3.21), the associated biomass level is

$$x_{MEY} = \frac{K}{2}\left(1 + \frac{c}{pqK}\right). \tag{3.31}$$

The corresponding harvest level is

$$h_{MEY} = \frac{rK}{4}\left(1 - \left(\frac{c}{pqK}\right)^2\right). \tag{3.32}$$

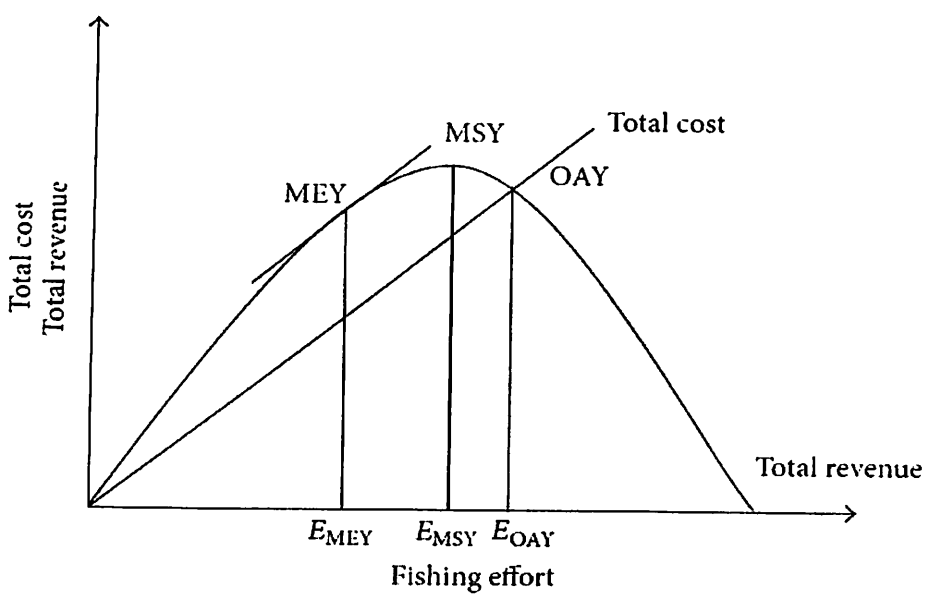

Figure 1: The Static Gordon-Schaefer Model

The total revenue curve is assumed to rise to a peak, and then to decline, as effort is increased (see Figure 1, sourced from Habib *et al.*, 2014). This is due to a specific consequence of the basic properties of a biological population. Precisely, high levels of harvesting effort (or harvest rates greater than MSY) can result in the depletion of the population to a level at which biological reproduction is severely reduced, ultimately leading to the extinction of the resource. When a population is fished to, say 10% of its virgin biomass, because of high inputs of effort, sustained catches can become greatly reduced—as has indeed often been the case (Clark, 2010).

Remarks

Figure 1 depicts $E_{OAY} > E_{MSY}$; however, in practice, E_{OAY} can be greater than or less than E_{MSY} depending on the price of fish and cost of effort. It is instructive to note that when effort level $E < E_{OAY}$, the net revenue is positive (revenue exceeds cost), thereby attracting more fishers into the industry. On the other hand, if the effort level $E > E_{OAY}$, the net revenue is negative (cost exceeds revenue), making fishers to abandon the industry. Therefore, there is always a tendency towards E_{OAY} under open access fishery.

Also, as already alluded to, when E_{OAY} is greater than E_{MSY} we have what is known as biological overfishing. This shows that open access fishery must not be a management tool as it can lead to both biological overfishing ($x_{OAY} < x_{MSY}$) and economic overfishing (net revenue is zero).

For the special case of very high costs or low prices, $E_{OAY} < E_{MSY}$ and $x_{OAY} > x_{MSY}$. Thus, in this instance, there is no biological overfishing, even though economic overfishing may be present.

Note that if $x_0 > x_{MSY}$, the fishery is said to be underexploited (or underfished); if $x_0 = x_{MSY}$, the fishery is considered fully exploited (or fully fished); and if $x_0 < x_{MSY}$, the fishery is said to be overexploited (or overfished).

It has to be observed that for most practical fishing costs, $E_{MEY} < E_{MSY}$ ($x_{MEY} > x_{MSY}$). However, for very low costs (or high prices) E_{MEY} is approximately equal to E_{MSY} (x_{MEY} is vey close to x_{MSY}). In fact, at zero costs, the values at MSY and MEY are identical. The following observation is also pertinent:

$$E_{MEY} = \frac{E_{OAY}}{2}$$

Assumptions of the model

The following are some of the assumptions inherent in the Gordon-Schaefer bioeconomic model.

1. The Schaefer catch relation, $h = qEx$ indicates that the exploited

population always distributes itself uniformly over the fishing area. In other words, catch per unit effort (CPUE) is proportional to stock size $x(t)$, with a constant catchability coefficient q. That is, $\frac{h}{E} = qx$.

2. Impact of variations of harvesting effort on the fish stock is instantaneous; no time-delays are allowed.

3. The carrying capacity K serves as an upper bound for the size of fish stock.

4. The catchability coefficient, q is constant. That is, improved fishing technology in the form of bigger boats, better engines, sophisticated fishing gears and navigational aids have no impact on the fishing activity.

5. The model is autonomous. That is, no parameter in the model explicitly depends on time. Additionally, the biological parameters—intrinsic growth rate r and carrying capacity K—as well as the economic parameters—price of a unit harvest p, cost of a unit fishing effort c and catchability coefficient q—remain fixed over the time horizon. Furthermore, the costs are linear in the fishing effort.

Limitations of the model

The limitations associated with the Gordon-Schaefer bioeconomic model include the following:

1. The model does not take cognisance of the age-structure of the fish stock. That is to say, juveniles and adults are lumped together as one in the model.

2. The catchability coefficient may actually not be constant in light of improved fishing technology.

3. The idea of uniform distribution of fish stock probably does not hold in practice. That is, CPUE is not an adequate measure of size of fish stock. For example, many small pelagics, such as sardinellas and anchovies, typically form large schools, which size is independent of the actual

population size. If these schools are readily located by fishermen, CPUE will remain relatively constant over all population levels (Mackinson, Sumaila & Pitcher, 1997).

4. Fluctuations in size of fish stocks may be attributable to intense overexploitation of the resource or may be due to natural phenomena. It is hard to exactly tell, between the two, the real cause of depletion of the resource.

5. The catch effort relation is given by $h = qEx$. For a fixed x, $h \to \infty$ as $E \to \infty$. Similarly, for a fixed E, $h \to \infty$ as $x \to \infty$. In other words, the harvest rate can be unbounded, in spite of the fact that the population size is constant, or the harvesting effort is constant (Clark, 2010; Patra, 2013; Suri, 2008).

Constant harvesting model

We turn our attention to the constant harvesting scenario by first presenting its basic biological model.

$$\frac{dx}{dt} = rx\left(1 - \frac{x}{K}\right) - h, \qquad x(0) = x_0. \tag{3.33}$$

To obtain the equilibrium points, we set Equation (3.33) to zero and solve the resulting quadratic equation to yield

$$x_1^* = \frac{K}{2}\left(1 - \sqrt{1 - \frac{4h}{rK}}\right), \qquad x_2^* = \frac{K}{2}\left(1 + \sqrt{1 - \frac{4h}{rK}}\right) \tag{3.34}$$

provided $h < \frac{rK}{4}$. The equilibrium points x_1^* and x_2^* are hyperbolic, with x_1^* unstable and x_2^* stable; and therefore the system is structurally stable. Invoking Theorem 3.2, the model undergoes saddle-node bifurcation at the point $h = \frac{rK}{4}$. That is, there is a single nonhyperbolic equilibrium point, $\frac{K}{2}$, which is semi-stable, thereby making the system to be structurally unstable. In other words, for any initial population $x_0 > \frac{K}{2}$, the population approaches $\frac{K}{2}$ as $t \to \infty$; and if $x_0 < \frac{K}{2}$,

the resource will eventually go into extinction in finite time. When $h > \frac{rK}{4}$, the model has no equilibrium point; and for any initial population, the resource will die out in finite time.

The equation for the sustainable yield is

$$h_S = rx\left(1 - \frac{x}{K}\right). \tag{3.35}$$

The MSY occurs when

$$\frac{dh_S}{dx} = r\left(1 - \frac{2x}{K}\right) = 0. \tag{3.36}$$

Thus, the biomass level at MSY is

$$x_{MSY} = \frac{K}{2}. \tag{3.37}$$

Additionally, substituting the value of the biomass level at MSY in Equation (3.37) into Equation (3.35) gives the value of MSY as

$$h_{MSY} = \frac{rK}{4}. \tag{3.38}$$

Therefore, h_{MSY} is the maximum amount that can be harvested while keeping the population constant. That is, $\frac{dx}{dt} = 0$.

Adding economic parameters unto the afore-mentioned biological model (3.33) gives the bioeconomic model. Therefore, the net revenue is given by

$$Net\ revenue = (p - c)h,$$

where p and c are price per unit harvest and cost per unit harvest, respectively.

Periodic harvesting model

A biological model for a population that undergoes periodic or oscillatory harvesting is

$$\frac{dx}{dt} = rx\left(1 - \frac{x}{K}\right) - h(1 + a\sin(bt)), \qquad x(0) = x_0, \tag{3.39}$$

where the non-autonomous harvest function is given by

$$h(t) = h(1 + a\sin(bt)).$$

The mean harvesting rate is represented by h and a is the amplitude of the sine function ($0 \leq a \leq 1$). Furthermore, the period is given by $P = \frac{2\pi}{b}$ and the frequency is $f = \frac{1}{P}$. When the modification on the frequency, $b = 2\pi$, then $P = f = 1$.

Benardete *et al.* (2008) state that, one way to find periodic solutions of a non-autonomous differential equation such as the one outlined in Equation (3.39) is to view it as a periodic perturbation of some autonomous differential equation

$$\frac{dx}{dt} = rx\left(1 - \frac{x}{K}\right) - h$$

whose behaviour is well understood.

Theorem 3.1 justifies the existence of periodic cycles for sufficiently small perturbations of h. The following proposition demonstrates the non-existence of periodic cycles of Equation (3.39) for large values of h.

Proposition 1. *If* $h > \frac{rK}{4}$, *then*

$$\frac{dx}{dt} = rx\left(1 - \frac{x}{K}\right) - h(1 + a\sin(2\pi t)), \qquad x(0) = x_0$$

has no periodic solution; and furthermore, all solutions diverge to $-\infty$.

Proof. From the fundamental theorem of calculus,

$$\begin{aligned} x(1) - x(0) &= \int_0^1 \frac{dx}{dt} dt \\ &= \int_0^1 \left[rx\left(1 - \frac{x}{K}\right) - h(1 + a\sin(2\pi t))\right] dt \\ &\leq \frac{rK}{4} - h, \end{aligned}$$

since

$$\max_x g(x) = \frac{rK}{4}, \quad \text{where } g(x) = rx\left(1 - \frac{x}{K}\right),$$

and

$$\int_0^1 h(1 + a\sin(2\pi t))\, dt = h.$$

So if $h > \frac{rK}{4}$, then $x(1) < x(0)$ implying $x(t)$ is not periodic.

In general, for all non-negative integers, n (n being the values of t)

$$x(n+1) - x(n) \leq \frac{rK}{4} - h < 0$$

showing that $x(t)$ diverges to $-\infty$. □

It is worth noting that since the model has a period of 1, it is periodic if $x(n+1) = x(n)$. Also, the objective functional for the periodic harvesting model is the same as that of the constant harvesting model.

Chapter Summary

The chapter has outlined some the underlying theory and concepts needed for a successful implementation of an optimisation process. This includes bifurcation theory and calculus of variations, the classical approach to solving optimisation problems. Theorems on equilibrium points and their stability properties are presented and discussed. The main model employed for the population dynamics of the fishery is the logistic model. Assumptions and limitations of this model are clearly spelt out.

Formulations of various types of optimal control problems are provided. This includes problems with linear controls, non-linear controls, bounded controls and states with fixed endpoints. Also considered were finite as well as infinite horizon optimal control problems.

The necessary and sufficient conditions for optimality of the model were discussed. Existence and uniqueness of the optimal control are guaranteed when the sufficiency conditions are met. The necessary conditions of the model are normally obtained through the application of Pontryagin's maximum principle. This principle makes use of a function called the Hamiltonian. When a discount term is present in the model, the optimality of the system could be determined employing either the present value Hamiltonian or the current value Hamiltonian. This study relies on the current value Hamiltonian because of the ease in analysis.

CHAPTER FOUR

PROPORTIONAL HARVESTING MODELS

Introduction

As already stated, Ghana's sardinella fishery is currently in a state of crisis. Present levels of harvests are among the lowest in recorded history. Thus, there is the need to come up with mathematical models that will help shed light on the prevailing precarious situation.

We shall begin by studying the canonical Gordon-Schaefer model. Afterwards, some modifications of the canonical model will be investigated with the aid of bifurcation and numerical analyses as they relate to the sardinella fishery in Ghana.

The Canonical Gordon-Schaefer Model

The dynamic optimisation version of the Gordon-Schaefer model can be presented in the following form:

$$\begin{aligned} \max_E Z(E) &= \int_0^\infty e^{-\delta t}(pqx(t) - c)E(t)\,dt \\ \text{subject to} \quad \frac{dx(t)}{dt} &= rx(t)\left(1 - \frac{x(t)}{K}\right) - qE(t)x(t) \\ x(0) &= x_0 \\ 0 \le E(t) &\le E_{max}, \end{aligned} \tag{4.1}$$

where E_{max} is the maximum effort capacity. The model aims to determine the effort strategy $E(t)$ that results in the largest possible net economic benefit as expressed by the present value integral Z of Model (4.1).

Bifurcation analysis

A bifurcation can be described as the change in the number of equilibrium points or periodic orbits, or in the stability properties of a dynamical system if a parameter is varied. The value of the parameter where the stability dynamics change is called a bifurcation point (Daci & Spaho, 2013).

As mentioned earlier, there are two equilibrium points associated with the state dynamics of the Model (4.1) when the effort is less than the bifurcation point. These are 0 and

$$x^* = K\left(1 - \frac{qE}{r}\right),$$

and the bifurcation point is given by $E = \frac{r}{q}$. The slope fields and solution curves of the state equation were plotted with the aid of the software dfield8 by John Polking. The Gordon-Schaefer model, as already alluded to, contains both biological and economic parameters. Therefore any numerical study of the model needs to obtain the values of these parameters.

Koranteng (as cited in Koranteng, 1998) stated:

> The multiplicity of gears and the problem of migration of fishers that characterise the artisanal fleet make assessment of its catch and fishing effort rather difficult. Consequently, assessment of the stocks of fish that the fleet exploits is also difficult (p.10).

Therefore, the biological data is sourced from a published work on a *Sardinella aurita* study conducted by the FAO in collaboration with the Nansen Programme (Nansen, 2001). As regards the economic data, the values are based on a field study conducted by the Marine Fisheries Research Division (MFRD) of the Fisheries Commission of Ghana (MFRD, 2008). For further details, see Bailey *et al.*, (2011), Fister and Panetta (2000), Akpalu and Vondolia (2011) and Lleonart and Merino (2009). The original economic data were denominated in United States dollars. Therefore to reflect current values, the original price and cost figures are adjusted for inflation using the CPI Inflation Calculator provided

by the United States Bureau of Labour Statistics on its website. See Brinson, Die, Bannerman and Diatta (2009) for further details. Table 1 presents the biological and economic parameter values used for the study.

Table 1: Parameter Values for Model

Parameter	Description	Value	Unit
δ	Discount rate	0.15	year^{-1}
q	Catchability coefficient	1.8×10^{-6}	trip^{-1}year^{-1}
r	Per capita growth rate	1.42	year^{-1}
K	Carrying capacity of ecosystem	1,000,000	tonnes
p	Ex-vessel price of fish	600	\$ tonne^{-1}
c	Cost per trip	195	\$ trip^{-1}year^{-1}

From the parameter values, the bifurcation point for the model is given by $E = 788,888.89$. That is, approximately 788,889 trips annually for the fishery. For ease of analysis, q, $E(t)$, K and $x(t)$ are scaled to a thousand units.

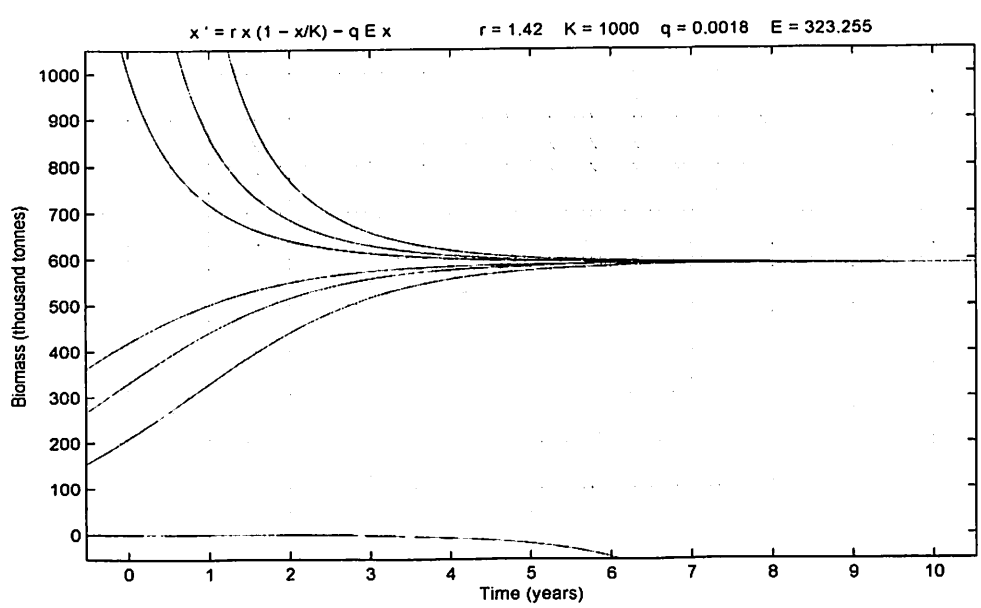

Figure 2: Solution Curves for $E = 323,255$

Figure 2 presents the solution curves for the case where $E = E_{MEY} = 323,255$ trips. It is observed that there are two hyperbolic equilibrium points: 0 and $x^* =$

$x_{MEY} = 590,278$ tonnes. For any initial population size or biomass level, $x_0 > x_{MEY}$, the population approaches the equilibrium population, x_{MEY} in the long run. Similarly, for $0 < x_0 < x_{MEY}$, the population asymptotically approaches x_{MEY}. Thus the biomass level 0 is unstable while x_{MEY} is stable (making the system structurally stable). Of course, biomass levels starting from the equilibrium levels, 0 and x_{MEY} remain there indefinitely. Hence, an effort level corresponding to E_{MEY} induces a long-term biomass level of more than a half the carrying capacity.

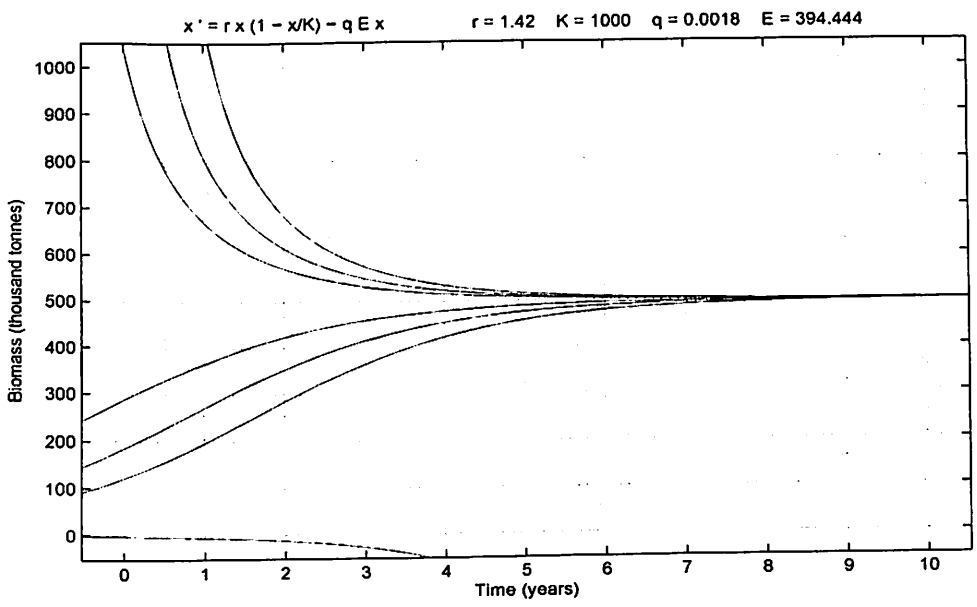

Figure 3: Solution Curves for $E = 394,444$

Solution curves corresponding to the situation where $E = E_{MSY} = 394,444$ trips are presented in Figure 3. It can be observed that there are two hyperbolic equilibrium points: 0 and $x^* = x_{MSY} = 500,000$ tonnes. For any initial biomass level, $x_0 > x_{MSY}$, the population approaches the equilibrium population, x_{MSY} in the long run. Similarly, for $0 < x_0 < x_{MSY}$, the population asymptotically approaches x_{MSY}. Thus the biomass level 0 is unstable while x_{MSY} is stable (making the system structurally stable). Of course, biomass levels starting from the equilibrium levels, 0 and x_{MSY} remain there indefinitely. Hence, an effort level corresponding to E_{MSY} induces a long-term biomass level of exactly half the carrying capacity.

Figure 4 shows the solution curves for the case where $E = E_{OAY} = 646,450$

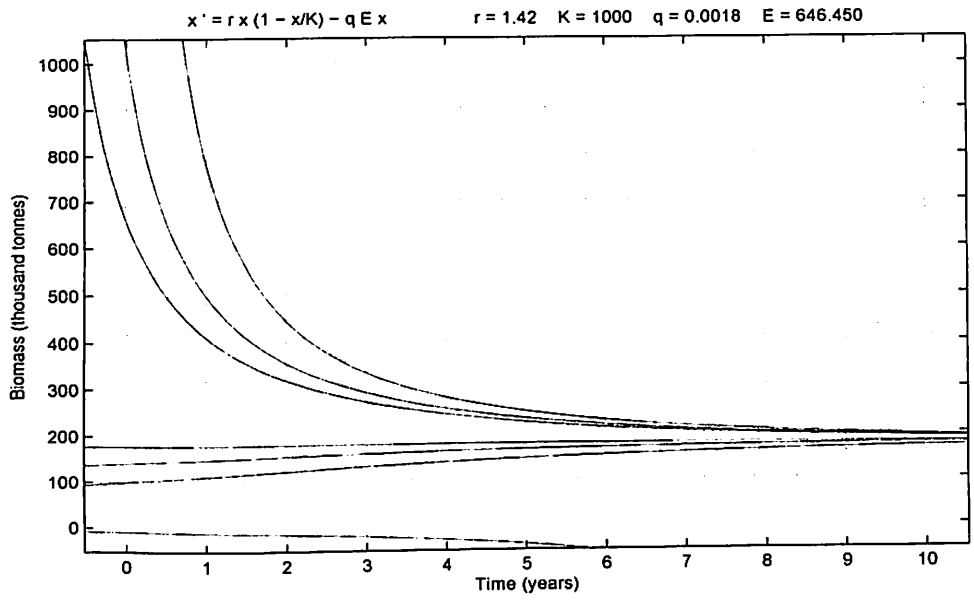

Figure 4: Solution Curves for $E = 646,450$

trips. Clearly, there are two hyperbolic equilibrium points: 0 and $x^* = x_{OAY} = 180,556$ tonnes. For any initial biomass level, $x_0 > x_{OAY}$, the population approaches the equilibrium population, x_{OAY} in the long run. Similarly, for $0 < x_0 < x_{OAY}$, the population asymptotically approaches x_{OAY}. Thus the biomass level 0 is unstable while x_{OAY} is stable (making the system structurally stable). Of course, biomass levels starting from the equilibrium levels, 0 and x_{OAY} remain there indefinitely. Hence, an effort level corresponding to E_{OAY} induces a long-term biomass level of about a fifth of the carrying capacity. However, as already mentioned, there is a question as to whether or not the fish stocks will persist at such a relatively low biomass level.

Solution curves corresponding to the case where $E = 788,889$ trips, the bifurcation point, are presented in Figure 5. For any initial biomass level, $x_0 > 0$, the population approaches the nonhyperbolic equilibrium population, 0 in the long run. Thus, at the transcritical bifurcation point, the single equilibrium biomass level 0, is semi-stable (making the system structurally unstable). Of course, biomass levels starting from the equilibrium level, 0 remain there indefinitely. Hence, for any initial biomass level, the long-term population of fish stock is towards extinction.

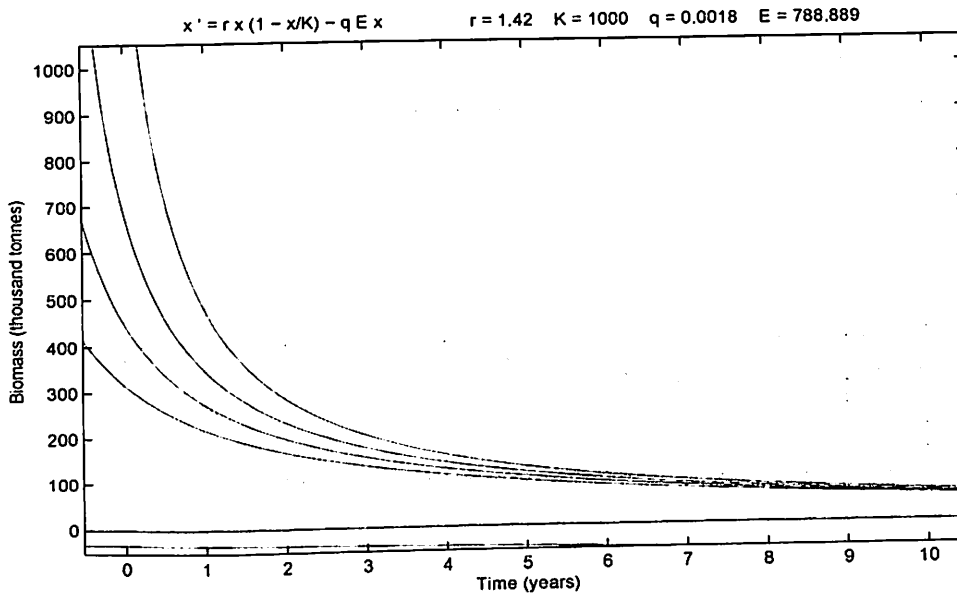

Figure 5: Solution Curves for $E = 788,889$

The case where effort level, $E = 1,183,333$ trips, is greater than the bifurcation point is shown in Figure 6. For any initial biomass level, $x_0 > 0$, the population approaches the hyperbolic equilibrium population, 0 in finite time. Thus, corresponding to this effort level exists a non-negative equilibrium biomass level 0, which is stable (making the system structurally stable). Hence, in this situation, whatever the initial fish population, the fish will die out as a result of overfishing or excessive harvesting in finite time.

In summary, fish stocks exploited below 788,889 trips (the bifurcation point) are more likely to persist. Specifically, exploited stocks at MEY and MSY levels, 323,255 and 394.444 trips, respectively, are almost guaranteed to persist. Moreover, at the OAY level of fishing effort (646,450 trips), the model predicts that the fish population will persist indefinitely at any level x_{OAY} no matter how low; and also the population will always recover if fishing ceases. As a matter of fact, many fish populations never recover from severe overfishing. Stocks exploited on or above the bifurcation point (1,183,333 trips) are more than likely to go into extinction, if not in finite time, then probably in the long run.

Regarding the artisanal fishery, as stated earlier, they are currently a little over 12,700 canoes operating within the sector targeting the four main fish species:

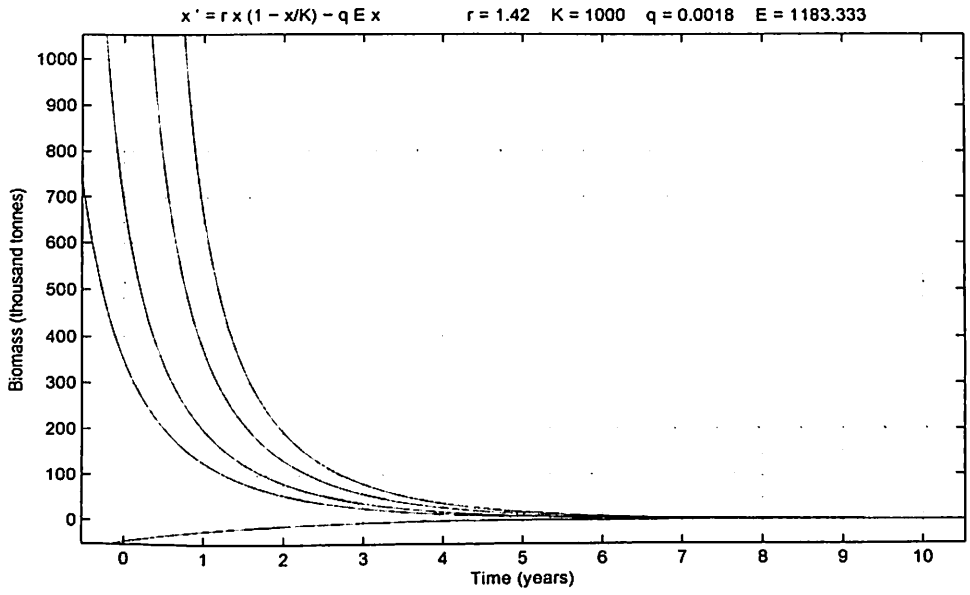

Figure 6: Solution Curves for $E = 1,183,333$

Sardinellas—aurita and *maderensis*, anchovies and mackerels. Assuming 40% of the boats are dedicated to *Sardinella aurita*, and also assuming 20 fishing days in a month (since most of the fishers along the coast do not fish on Tuesdays, and also excluding days fishers use to mend their broken nets as well as days of adverse weather conditions), then we have a total of 1,219,200 fishing days in a year. Furthermore, equating one trip to one fishing day, then we have 1,219,200 trips undertaken annually by the fishermen exploiting, in particular, the *Sardinella aurita*. Juxtaposing these current effort levels by the artisanal fishermen with the preceding reference points, they seem way above the bifurcation point of the fishery. In fact, the current effort levels are more than three times the effort needed at MSY. This can only mean one thing—if current effort levels are not checked, the long-term sustainability of the resource will be in serious jeopardy, attested to by current very low yields.

Annual net revenue

Recall the net revenue for the static model is given by

$$\pi = ph - cE\,.$$

Therefore, substituting the values of the effort and harvest levels at the three

equilibrium reference points, MEY, MSY and OAY, into the net revenue equation, we can compute the annual net revenue, as shown in Table 2.

Table 2: Annual Net Revenue at MEY, MSY and OAY Levels of Harvesting

Reference point	MEY	MSY	OAY
x	590,278	500,000	180,556
E	323,225	394,444	646,450
h	343,427	355,000	210,096
Sustainable net revenue (\$ year^{-1})	143,027,325	136,083,420	0

Table 2 validates theoretical results. At MEY levels, we have the maximum revenue as well the highest fish stock size. Thus, apart from providing the most revenue, it is the most conservationist among the three. Of course, the level at MSY provides the highest yield; and at the OAY level, it provides the most effort, lowest fish stock size, lowest yield, and of course, zero revenue. Note that the sustainable net revenue for OAY is exactly zero when all the significant digits of h and E are used in the computation.

Optimality of the model

The characterisation of the optimal control is sought for in this section. Also, the model is analysed to determine whether or not the singular path is attainable by the control. The goal, as stated earlier, is to maximise the discounted present value of future net revenues. Thus, we seek an optimal control E_δ such that

$$Z(E_\delta) = \max\{Z(E) \,|\, E \in U\},$$

where the control set, which is Lebesgue measurable for an infinite time horizon, is defined by

$$U = \{E(t) \,|\, 0 \leq E(t) \leq E_{max},\ t \in [0,\infty)\}.$$

To derive the necessary conditions for the optimal control, Pontryagin's maximum principle (Pontryagin *et al.*, 1962) is employed. The current value Hamiltonian for the optimal control problem (4.1) is

$$H(t,x,E,\lambda) = (pqx - c)E + \lambda\left[rx\left(1 - \frac{x}{K}\right) - qEx\right]. \tag{4.2}$$

The adjoint variable λ is governed by

$$\begin{aligned} \lambda' &= \delta\lambda - \frac{\partial H}{\partial x} \\ &= \delta\lambda - pqE - \lambda\left(r - \frac{2rx}{K} - qE\right). \end{aligned} \tag{4.3}$$

The switching function is defined by

$$\begin{aligned} \psi(t) &= \frac{\partial H}{\partial E} \\ &= (pqx - c) - \lambda qx. \end{aligned} \tag{4.4}$$

The characterisation of the optimal control is

$$\begin{cases} E_\delta = 0 & \text{if} \quad \psi(t) < 0, \\ 0 < E_\delta < E_{max} & \text{if} \quad \psi(t) = 0, \\ E_\delta = E_{max}, & \text{if} \quad \psi(t) > 0. \end{cases} \tag{4.5}$$

Singularity analysis of the model

This is to enable us determine whether the optimal control would be bang-bang or follow a singular path. For a singular control, we assume that there is an interval I for all $t \in I \subset [0,\infty)$ such that

$$\psi(t) = 0. \tag{4.6}$$

Thus, from Equations (4.4) and (4.6),

$$(pqx - c) - \lambda qx = 0. \tag{4.7}$$

So, solving for λ we find

$$\lambda = p - \frac{c}{qx}. \tag{4.8}$$

Differentiating Equation (4.8) with respect to t, substituting for the state equation in Model (4.1) and simplifying, it follows that

$$\lambda' = \frac{crK - cqEK - crx}{qxK}. \tag{4.9}$$

By plugging the λ expression in Equation (4.8) into the adjoint equation (4.3), we get

$$\lambda' = \frac{\delta pqxK + 2pqrx^2 + crK - pqrxK - cqEK - \delta cK - 2crx}{qxK}. \tag{4.10}$$

Setting the expressions in Equations (4.9) and (4.10) equal to each other and simplifying, we obtain the positive optimal biomass level as

$$x_\delta = \frac{K}{4}\left[\left(1 + \frac{c}{pqK} - \frac{\delta}{r}\right) + \sqrt{\left(1 + \frac{c}{pqK} - \frac{\delta}{r}\right)^2 + \frac{8\delta c}{pqrK}}\right]. \tag{4.11}$$

To digress, we can also obtain the optimal biomass level by the application of calculus of variations (see Appendix).

The effort level corresponding to x_δ is found from the state equation in Model (4.1), after noting that $x' = 0$, since x_δ is a constant. Thus

$$E_\delta = \frac{r}{q}\left(1 - \frac{x_\delta}{K}\right). \tag{4.12}$$

The corresponding harvest level is

$$h_\delta = qE_\delta x_\delta. \tag{4.13}$$

The optimal sustainable net revenue is given by

$$\pi = ph_\delta - cE_\delta. \tag{4.14}$$

Therefore, the discounted present value of the future net revenues is

$$\begin{aligned} Z(E_\delta) &= \int_0^\infty e^{-\delta t}\pi\, dt \\ &= \frac{1}{\delta}\pi \qquad (\delta \neq 0). \end{aligned} \tag{4.15}$$

Hence, the optimal fishing effort is

$$E_\delta = \begin{cases} 0 & \text{if} \quad \lambda > p - \dfrac{c}{qx}, \\ \dfrac{r}{q}\left(1 - \dfrac{x_\delta}{K}\right) & \text{if} \quad \lambda = p - \dfrac{c}{qx}, \\ E_{max} & \text{if} \quad \lambda < p - \dfrac{c}{qx}. \end{cases} \tag{4.16}$$

This implies that the optimal control comprises both the extreme controls and the singular control. The extreme controls indicate that the resource should be harvested (by exerting up to the maximum available effort rate) if and only if the net revenue per unit harvest (or the marginal net revenue of harvest) exceeds the current value shadow price of the resource (or the marginal net revenue of stock) (Dubey *et al.*, 2003; Kar & Chakraborty, 2009).

In addition, the harvested resource could follow the optimum sustainable yield (OSY) path (or singular path) if the current value shadow price exactly equals the net revenue per unit harvest. Thus the OSY parameters are E_δ, x_δ and h_δ.

Sometimes, the optimal control alternates between the singular and bang-bang controls known as a bang-singular control (also referred to as singular control); see Kar and Matsuda (2008) and Lenhart and Workman (2007).

Alternatively, from Equations (4.6) and (4.7), when $\psi(t) = 0$,

$$\lambda qx = pqx - c = \frac{\partial \pi}{\partial E}.$$

This implies, the product of the current value shadow price, catchability and stock size equals the fishermen's net revenue per unit of effort (or the marginal net revenue of effort) at the OSY level.

It is normal in optimal control problems to ensure the existence of the optimality system. In this vein, it should be noted that the state equation, which is logistic with harvesting is a priori bounded. Also, the state equation and the objective functional are both linear in the control E. Therefore, by standard arguments, an optimal control as well as the optimal state exists (Fleming & Rishel, 1995; Joshi, Lenhart, Hota & Agusto, 2015).

Table 3 features the results of harvesting at OSY levels. It shows that when the discount rate is zero the OSY levels are identical to the MEY levels of the model. As the discount rate increases, effort rate increases while the biomass and the net revenue decrease. However, the harvest increases up to a point (attaining its maximum where the biomass level is near x_{MSY}), then starts decreasing. When the discount rate approaches infinity, the levels of OSY mirror those of OAY. In order

to avoid this undesirable situation, a strong regulatory scheme must be strictly enforced to curb the excessive harvesting of the resource (Kar & Chakraborty, 2009).

Table 3: Annual Net Revenue at OSY Levels of Harvesting

δ	x_δ	E_δ	h_δ	Sustainable net revenue (\$ year^{-1})
0	590,278	323,225	343,427	143,027,325
0.05	578,170	332,777	346,323	142,902,285
0.10	566,293	342,146	348,759	142,536,930
0.15	554,654	351,328	350,758	141,945,840
0.20	543,261	360,317	352,343	141,143,985
0.25	532,119	369,106	353,535	140,145,330
0.50	480,392	409,913	354,454	132,739,365
0.75	435,645	445,214	349,119	122,654,670
0.95	404,926	469,447	342,165	113,756,835
∞	180,556	646,450	210,096	0

Note that the optimal sustainable population size, x_δ (represented by Equation (4.11)) contains x_{MSY}, x_{MEY} and x_{OAY} as special cases. That is, x_{MSY} is optimal under zero costs and zero discounting, x_{MEY} is optimal under zero discounting and x_{OAY} is optimal at infinite discounting. In other words, with zero future discounting, the optimal harvest strategy would be to maximise long-term economic benefits (or net revenue), which corresponds to MEY.

It can also be deduced that

$$x_\delta < x_{MEY} \quad \text{if } \delta > 0,$$

and also, as attested to by Table 3,

$$x_\delta \text{ is a decreasing function of } \delta.$$

Higher discount rates imply lower levels of conservation. In fact, as already ob-

served from the table,

$$\lim_{\delta \to \infty} x_\delta = x_{OAY}.$$

Scott (1955) was the first to argue that infinite discounting leads to the same outcome as OAY. In other words, under high discounting, future revenues count for very little, so present revenues are maximised, and this implies rapid harvesting down to x_{OAY}. As another way of looking at it, under open access competition, resource users must completely discount the future because they cannot expect positive returns in the long run (Clark, 2010). The sensitivity of x_δ to various economic parameters is listed in Table 4.

Table 4: Sensitivity of x_δ to Economic Parameters

Parameter	Sensitivity to x_δ
price, p	–
effort cost, c	+
discount rate, δ	–

From the table, it can be seen that the optimal population size, x_δ increases if the cost of fishing effort increases. On the other hand, x_δ decreases if the price per unit harvest, or the discount rate increases.

Numerical simulations

Since the MEY, MSY and OAY are the static equilibrium reference points, we next employ simulations to further explore the dynamic reference point, OSY. Therefore, the optimality system is implemented using an iterative method involving the Runge-Kutta Fourth order scheme. The modified code, originally developed by Lenhart and Workman (2007), is implemented in Matlab.

We present simulations results corresponding to OSY (which is optimal under dynamic conditions). First, we shall consider the transient (or short-run) case

where T is finite; and second, extend it to the equilibrium (or long-run) scenario where $T \to \infty$.

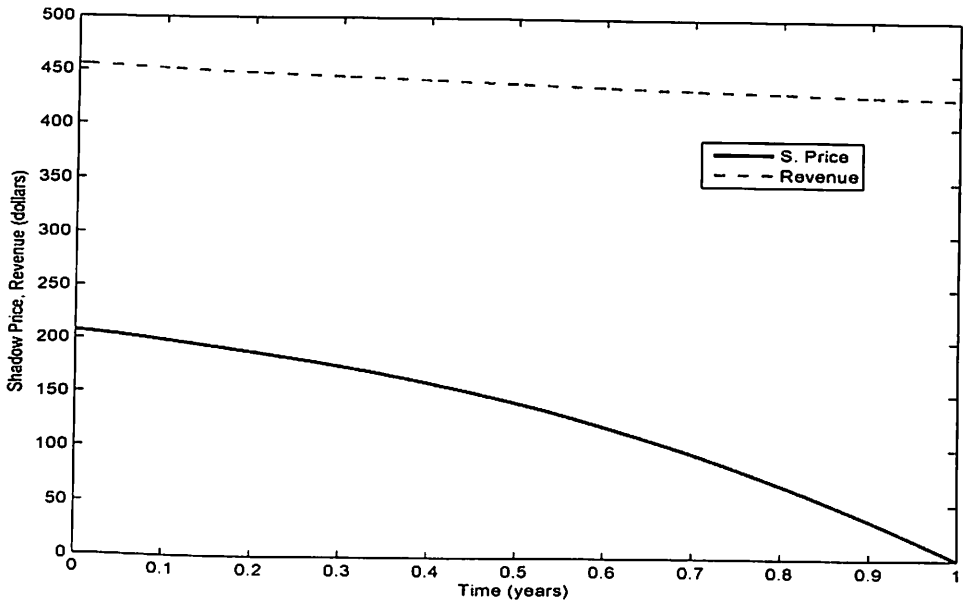

Figure 7: Shadow Price and Net Revenue for $E_{max} = 351,328$, $x_0 = 750,000$ and $T = 1$

Figure 7 depicts fishing at a maximum effort rate of 351,328 trips, $x_0 = 750,000$ tonnes and $T = 1$ year, where the shadow price appears to be decreasing and concave and the net revenue per unit harvest is monotonically decreasing. At the start of the harvesting period, the shadow price, US \$207.56 is significantly lower than the net revenue, US \$455.56. This signifies that the revenue due an additional tonne of fish being added to the biomass is less than the expected revenue from harvesting the fish. So at this instance it is prudent to fish close to the maximum rate of effort. As time progresses the shadow price experiences a gradual decline in value to zero while the net revenue also gradually decreases to US \$427.40. The shadow price is always lower than the net revenue for the one-year horizon. Thus the optimal strategy is bang-bang without switching; that is, fishing at a rate close to the maximum rate throughout the time horizon (see Figure 8).

Simulation results for the fishing effort and stock size relating to the case where $E_{max} = 351,328$ trips are presented in Figure 8. In Figure 8 (a), it is observed that when the maximum effort rate E_{max} is set at OSY level, the optimal

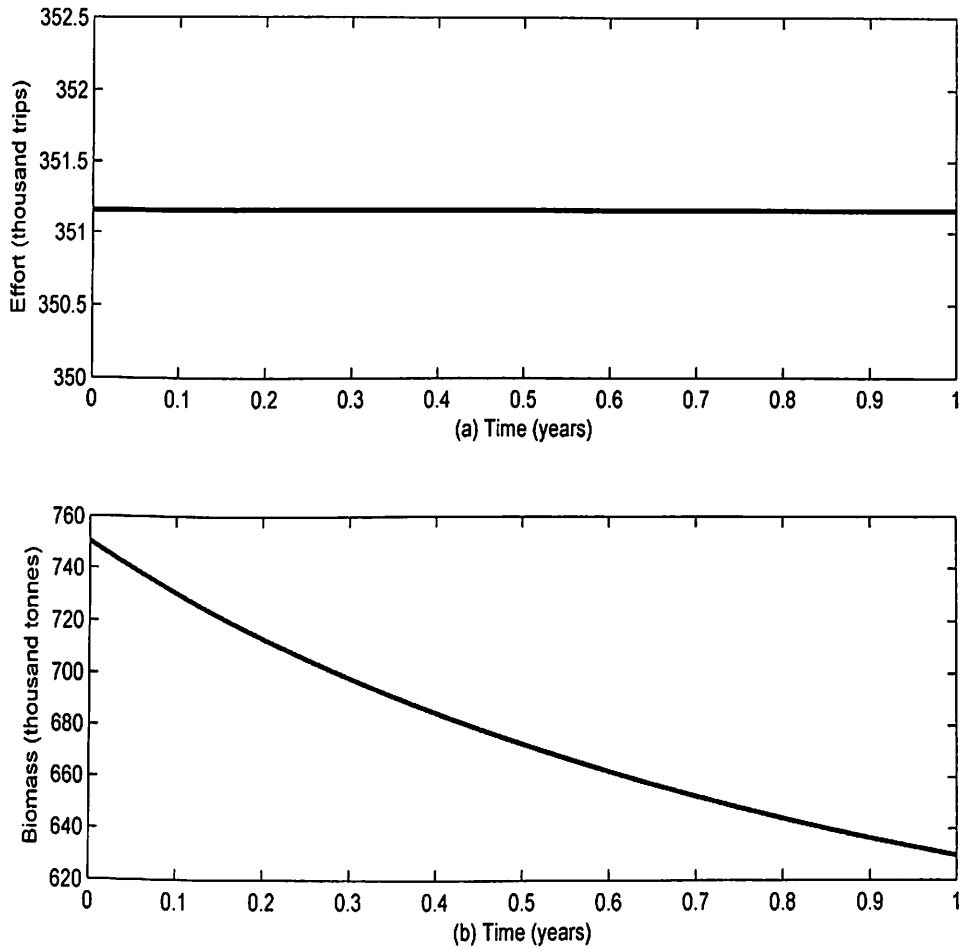

Figure 8: (a) Effort and (b) Biomass Levels for $E_{max} = 351,328$, $x_0 = 750,000$ and $T = 1$

effort rate follows a path of around $351,160$ trips for the one-year horizon, and the biomass level ends well above the x_δ level of $554,654$ tonnes; see Figure 8 (b).

Assuming an initial population size of $750,000$ tonnes, the performance criterion, which is the total net revenue over the time horizon (in this instance, one year) corresponding to the given rate of fishing effort is computed as US $\$175,870,000$.

Figure 9 depicts fishing at a maximum effort rate of $351,328$ trips (OSY effort rate), $x_0 = 750,00$ tonnes and $T = 20$ years, where the shadow price initially increases, appears to remain constant, then decreases; while the net revenue per unit harvest initially decreases up a point, then appears to remain constant. At the start of the harvesting period, the shadow price, US \$306.68 is significantly lower than the net revenue, US \$455.56. This signifies that the revenue due an additional

tonne of fish being added to the biomass is less than the expected revenue from harvesting the fish. So at this instance it is prudent to harvest. As time progresses the shadow price appears to stabilise and intersect with the net revenue for the majority of the time horizon. Thereafter, the shadow price experiences a sharp fall to a value of zero at the time horizon, $T = 20$ years; while the net revenue appears to remain constant, and finally ending at US \$404.76. The optimal control alternates between the singular and bang-bang controls. This shows that for a long-term time horizon (or under equilibrium conditions), it is optimal to exert the effort at the OSY level ($E_\delta = 351,328$ trips; see Figure 10).

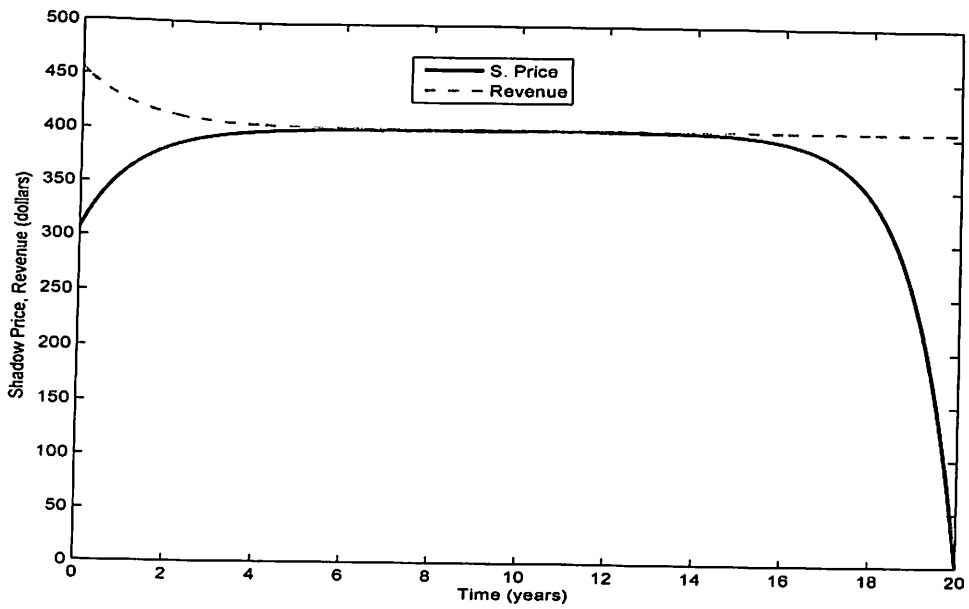

Figure 9: Shadow Price and Net Revenue for $E_{max} = 351,328$, $x_0 = 750,000$ and $T = 20$

In Figure 10, the simulation is set at twenty years to test for the equilibrium conditions. The optimal effort rate appears very close to the OSY level (Figure 10 (a)); and also, the biomass level approaches x_δ level of 554,654 tonnes as the time approaches infinity (Figure 10 (b)). For this particular fishery, it takes less than twenty years for the equilibrium status to be achieved, assuming that the initial fish stock size at the onset of the exploitation of the resource is at 75% of the carrying capacity.

The total net revenue over twenty years corresponding to the given initial pop-

ulation size and rate of fishing effort has a value of US$967,990,000. It is worth noting that, if $E_{max} > E_{\delta}$, the iterates of the simulation process fail to converge as $T \rightarrow \infty$. In other words, the model does not attain dynamic equilibrium status for rates of fishing effort exceeding the effort rate corresponding to OSY. This validates the assertion that OSY is optimal under dynamic conditions.

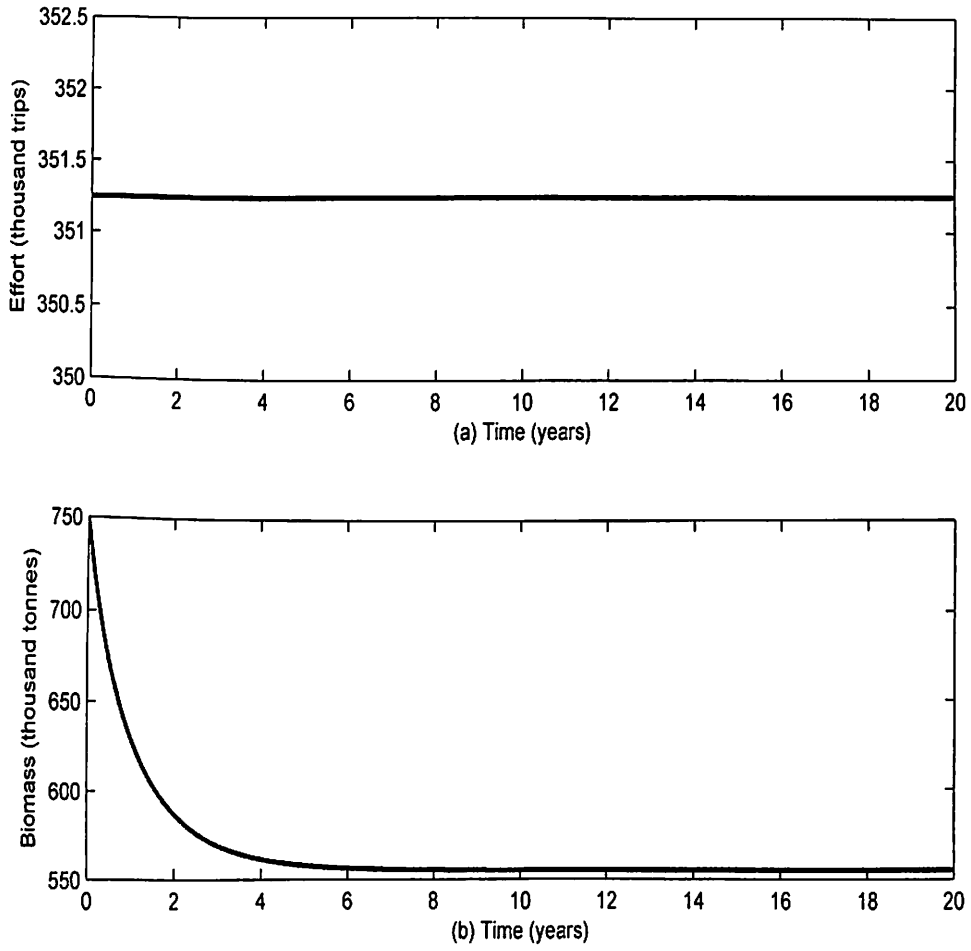

Figure 10: (a) Effort and (b) Biomass Levels for $E_{max} = 351,328$, $x_0 = 750,000$ and $T = 20$

We next turn our attention to the situation where the assumption is that the fishery has been fished down to the MSY levels (which is not far-fetched, given the current low yields of sardinella). Thus, simulations are carried out with an initial fish stock size of 550,000 tonnes (close to x_{MSY}).

Simulation results for the fishing effort and stock size relating to the case where $E_{max} = 351,328$ trips, $x_0 = 550,000$ and $T = 1$ year are presented in Figure 11. In Figure 11 (a), it is observed that when the maximum effort rate E_{max} is

set at OSY level, the optimal effort rate follows a path of around 351,160 trips for the one-year horizon, and the biomass level increases from the given initial value to about 552,550 tonnes; see Figure 11 (b).

Assuming an initial population size of 550,000 tonnes, the total net revenue over the one-year horizon corresponding to the given rate of fishing effort is computed as US$130,650,000.

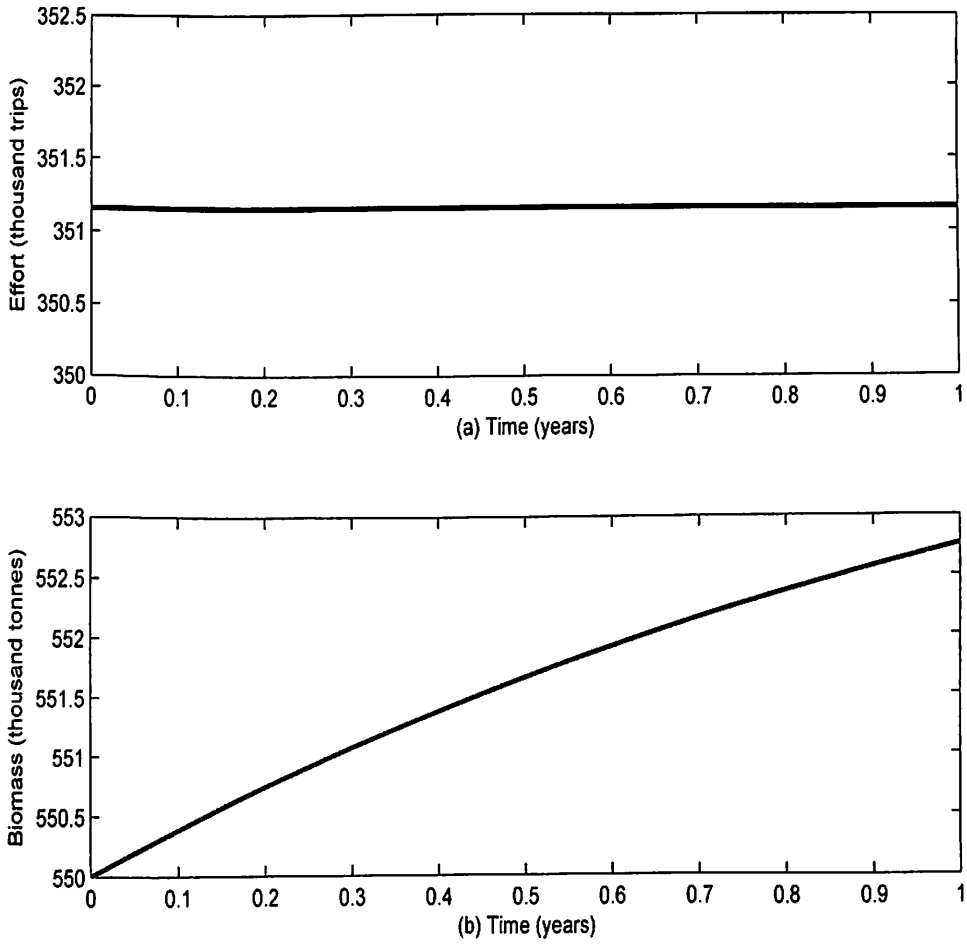

Figure 11: (a) Effort and (b) Biomass Levels for $E_{max} = 351,328$, $x_0 = 550,000$ and $T = 1$

Figure 12 depicts fishing at a maximum effort rate of 351,328 trips, $x_0 = 550,000$ tonnes and $T = 5$ years, where the shadow price appears concave and decreasing, while the net revenue monotonically increases. At the start of the harvesting period, the shadow price, US $402.51 is marginally lower than the net revenue, US $403.03. This signifies that the revenue due an additional tonne of fish being added to the biomass is marginally less than the expected revenue

from harvesting the fish. So at this instance it is prudent to harvest, but not at the maximum effort rate. As time progresses the shadow price decreases to a value of zero at the time horizon, $T = 5$ years, while the net revenue appears to marginally increase to US \$404.70. This shows that for the initial time when the shadow price and the net revenue appeared identical, it was not optimal to exert the maximum effort rate. However, within the short-term time horizon of $T = 5$ years, the difference between them became significant and it was therefore optimal to immediately switch to exerting the maximum effort rate available (see Figure 13).

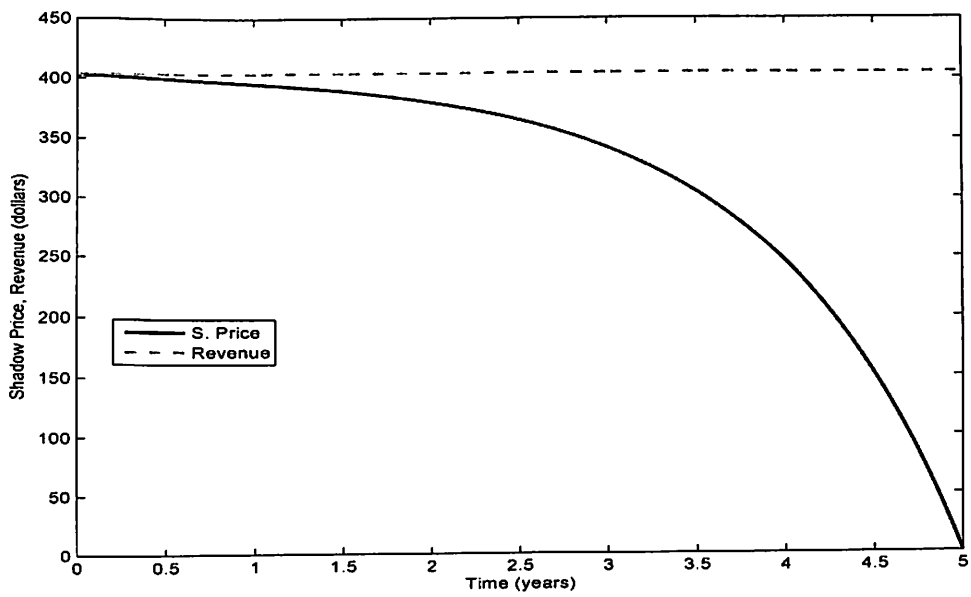

Figure 12: Shadow Price and Net Revenue for $E_{max} = 351,328$, $x_0 = 550,000$ and $T = 5$

The case when the time horizon is five years and $x_0 = 550,000$ is shown in Figure 13. In Figure 13 (a), it is observed that when the maximum effort rate $E_{max} = 351,328$, the optimal effort rate initially starts at around 327,990 trips and soon switches to the maximum effort rate of 351,328 trips (making the upper constraint on effort to be binding) for the majority of the five-year period. Similarly, the biomass level initially starts at 550,000 tonnes and then soon experiences a very sharp increase to around 551,500 tonnes; thereafter, increasing gradually to a maximum level of about 554,550 tonnes; see Figure 13 (b).

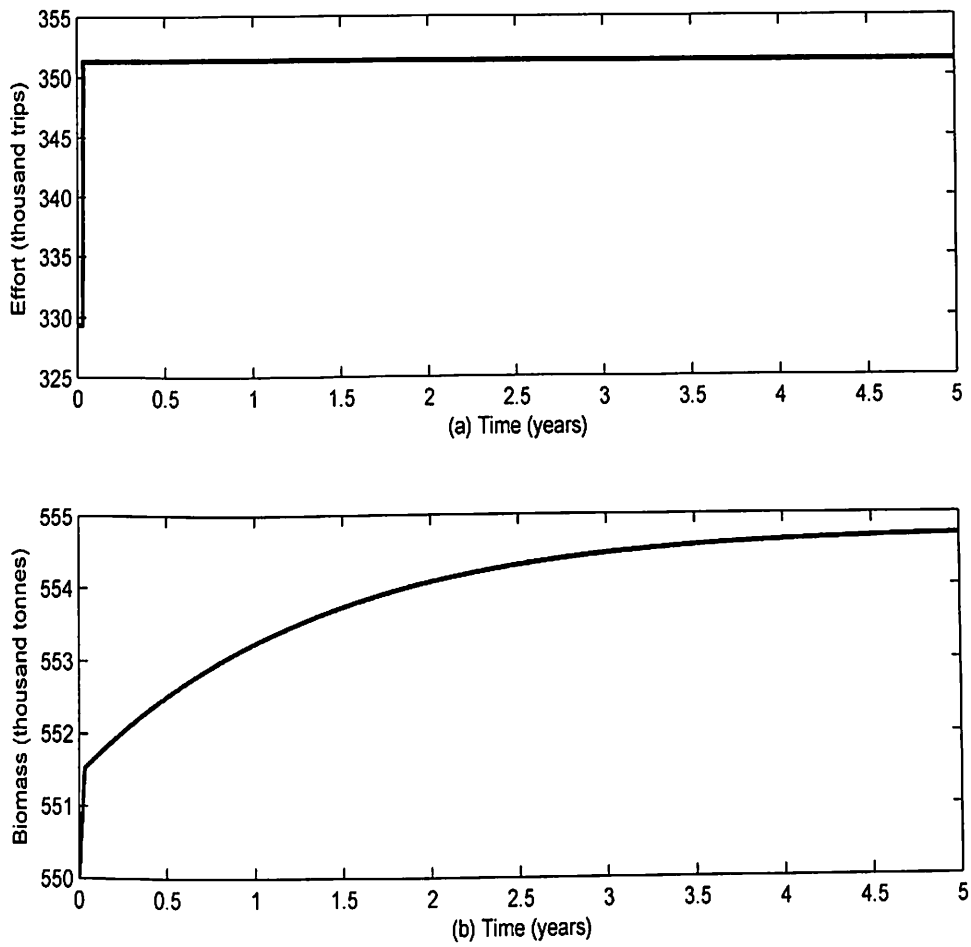

Figure 13: (a) Effort and (b) Biomass Levels for $E_{max} = 351,328$, $x_0 = 550,000$ and $T = 5$

For an initial population size of 550,000 tonnes, the total net revenue over five years corresponding to the given rate of fishing effort has a value of US \$497,760,000.

There was the observation that, for the given initial population size and effort rate, the model does not go beyond a time horizon of five years. That is, when $x_0 = 550,000$ ($x_0 < x_\delta$) and $E_{max} = 351,328$ (with $\delta = 0.15$), the iterates failed to converge beyond five years. However, to achieve sustainability at $x_0 = 550,000$, the maximum fishing effort, E_{max} must be set at 175,664; that is, 50% of $E_\delta = 351,328$ (see Figure 14).

For an initial population size of 550,000 tonnes, the total net revenue for a period of 20 years (corresponding to the rate of fishing effort set at 175,664 trips) has a value of US\$676,930,000, which is equivalent to a 30% reduction in the

net revenue for $x_0 = 750,000$ and $E_{max} = 351,328$ for the same time horizon. Thus, any decrease in fishing effort—cutting down on the number of canoes or reducing the number of days fished—leads to loss of jobs in the artisanal sector; or a decrease in income to the individual fishers, assuming the same number of fishers in employment remained constant.

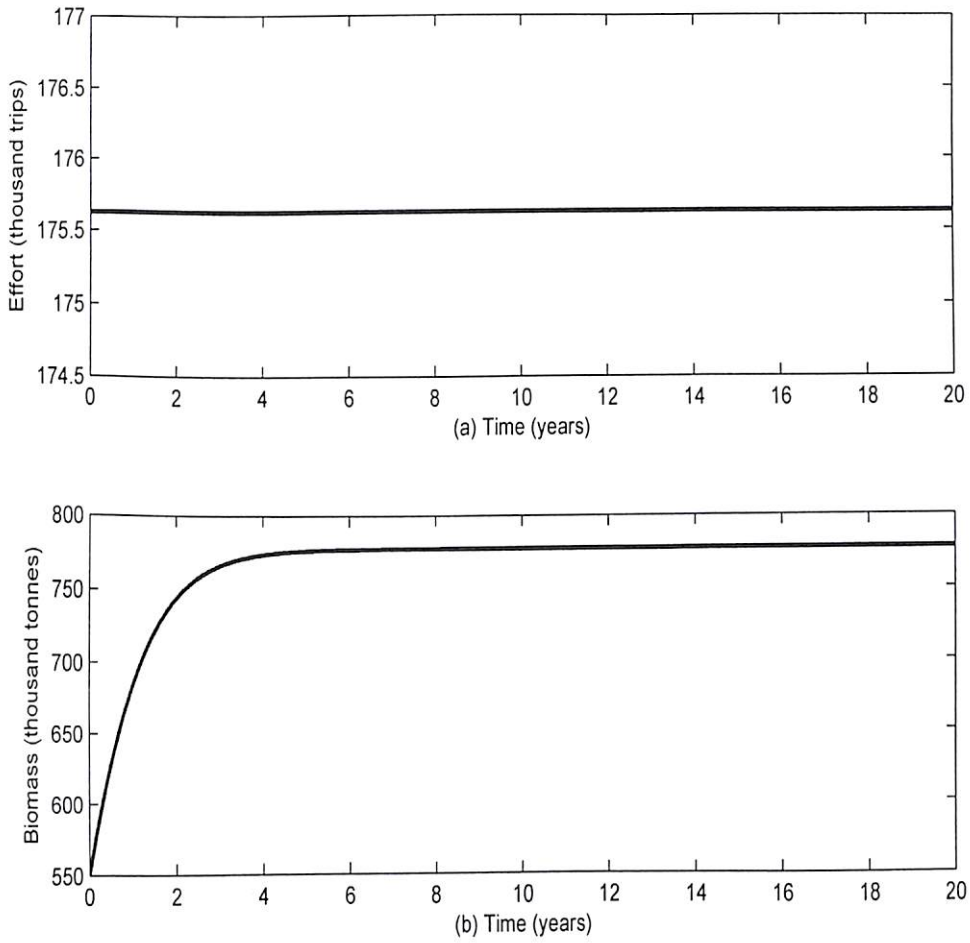

Figure 14: (a) Effort and (b) Biomass Levels for $E_{max} = 175,664$, $x_0 = 550,000$ and $T = 20$

It is instructive to note that the total net revenue is sensitive to the initial population size. For instance, for an initial population size of 750,000 tonnes and a discount rate of 15%, the total net revenue for a year is US$175,870,000, which is greater than the annual sustainable net revenue (under equilibrium conditions, where $x_0 = x_\delta = 554,654$ is assumed) of US$141,945,981 (see Table 3). Also, for an initial population size of 550,000 tonnes, the total net revenue for a year is US$130,650,000, which is less than the annual sustainable net revenue under

SAM JONAH LIBRARY
UNIVERSITY OF CAPE COAST

equilibrium conditions.

Figure 15 depicts fishing at a maximum effort rate of 800,000 trips, $x_0 =$ 200,00 tonnes and $T = 1$ year, where the shadow price appears to be decreasing and the net revenue per unit harvest initially increases up a point, then decreases. At the start of the harvesting period, the shadow price, US \$392.56 is significantly higher than the net revenue, US \$58.33. This signifies that the revenue due an additional tonne of fish being added to the biomass is greater than the expected revenue from harvesting the fish. So at this instance it is prudent not to harvest. As time progresses the shadow price experiences a gradual decline in value while the net revenue sharply increases until the two intersect at US \$297.46 with switching time $t^* = 0.56$ year. Thereafter, the shadow prices experiences a sharp fall to a value of zero at the time horizon, $T = 1$ year, while the net revenue gradually declines to US \$227.65 . Thus, after 6.7 months (the switching time) it is now optimal to harvest the fish stocks as the net revenue would be greater than the shadow price.

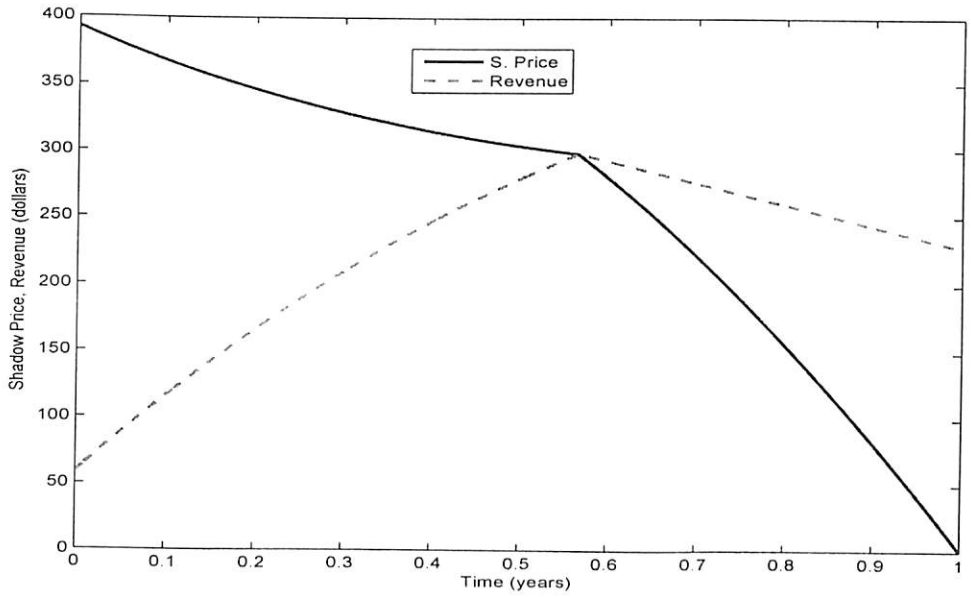

Figure 15: Shadow Price and Net Revenue for $E_{max} = 800,000$, $x_0 = 200,000$ and $T = 1$

Simulation results for the fishing effort strategy and biomass level relating to the case where $E_{max} = 800,000$ trips, $x_0 = 200,000$ tonnes and $T = 1$ year

are presented in Figure 16. In Figure 16 (a), it is observed that the switching time occurs at $t^* = 0.56$ year (see Figure 15) indicating that for the initial 6.7 months of the year, no fishing effort should be applied (or harvesting occurring). Thereafter, the maximum rate of fishing effort should be applied. A significant change in the growth of fish stocks can be observed once the maximum rate of fishing effort is exerted (Figure 16 (b)). The biomass level ends at around 290,000 tonnes. Thus the optimal effort strategy recommends the bang-bang approach.

Assuming an initial population size of one-fifth the carrying capacity, 200,000 tonnes, the total net revenue over the one-year horizon corresponding to a high rate of fishing effort of more than twice the MSY level (800,000 trips) is computed as US $623,710,000.

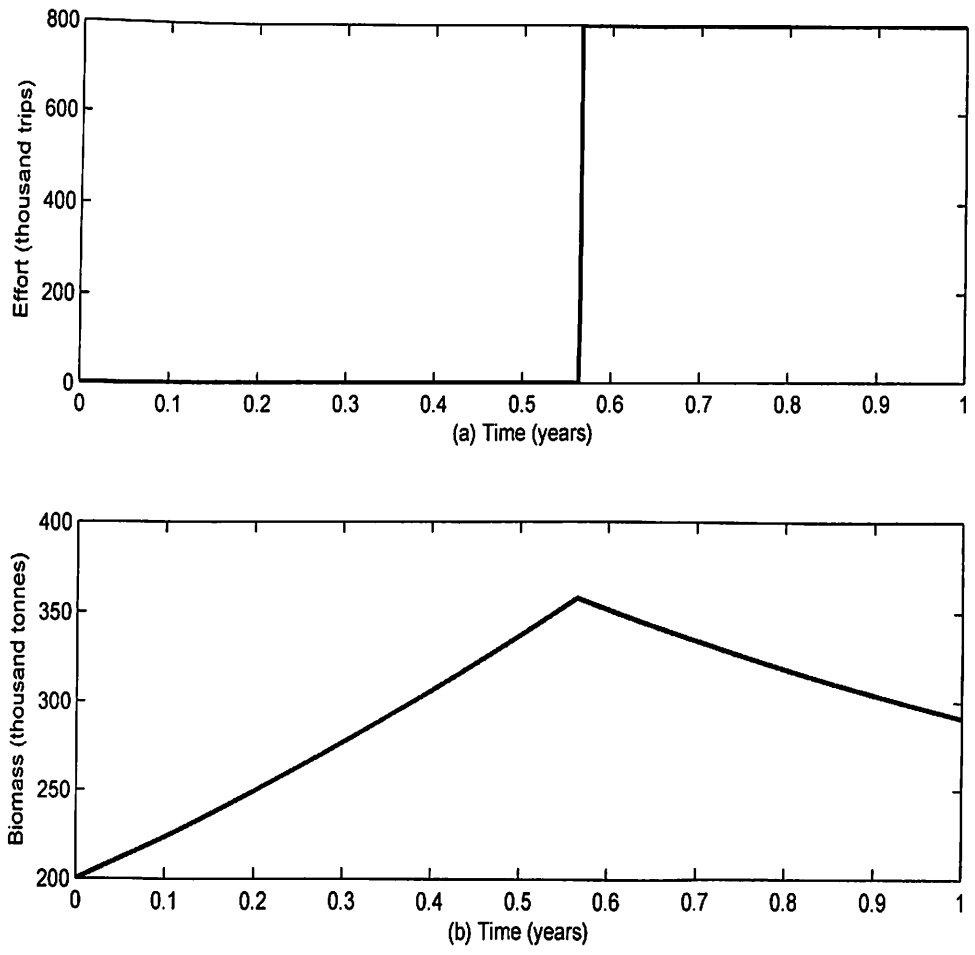

Figure 16: (a) Effort and (b) Biomass Levels for $E_{max} = 800,000$, $x_0 = 200,000$ and $T = 1$

This extreme scenario vividly depicts the current sardinella fishery situation

in Ghana. The fishery is open access (very high effort rates) and the present low yields presume a low level of stock size (biomass depleted beyond MSY levels). The model strongly recommends that in a crisis situation, as the sardinella fishery in Ghana evidently is, closed fishing seasons must be implemented. At least six months of no fishing activity every year would go a long way to restoring the fish stocks to appreciable levels.

Model summary

This section looked into the fishing effort strategies of the sardinella fishery under the canonical Gordon-Schaefer model in order to determine the optimal strategy. The appropriate biological model was formulated and subjected to bifurcation analysis. The results show that the rate of fishing effort corresponding to levels of MSY and MEY has a positive impact on fish stocks as compared to the OAY level. Characterisation of the optimal effort rate of fishing gives room for both the bang-bang and singular controls. However, in almost all the simulations carried out, the optimal strategy recommended is the bang-bang (without switching) approach, or switching between the bang-bang and singular controls. That is, the optimal fishing effort is very close to E_{max}, thereby making the constraints on effort to be nearly binding. It is also observed that it is biologically feasible and economically beneficial to harvest at positive levels, therefore the optimal effort never falls to zero (except for the extreme scenario).

From the simulation results, the recommended rate of fishing effort is at the OSY level, with an initial fish stock size of at least $x^* = 554,654$ tonnes. As clearly portrayed in the simulations, with discounting, if the initial stock size is below the OSY level, then there must be a reduction of effort in order to attain sustainability. This can only be achieved if the fisheries managers impose and enforce tough regulations to sanitise the fishing industry. As a starting point, a limit must be imposed on the number of fishing vessels exploiting the fisheries at any given time; or alternatively, cutting down on the number of fishing days in a year (closed seasons). Experts in fisheries are of the opinion that closed fishing

seasons are easier to implement and monitor than cutting down on the number of fishing vessels. That is, in a closed fishing season, any fishing boat operating is violating the law and can be easily identified and sanctioned.

The upper bound on the number of trips in any given year (or fishing days) must be at the level of E_{OSY} in order to ensure the sustainability of the resource.

Optimal Yield Model

We present a model that seeks the optimal effort strategy in order to attain the maximum harvest (or yield). The model is given as

$$\begin{aligned} \max_E Z(E) &= \int_0^\infty qEx\,dt \\ \text{subject to} \quad \frac{dx}{dt} &= rx\left(1-\frac{x}{K}\right) - qEx \\ x(0) &= x_0 \\ 0 \le E &\le E_{max}\,. \end{aligned} \tag{4.17}$$

Optimality of the model

The characterisation of the optimal control is sought for in this section. In this regard, the model will be analysed for the determination of a singular path and/or the boundary solutions. This is to enable us establish the conditions necessary for optimality by the use of Pontryagin's maximum principle. The Hamiltonian for the optimal control problem (4.17) can be expressed as

$$H = qEx + \lambda\left[rx\left(1-\frac{x}{K}\right) - qEx\right]. \tag{4.18}$$

The adjoint variable λ is governed by

$$\begin{aligned} \lambda' &= -\frac{\partial H}{\partial x} \\ &= -qE - \lambda\left(r - \frac{2rx}{K} - qE\right). \end{aligned} \tag{4.19}$$

The switching function is defined by

$$\begin{aligned}\psi(t) &= \frac{\partial H}{\partial E} \\ &= qx(1-\lambda)\,. \end{aligned} \tag{4.20}$$

The characterisation of the optimal control is

$$\begin{cases} E_\delta = 0 & \text{if} \quad \psi(t) < 0\,, \\ 0 < E_\delta < E_{max} & \text{if} \quad \psi(t) = 0\,, \\ E_\delta = E_{max}, & \text{if} \quad \psi(t) > 0\,. \end{cases} \tag{4.21}$$

Singularity analysis of the model

This is to enable us determine whether the optimal control would be bang-bang or follow a singular path. For a singular control, we assume that there is an interval I for all $t \in I \subset [0,\infty)$ such that

$$\psi(t) = 0\,. \tag{4.22}$$

Thus, from Equations (4.20) and (4.22),

$$qx(1-\lambda) = 0\,. \tag{4.23}$$

So, solving for λ we find

$$\lambda = 1\,. \tag{4.24}$$

Differentiating Equation (4.24) with respect to t, it follows that

$$\lambda' = 0\,. \tag{4.25}$$

By plugging the λ expression in Equation (4.24) into the adjoint equation (4.19), we get

$$\lambda' = \frac{2rx}{K} - r\,. \tag{4.26}$$

Setting the expressions in Equations (4.25) and (4.26) equal to each other and simplifying, we obtain the optimal biomass level as

$$x_\delta = \frac{K}{2}\,. \tag{4.27}$$

The effort level corresponding to x_δ is found from the state equation in Model (4.17), after noting that $x' = 0$, since x_δ is a constant. Thus

$$E_\delta = \frac{r}{2q}. \tag{4.28}$$

The corresponding harvest level is

$$h_\delta = \frac{rK}{4}. \tag{4.29}$$

Hence, the optimal fishing effort is

$$E_\delta = \begin{cases} 0 & \text{if} \quad \lambda > 1, \\ \dfrac{r}{2q} & \text{if} \quad \lambda = 1, \\ E_{max} & \text{if} \quad \lambda < 1. \end{cases} \tag{4.30}$$

This implies that the optimal control comprises both the extreme controls and the singular control. The marginal yield, λ may be viewed as the additional yield associated with an increase in stock size of one tonne. Thus, the extreme controls indicate that the resource should be harvested (by exerting an effort rate up to the available maximum) if and only if the marginal yield is less than one tonne.

In addition, the harvested resource could follow the OSY path (or singular path) if the marginal yield exactly equals a tonne. Thus the OSY parameters are E_δ, x_δ and h_δ, which are exactly the same parameters at the MSY level.

Numerical simulations

We present simulations results corresponding to OSY. Recall that at this equilibrium point the model is optimal under dynamic conditions. Simulation results for the fishing effort and fish stock size relating to the case where $E_{max} = 394,444$ trips and $T = 1$ year are presented in Figure 17. In Figure 17 (a), it is observed that when the maximum effort rate E_{max} is set at the MSY level, the optimal effort rate follows a path of around $394,250$ trips for the one-year horizon , and the biomass level ends well above the x_{MSY} level, to a value of around $600,000$ tonnes; see Figure 17 (b).

Assuming an initial population size of 750.000 tonnes, the total yield (the performance criterion) over the one-year horizon corresponding to the given rate of fishing effort is computed as 468, 129 tonnes.

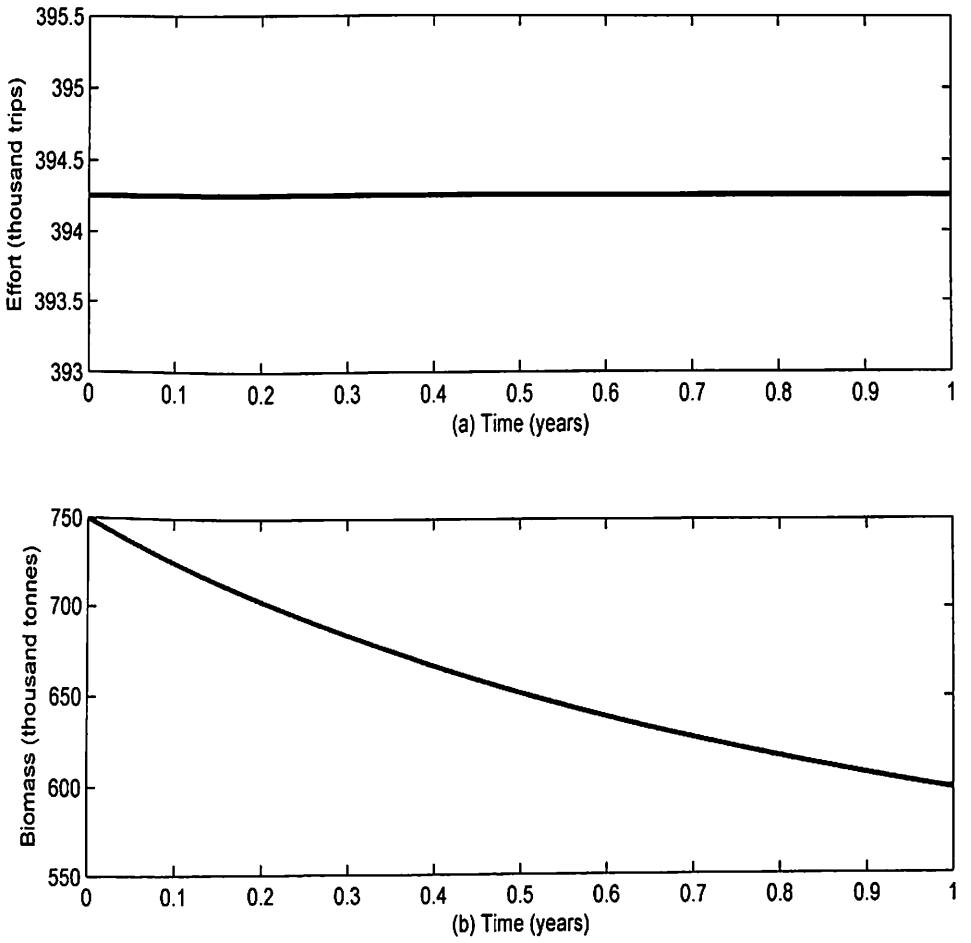

Figure 17: (a) Effort and (b) Biomass Levels for $E_{max} = 394,444$, $x_0 = 750,000$ and $T = 1$

Simulation results for the fishing effort and stock size relating to the case where $E_{max} = 394,444$ trips and $T = 20$ years are presented in Figure 18. In Figure 18 (a), it is observed that when the maximum effort rate E_{max} is set at the MSY level, the optimal effort rate follows almost the maximum trajectory of around 394,444 trips (implying $E_\delta = E_{MSY}$ is optimal under equilibrium conditions) throughout the twenty-year horizon, and the biomass level ends at the x_{MSY} level of 500.000 tonnes (Figure 18 (b)). For an initial population size of 750,000 tonnes, the total yield over the twenty-year horizon corresponding to the given rate of fishing effort is computed as 7,304,200 tonnes.

Assuming an initial population size of 750.000 tonnes, the total yield (the performance criterion) over the one-year horizon corresponding to the given rate of fishing effort is computed as 468, 129 tonnes.

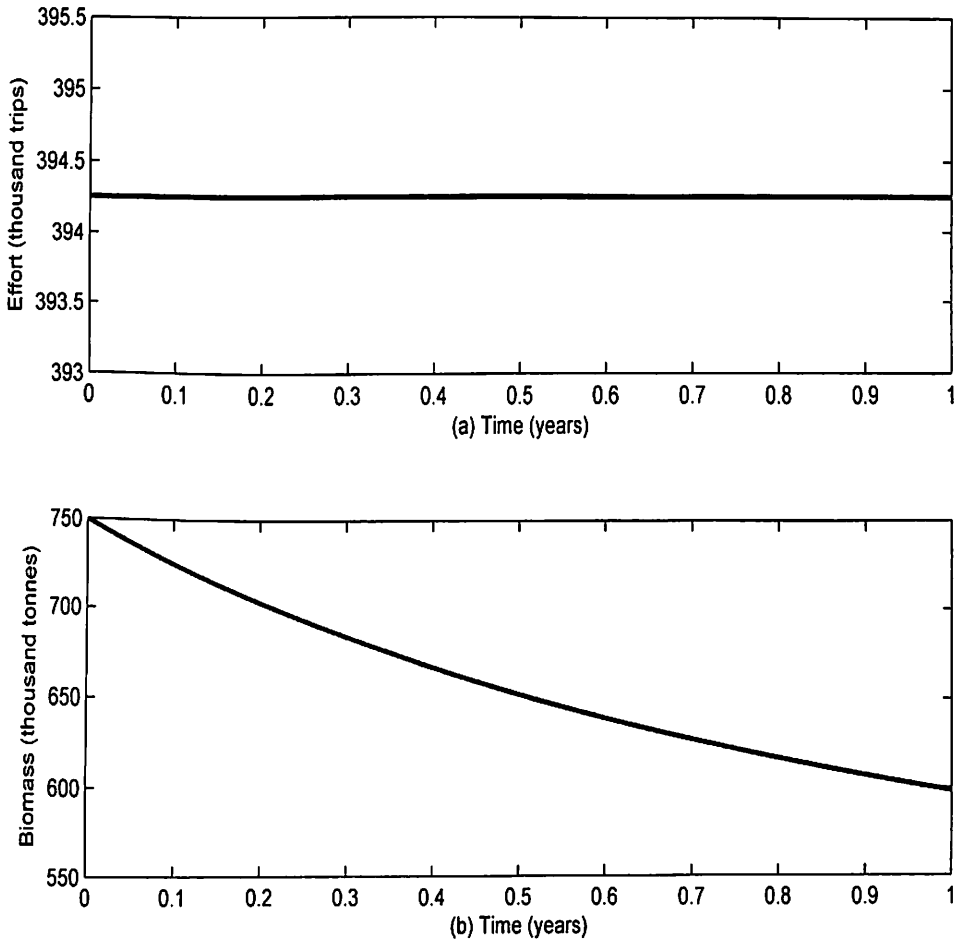

Figure 17: (a) Effort and (b) Biomass Levels for $E_{max} = 394,444$, $x_0 = 750,000$ and $T = 1$

Simulation results for the fishing effort and stock size relating to the case where $E_{max} = 394,444$ trips and $T = 20$ years are presented in Figure 18. In Figure 18 (a), it is observed that when the maximum effort rate E_{max} is set at the MSY level, the optimal effort rate follows almost the maximum trajectory of around 394,444 trips (implying $E_\delta = E_{MSY}$ is optimal under equilibrium conditions) throughout the twenty-year horizon, and the biomass level ends at the x_{MSY} level of 500.000 tonnes (Figure 18 (b)). For an initial population size of 750,000 tonnes, the total yield over the twenty-year horizon corresponding to the given rate of fishing effort is computed as 7,304,200 tonnes.

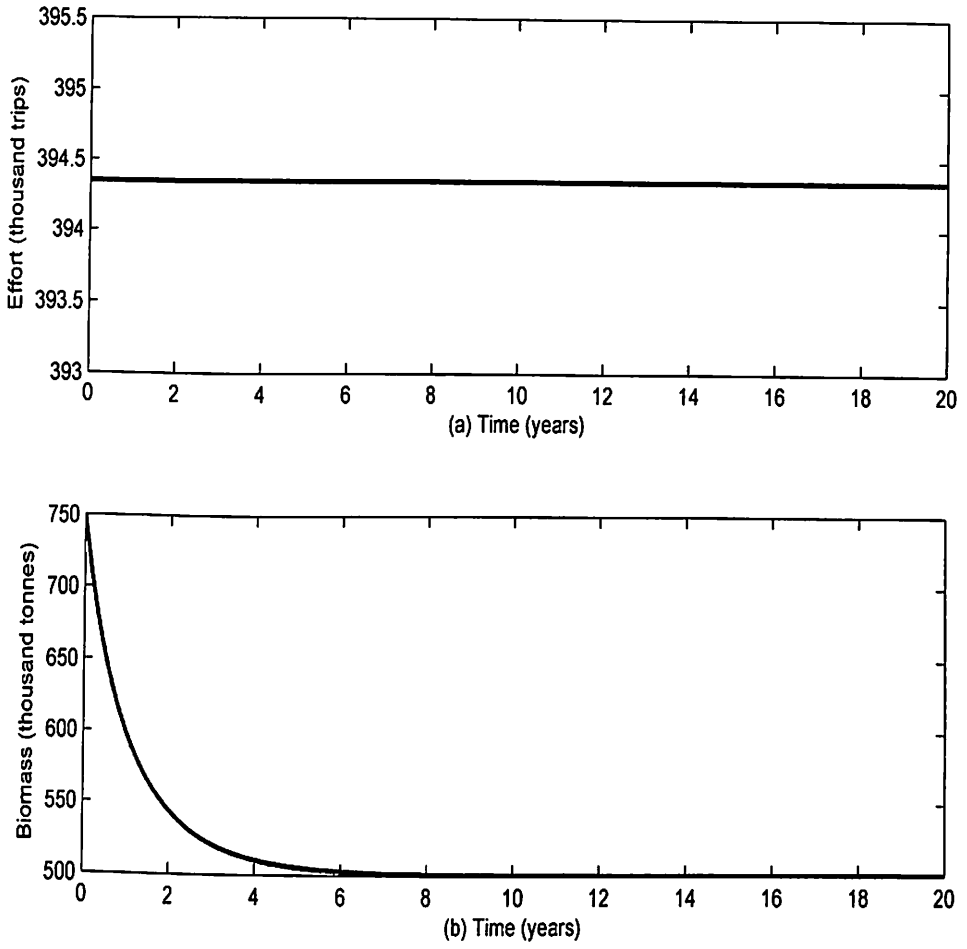

Figure 18: (a) Effort and (b) Biomass Levels for $E_{max} = 394,444$, $x_0 = 750,000$ and $T = 20$

Simulation results for the fishing effort and stock size relating to the case where $E_{max} = 394,444$ trips, $T = 1$ year, $x_0 = 550,000$ tonnes and $x_0 = 750,000$ tonnes are presented in Figure 19. In Figure 19 (a), it is observed that when the maximum effort rate E_{max} is set at the MSY level, the optimal effort rate appears to follow the same path of around 394,250 trips for the one-year horizon for the different initial biomass levels. However, the fish biomass levels follow different trajectories. The biomass decreases for the higher initial value to a value of around 600,000 tonnes, and decreases also for the lower initial value of 550,000 tonnes to a value of around 525,000 tonnes (Figure 19 (b)). For an initial stock size of 550,000 tonnes, the total yield over the one-year horizon corresponding to the given rate of fishing effort is computed as 379,710 tonnes. This represents a 19% reduction of the value at $x_0 = 750,000$ tonnes.

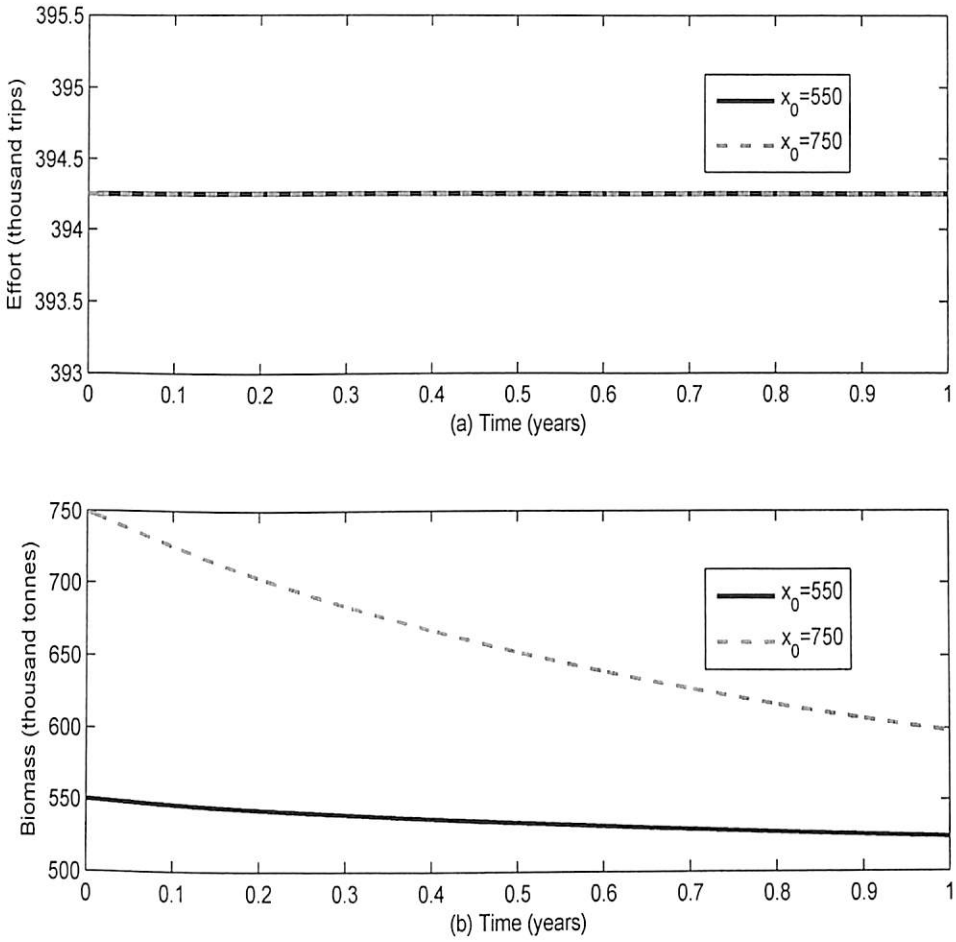

Figure 19: (a) Effort and (b) Biomass Levels for $E_{max} = 394,444$, $x_0 = 550,000$; $750,000$ and $T = 1$

Simulation results for the fishing effort and stock size relating to the case where $E_{max} = 394,444$ trips, $T = 20$ years, $x_0 = 550,000$ tonnes and $x_0 = 750,000$ tonnes are presented in Figure 20. In Figure 20 (a), it is observed that when the maximum effort rate E_{max} is set at the MSY level, the optimal effort rate appears to follow the same almost maximum trajectory of around $394,444$ trips throughout the twenty-year horizon for the different initial biomass levels. However, the fish biomass levels follow different trajectories. The biomass decreases for the higher initial value to a value of a around $500,000$ tonnes, and decreases also for the lower initial value of $550,000$ tonnes to around $500,000$ tonnes (Figure 20 (b)). For an initial stock size of $550,000$ tonnes, the total yield over the twenty-year horizon corresponding to the given rate of fishing effort is computed as $7,149,100$ tonnes. This is only a 2% reduction of the value at $x_0 = 750,000$ tonnes.

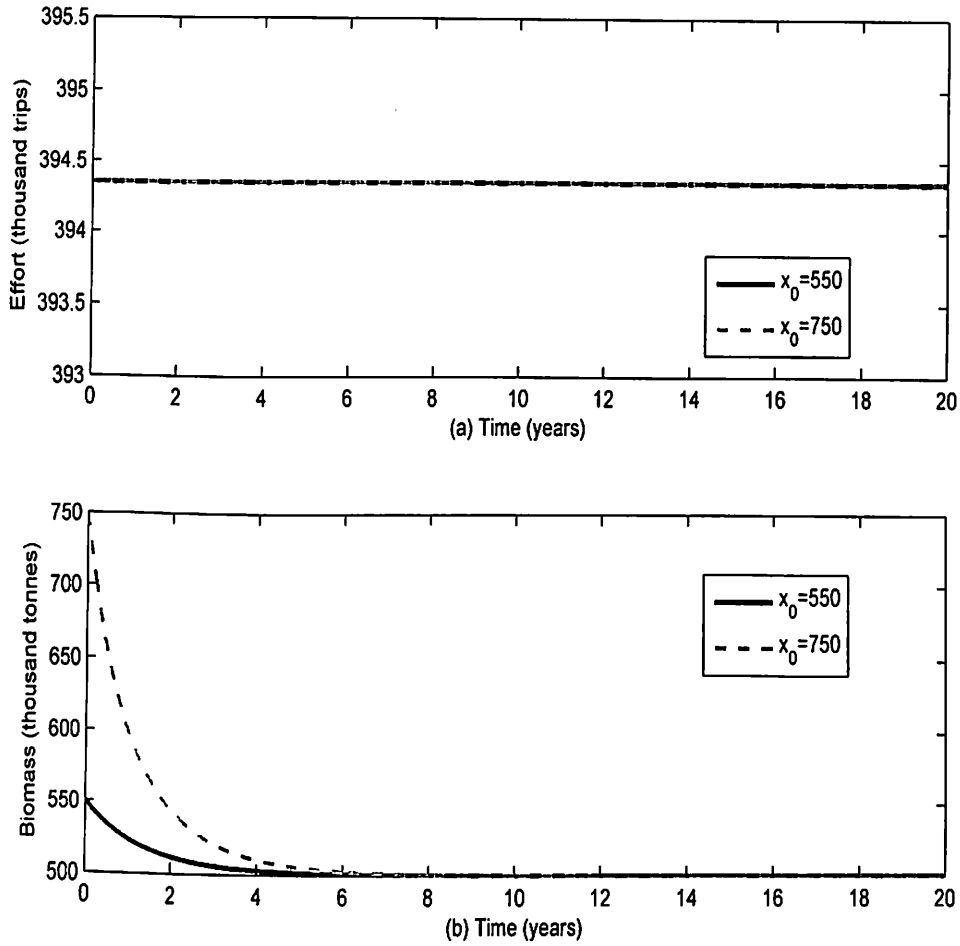

Figure 20: (a) Effort and (b) Biomass Levels for $E_{max} = 394,444$, $x_0 = 550,000$; $750,000$ and $T = 20$

Simulation results for the fishing effort and stock size relating to the case where $E_{max} = 500,000$ trips, $x_0 = 750,000$ tonnes and $T = 3.5$ years are presented in Figure 21. In Figure 21 (a), it is observed that when the maximum effort rate E_{max} is set at about 27% higher than the MSY level, the optimal effort rate follows a path of around $499,900$ trips throughout the three and half-year horizon, and the biomass level ends at a value of around $400,000$ tonnes (Figure 21 (b)).

Assuming an initial population size of $750,000$ tonnes, the total yield over the three and half-year horizon corresponding to the given rate of fishing effort is computed as $1.553,200$ tonnes. It is instructive to note that, when the fishing effort is set at $500,000$ trips and $x_0 = 750,000$ tonnes, the iterates failed to converge beyond three and half years.

Simulation results for the fishing effort and stock size relating to the case

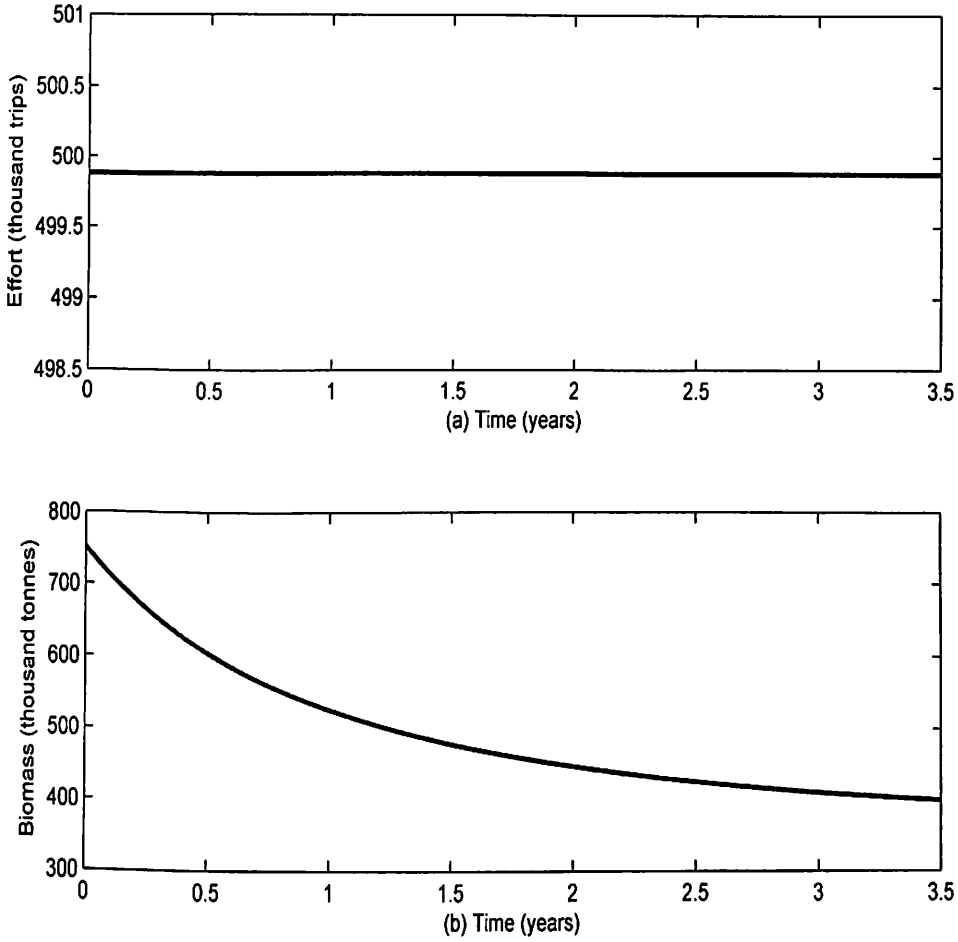

gure 21: (a) Effort and (b) Biomass Levels for $E_{max} = 500,000$, $x_0 = 750,000$ and $T = 3.5$

re $E_{max} = 500,000$ trips, $x_0 = 550,000$ tonnes and $T = 2.5$ years are pre-d in Figure 22. In Figure 22 (a), it is observed that when the maximum effort

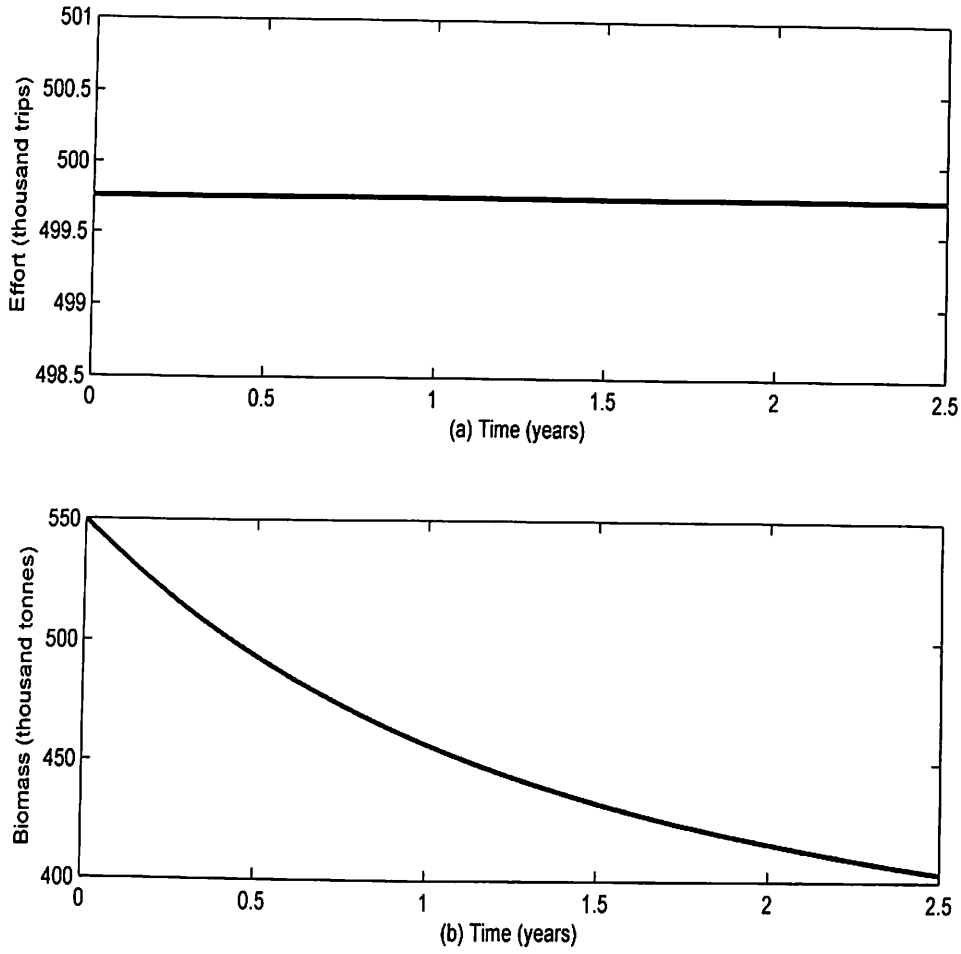

Figure 22: (a) Effort and (b) Biomass Levels for $E_{max} = 500,000$, $x_0 = 550,000$ and $T = 2.5$

200,000 tonnes and $T = 1$ year, where the marginal yield appears to be concave and the change in biomass, constant. At the start of the harvesting period, the marginal yield, 1.09 tonnes, is slightly higher than the biomass change of one tonne. This signifies that the additional tonne of fish stock being added to the biomass is less than the marginal yield. So at this instance it is prudent not to harvest. As time progresses the marginal yield experiences a sharp decline in value while the change in biomass stays constant until the two intersect at the switching time $t^* = 0.1$ year. Thereafter, the marginal yield continues to fall to a value of zero at the time horizon, $T = 1$ year. Thus, after 1.2 months (the switching time) it is now optimal to harvest the fish stock as the biomass change of a tonne would be greater than the marginal yield.

Simulation results for the fishing effort strategy and biomass level relating to

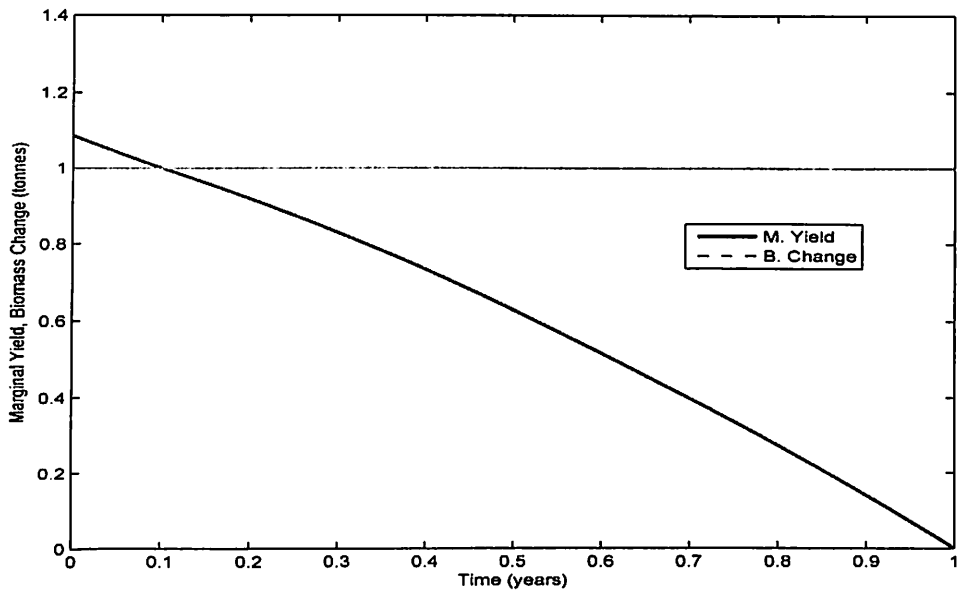

Figure 23: Marginal Yield and Biomass Change for $E_{max} = 800,000$ and $T = 1$

the case where $E_{max} = 800,000$ trips, $x_0 = 200,000$ tonnes and $T = 1$ year are presented in Figure 24. In Figure 24 (a) it is observed that the switching time occurs at $t^* = 0.1$ year (see Figure 23) indicating that for the initial 1.2 months of the year, no fishing effort should be applied (or harvesting occurring). Thereafter, the maximum rate of fishing effort should be applied. A significant change in the growth of fish stock can be observed once the maximum rate of fishing effort is exerted (Figure 24 (b)). The biomass level ends a little above 170,000 tonnes. Thus the optimal effort strategy recommends the bang-bang approach.

Assuming an initial population size of one-fifth the carrying capacity, 200,000 tonnes, the total yield over the one-year horizon corresponding to a high rate of fishing effort of more than twice the MSY level (800,000 trips) is computed as 252,851 tonnes.

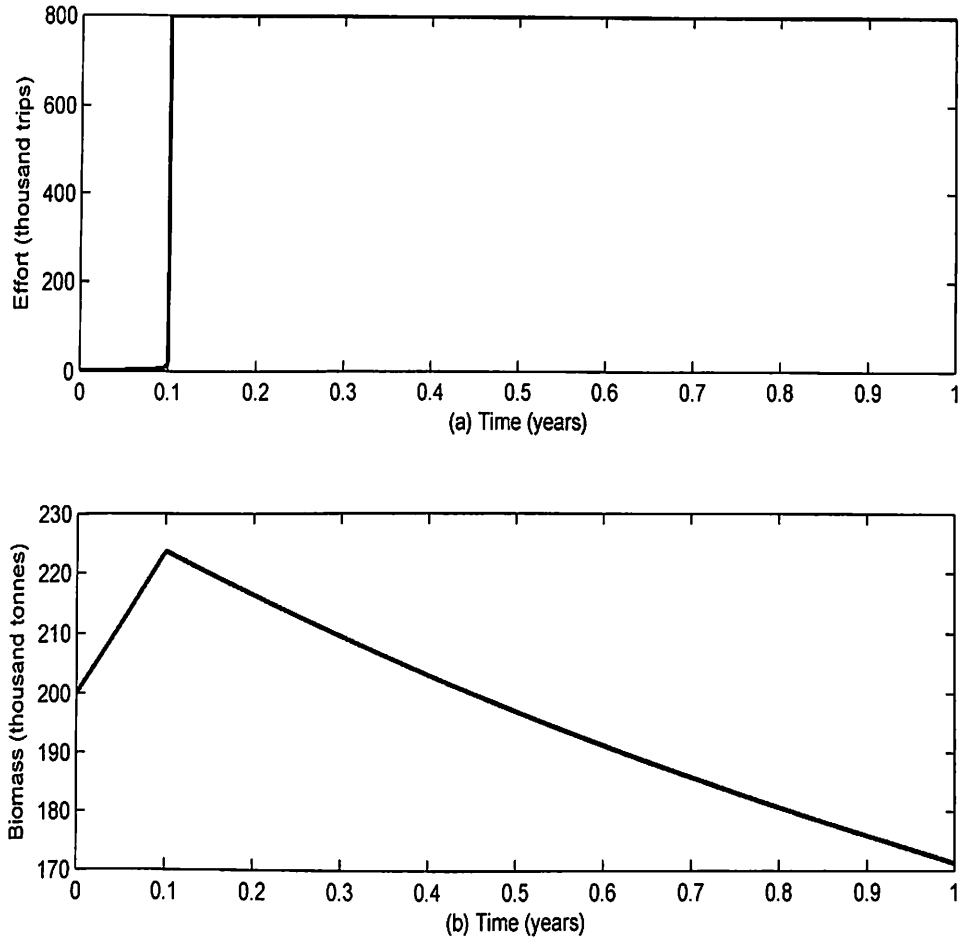

Figure 24: (a) Effort and (b) Biomass Levels for $E_{max} = 800,000$, $x_0 = 200,000$ and $T = 1$

Model summary

This section looked into the fishing effort strategies of the sardinella fishery under the optimal yield model in order to determine the optimal strategy. Characterisation of the optimal rate of fishing gives room for both the bang-bang and singular controls. The boundary controls indicate that the fish stocks should only be exploited if and only if the marginal yield is less than one tonne, and the singular path recommended the effort rate at the MSY level.

However, in almost all the simulations carried out, the optimal strategy recommended is along the boundary controls (bang-bang approach without switching). That is, the optimal fishing effort is mostly near E_{max}, thereby making the constraints on effort to be almost binding. It is also observed in one extreme scenario

that the bang-bang approach with switching was possible for the fishery. From most of the simulation results, the recommended level of rate of fishing effort is at the E_{max} level, with an initial fish stock size of at least 55% of the carrying capacity.

The Craven Model

We present a model originally developed by Craven (1995) to take into account the diminishing returns to revenue when there is a large amount of fish to sell. Ordinarily, a bumper harvest should be an occasion of merriment. However, in many developing countries, with Ghana not being an exception, fishermen do not benefit from large yields because of non-existent or inadequate storage facilities. Rather, the increased catches only serve to depress the ex-vessel price of the landed fish.

Thus the model proposed by Craven (1995) includes an additional revenue term in the objective functional, and is expressed as

$$\begin{aligned} \max_u Z(u) &= \int_0^\infty e^{-\delta t}(p_1 ux - p_2(ux)^2 - cu)\,dt \\ \text{subject to} \quad & \frac{dx}{dt} = rx\left(1 - \frac{x}{K}\right) - ux \\ & x(0) = x_0 \\ & 0 \le u \le u_{max}, \end{aligned} \tag{4.31}$$

where u is the level of harvesting, p_1 is the price of landed fish, p_2 represents the diminishing returns when there is a large quantity of fish to sell and c represents the cost per level of harvesting.

The biomass dynamics

There are two equilibrium points for the state equation in Model (4.31); namely, 0 and a positive equilibrium point

$$x^* = K\left(1 - \frac{u}{r}\right), \tag{4.32}$$

provided $u < r$. The equilibrium point x^* is hyperbolic, and therefore the system is structurally stable. Invoking Theorem 3.3, the model undergoes transcritical bifurcation at the point $u = r$. That is, there is a single nonhyperbolic equilibrium point, 0, which makes the system structurally unstable. In other words, for any initial population x_0, the resource will eventually go into extinction. When $u > r$, there is a single non-negative hyperbolic equilibrium point, 0. Of course, it is stable, and the system structurally stable. Thus, for any initial population level, the resource will die out in finite time.

To determine the MSY levels, we begin by substituting Equation (4.32) into the harvest equation $h = ux$, with $x = x^*$, giving the sustainable yield

$$h_S = uK\left(1 - \frac{u}{r}\right). \tag{4.33}$$

The level of harvesting that maximises the sustainable yield h_S is found as

$$u_{MSY} = \frac{r}{2}. \tag{4.34}$$

The value of MSY, denoted h_{MSY}, is found by plugging Equation (4.34), with $u = u_{MSY}$, into Equation (4.33). Hence,

$$h_{MSY} = \frac{rK}{4}, \tag{4.35}$$

and the biomass level at the MSY is

$$x_{MSY} = \frac{K}{2}. \tag{4.36}$$

Bifurcation analysis

Solution curves depicting the effects of the various levels of harvesting on the fish stock are presented and discussed. The curves corresponding to the situation where the harvest level, $u = u_{MSY} = 0.71$ per year are presented in Figure 25. It can be observed that there are two hyperbolic equilibrium points: 0 and $x^* = x_{MSY} = 500{,}000$ tonnes. For any initial biomass level, $x_0 > x_{MSY}$, the population approaches the equilibrium population, x_{MSY} in the long run. Similarly, for $0 <$

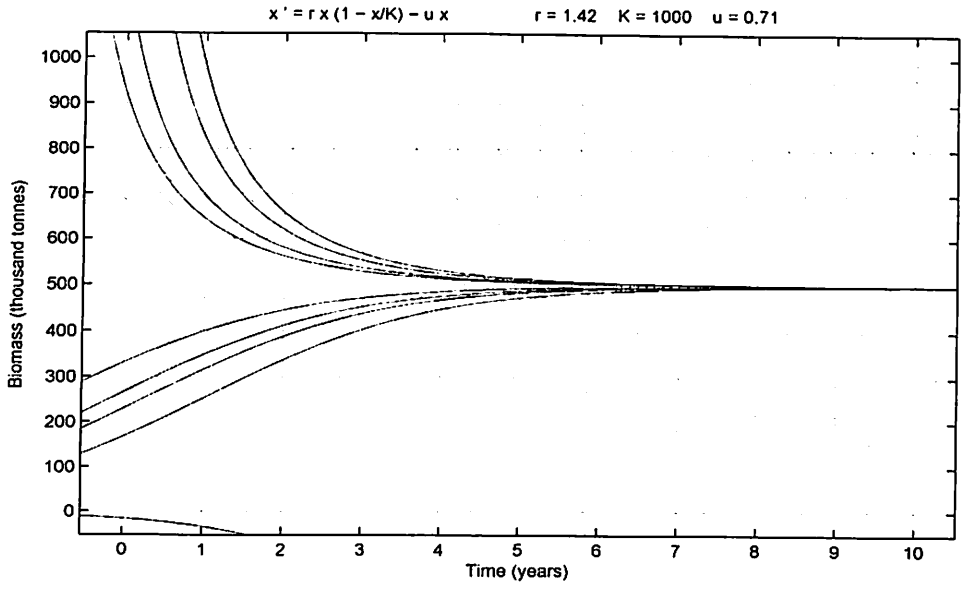

Figure 25: Solution Curves for $u = 0.71$

$x_0 < x_{MSY}$, the population asymptotically approaches x_{MSY}. Thus the biomass level 0 is unstable while x_{MSY} is stable (making the system structurally stable). Of course, biomass levels starting from the equilibrium levels, 0 and x_{MSY} remain there indefinitely. Hence, a harvest level corresponding to u_{MSY} induces a long-term biomass level of exactly half the carrying capacity.

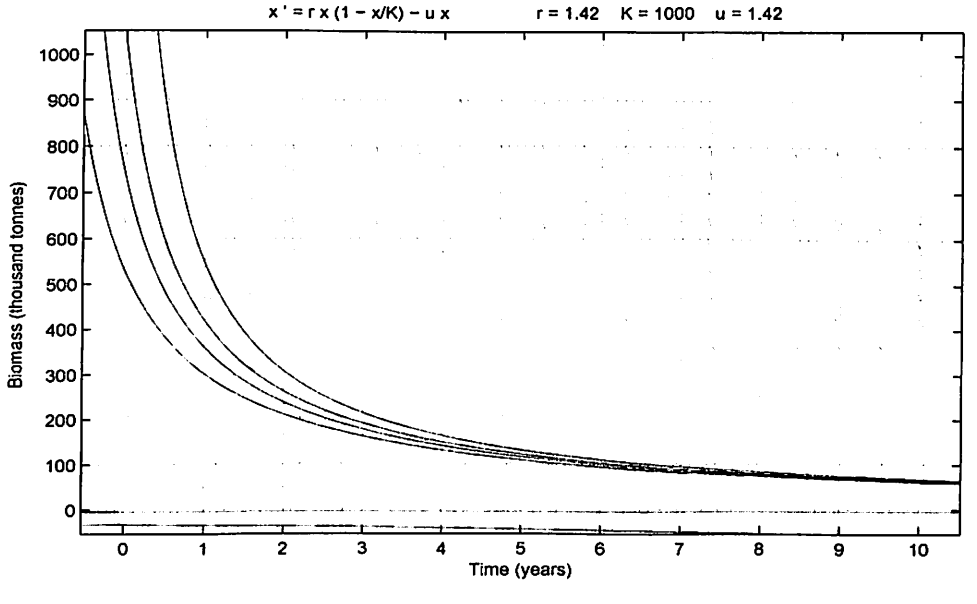

Figure 26: Solution Curves for $u = 1.42$

Solution curves corresponding to the case where the harvest level, $u = 1.42$ per year, the bifurcation point, are presented in Figure 26. For any initial biomass

level, $x_0 > 0$, the population approaches the nonhyperbolic equilibrium population, 0 in the long run. Thus, at the bifurcation point, the single equilibrium biomass level 0, is semi-stable (making the system structurally unstable). Of course, biomass levels starting from the equilibrium level, 0 remain there indefinitely. Hence, for any initial biomass level, the long-term population of fish stock is towards extinction.

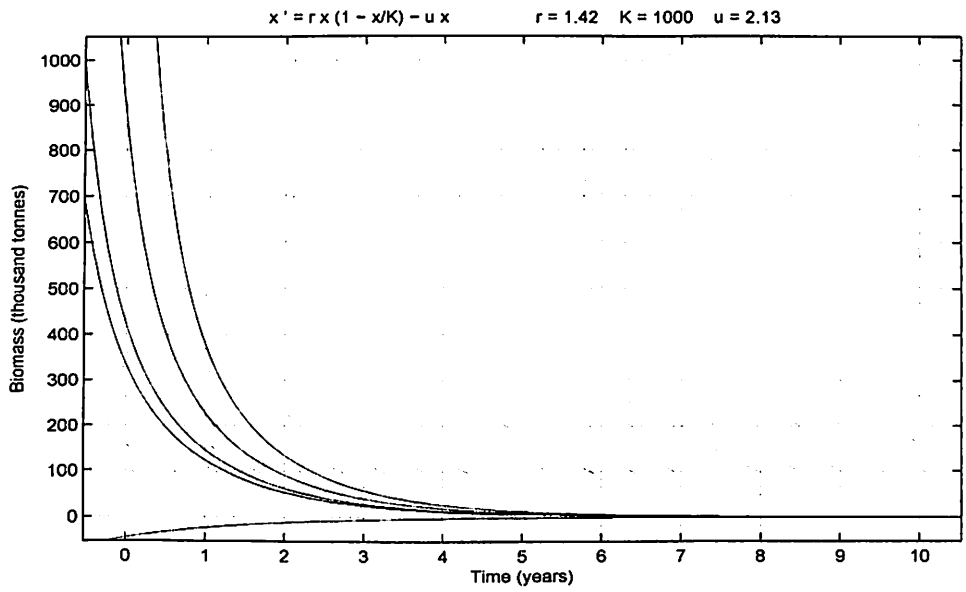

Figure 27: Solution Curves for $u = 2.13$

The case where the harvest level, $u = 2.13$ per year is about 50% greater than the bifurcation point is shown in Figure 27. For any initial biomass level, $x_0 > 0$, the population approaches the hyperbolic equilibrium population, 0 in finite time. Thus, corresponding to this harvest level exists a non-negative equilibrium biomass level 0, which is stable (making the system structurally stable). Hence, in this situation, whatever the initial fish population, the fish will die out as a result of overfishing or excessive harvesting in finite time.

The bioeconomic model

Incorporating economic parameters as proposed by Craven (1995) into the Schaefer model with yield, h depending on the level of harvesting, u gives the bioeconomic model (4.31).

In practical terms, $u = qE$; and the cost per level of harvesting, c is computed from the cost per rate of fishing effort, $c(E) = \$195/\text{trip/year}$ (other parameter values taken from Table 1) as follows:

$$\begin{aligned} c &= \frac{c(E)}{q} \\ &= \$1.0833 \times 10^8 . \end{aligned}$$

Additionally, p_1 takes the value of the linear price $p = \$600/\text{tonne}$ whereas p_2 is computed as

$$\begin{aligned} p_2 &= \frac{0.15 p_1}{u_{MSY} x_{MSY}} \\ &= \$2.54 \times 10^{-4}/\text{tonne}^2\,\text{year} . \end{aligned}$$

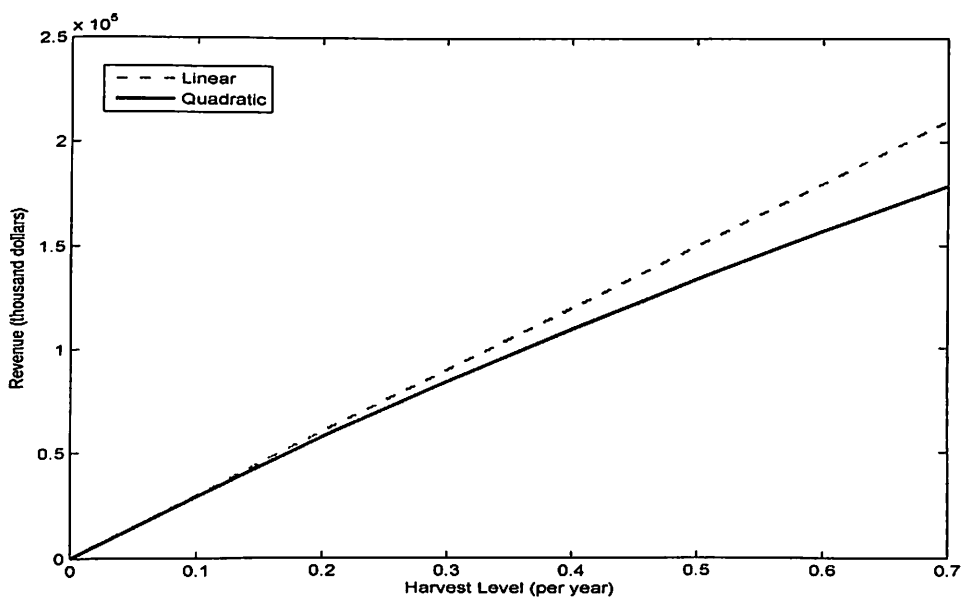

Figure 28: Linear and Quadratic Revenues

The linear and quadratic revenues are depicted in Figure 28. The diminishing returns on the linear revenues are such that when the level of harvesting is at the MSY reference point, the quadratic gross revenues are 15% less than the linear revenues.

Table 5: Annual Net Revenue at the Static Reference Points

Reference point	MEY	MSY	OAY
x	626,761	500,000	197,183
u	0.53	0.71	1.14
h	332,183	355,000	224,789
Sustainable net revenue ($\$ year^{-1})	124,056,182	104,072,984	0

Table 5 shows that, at the MEY levels, we have the maximum revenue as well the highest fish stock size. Thus, apart from providing the most revenue, it is the most conservationist among the three. Of course, the level at MSY provides the highest yield; and at the OAY level, it provides the most effort, lowest fish stock size, lowest yield, and of course, zero revenue. Therefore, this is a situation fisheries managers must guard against.

Optimality of the model

The sufficiency conditions are investigated and discussed in this section. In particular, the existence of an optimal control is determined. Also, the characterisation of the optimal control as well as the existence and uniqueness of the optimality system is sought. The goal is to maximise the present value of the net revenue. Thus, we seek an optimal control u_δ such that

$$Z(u_\delta) = \max\{Z(u) \,|\, u \in U\},$$

where the control set is Lebesgue measurable for an infinite time horizon and defined by

$$U = \{u(t) \,|\, 0 \leq u(t) \leq u_{max},\ t \in [0,\infty)\}.$$

As already intimated, in the solution of an optimal control problem, necessary and sufficient conditions of the problem need to be investigated and verified. We examine the conditions that are sufficient for the existence of an optimal control to the underlying problem.

Theorem 4.1. *There exists an optimal control u_δ that maximises the objective functional $Z(u)$ over the control set U.*

The proof of theorem is similar to that of Theorem 4.5 on page 153.

Characterisation of the optimal control

The optimal control will be characterised—obtaining an explicit formulation for the optimal control level—as well as the optimality system determined. Since the existence of an optimal control to Model (4.31) has already been established, to derive the necessary conditions for the optimal control, a version of Pontryagin's maximum principle (Pontryagin *et al.*, 1962) is employed.

Theorem 4.2. *Given an optimal control u_δ and a solution to the corresponding state equation, there exists an adjoint variable λ satisfying*

$$\lambda' = \left(\delta - r + \frac{2rx}{K}\right)\lambda - (p_1 - 2p_2ux - \lambda)u \tag{4.37}$$

and the transversality condition,

$$\lim_{t\to\infty} \lambda(t) = 0.$$

Furthermore, u_δ can be presented as

$$u_\delta = \min\left(u_{max}, \left(\frac{(p_1 - \lambda)x - c}{2p_2x^2}\right)^+\right).$$

Proof. The current value Hamiltonian for the optimal control problem (4.31) is

$$H = p_1ux - p_2(ux)^2 - cu + \lambda\left[rx\left(1 - \frac{x}{K}\right) - ux\right]. \tag{4.38}$$

Therefore, we obtain Equation (4.37) from the adjoint equation

$$\lambda' = \delta\lambda - \frac{\partial H}{\partial x}.$$

The optimality condition is given by

$$\frac{\partial H}{\partial u} = p_1x - 2p_2ux^2 - c - \lambda x = 0.$$

Thus,

$$u_\delta = \frac{(p_1 - \lambda)x - c}{2p_2x^2}. \tag{4.39}$$

The characterisation of the optimal control is

$$\begin{cases} u_\delta = 0 & \text{if} \quad \frac{\partial H}{\partial u} < 0, \\ 0 \le u_\delta \le u_{max} & \text{if} \quad \frac{\partial H}{\partial u} = 0, \\ u_\delta = u_{max} & \text{if} \quad \frac{\partial H}{\partial u} > 0. \end{cases} \tag{4.40}$$

By standard control arguments involving the bounds on the control, we have

$$u_\delta = \begin{cases} 0 & \text{if} \quad \lambda > p_1 - \frac{c}{x}, \\ \frac{(p_1 - \lambda)x - c}{2p_2x^2} & \text{if} \quad p_1 - \frac{(c + 2p_2u_{max}x^2)}{x} \le \lambda \le p_1 - \frac{c}{x}, \\ u_{max}; & \text{if} \quad \lambda < p_1 - \frac{(c + 2p_2u_{max}x^2)}{x}. \end{cases} \tag{4.41}$$

This implies that the optimal control comprises both the boundary solutions (or binding constraints) and the interior solution. The boundary solutions indicate that the resource should be harvested if and only if the marginal revenue of harvest as a result of the application of maximum level of harvesting exceeds the current value shadow price of the resource.

In compact notation,

$$u_\delta = \min\left(u_{max}, \left(\frac{(p_1 - \lambda)x - c}{2p_2x^2}\right)^+\right).$$

The optimality system comprises the state equation coupled with the adjoint equation and the initial and transversality conditions together with the characterisation of the optimal control.

Therefore,

$$\begin{aligned} x' &= rx\left(1 - \frac{x}{K}\right) - \min\left(u_{max}, \left(\frac{(p_1 - \lambda)x - c}{2p_2x^2}\right)^+\right)x, \\ \lambda' &= \left(\delta - r + \frac{2rx}{K}\right)\lambda \\ &\quad - \left(p_1 - 2p_2 \min\left(u_{max}, \left(\frac{(p_1 - \lambda)x - c}{2p_2x^2}\right)^+\right)x - \lambda\right) \\ &\quad \times \min\left(u_{max}, \left(\frac{(p_1 - \lambda)x - c}{2p_2x^2}\right)^+\right), \end{aligned}$$

$$\text{with} \quad x(0) = x_0 \quad \text{and} \quad \lim_{t \to \infty} \lambda(t) = 0. \qquad \square$$

The existence of the optimal control has already been established by Theorem 3.12. We wish to ensure the uniqueness of the so established optimal control. The arguments espoused in Theorem 4.5 for the uniqueness suffice.

Numerical simulations

We shall subject the model to numerical analyses by way of simulations and graphical illustrations. First, a number of simulations are performed with the maximum level of harvesting set at the MEY and OAY levels while varying the initial stock level. The maximum level of harvesting maintained at the MSY level is considered second. Simulations will be carried out at a fixed initial biomass level while varying the level of harvesting.

Simulation results for the harvest level and stock size relating to the case where $u_{max} = 0.53$ per year, $x_0 = 550,000$ tonnes, $x_0 = 750,000$ tonnes and $T = 1$ year are presented in Figure 29. In Figure 29 (a), it is observed that when the maximum harvest level u_{max} is set at the MEY level, the optimal harvest level appears to follow the same boundary path of around 0.53 for the one-year horizon for the different initial biomass levels. However, the fish biomass levels follow different trajectories. The biomass decreases for the higher initial value to about 670,000 tonnes, and increases for the lower initial value of 550,000 tonnes to about 590,000 tonnes (Figure 29 (b)).

Assuming an initial population size of 550,000 tonnes, the total net revenue over the one-year horizon corresponding to the given level of harvesting is computed as US$94,218,000; a decrease of 23% of the net revenue, US$121,870,000 for $x_0 = 750,000$ tonnes.

Simulation results for the harvest level and stock size relating to the case where $u_{max} = 0.53$ per year and $T = 20$ years are presented in Figure 30. In Figure 30 (a) it is observed that when the maximum harvest level u_{max} is set at the MEY level, the optimal harvest level appears to follow the same boundary path of the maximum MEY level throughout the twenty-year horizon for the different initial biomass levels. However, the fish biomass levels follow different trajectories. The

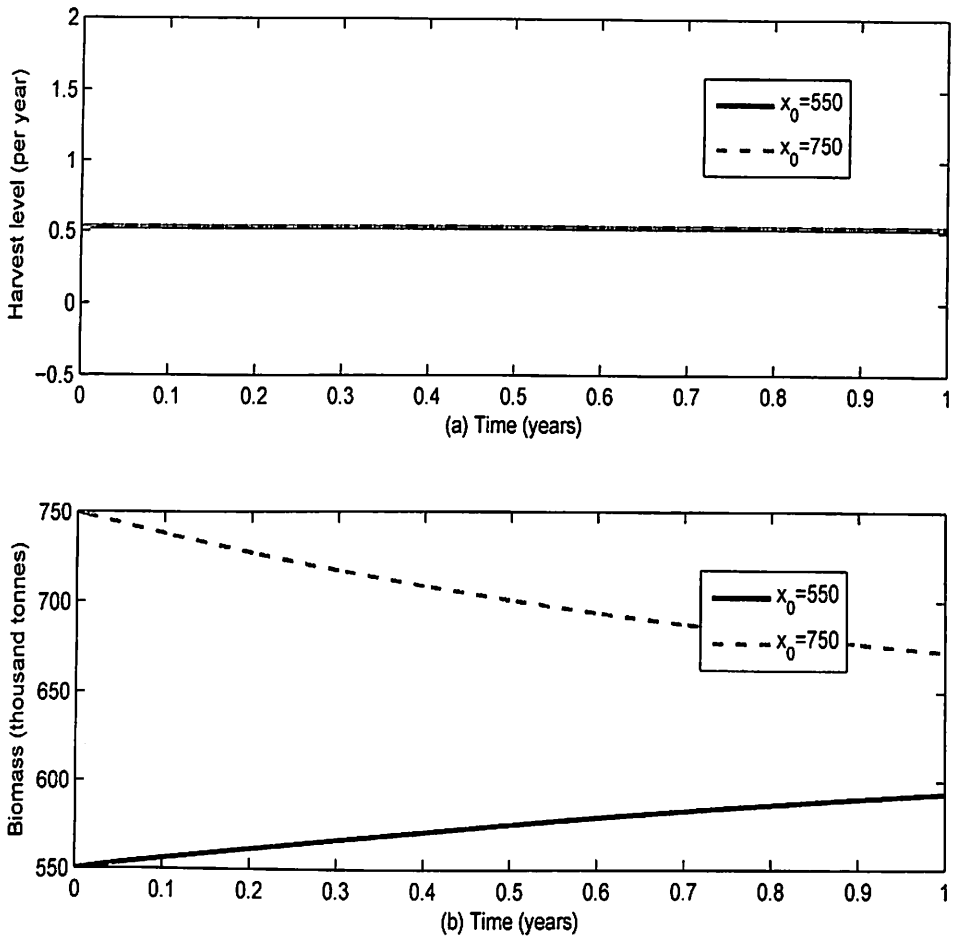

Figure 29: (a) Harvest and (b) Biomass Levels for $x_0 = 550,000; 750,000$, $u_{max} = 0.53$ and $T = 1$

biomass decreases for the higher initial value and increases for the lower initial value of 550,000 tonnes to the common equilibrium value of around 626,943 tonnes (Figure 30 (b)). It is interesting to observe that the fishery will attain equilibrium status even at lower initial biomass levels provided that the level of harvesting is kept at the MEY level.

Assuming an initial population size of 550,000 tonnes, the total net revenue over the twenty-year horizon corresponding to the given harvest level is computed as US$703,260,000; a decrease of 6% of the net revenue, US$745,790,000 for $x_0 = 750,000$ tonnes.

Simulation results for the harvest level and stock size relating to the case where $u_{max} = 1.14$ per year, $x_0 = 550,000$ tonnes, $x_0 = 750,000$ tonnes and $T = 1$ year are presented in Figure 31. In Figure 31 (a), it is observed that when the maximum

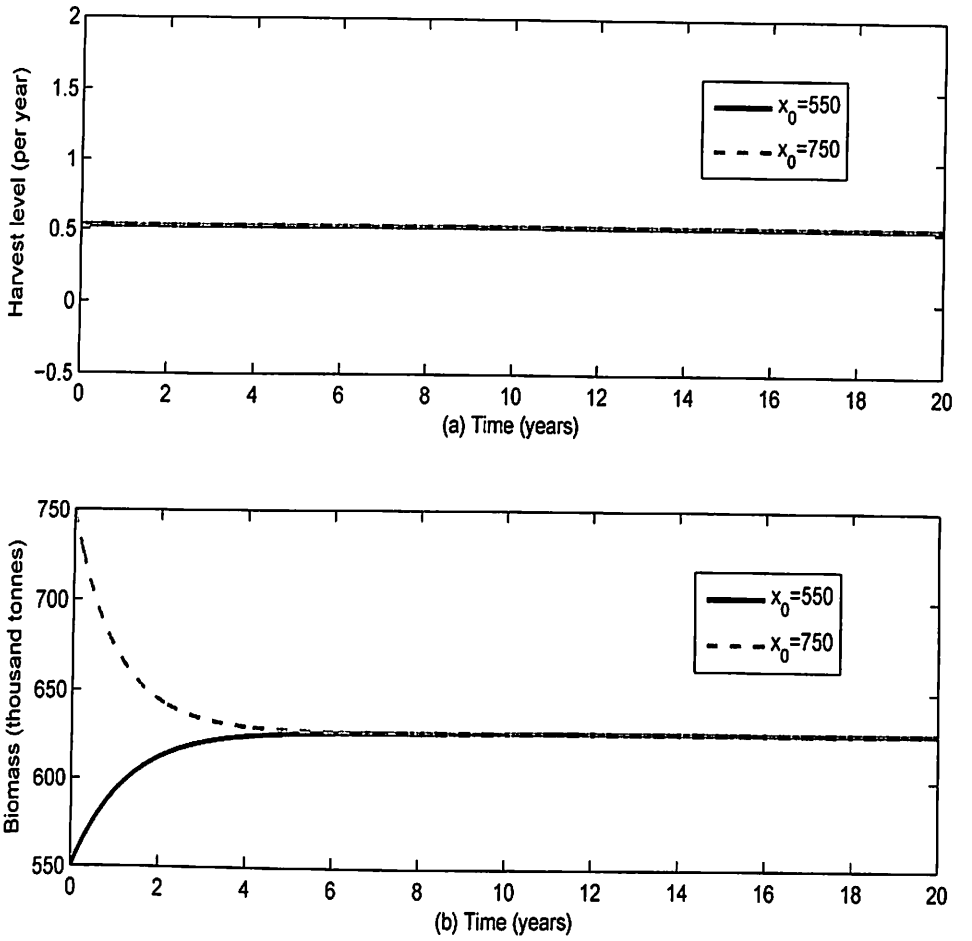

Figure 30: (a) Harvest and (b) Biomass Levels for $x_0 = 550,000$; $750,000$, $u_{max} = 0.53$ and $T = 20$

harvest level u_{max} is set at the OAY level, the optimal harvest level appears to initially follow different paths, starting from around 0.72 per year and 0.82 per year respectively for $x_0 = 550,000$ tonnes and $x_0 = 750,000$ tonnes. Thereafter, the harvest levels intersect at almost 1.14 per year and remain constant till the final horizon. Furthermore, the fish biomass levels follow significantly different trajectories. The biomass decreases for the higher initial biomass level to about 483,045 tonnes, and decreases also for the lower initial level of 550,000 tonnes to below 428,409 tonnes (Figure 31 (b)).

Assuming an initial population size of 550,000 tonnes, the total net revenue over the one-year horizon corresponding to the given level of harvesting is computed as US$114,460,000; a decrease of 23% of the net revenue, US$148,850,000 for $x_0 = 750,000$ tonnes.

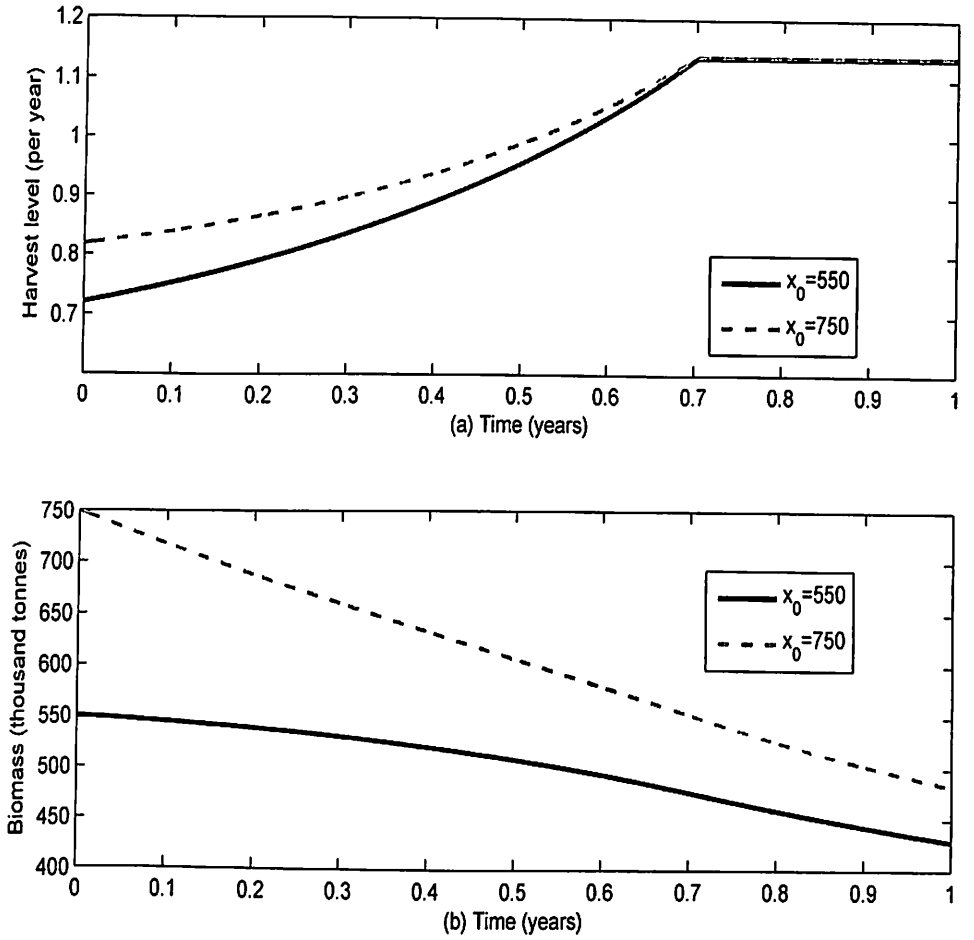

Figure 31: (a) Harvest and (b) Biomass Levels for $x_0 = 550,000$; $750,000$, $u_{max} = 1.14$ and $T = 1$

Simulation results for the harvest level and stock size relating to the case where $u_{max} = 1.14$ per year and $T = 20$ years are presented in Figure 32. In Figure 32 (a), it is observed that when the maximum harvest level u_{max} is set at the OAY level, the optimal harvest level appears to initially follow different paths, starting from around 0.51 per year and 0.68 per year respectively for $x_0 = 550,000$ tonnes and $x_0 = 750,000$ tonnes. Thereafter, the harvest levels intersect at about 0.57 per year, before rising and ending at 1.14 per year at the final horizon. Furthermore, the fish biomass levels initially follow different trajectories before intersecting at 596,360 tonnes for a majority of the time horizon. Thereafter, the biomass decreases for both initial values to a common value of around 431,062 tonnes (Figure 32 (b)).

Assuming an initial population size of 550,000 tonnes, the total net revenue over the twenty-year horizon corresponding to the given level of harvesting is

computed as US$707,130,000. The net revenue for $x_0 = 750,000$ tonnes is computed as US $752,680,000; an increase of 6%.

It is instructive to note that when the level of harvesting is pegged at the OAY level, the iterates still converge. This is as a result of the harvest level, 1.14 per year being less the bifurcation point of the model, 1.42 per year. Additionally, for the majority of the time horizon, the optimal harvest level is at most about 0.57 per year. This is far less than the maximum harvest level, which is set at 1.14 per year.

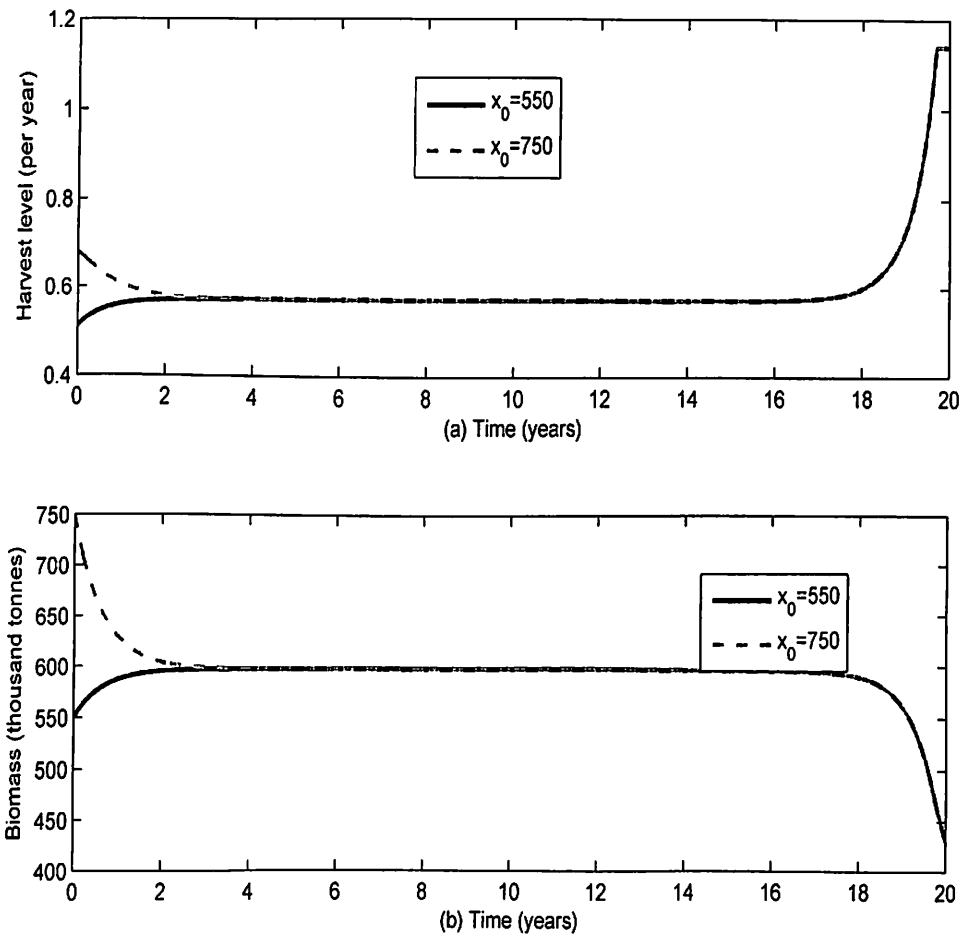

Figure 32: (a) Harvest and (b) Biomass Levels for $x_0 = 550,000$; 750,000, $u_{max} = 1.14$ and $T = 20$

Simulation results for the harvest level and stock size relating to the case where $x_0 = 550,000$ tonnes, $u_{max} = 0.53$ per year, $u_{max} = 0.71$ per year and $T = 1$ year are presented in Figure 33. In Figure 33 (a), it is observed that when the maximum harvest level u_{max} is set at the MEY and MSY levels, the optimal harvest

level appears to follow different paths of nearly 0.53 and 0.71 corresponding respectively to the MEY and MSY levels for the one-year horizon . Furthermore, the fish biomass levels follow different trajectories. The biomass increases for the harvest level at MEY to around 593,000, and decreases for the harvest level at MSY to about 524,000 tonnes (Figure 33 (b)).

Assuming an initial population size of 550,000 tonnes, the total net revenue over the one-year horizon corresponding to the harvest levels at MEY and MSY are computed as US$94,218,000 and US$106,240,000, respectively. That is, before equilibrium is attained, the net revenue at the MSY level is 11% greater than the net revenue at the MEY level.

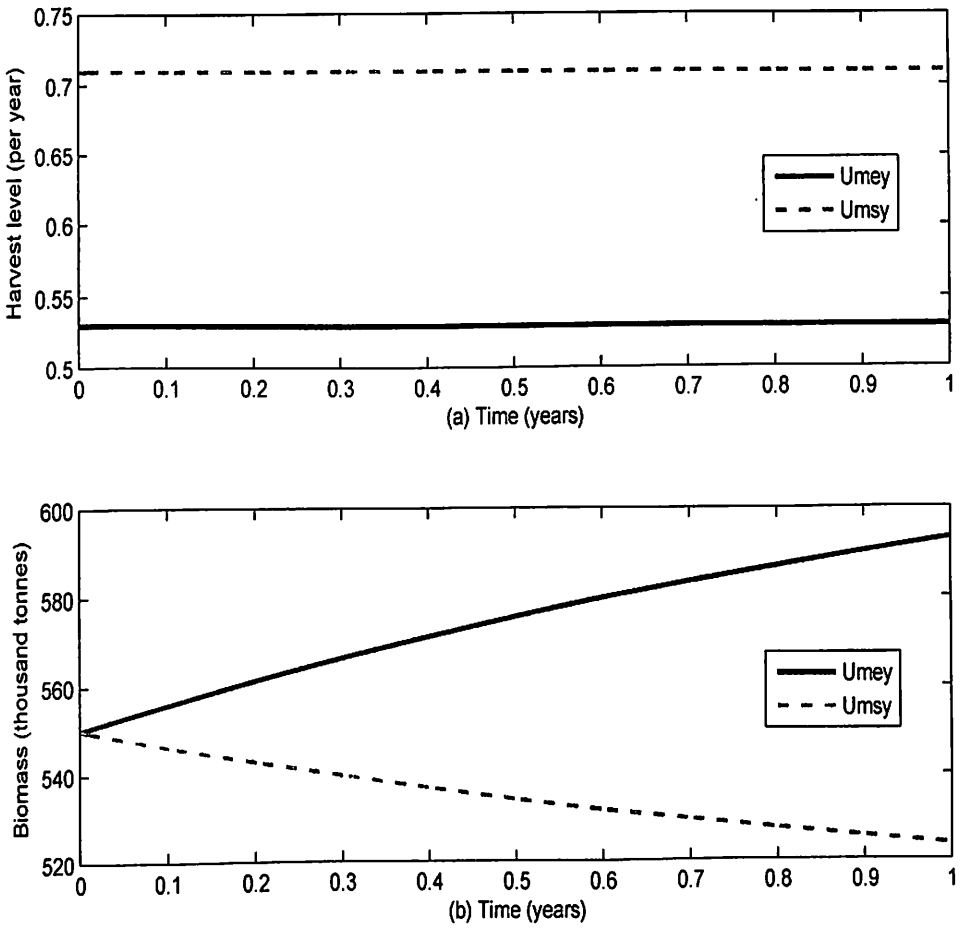

Figure 33: (a) Harvest and (b) Biomass Levels for $x_0 = 550,000$, $u_{max} = 0.53$, 0.71 and $T = 1$

Simulation results for the harvest level and stock size relating to the case where $x_0 = 550,000$ tonnes, $T = 20$ years, $u_{max} = 0.53$ per year and $u_{max} = 0.71$ per year

are presented in Figure 34. In Figure 34 (a), it is observed that when the maximum harvest level u_{max} is set at the MEY and MSY levels, the optimal harvest level appears to follow different paths. The harvest level for MEY is at the equilibrium value of 0.53 per year throughout the twenty-year horizon. On the other hand, the harvest level for MSY starts at a lower value of 0.51 per year and rises to 0.57 per year for the majority of the time horizon. It eventually rises again and ends at the maximum value, 0.71.

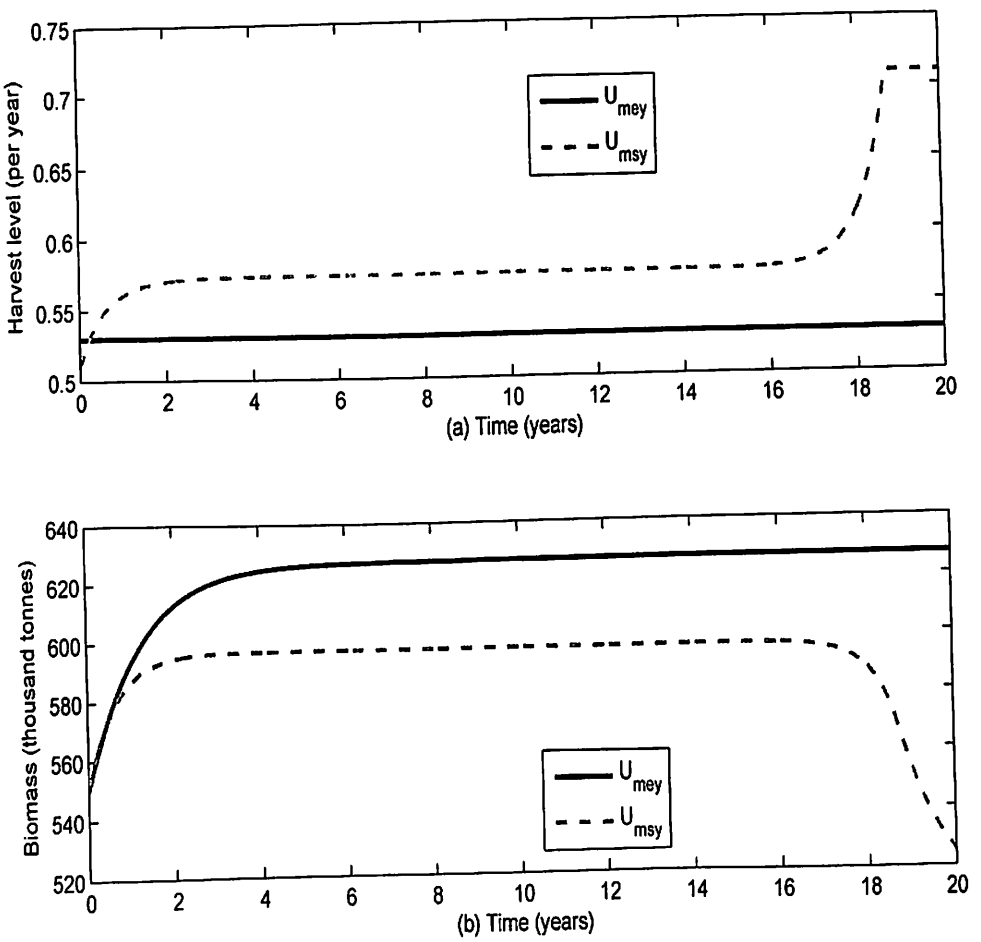

Figure 34: (a) Harvest and (b) Biomass Levels for $x_0 = 550{,}000$, $u_{max} = 0.53$, 0.71 and $T = 20$

Furthermore, the fish biomass levels follow different trajectories. The biomass increases for harvest level at MEY to its equilibrium value of around 626,943 tonnes. For the harvest level at MSY, the biomass increases to 596,823 tonnes for the majority of the time horizon before finally decreasing to 525,127 tonnes (Figure 34 (b)).

Assuming an initial population size of 550,000 tonnes, the total net revenue over the twenty-year horizon corresponding to the harvest levels at MEY and MSY are computed as US$703,260,000 and US$706,900,000, respectively. The net revenue at MSY is about 1% greater than the revenue at MEY.

Model summary

This section looked into the level of harvesting strategies of the sardinella fishery under the Craven model in order to determine the optimal strategy. Dynamics of the biomass were modelled using the Schaefer equation (with level of harvesting as the control instead of effort). Bifurcation analysis was performed on this model to determine the maximum sustainable harvest as well as the bifurcation point. However, the objective functional of the canonical Gordon-Schaefer model was subjected to a modification. Instead of the linear revenues in the model, an objective functional of quadratic revenues proposed by Craven (1995) was preferred. The new reference points under this modified model—the MEY and OAY—were determined and numerically illustrated.

Numerical simulations were performed on the Craven model to highlight further useful insights. The model was found to attain equilibrium status when the level of harvesting is set at the MEY level. The model was also found to converge at both the MSY and OAY levels. However, at these harvest levels, the optimal control is mostly at the interior as opposed to the boundary (signifying harvesting, but not at the maximum level).

The harvest levels at MEY and MSY levels were compared at two different time-horizons. It was observed that at both horizons, the total net revenue for MSY was greater than the revenue for MEY. However, the final biomass level for MEY is greater than the level for MSY at a common initial biomass level of 55% of the carrying capacity.

Assuming an initial population size of 550,000 tonnes, the total net revenue over the twenty-year horizon corresponding to the harvest levels at MEY and MSY are computed as US$703,260,000 and US$706,900,000, respectively. The net revenue at MSY is about 1% greater than the revenue at MEY.

Model summary

This section looked into the level of harvesting strategies of the sardinella fishery under the Craven model in order to determine the optimal strategy. Dynamics of the biomass were modelled using the Schaefer equation (with level of harvesting as the control instead of effort). Bifurcation analysis was performed on this model to determine the maximum sustainable harvest as well as the bifurcation point. However, the objective functional of the canonical Gordon-Schaefer model was subjected to a modification. Instead of the linear revenues in the model, an objective functional of quadratic revenues proposed by Craven (1995) was preferred. The new reference points under this modified model—the MEY and OAY—were determined and numerically illustrated.

Numerical simulations were performed on the Craven model to highlight further useful insights. The model was found to attain equilibrium status when the level of harvesting is set at the MEY level. The model was also found to converge at both the MSY and OAY levels. However, at these harvest levels, the optimal control is mostly at the interior as opposed to the boundary (signifying harvesting, but not at the maximum level).

The harvest levels at MEY and MSY levels were compared at two different time-horizons. It was observed that at both horizons, the total net revenue for MSY was greater than the revenue for MEY. However, the final biomass level for MEY is greater than the level for MSY at a common initial biomass level of 55% of the carrying capacity.

A Model with Isoperimetric Constraint

According to Clark (2010), the management of a fishery becomes necessary as a result of the undesirable consequences of open access exploitation of the resource. Historically, the emphasis of management has been on preventing overfishing. By capping annual catches, fishery managers can prevent stock depletion, or in the case of already depleted stock, can arrange for stock rehabilitation. The usual management objective has been catches set at the MSY level, possibly with a safety factor to allow for the inevitable uncertainties in stock estimates and annual catch levels. The annual catch quota set with such an objective in mind is called the total allowable catch (TAC).

TAC-regulated management has at least the effect of preventing overfishing, even though this can prove difficult if fishing capacity is large. The problem has to do with individual fishermen's economic incentive under conditions of competitive access to the resource (Clark, 2010).

A model is proposed that seeks to determine the discounted total net revenue from not only harvesting the fish stocks, but also maintaining the TAC. That is, the model has as one of its constraints the total yield in a given time horizon.

The proposed model has a quadratic objective functional signifying the costs are not linear in effort, and can be expressed as

$$\begin{aligned} \max_E Z(E) &= \int_0^T e^{-\delta t}(pqx - c_1 - \frac{c_2}{2}E)E\,dt \\ \text{subject to} \quad & \frac{dx}{dt} = rx\left(1 - \frac{x}{K}\right) - qEx \\ & \int_0^T qEx\,dt = B \\ & x(0) = x_0 \\ & 0 \leq E \leq E_{max}, \end{aligned} \tag{4.42}$$

where B is the TAC in the finite time horizon, T.

The Model (4.42) contains an isoperimetric constraint and can thus be trans-

formed into a two-dimensional model of the form:

$$\begin{aligned}
\max_E Z(E) &= \int_0^T e^{-\delta t}(pqx - c_1 - \frac{c_2}{2}E)E\,dt \\
\text{subject to} \quad & \frac{dx}{dt} = rx\left(1 - \frac{x}{K}\right) - qEx \\
& \frac{dz}{dt} = qEx \\
& x(0) = x_0 \\
& z(0) = 0, \quad z(T) = B \\
& 0 \le E \le E_{max},
\end{aligned} \tag{4.43}$$

where the state variable, $z(t)$ denotes the TAC at any time, t. Obviously, the TAC at the initial time is zero and the TAC at the final time is fixed (in this instance, the value is B).

Optimality of the model

The sufficiency conditions are investigated and discussed in this section. In particular, the existence of an optimal control is determined. Also, the characterisation of the optimal control as well as the existence and uniqueness of the optimality system is sought. The goal is to maximise the present value of the net revenue. Thus, we seek an optimal control E_δ such that

$$Z(E_\delta) = \max\{Z(E) \,|\, E \in U\},$$

where the control set is Lebesgue measurable for a finite time horizon, T and defined by

$$U = \{E(t) \,|\, 0 \le E(t) \le E_{max},\ t \in [0,T]\}.$$

As mentioned earlier, in the solution of an optimal control problem, necessary and sufficient conditions of the problem need to be investigated and verified. We examine the conditions that are sufficient for the existence of an optimal control to the underlying problem.

Theorem 4.3. *There exists an optimal control E_δ that maximises the objective functional $Z(E)$ over the control set U.*

The proof of theorem is similar to that of Theorem 4.5 on page 153.

Characterisation of the optimal control

The optimal control will be characterised—obtaining an explicit formulation for the optimal control level—as well as the optimality system determined. Since the existence of an optimal control to Model (4.43) has already been established, to derive the necessary conditions for the optimal control, a version of Pontryagin's maximum principle (Pontryagin *et al.*, 1962) is employed.

Theorem 4.4. *Given an optimal control u_δ and a solution to the corresponding state system, there exists adjoint variables λ_1 and λ_2 satisfying*

$$\lambda_1' = \left(\delta - r + \frac{2rx}{K}\right)\lambda_1 - (p - \lambda_1 + \lambda_2)qE\,, \tag{4.44}$$

$$\lambda_2' = \delta\lambda_2\,, \tag{4.45}$$

and the transversality condition,

$$\lambda_1(T) = 0\,.$$

Furthermore, E_δ can be presented as

$$E_\delta = \min\left(E_{max}, \left(\frac{(p - \lambda_1 + \lambda_2)qx - c_1}{c_2}\right)^+\right).$$

Proof. The current value Hamiltonian for the optimal control problem (4.43) is

$$H = (pqx - c_1 - \frac{c_2}{2}E)E + \lambda_1\left[rx\left(1 - \frac{x}{K}\right) - qEx\right] + \lambda_2 qEx\,. \tag{4.46}$$

Therefore, we obtain Equations (4.44) and (4.45) from the respective adjoint equations

$$\lambda_1' = \delta\lambda_1 - \frac{\partial H}{\partial x}\,,$$
$$\lambda_2' = \delta\lambda_2 - \frac{\partial H}{\partial z}\,.$$

The optimality condition is given by

$$\frac{\partial H}{\partial E} = (p - \lambda_1 + \lambda_2)qx - c_1 - c_2 E = 0\,.$$

Thus,

$$E_\delta = \frac{(p-\lambda_1+\lambda_2)qx - c_1}{c_2}. \tag{4.47}$$

The characterisation of the optimal control is

$$\begin{cases} E_\delta = 0 & \text{if} \quad \frac{\partial H}{\partial E} < 0, \\ 0 \le E_\delta \le E_{max} & \text{if} \quad \frac{\partial H}{\partial E} = 0, \\ E_\delta = E_{max} & \text{if} \quad \frac{\partial H}{\partial E} > 0. \end{cases} \tag{4.48}$$

By standard control arguments involving the bounds on the control, we have

$$E_\delta = \begin{cases} 0 & \text{if} \quad \lambda_1 - \lambda_2 > p - \frac{c_1}{qx}, \\ \frac{(p-\lambda_1+\lambda_2)qx - c_1}{c_2} & \text{if } p - \frac{(c_1+c_2E_{max})}{qx} \le \lambda_1 - \lambda_2 \le p - \frac{c_1}{qx}, \\ E_{max} & \text{if} \quad \lambda_1 - \lambda_2 < p - \frac{(c_1+c_2E_{max})}{qx}. \end{cases} \tag{4.49}$$

This implies that the optimal control comprises both the boundary solutions (or binding constraints) and the interior solution. The boundary solutions indicate that the resource should be harvested if and only if the marginal net revenue of harvest as a result of applying the maximum effort exceeds the difference of the shadow price of fish stock and the shadow price of the introduced state variable, TAC. The shadow price of fish stock is positive (only zero at the terminal time), implying an additional tonne of stock will increase net revenue. On the hand, the shadow price of TAC is negative, reflecting the fact that any additional tonne of catch (beyond the TAC) will depress net revenue (the costs will exceed revenues).

Furthermore, the interior solution is applicable if the difference of the shadow prices lies between the two marginal revenues. In compact notation,

$$E_\delta = \min\left(E_{max}, \left(\frac{(p-\lambda_1+\lambda_2)qx - c_1}{c_2}\right)^+\right).$$

The optimality system comprises the state equations and the adjoint equations with the initial and transversality conditions, together with the characterisation of the optimal control.

Therefore,

$$x' = rx\left(1-\frac{x}{K}\right) - q\min\left(E_{max}, \left(\frac{(p-\lambda_1+\lambda_2)qx-c_1}{c_2}\right)^+\right)x,$$

$$z' = q\min\left(E_{max}, \left(\frac{(p-\lambda_1+\lambda_2)qx-c_1}{c_2}\right)^+\right)x,$$

$$\lambda_1' = \left(\delta - r + \frac{2rx}{K}\right)\lambda_1 - (p-\lambda_1+\lambda_2)q\min\left(E_{max}, \left(\frac{(p-\lambda_1+\lambda_2)qx-c_1}{c_2}\right)^+\right),$$

$$\lambda_2' = \delta\lambda_2,$$

$$\text{with} \quad x(0) = x_0, \quad z(0) = 0, \quad z(T) = B \quad \text{and} \quad \lambda_1(T) = 0. \qquad \square$$

The existence of the optimal control has already been established by Theorem 3.12. We wish to ensure the uniqueness of the so established optimal control. The arguments espoused in Theorem 4.5 for the uniqueness suffice.

Numerical simulations

Solving optimal control problems in which a state variable has both the initial state and terminal state fixed can be a bit challenging. The forward-backward sweep method employed so far cannot deal with such problems. A modification to this method, called the Adapted Forward-Backward Sweep method is implemented for such problems. For further details, see Lenhart and Workman (2007).

We shall subject the model to numerical simulations and the results illustrated graphically. First, a number of simulations are performed with the TAC at the MSY level and the maximum rate of fishing effort set at more than twice the MSY level. Second, the maximum rate of fishing effort is maintained at almost twice the MSY level, while simulations are carried out varying the TAC for a given time horizon.

Simulation results for the effort, biomass and total harvest levels relating to the case where $x_0 = 750{,}000$ tonnes, $z(T) = 355{,}000$ tonnes, $E_{max} = 800{,}000$ trips and $T = 1$ year are presented in Figure 35. In Figure 35 (a), it is observed that when the maximum harvest level E_{max} is set at more than twice the MSY level, the

optimal effort level appears convex, starting from 309,443 trips to 305,628 trips, with a minimum value of 263,255 trips for the one-year horizon. Furthermore, the fish biomass decreases to a value of around 685,733 tonnes (Figure 35 (b)). The Total harvest plot (Figure 35 (c)), shows that the TAC is linear, from initially zero to 355,000 tonnes, which is the annual harvest at the MSY level.

Assuming an initial population size of 750,000 tonnes and a TAC of 355,000 tonnes, the total net revenue over the one-year horizon corresponding to the given effort rate is computed as US$139,040,000.

The TAC plot is just a straight line from $z(0) = 0$ to $z(1) = 355{,}000$. In subsequent plots, this will be replaced by the Harvest plot. The harvest rate plot component of Figure 35 is presented in Figure 36. It shows that the harvest rate is convex, starting from an initial value of about 417,747 tonnes per year to about 377,242 tonnes per year, with the minimum being 335,236 tonnes per year.

Simulation results for the effort, biomass and total harvest levels relating to the case where $x_0 = 550{,}000$ tonnes, $z(T) = 355{,}000$ tonnes, $E_{max} = 800{,}000$ trips and $T = 1$ year are presented in Figure 37. In Figure 37 (a), it is observed that when the maximum harvest level E_{max} is set at more than twice the MSY level, the optimal effort starts at 181,980 trips and increases monotonically to 569,964 trips for the one-year horizon. However, the fish biomass is concave, starting from 550,000 tonnes to around 541,611 tonnes, with a maximum of 590,207 tonnes (Figure 37 (b)). In Figure 37 (c), the harvest rate monotonically increases to about 555,658 tonnes per year, from an initial value of around 180,161 tonnes per year.

Assuming an initial population size of 550,000 tonnes and a TAC of 355,000 tonnes, the total net revenue over the one-year horizon corresponding to the given effort rate is computed as US$119,500,000.

Simulation results for the effort, biomass and total harvest levels relating to the case where $x_0 = 1{,}000{,}000$ tonnes, $z(T) = 400{,}000$ tonnes, $E_{max} = 800{,}000$ trips and $T = 1$ year are presented in Figure 38. In Figure 38 (a), it is observed that when the maximum harvest level E_{max} is set at more than twice the MSY level, the optimal effort starts at 475,400 trips and decreases monotonically to 161,700

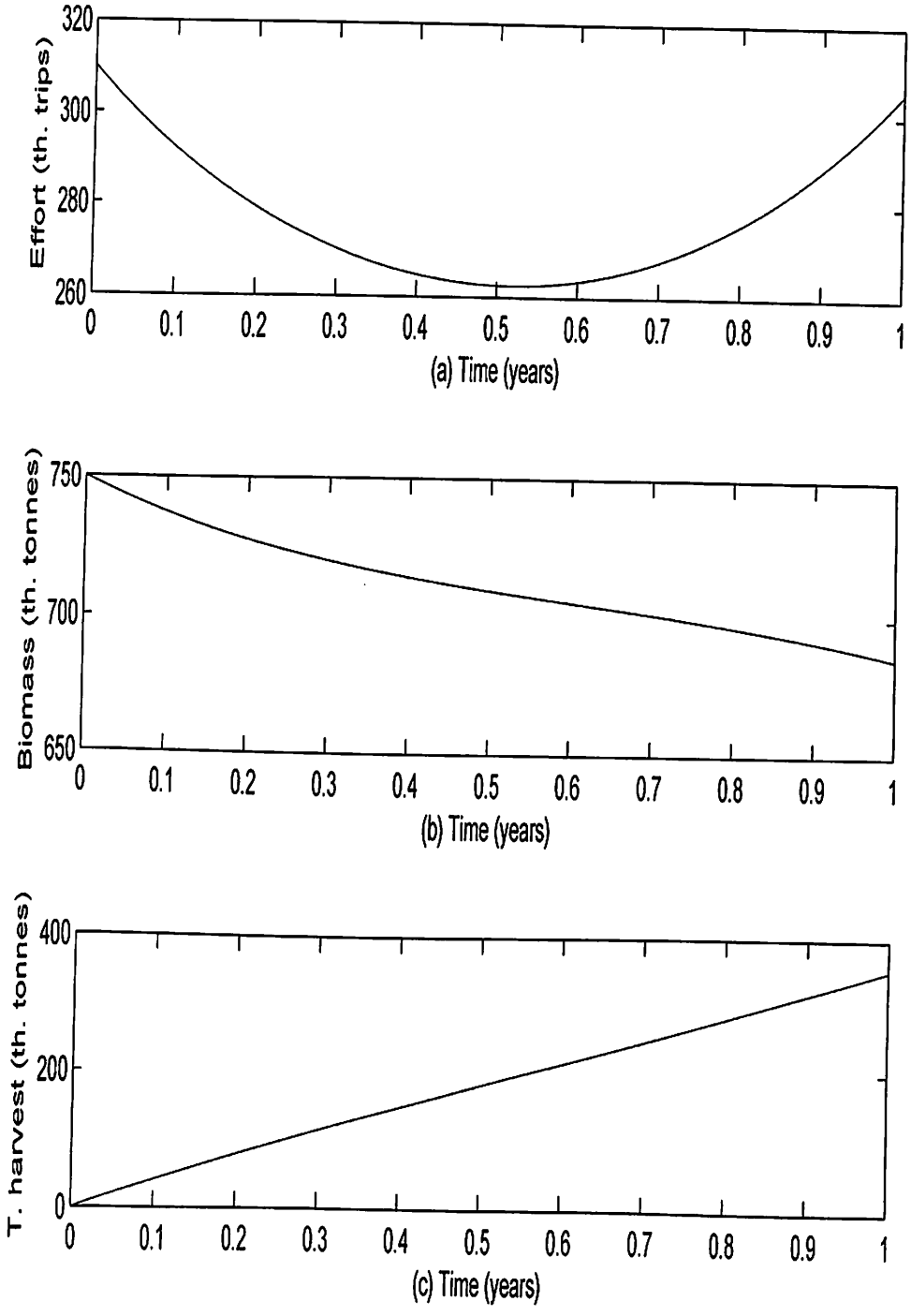

Figure 35: (a) Effort, (b) Biomass and (c) Total Harvest Levels for $x_0 = 750,000$, $z(T) = 355,000$, $E_{max} = 800,000$ and $T = 1$

trips for the one-year horizon. Furthermore, the fish biomass decreases to about 789,500 tonnes (Figure 38 (b)). In Figure 38 (c), the harvest rate decreases to around 229,800 tonnes per year, from an initial value of about 855,800 tonnes per year.

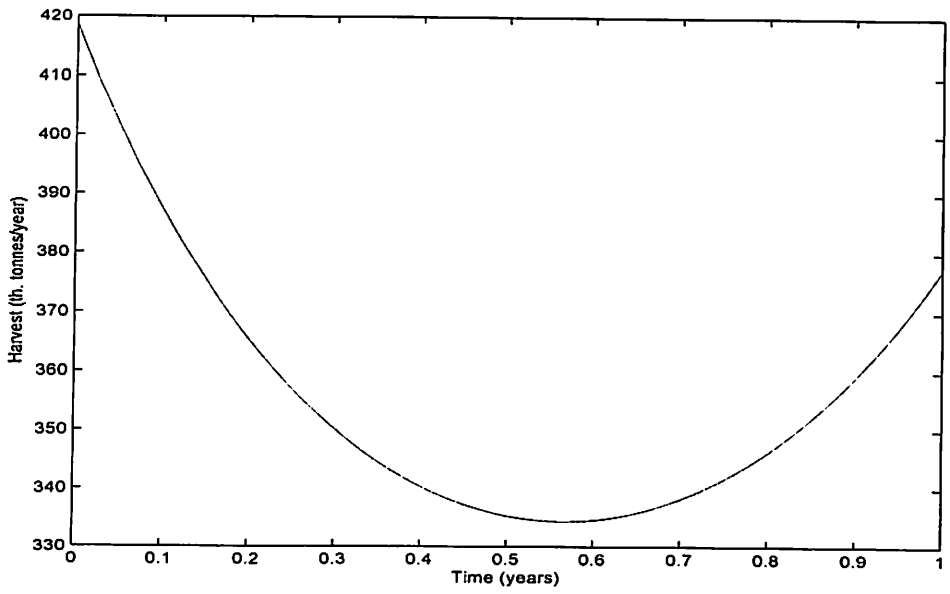

Figure 36: Harvest Level for $x_0 = 750,000$, $z(T) = 355,000$, $E_{max} = 800,000$ and $T = 1$

Assuming an initial population size of 1,000,000 tonnes (the carrying capacity) and a TAC of 400,000 tonnes, the total net revenue over the one-year horizon corresponding to the given effort rate is computed as US$169,970,000.

Simulation results for the effort, biomass and total harvest levels relating to the case where $x_0 = 750,000$ tonnes, $z(T) = 400,000$ tonnes, $E_{max} = 800,000$ trips and $T = 1$ year are presented in Figure 39. In Figure 39 (a), it is observed that when the maximum harvest level E_{max} is set at more than twice the MSY level, the optimal effort appears convex, starting from 347,571 trips to 380,660 trips, with a minimum value of 298,256 trips for the one-year horizon. On the other hand, the fish biomass decreases to about 650,187 tonnes (Figure 39 (b)). In Figure 39 (c), the harvest rate appears convex, starting from 469,221 tonnes per year to 445,501 tonnes per year, with a minimum value of 372,986 tonnes per year.

Assuming an initial population size of 750,000 tonnes and a TAC of 400,000 tonnes, the total net revenue over the one-year horizon corresponding to the given effort rate is computed as US$153,240,000.

Simulation results for the effort, biomass and total harvest levels relating to the case where $x_0 = 500,000$ tonnes, $z(T) = 250,000$ tonnes, $E_{max} = 800,000$ trips

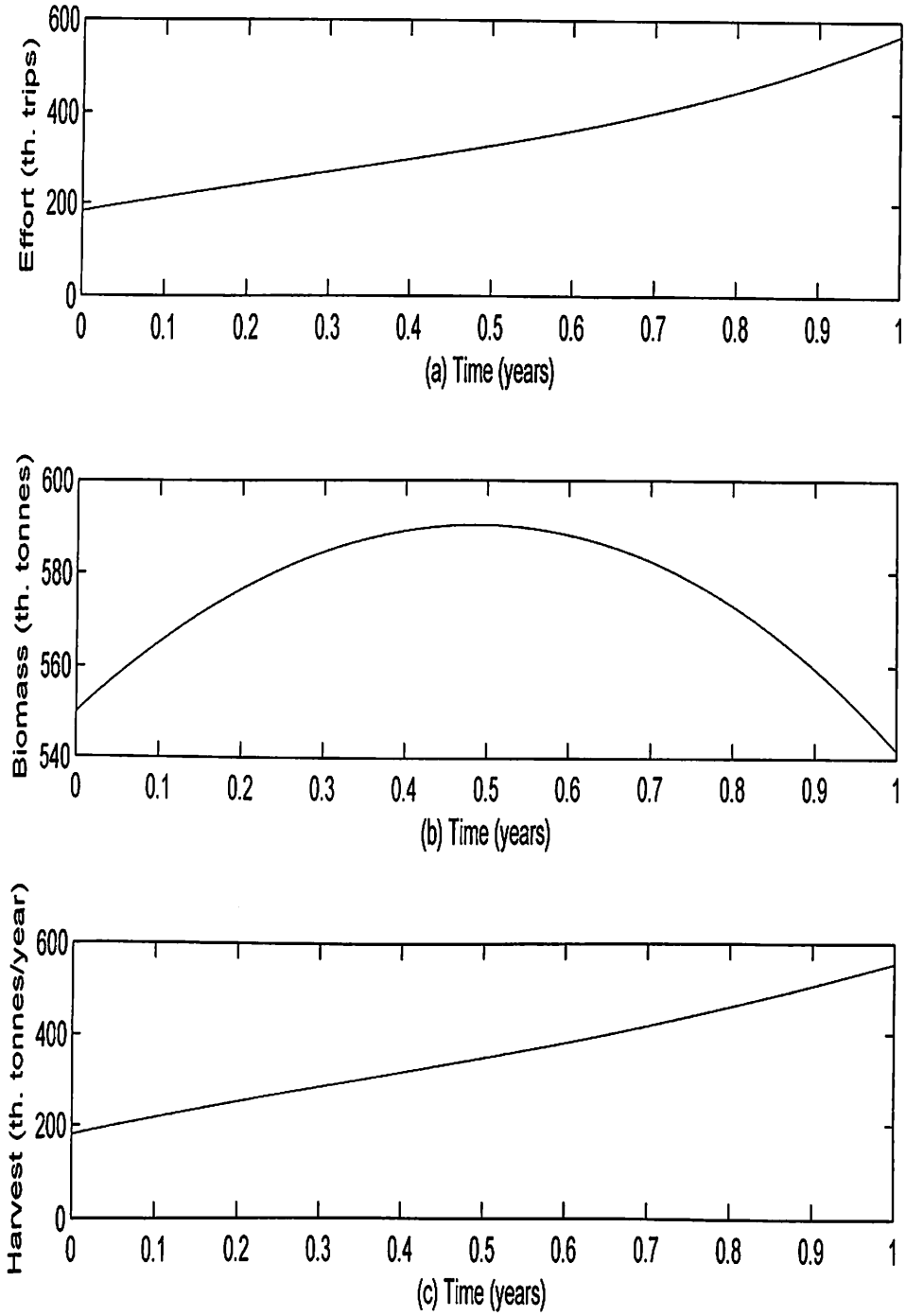

Figure 37: (a) Effort, (b) Biomass and (c) Harvest Levels for $x_0 = 550,000$, $z(T) = 355,000$, $E_{max} = 800,000$ and $T = 1$

and $T = 1$ year are presented in Figure 40. In Figure 40 (a), it is observed that when the maximum harvest level E_{max} is set at more than twice the MSY level, the optimal effort starts at 71,647 trips and increases monotonically to 406,874 trips for the one-year horizon. However, the fish biomass is concave, starting from

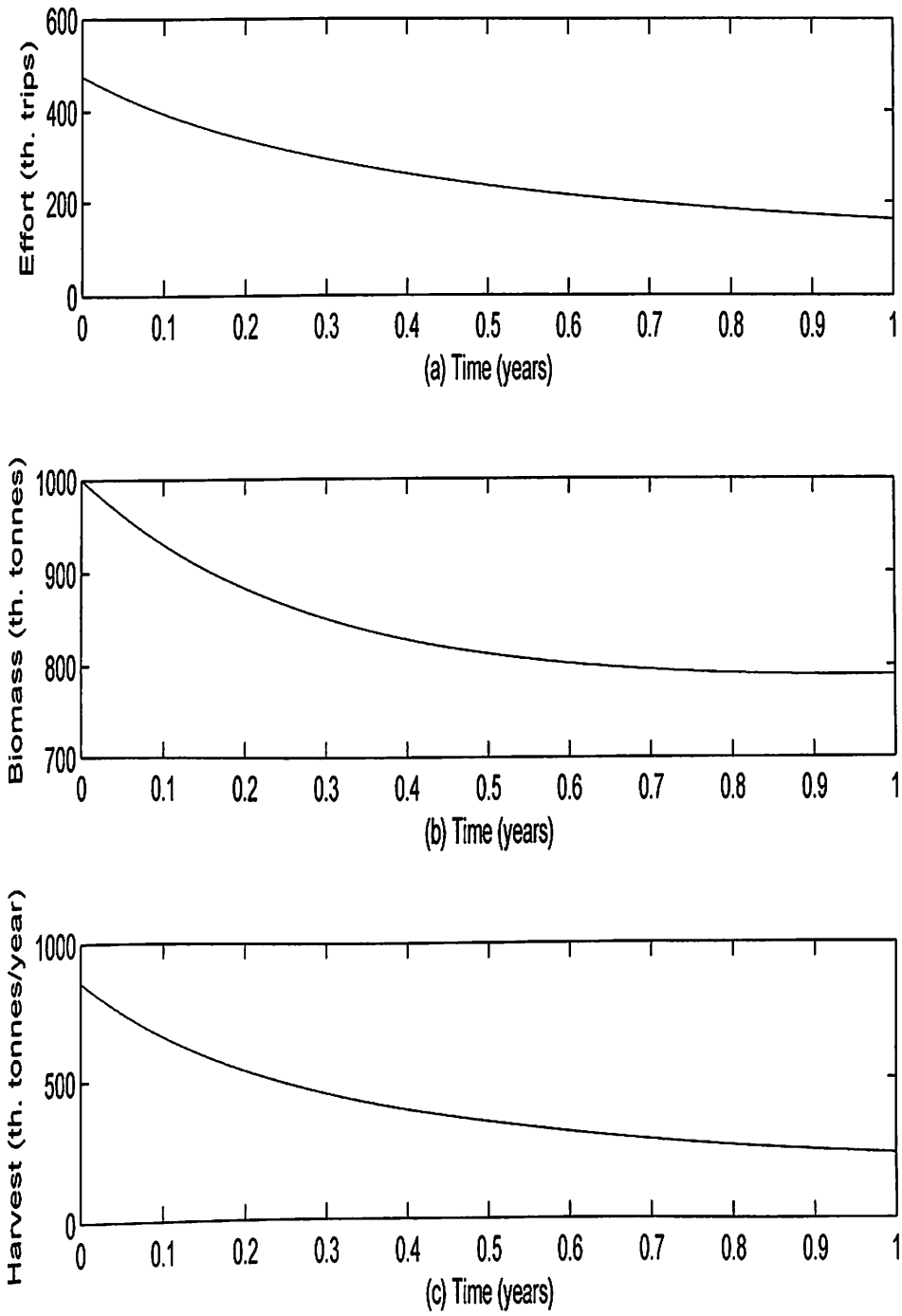

Figure 38: (a) Effort, (b) Biomass and (c) Harvest Levels for $x_0 = 1,000,000$, $z(T) = 400,000$, $E_{max} = 800,000$ and $T = 1$

500,000 tonnes to around 594,862 tonnes, with a maximum of 605,600 tonnes (Figure 40 (b)). In Figure 40 (c), the harvest rate monotonically increases to about 435,660 tonnes per year, from an initial value of around 64,483 tonnes per year.

Assuming an initial population size of 500,000 tonnes and a TAC of 250,000

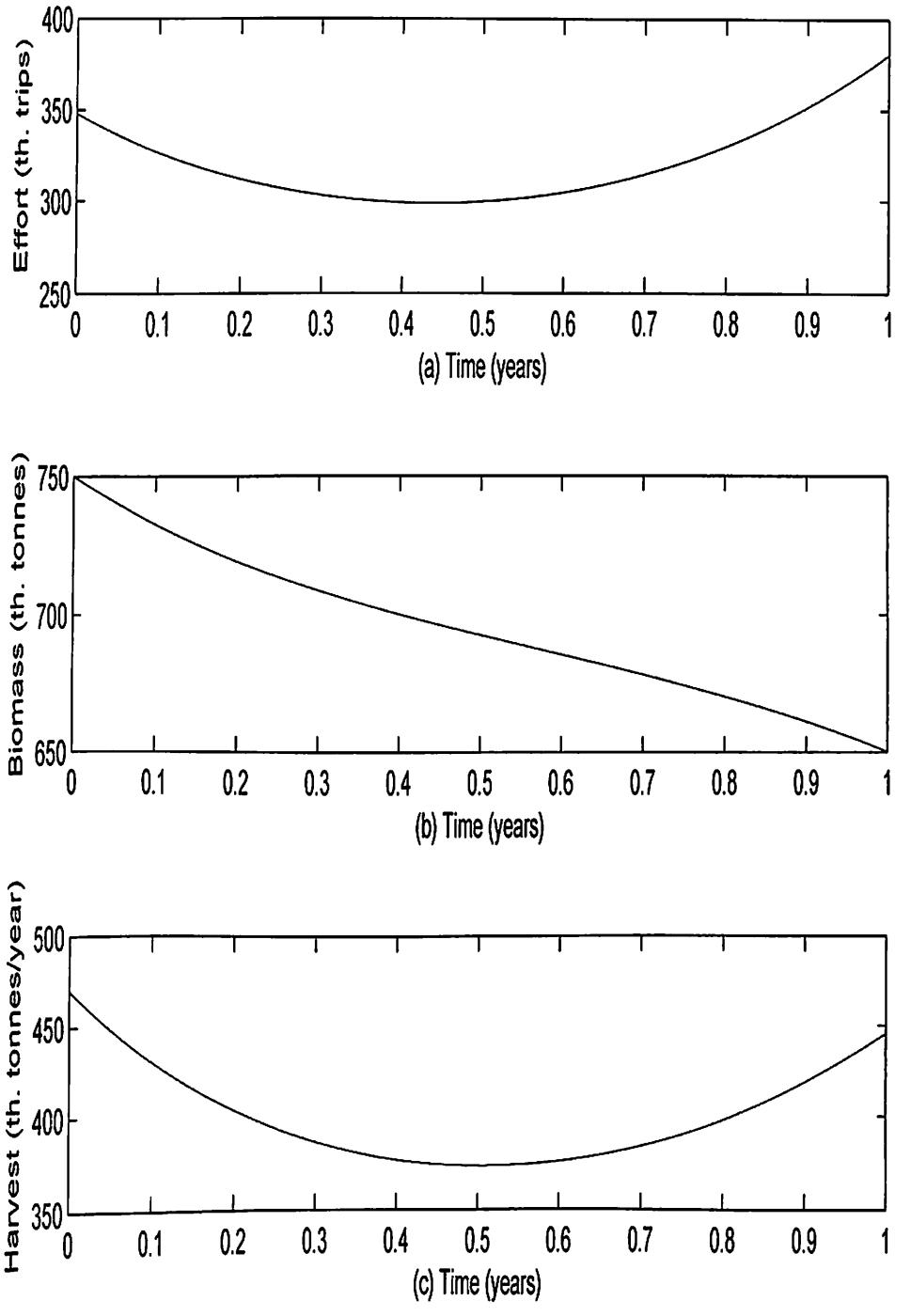

Figure 39: (a) Effort, (b) Biomass and (c) Harvest Levels for $x_0 = 750,000$, $z(T) = 400,000$, $E_{max} = 800,000$ and $T = 1$

tonnes, the total net revenue over the one-year horizon corresponding to the given effort rate is computed as US$87,667,000.

Simulation results for the effort, biomass and total harvest levels relating to the case where $x_0 = 500,000$ tonnes, $z(T) = 350,000$ tonnes, $E_{max} = 800,000$ trips

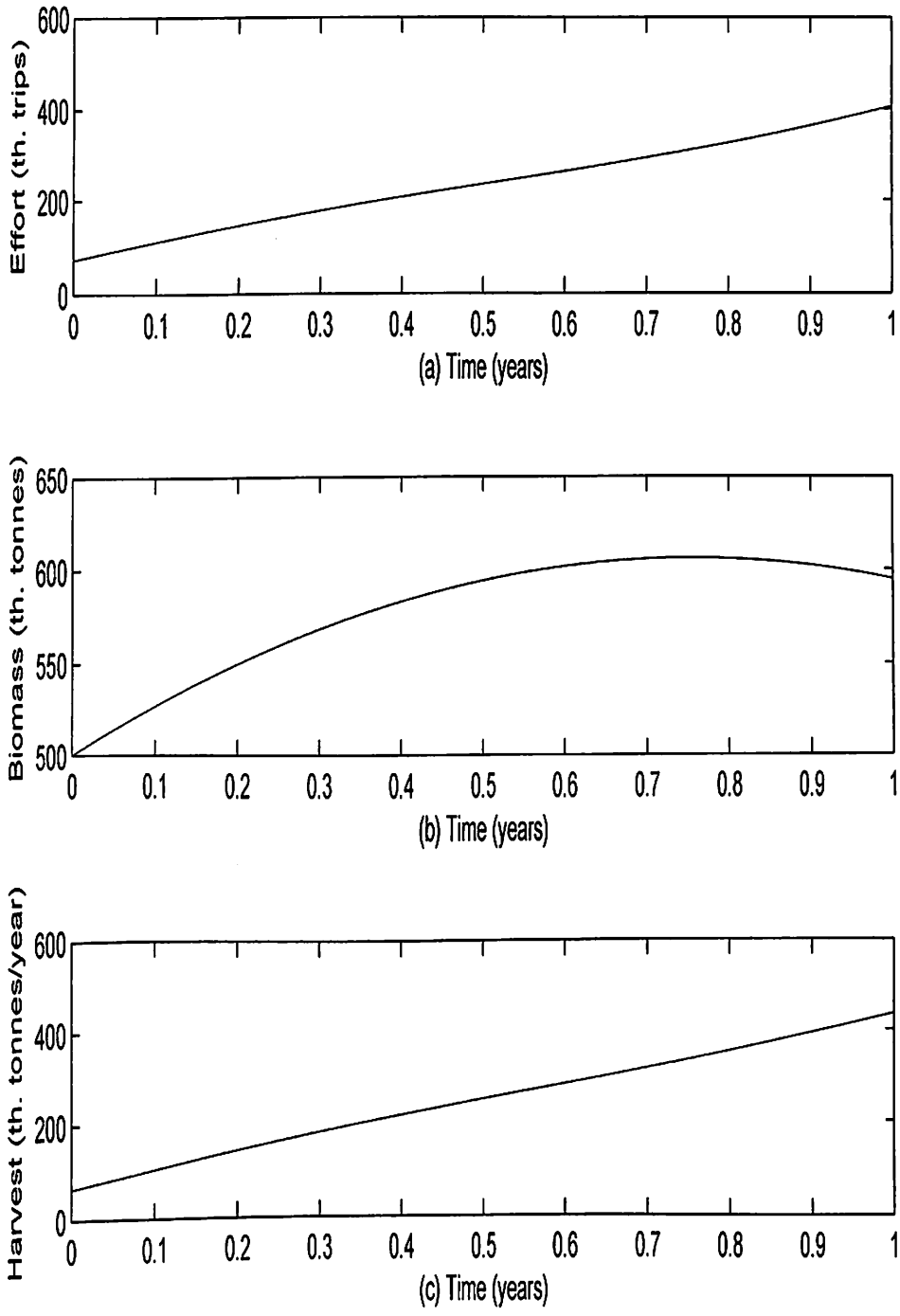

Figure 40: (a) Effort, (b) Biomass and (c) Harvest Levels for $x_0 = 500,000$, $z(T) = 250,000$, $E_{max} = 800,000$ and $T = 1$

and $T = 1$ year are presented in Figure 41. In Figure 41 (a), it is observed that when the maximum harvest level E_{max} is set at more than twice the MSY level, the optimal effort starts at 137,769 trips and increases to about 654,406 trips for the one-year horizon. However, the fish biomass is concave, starting from 500,000

tonnes to around 502,411 tonnes, with a maximum of 557,859 tonnes (Figure 41 (b)). In Figure 41 (c), the harvest rate increases to about 591,805 tonnes per year, from an initial value of around 123,992 tonnes per year.

Assuming an initial population size of 550,000 tonnes and a TAC of 350,000

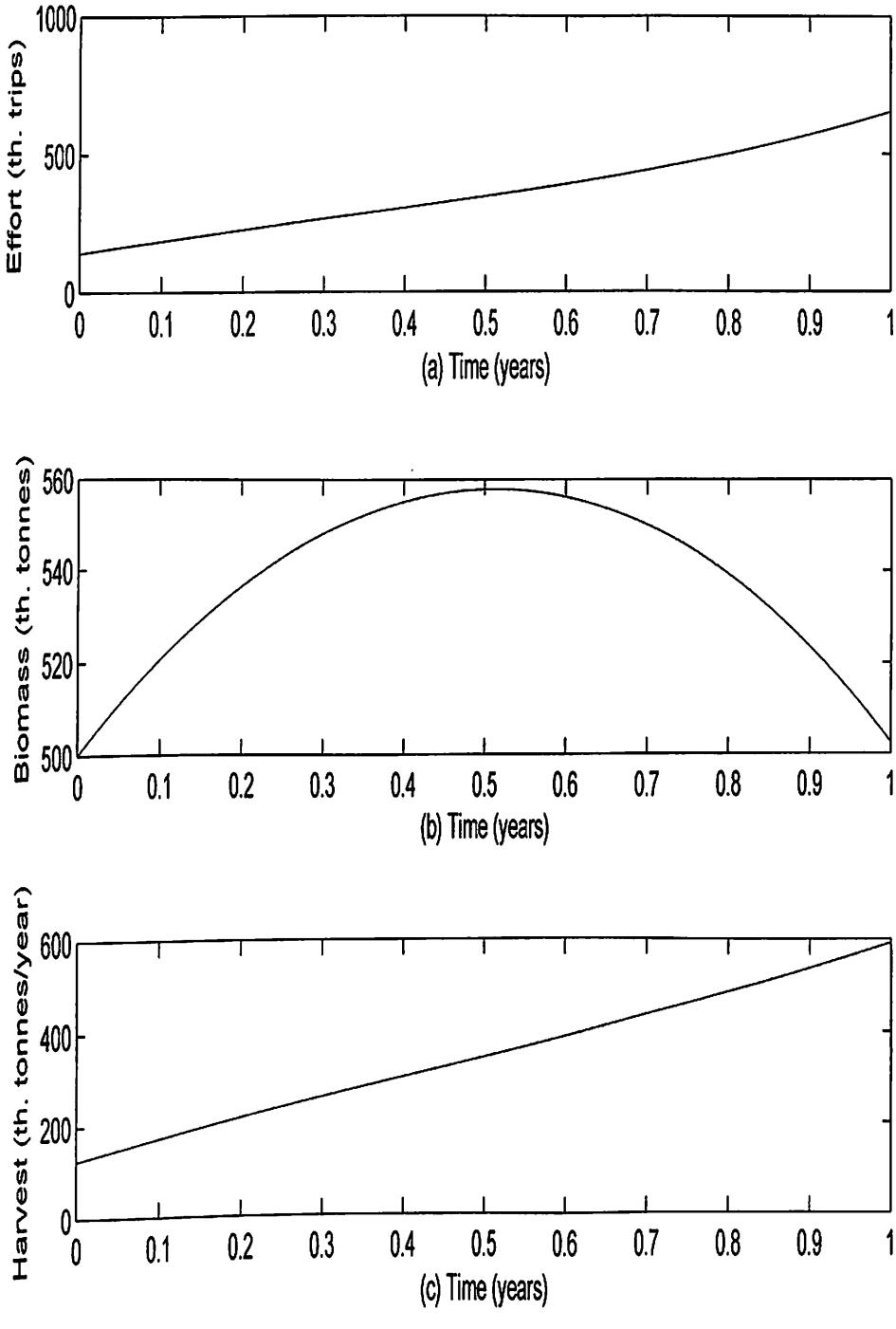

Figure 41: (a) Effort, (b) Biomass and (c) Harvest Levels for $x_0 = 500,000$, $z(T) = 350.000$, $E_{max} = 800,000$ and $T = 1$

tonnes, the total net revenue over the one-year horizon corresponding to the given effort rate is computed as US$110,840,000.

Model summary

This section looked into the fishing effort strategies of the sardinella fishery under a model incorporating TAC in order to determine the optimal strategy. Dynamics of the biomass were modelled using the Schaefer equation. However, the objective functional of the canonical Gordon-Schaefer model was subjected to a modification. Instead of the linear costs in the model, the objective functional assumed quadratic costs.

Numerical simulations were performed on the model to highlight further useful insights. As already alluded to, because one of the state variables has a fixed endpoint as well as a fixed initial point, convergence of the iterates for a lot of parameter values was not achievable. For those that achieved convergence, the model recommended a relatively small effort rate out of the maximum allowable in order to realise a TAC set at the MSY level. Even assuming an initial biomass level of the full carrying capacity did not seem to affect the magnitude of the optimal fishing rate in relation to the maximum rate available. That is, in order to ensure sustainability of the resource, there needs to be a drastic reduction in effort. This can be achieved through seasonal closures.

It was further observed that for the same TAC, a lower initial biomass level requires a higher effort rate at the final horizon than for a higher initial biomass level. Also, for the same initial biomass level, a higher TAC requires a higher average effort rate.

A Model with Modified Catchability

The present precarious situation of Ghana's sardinella fishery has been amply documented and discussed. However, the role of unorthodox fishing practices, especially the use of under-sized mesh fishing gears by fishermen in exacerbating

the problem has not been examined to a large extent by researchers in the field of fishery science.

The assumption of constant catchability coefficient in the Gordon-Schaefer model is at variance with technological aspects of the evolution of fishing power. Improvements in fishing gear design such as the use of synthetic fibres, and technologies for fish detection, with increased precision in the application of fishing power, are rarely explicitly considered when standardising fishing effort (Caddy, 1996, 1999; Defeo & Caddy, 2001).

Therefore, a bioeconomic model is developed to assess the possible impact of the use of these unapproved fishing gears (call it a crude form of technology) on specifically the catchability of the sardinella. In the second section of the Chapter, the optimal control model is formulated comprising the biomass dynamics (with bifurcation analysis) as well as the complete bioeconomic model. Optimality of the model, which consists of the characterisation of the optimal control as well as the existence and uniqueness of the optimality system is discussed in the third section. Numerical and graphical illustrations of the model are portrayed in the fourth section while the last section deals with the summary and conclusion.

Model formulation

The formulation of the model takes into account the biological considerations as well as the economic objectives of fisheries management. The biological growth dynamics with harvesting makes use of the Schaefer model

$$\frac{dx}{dt} = rx\left(1 - \frac{x}{K}\right) - qEx, \qquad x(0) = x_0 .$$

As mentioned earlier, there are two equilibrium points associated with the state dynamics of the model when the effort is less than the bifurcation point. These are 0 and $x^* = K\left(1 - \frac{qE}{r}\right)$, and the bifurcation point is given by $E = \frac{r}{q}$.

Sensitivity analysis

Sensitivity analysis on the catchability coefficient of the model will be performed to simulate the effects of IUU fishing on the sardinella stocks.

The constant catchability coefficient q is replaced by $q(1+\theta)$, where θ, a proportion of the catchability, is a measure of the effect of IUU fishing—under-sized mesh gears, light fishing, explosives and chemicals—on biomass levels. The values of θ will range from 0 (no IUU fishing) to 1 (extreme IUU fishing). For further details, see Mackinson, Sumaila and Pitcher (1997) and Habib *et al.* (2014).

Therefore,

$$E^{\theta}_{MSY} = \frac{r}{2q(1+\theta)} = \frac{1}{1+\theta}E_{MSY}\,.$$

The harvests will now become

$$\begin{aligned} h_{\theta} &= q(1+\theta)Ex \\ &= qEx(1+\theta) \\ &= h(1+\theta)\,. \end{aligned}$$

This implies that, to ensure sustainability of the resource (attaining equilibrium) at the MSY level when the catchability is increased by θ (a multiplier of q), the accompanying effort level E^{θ}_{MSY} should be reduced to a value that is $\frac{1}{1+\theta}$ of the E_{MSY}. Otherwise, the harvests h_{θ} would be a proportion θ greater than the harvests without any increase in catchability, h.

Consequently, if

$$h_{\theta} > h_{MSY}\,,$$

then the long-term sustainability of the fishery will be seriously jeopardised.

Bifurcation analysis

We shall present the solution curves for the scenario depicting the effects of the variation in catchability on the fish stock. The equilibrium points and the associated stability properties of the model will be clearly highlighted in the ensuing figures.

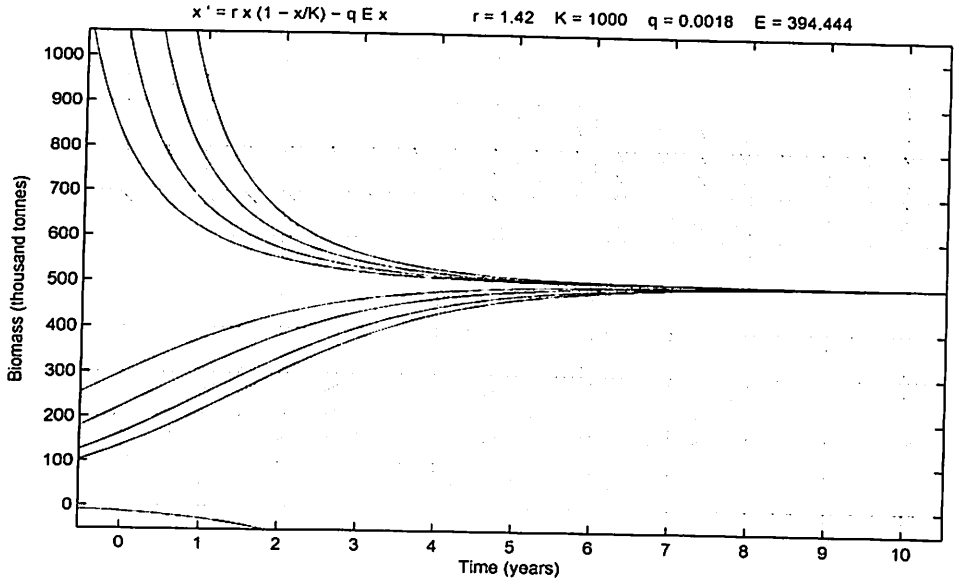

Figure 42: Solution Curves for $E = 394.444$

Solution curves corresponding to the situation where $E = E_{MSY} = 394{,}444$ trips (with no variation in catchability) are presented in Figure 42. It can be observed that there are two hyperbolic equilibrium points: 0 and $x^* = x_{MSY} = 500{,}000$ tonnes. For any initial biomass level, $x_0 > x_{MSY}$, the population approaches the equilibrium population, x_{MSY} in the long run. Similarly, for $0 < x_0 < x_{MSY}$, the population asymptotically approaches x_{MSY}. Thus the biomass level 0 is unstable while x_{MSY} is stable (making the system structurally stable). Of course, biomass levels starting from the equilibrium levels, 0 and x_{MSY} remain there indefinitely. Hence, an effort level corresponding to E_{MSY} induces a long-term biomass level of exactly half the carrying capacity.

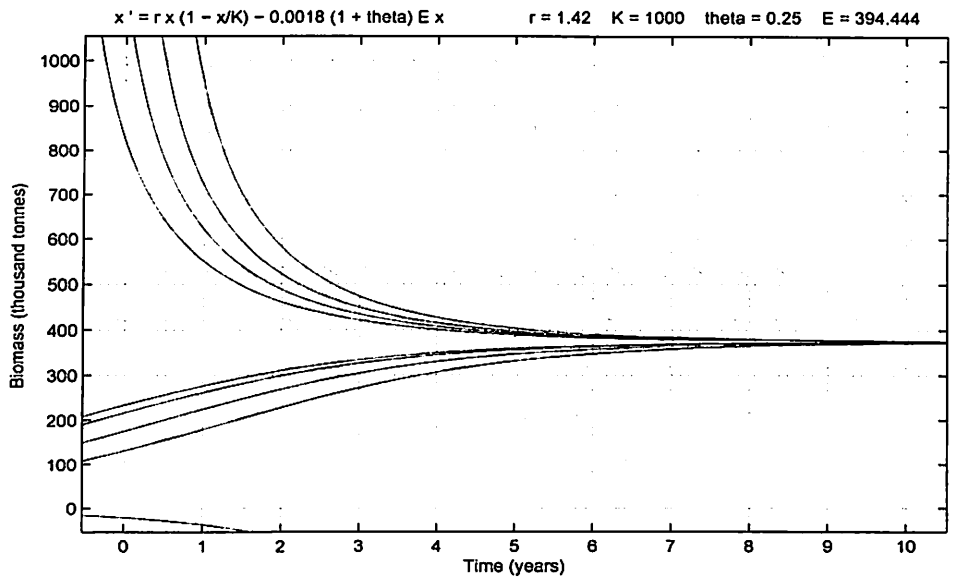

Figure 43: Solution Curves for $E = 394.444$ with $\theta = 0.25$

Solution curves corresponding to the situation where $E = E_{MSY} = 394,444$ trips, with a variation in catchability, $\theta = 0.25$, are presented in Figure 43. It can be observed that there are two hyperbolic equilibrium points: 0 and $x_\theta = 375,000$ tonnes. For any initial biomass level, $x_0 > x_\theta$, the population approaches the equilibrium population, x_θ in the long run. Similarly, for $0 < x_0 < x_\theta$, the population asymptotically approaches x_θ. Thus the biomass level 0 is unstable while x_θ is stable (making the system structurally stable). Of course, biomass levels starting from the equilibrium levels, 0 and x_θ remain there indefinitely. Hence, an increase in catchability of 25% is equivalent to fishing at an effort rate of one and a quarter times the effort rate at E_{MSY}. This induces a long-term decline in fish stock to a level that is 75% of x_{MSY}.

Solution curves corresponding to the situation where $E = E_{MSY} = 394,444$ trips, with a variation in catchability, $\theta = 0.5$, are presented in Figure 44. It can be observed that there are two hyperbolic equilibrium points: 0 and $x_\theta = 250,000$ tonnes. For any initial biomass level, $x_0 > x_\theta$, the population approaches the equilibrium population, x_θ in the long run. Similarly, for $0 < x_0 < x_\theta$, the population asymptotically approaches x_θ. Thus the biomass level 0 is unstable while x_θ is stable (making the system structurally stable). Of course, biomass levels starting

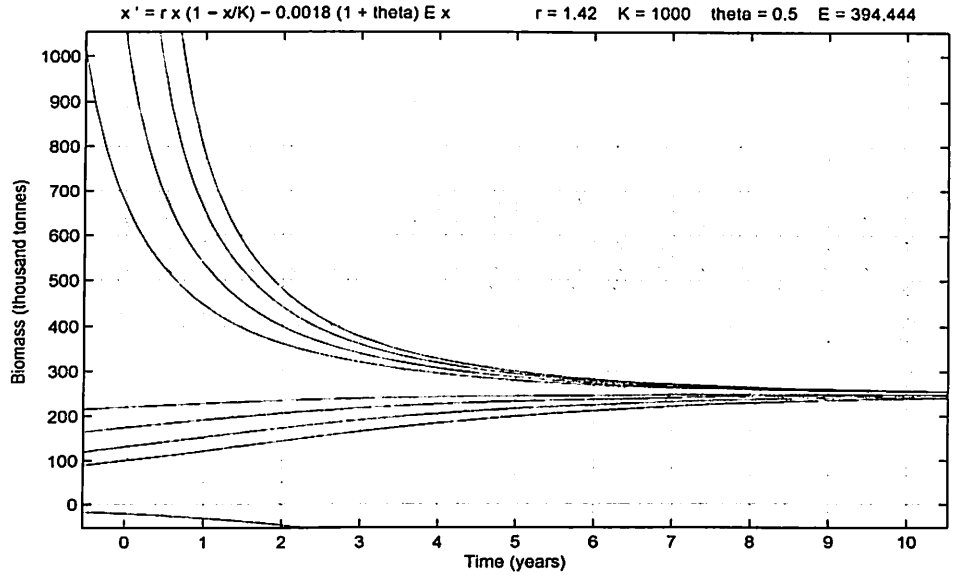

Figure 44: Solution Curves for $E = 394.444$ with $\theta = 0.5$

from the equilibrium levels, 0 and x_θ remain there indefinitely. Hence, an increase in catchability of 50% is equivalent to fishing at an effort rate of one and a half times the effort rate at E_{MSY}. This induces a long-term decline in fish stocks to a level that is 50% of x_{MSY}.

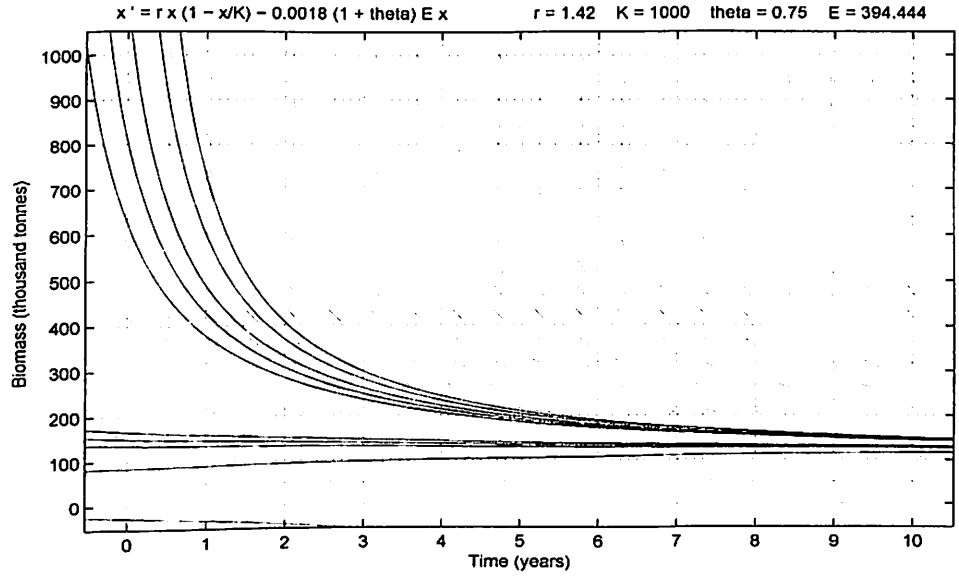

Figure 45: Solution Curves for $E = 394.444$ with $\theta = 0.75$

Solution curves corresponding to the situation where $E = E_{MSY} = 394,444$ trips, with a variation in catchability, $\theta = 0.75$, are presented in Figure 45. It can be observed that there are two hyperbolic equilibrium points: 0 and $x_\theta = 125,000$

tonnes. For any initial biomass level, $x_0 > x_\theta$, the population approaches the equilibrium population, x_θ in the long run. Similarly, for $0 < x_0 < x_\theta$, the population asymptotically approaches x_θ. Thus the biomass level 0 is unstable while x_θ is stable (making the system structurally stable). Of course, biomass levels starting from the equilibrium levels, 0 and x_θ remain there indefinitely. Hence, an increase in catchability of 75% is equivalent to fishing at an effort rate of one and three-quarters times the effort rate at E_{MSY}. This induces a long-term decline in fish stocks to a level that is 25% of x_{MSY}. The question of persistence of the fish stock again arises when the final biomass level for this effort strategy is such low.

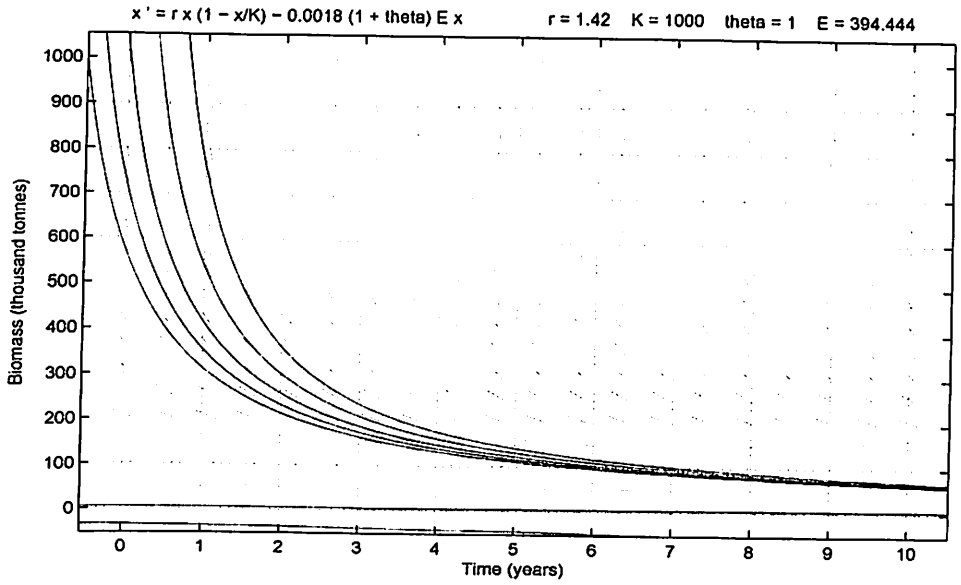

Figure 46: Solution Curves for $E = 394.444$ with $\theta = 1$

Solution curves corresponding to the case where $E = 394{,}444$ trips, with a variation in catchability, $\theta = 1$, are presented in Figure 46. This implies that an increase in catchability of 100% is equivalent to fishing at an effort rate that is twice the effort rate at E_{MSY}. Fishing at two times of E_{MSY} corresponds to the bifurcation point of the model. Thus, for any initial biomass level, $x_0 > 0$, the population approaches the nonhyperbolic equilibrium population, 0 in the long run. Thus, at the bifurcation point ($2 \times E_{MSY}$), the single equilibrium biomass level 0, is semi-stable (making the system structurally unstable). Of course, biomass levels starting from the equilibrium level, 0 remain there indefinitely. Hence,

for any initial biomass level, the long-term population of fish stock is towards extinction.

The bioeconomic model

Incorporating economic parameters into the afore-mentioned biological model (Schaefer model) gives the bioeconomic model. The net revenue is the difference of total sustainable revenue TR_S and total cost TC, where TC is taken to be a quadratic function of E. That is,

$$TC = c_1 E + \frac{c_2}{2} E^2 .$$

As Hanson and Ryan (1998) state, the additional quadratic cost term $\frac{c_2}{2}E^2$, appropriately scaled, may be viewed as a perturbation on the more typically employed linear costs as well as a technique to avoid complexities inherent in the application of singular controls. It is assumed that both c_1 and c_2 are strictly positive, so that costs are a monotonically increasing function and grow rapidly than a linear function of effort. Such a cost function is, however, commonplace and has been employed in fisheries studies by a number of authors (Koenig, 1984; Lewis, 1981, 1982; Sancho & Mitchell, 1977). As emphasised by Sancho and Mitchel (1975) and Holt, Modigliani, Muth and Simon (1960), quadratic costs appear more to reflect reality, as opposed to linear costs.

Open access yield

Operating under an open-access regimen where there is little or no regulation of the resource, effort E tends to a level where the sustainable economic rent or net revenue π_S is zero. That is,

$$\begin{aligned} \pi_S &= ph_S - c_1 E - \frac{c_2}{2} E^2 \\ &= pqEK\left(1 - \frac{qE}{r}\right) - c_1 E - \frac{c_2}{2} E^2 , \end{aligned} \tag{4.50}$$

where p is the price per unit harvest and c_1 and c_2 are the cost components relating to the effort.

Letting Equation (4.50) go to zero gives

$$E_{OAY} = \frac{2r(pqK - c_1)}{2pq^2K + rc_2}. \tag{4.51}$$

where $pqK > c_1$. Notice that E_{OAY} reduces to what was obtained for the linear cost when $c_2 = 0$.

To get the biomass level x_{OAY} associated with E_{OAY}, we have

$$x_{OAY} = K\left(1 - \frac{qE_{OAY}}{r}\right). \tag{4.52}$$

The associated harvest level is

$$h_{OAY} = qE_{OAY}x_{OAY}. \tag{4.53}$$

Maximum economic yield

The level of harvesting that maximises the net revenue is the MEY. The effort level that maximises the sustainable net revenue is found from Equation (4.50) as

$$E_{MEY} = \frac{r(pqK - c_1)}{2pq^2K + rc_2}. \tag{4.54}$$

Also, E_{MEY} reduces to what was obtained for the linear cost when $c_2 = 0$, as well as being 50% of E_{OAY}.

The associated biomass level is

$$x_{MEY} = K\left(1 - \frac{qE_{MEY}}{r}\right), \tag{4.55}$$

and the corresponding harvest level is

$$h_{MEY} = qE_{MEY}x_{MEY}. \tag{4.56}$$

Therefore, the optimal control problem is to maximise the present value (or discounted value) of the net revenue, and can be expressed as

$$\begin{aligned} \max_E Z(E) &= \int_0^\infty e^{-\delta t}\left(pqx - c_1 - \frac{c_2}{2}E\right)E\,dt \\ \text{subject to} \quad \frac{dx}{dt} &= rx\left(1 - \frac{x}{K}\right) - qEx \\ x(0) &= x_0 \\ 0 \le E &\le E_{max}. \end{aligned} \tag{4.57}$$

Optimality of the model

The sufficiency conditions are investigated and discussed in this section. In particular, the existence of an optimal control is determined. Also, the characterisation of the optimal control as well as the existence and uniqueness of the optimality system is sought. The goal is to maximise the present value of the net revenue. Thus, we seek an optimal control E_δ such that

$$Z(E_\delta) = \max\{Z(E) \,|\, E \in U\},$$

where the control set is Lebesgue measurable for an infinite time horizon and defined by

$$U = \{E(t) \,|\, 0 \leq E(t) \leq E_{max},\ t \in [0,\infty)\}.$$

As already intimated, in the solution of an optimal control problem, necessary and sufficient conditions of the problem need to be investigated and verified. We examine the conditions that are sufficient for the existence of an optimal control to the underlying problem.

Theorem 4.5. *There exists an optimal control E_δ that maximises the objective functional $Z(E)$ over the control set U.*

Proof. To prove the given theorem, we invoke a sufficiency result proposed by Fleming and Rishel (1975), Theorem 3.12.

To verify the conditions of Theorem 3.12, we first refer to an existence and uniqueness of the solution of the state equation with bounded coefficients guaranteed by Picard-Lindelof, Theorem 3.5. This gives condition 1 of Theorem 3.12.

For verification of condition 2, by definition, the control set U is closed and convex. In order to verify condition 3, first, the boundedness of the solution to the state equation is determined using the comparison theory of differential equations and the theorem on differential inequalities. Since

$$x' = rx\left(1 - \frac{x}{K}\right) - qEx \leq rx\left(1 - \frac{x}{K}\right)$$

for $0 \leq t < \infty$ and $x_0 > 0$, then

$$x' \leq rx\left(1 - \frac{x}{K}\right).$$

Thus,

$$x(t) \leq \frac{x_0 K}{x_0 + (K - x_0)e^{-rt}}.$$

Therefore, as $t \to \infty$

$$x \leq K.$$

Second, the right hand side of the state equation can be written as

$$S(t,x,E) = rx\left(1 - \frac{x}{K}\right) - qEx \leq rx \leq rK.$$

Hence the bound on the right hand side is given by

$$S(t,x,E) \leq rK.$$

Next, we show that the integrand of the objective functional, $L(t,x,E) = pqxE - c_1E - \frac{c_2}{2}E^2$ is concave on U. First, using the convex property of E; for $0 \leq m \leq 1$ and E_1, $E_2 \in U$, it implies that

$$mE_1^2 + (1-m)E_2^2 \geq [mE_1 + (1-m)E_2]^2.$$

Thus the objective is to show that

$$mL(t,x,E_1) + (1-m)L(t,x,E_2) \leq L(t,x,mE_1 + (1-m)E_2).$$

Commence the proof by noting that the difference of $mL(t,x,E_1) + (1-m)L(t,x,E_2)$ and $L(t,x,mE_1 + (1-m)E_2)$ is given by

$$\begin{aligned}
&mL(t,x,E_1) + (1-m)L(t,x,E_2) - L(t,x,mE_1 + (1-m)E_2) \\
&= mpqxE_1 - mc_1E_1 - m\frac{c_2}{2}E_1^2 + (1-m)pqxE_2 - (1-m)c_1E_2 - (1-m)\frac{c_2}{2}E_2^2 \\
&\quad - pqx[mE_1 + (1-m)E_2] + c_1[mE_1 + (1-m)E_2] + \frac{c_2}{2}[mE_1 + (1-m)E_2]^2.
\end{aligned}$$

Simplifying, this implies the right-hand-side is given by

$$-\frac{c_2}{2}\{mE_1^2 + (1-m)E_2^2 - [mE_1 + (1-m)E_2]^2\} \leq 0,$$

SAM JONAH LIBRARY
UNIVERSITY OF CAPE COAST
CAPE COAST

since from the convexity of E,

$$mE_1^2 + (1-m)E_2^2 - [mE_1 + (1-m)E_2]^2 \geq 0.$$

Hence,

$$mL(t,x,E_1) + (1-m)L(t,x,E_2) \leq L(t,x,mE_1 + (1-m)E_2).$$

This satisfies condition 4.

Finally, to verify condition 5, we note that x and E are bounded. So there exists a $B > 0$ such that $x \leq B$ and $E \leq B$ on $[0,\infty)$, where $B = \max(K, E_{max})$. Therefore,

$$\begin{aligned} pqxE - c_1E - \frac{c_2}{2}E^2 &\leq pqB^2 - \frac{c_2}{2}E^2 \\ &\leq w_1 - w_2E^2, \end{aligned}$$

where

$$w_1 = pqB^2, \quad w_2 = \frac{c_2}{2} \quad \text{and} \quad \eta = 2. \qquad \square$$

Characterisation of optimal control

The optimal control will be characterised—obtaining an explicit formulation for the optimal control level—as well as the optimality system determined. Since the existence of an optimal control to Problem (4.57) has already been established, to derive the necessary conditions for the optimal control, a version of Pontryagin's maximum principle (Pontryagin *et al.*, 1962) is employed.

Theorem 4.6. *Given an optimal control E_δ and a solution to the corresponding state equation, there exists an adjoint variable λ satisfying*

$$\lambda' = \left(\delta - r + \frac{2rx}{K}\right)\lambda - (p-\lambda)qE \tag{4.58}$$

and the transversality condition,

$$\lim_{t\to\infty} \lambda(t) = 0.$$

Furthermore, E_δ can be presented as

$$E_\delta = \min\left(E_{max}, \left(\frac{(p-\lambda)qx - c_1}{c_2}\right)^+\right),$$

where the notation is given by

$$n^+ = \begin{cases} n & \text{if} \quad n > 0, \\ 0 & \text{if} \quad n \leq 0. \end{cases}$$

(Fister & Panetta, 2000; Royden, 1988)

Proof. The current value Hamiltonian for the optimal control problem (4.57) is

$$H = \left(pqx - c_1 - \frac{c_2}{2}E\right)E + \lambda\left[rx\left(1 - \frac{x}{K}\right) - qEx\right]. \tag{4.59}$$

Therefore, we obtain Equation (4.58) from the adjoint equation

$$\lambda' = \delta\lambda - \frac{\partial H}{\partial x}.$$

The optimality condition is given by

$$\frac{\partial H}{\partial E} = pqx - c_1 - c_2E - \lambda qx = 0.$$

Thus,

$$E_\delta = \frac{(p-\lambda)qx - c_1}{c_2}. \tag{4.60}$$

The characterisation of the optimal control is

$$\begin{cases} E_\delta = 0 & \text{if} \quad \frac{\partial H}{\partial E} < 0, \\ 0 \leq E_\delta \leq E_{max} & \text{if} \quad \frac{\partial H}{\partial E} = 0, \\ E_\delta = E_{max} & \text{if} \quad \frac{\partial H}{\partial E} > 0. \end{cases} \tag{4.61}$$

By standard control arguments involving the bounds on the control, we have the following,

$$E_\delta = 0 \qquad \text{if} \qquad \frac{\partial H}{\partial E} < 0.$$

This implies

$$pqx - c_1 - c_2E - \lambda qx < 0,$$

and so

$$\frac{(p-\lambda)qx-c_1}{c_2} < E_\delta = 0.$$

Thus,

$$\frac{(p-\lambda)qx-c_1}{c_2} < 0.$$

Similarly,

$$E_\delta = E_{max} \qquad \text{if} \qquad \frac{\partial H}{\partial E} > 0.$$

This implies

$$pqx - c_1 - c_2E - \lambda qx > 0,$$

and so

$$\frac{(p-\lambda)qx-c_1}{c_2} > E_\delta = E_{max}.$$

Thus,

$$\frac{(p-\lambda)qx-c_1}{c_2} > E_{max}.$$

Hence,

$$E_\delta = \begin{cases} 0 & \text{if} \quad \dfrac{(p-\lambda)qx-c_1}{c_2} < 0, \\ \dfrac{(p-\lambda)qx-c_1}{c_2} & \text{if} \quad 0 \le \dfrac{(p-\lambda)qx-c_1}{c_2} \le E_{max}, \\ E_{max}, & \text{if} \quad \dfrac{(p-\lambda)qx-c_1}{c_2} > E_{max}. \end{cases}$$

This implies

$$E_\delta = \begin{cases} 0 & \text{if} \quad \lambda > p - \dfrac{c_1}{qx}, \\ \dfrac{(p-\lambda)qx-c_1}{c_2} & \text{if} \quad p - \dfrac{(c_1+c_2E_{max})}{qx} \le \lambda \le p - \dfrac{c_1}{qx}, \\ E_{max}, & \text{if} \quad \lambda < p - \dfrac{(c_1+c_2E_{max})}{qx}. \end{cases} \tag{4.62}$$

Therefore, the optimal control comprises both the boundary solutions (or binding constraints) and the interior solution. The boundary solutions indicate that the resource should be harvested if and only if the marginal revenue of harvest due to the application of maximum fishing effort exceeds the current value shadow price of the resource. In compact notation,

$$E_\delta = \min\left(E_{max}, \left(\frac{(p-\lambda)qx-c_1}{c_2}\right)^+\right).$$

The optimality system comprises the state equation coupled with the adjoint equation and the initial and transversality conditions together with the characterisation of the optimal control.

Therefore,

$$x' = rx\left(1-\frac{x}{K}\right) - q\min\left(E_{max}, \left(\frac{(p-\lambda)qx - c_1}{c_2}\right)^+\right)x,$$

$$\lambda' = \left(\delta - r + \frac{2rx}{K}\right)\lambda - (p-\lambda)q\min\left(E_{max}, \left(\frac{(p-\lambda)qx - c_1}{c_2}\right)^+\right),$$

$$\text{with} \quad x(0) = x_0 \quad \text{and} \quad \lim_{t\to\infty}\lambda(t) = 0. \qquad \square$$

The existence of the optimal control has already been established by Theorem 3.12. We wish to ensure the uniqueness of the so established optimal control.

Given the a priori boundedness of the state and adjoint equations; and also the state equation being continuously differentiable, then through the application of the mean value theorem the state equation satisfies the Lipschitz condition with regard to the state variable. Thus, we obtain the uniqueness of the optimality system for small time intervals. There is a restriction on the length of the time interval in order to guarantee the uniqueness of the optimality system. This small time condition is due to the opposite time orientations of the state and adjoint equations; the state equation has initial value, and the adjoint equation has a terminal value.

Furthermore, the uniqueness of the solutions of the optimality system guarantees uniqueness of the optimal control (Lenhart & Workman, 2007; Okosun, Makinde & Takaidza, 2013).

Numerical simulations

The model will be subjected to numerical analyses and the results illustrated graphically. First, a number of simulations are performed with the maximum effort set at the MEY and OAY levels, while varying the initial stock level. Initially, we shall consider the transient case where T is finite, and then extend it to the equilibrium scenario where $T \to \infty$.

The maximum effort maintained at an appropriate sustainable yield level is considered second. Simulations will be carried out while varying the catchability coefficient of the model to take into account the illegal and unapproved fishing methods employed by the fishermen. The catchability coefficient can be thought of conceptually as the probability of any single fish being caught. Catchability is also called fishing power, or sometimes gear efficiency (Hilborn & Walters, 1992).

The linear and quadratic costs are depicted in Figure 47. The perturbation in the linear costs is such that when the effort is at the MSY level, the quadratic costs are 25% greater than the linear costs.

In the simulations, c_1 takes the value of the linear cost $c = \$195/\text{trip/year}$ whereas c_2 is computed as

$$\begin{aligned} c_2 &= 2\left(\frac{0.25c_1}{E_{MSY}}\right) \\ &= \$2.47 \times 10^{-4}/\text{trip}^2/\text{year}. \end{aligned}$$

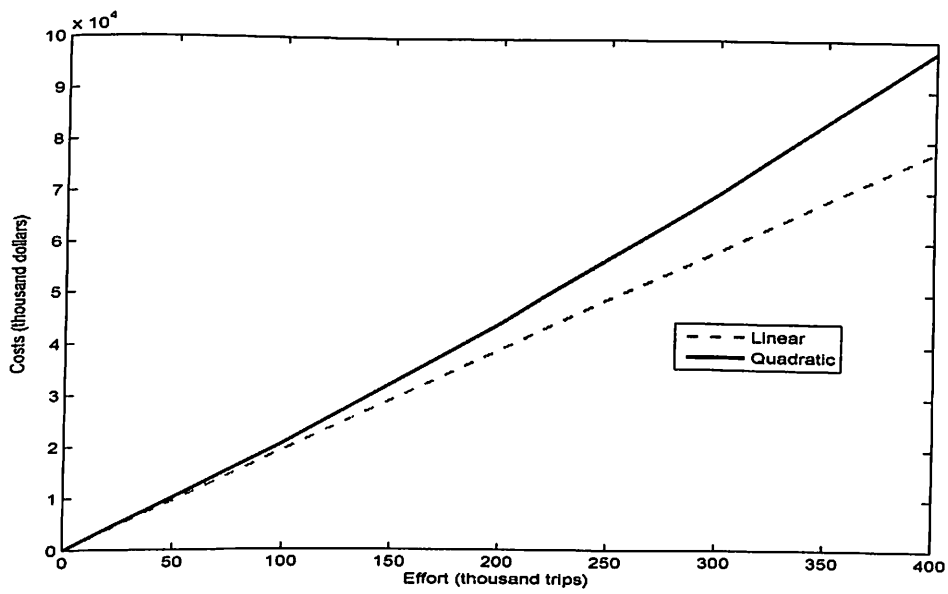

Figure 47: Linear and Quadratic Costs

The initial simulations are based on the Schaefer model assumption of constant catchabilty ($\theta = 0$); later simulations will incorporate sensitivity analysis of the catchability. Simulation results for the fishing effort and stock size relating to the case where $E_{max} = 296,380$ trips, $T = 1$ year, $x_0 = 550,000$ tonnes and $x_0 =$

750,000 tonnes are presented in Figure 48. In Figure 48 (a), it is observed that when the maximum effort rate E_{max} is set at the MEY level, the optimal effort rate appears to follow the same path of around 296,250 trips for the one-year horizon for the different initial biomass levels. However, the fish biomass levels follow different trajectories. The biomass decreases for the higher initial value to about 670,000 tonnes, and increases for the lower value of 550,000 tonnes to about 578,000 tonnes (Figure 48 (b)).

Assuming an initial population size of 550,000 tonnes, the total net revenue over the one-year horizon corresponding to the given rate of fishing effort is computed as US$106,430,000; a decrease of 29% of the net revenue for $x_0 = 750,000$ tonnes.

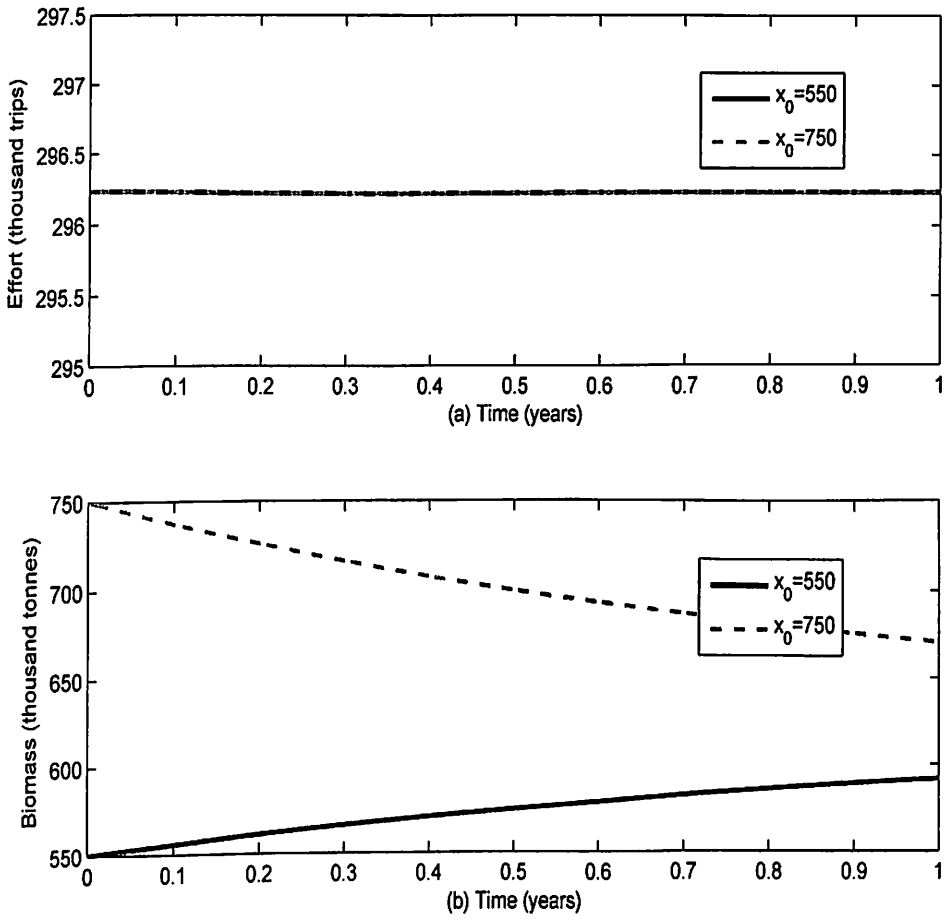

Figure 48: (a) Effort and (b) Biomass Levels for $E_{max} = 296,380$, $x_0 = 550,000$; 750,000 and $T = 1$

Simulation results for the fishing effort and stock size relating to the case

where $E_{max} = 296,380$ trips and $T = 20$ years are presented in Figure 49. In Figure 49 (a), it is observed that when the maximum effort rate E_{max} is set at the MEY level, the optimal effort rate appears to initially follow different trajectories for the initial biomass levels. The lower initial biomass level effort rate starts at 245,827 trips. However, the effort rates soon follow the same path very close to the MEY level throughout the twenty-year horizon for both initial biomass levels. However, the fish biomass levels follow different trajectories. The biomass decreases for the higher initial value and increases for the lower initial value of 550,000 tonnes to the equilibrium value of around 624,000 tonnes (Figure 49 (b)).

It is interesting to observe that the fishery will attain equilibrium status even at lower initial biomass levels provided that the rate of fishing effort is kept at the MEY level.

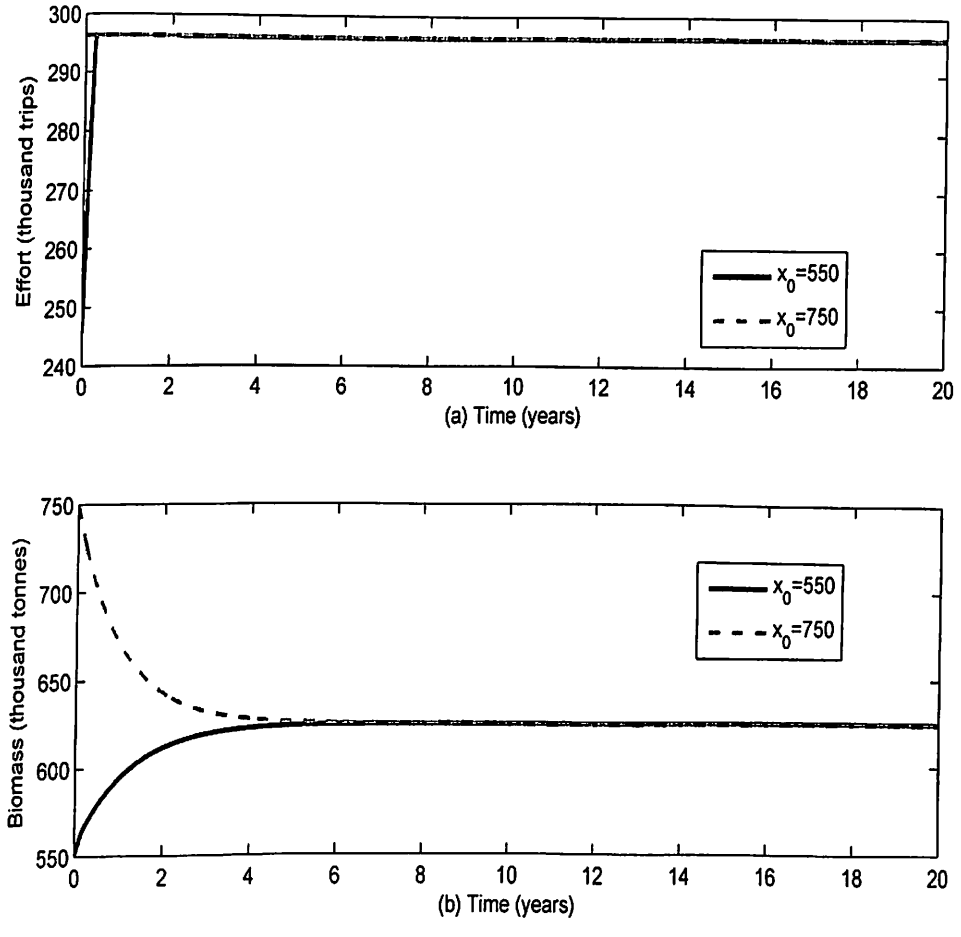

Figure 49: (a) Effort and (b) Biomass Levels for $E_{max} = 296,380$, $x_0 = 550,000$; $750,000$ and $T = 20$

Assuming an initial population size of 550,000 tonnes, the total net revenue over the twenty-year horizon corresponding to the given rate of fishing effort is computed as US$806,620,000; a decrease of 7% of the net revenue for $x_0 =$ 750,000 tonnes.

Simulation results for the fishing effort and stock size relating to the case where $E_{max} = 592,761$ trips, $T = 1$ year, $x_0 = 550,000$ tonnes and $x_0 = 750,000$ tonnes are presented in Figure 50. In Figure 50 (a), it is observed that when the maximum effort rate E_{max} is set at the OAY level, the optimal effort rate appears to initially follow different trajectories for the initial biomass levels. The lower initial biomass level effort rate starts at 325,341 trips. However, the effort rates soon follow the same path of nearly 592,200 trips for the one-year horizon for both initial biomass levels. On the other hand, the fish biomass levels follow different trajectories. The biomass decreases for the higher initial value to about 470,000 tonnes, and decreases also for the lower initial value of 550,000 tonnes to a little above 440,000 tonnes (Figure 50 (b)).

Assuming an initial population size of 550,000 tonnes, the total net revenue over the one-year horizon corresponding to the given rate of fishing effort is computed as US$134,000,000; a decrease of 33% of the net revenue for $x_0 = 750,000$ tonnes.

Simulation results for the fishing effort and stock size relating to the case where $E_{max} = 592,761$ trips and $T = 1.5$ years are presented in Figure 51. In Figure 51 (a), it is observed that when the maximum effort rate E_{max} is set at the OAY level, the optimal effort rate appears to follow the same path of almost 592,761 trips for both initial biomass levels throughout the one and half-year horizon; except for a period where it is convex, attaining a minimum value of 498,056 trips. However, the fish biomass levels follow different trajectories. The biomass decreases for the higher initial value to a little below 450,000 tonnes, and also decreases for the initial lower value of 550,000 tonnes to around 445,000 tonnes; see Figure 51 (b).

Assuming an initial population size of 550,000 tonnes, the total net revenue

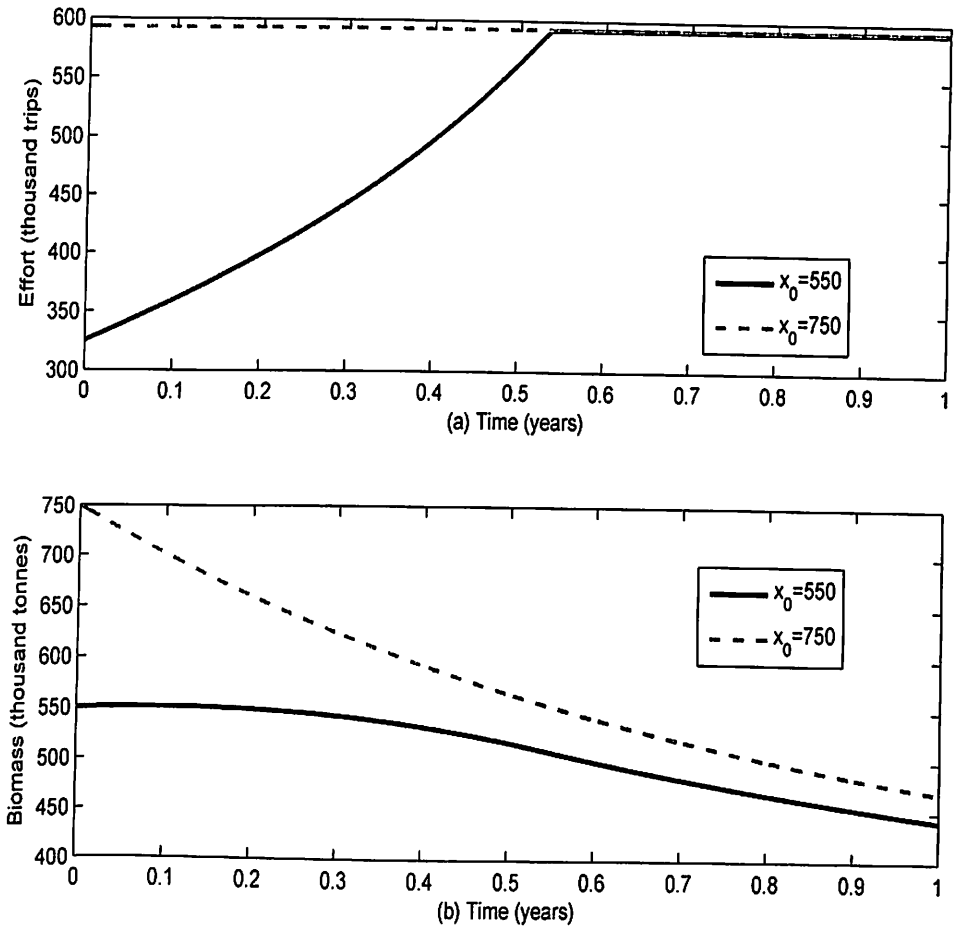

Figure 50: (a) Effort and (b) Biomass Levels for $E_{max} = 592,761$, $x_0 = 550,000$; $750,000$ and $T = 1$

over the one and half-year horizon corresponding to the given rate of fishing effort is computed as US$185,260,000; a decrease of 30% of the net revenue for $x_0 = 750,000$ tonnes.

It is instructive to note that when the rate of fishing effort is pegged at the OAY level, the iterates failed to converge beyond a time horizon of three years no matter the initial biomass level.

In the standard Gordon-Schaefer model (where $\theta = 0$ and $c_2 = 0$) the OSY is computed as 351,328 trips per annum. Therefore to ensure sustainability of the resource, the annual rate of effort of the quadratic model should be less than 351,328 trips (since the higher fishing costs in the quadratic model has the tendency to reduce effort rate). For the quadratic model, set the sustainable yield (SY) at 315,000 trips per annum.

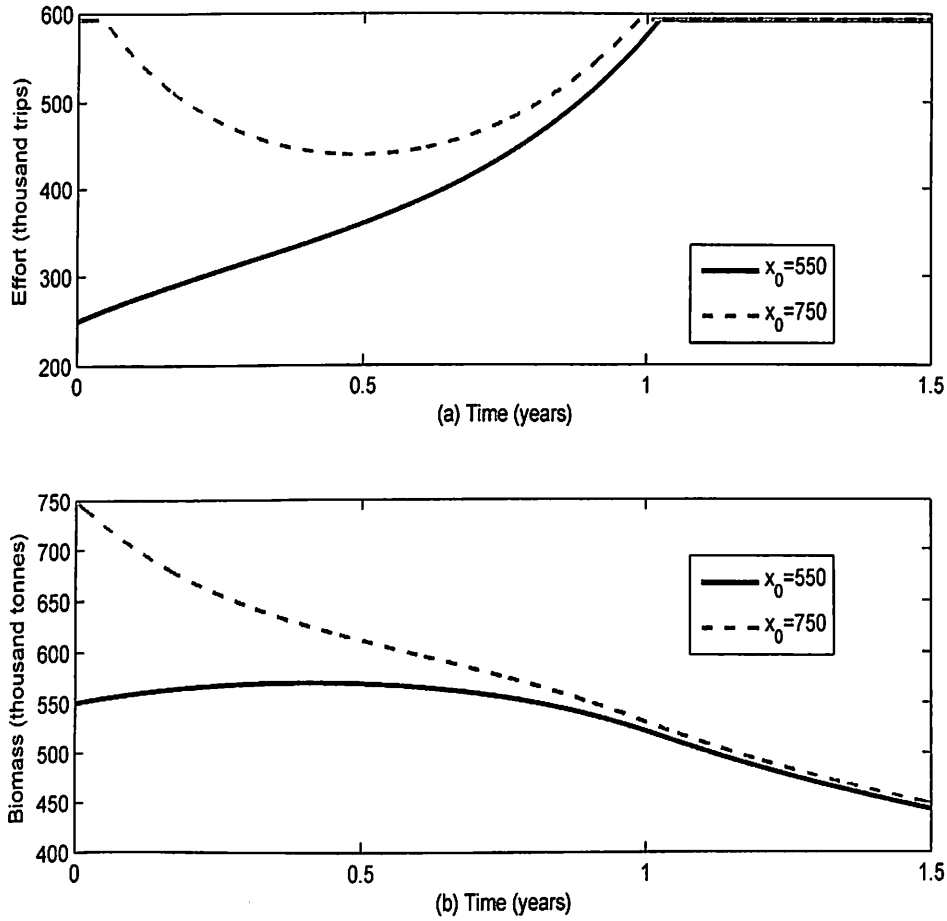

Figure 51: (a) Effort and (b) Biomass Levels for $E_{max} = 592,761$, $x_0 = 550,000$; $750,000$ and $T = 1.5$

Simulation results for the fishing effort and stock size relating to the case where $x_0 = 750,000$ tonnes, $T = 1$ year, $E_{max} = 296,380$ trips and $E_{max} = 315,000$ trips are presented in Figure 52. In Figure 52 (a), it is observed that when the maximum effort rate E_{max} is set at the MEY and SY levels, the optimal effort rate appears to follow different paths of nearly $296,380$ and $315,000$ trips corresponding respectively to the MEY and SY levels for the one-year horizon . Furthermore, the fish biomass levels follow different trajectories. The biomass decreases for both effort levels, to a value of around $670,000$ tonnes for the MEY, and a value of a little below $657,000$ tonnes for SY (Figure 52 (b)).

Assuming an initial population size of $750,000$ tonnes, the total net revenues over the one-year horizon corresponding to the effort levels at MEY and SY are computed as US$145,460,000 and US$151,300,000, respectively.

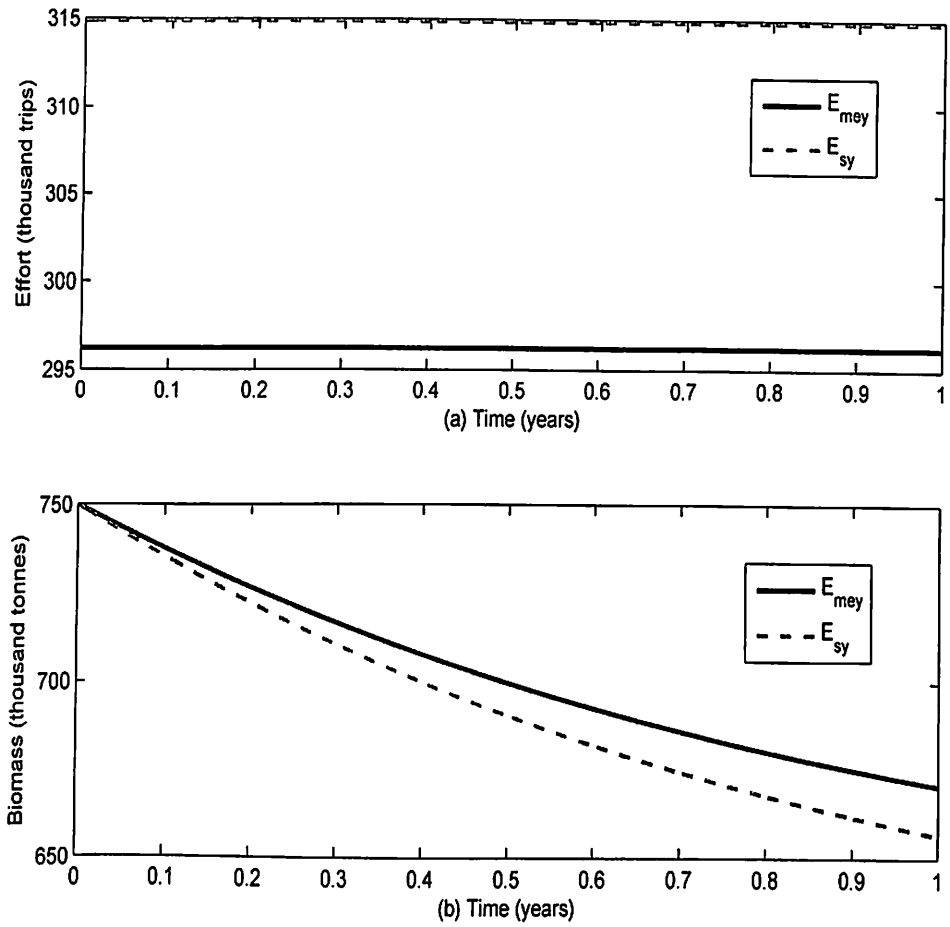

Figure 52: (a) Effort and (b) Biomass levels for $E_{max} = 296,380$; $315,000$, $x_0 = 750,000$ and $T = 1$

Simulation results for the fishing effort and stock size relating to the case where $x_0 = 750,000$ tonnes, $T = 20$ years, $E_{max} = 296,380$ trips, and $E_{max} = 315,000$ trips are presented in Figure 53. In Figure 53 (a), it is observed that when the maximum effort rate E_{max} is set at the MEY and SY levels, the optimal effort rate appears to follow different paths corresponding to almost the equilibrium values at the MEY and SY levels throughout the twenty-year horizon. Furthermore, the fish biomass levels follow different trajectories. The biomass decreases for both effort levels, to their equilibrium levels of about $624,000$ tonnes for the MEY, and about $600,000$ tonnes for SY (Figure 53 (b)).

Assuming an initial population size of $750,000$ tonnes, the total net revenues over the twenty-year horizon corresponding to the effort levels at MEY and SY are computed as US\$$866,530,000$ and US\$$873,300,000$, respectively.

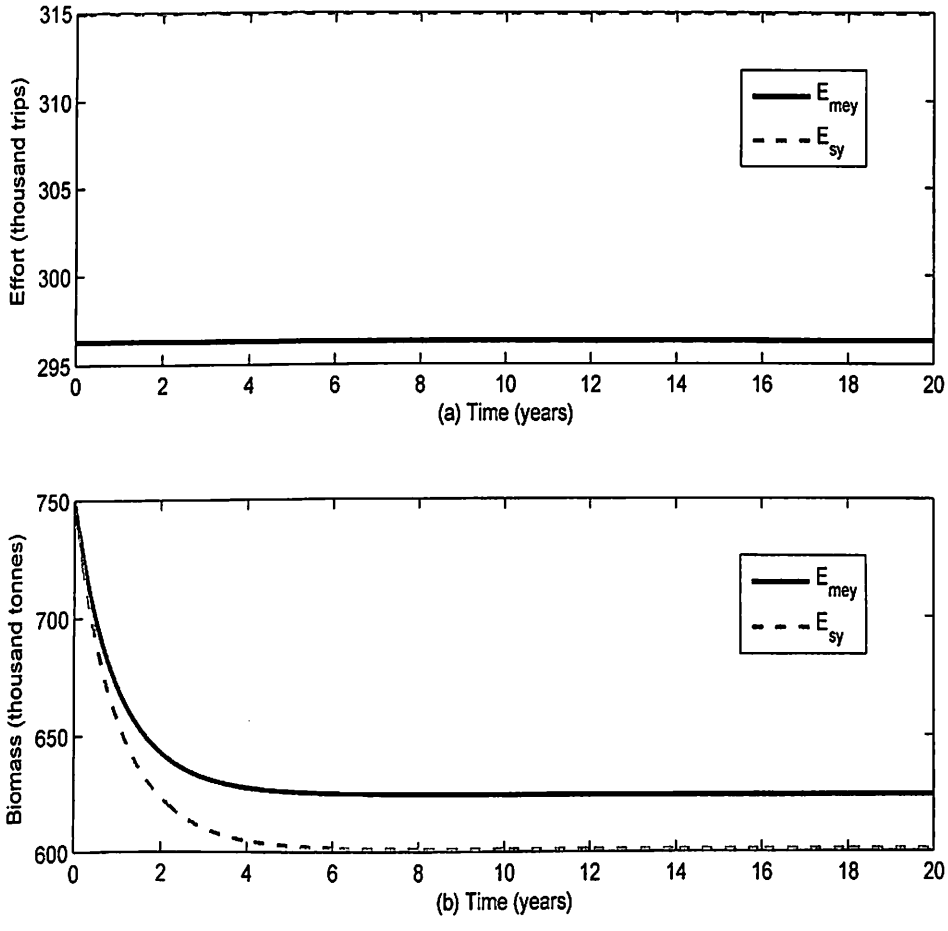

Figure 53: (a) Effort and (b) Biomass Levels for $E_{max} = 296,380$; $315,000$, $x_0 = 750,000$ and $T = 20$

Simulation results for the fishing effort and stock size relating to the case where $x_0 = 550,000$ tonnes, $T = 1$ year, $E_{max} = 296,380$ trips, and $E_{max} = 315,000$ trips are presented in Figure 54. In Figure 54 (a), it is observed that when the maximum effort rate E_{max} is set at the MEY and SY levels, the optimal effort rate appears to follow different paths of around $296,200$ and $315,000$ trips corresponding respectively to the MEY and SY levels throughout the one-year horizon. Furthermore, the fish biomass levels follow different trajectories. The biomass increases for the effort level at MEY to a value of around $592,000$ tonnes, and also increases for the effort level at SY to a value of about $578,000$ tonnes (Figure 54 (b)).

Assuming an initial population size of $550,000$ tonnes, the total net revenues over the one-year horizon corresponding to the effort levels at MEY and SY are

computed as US$106,430,000 and US$110,140,000, respectively.

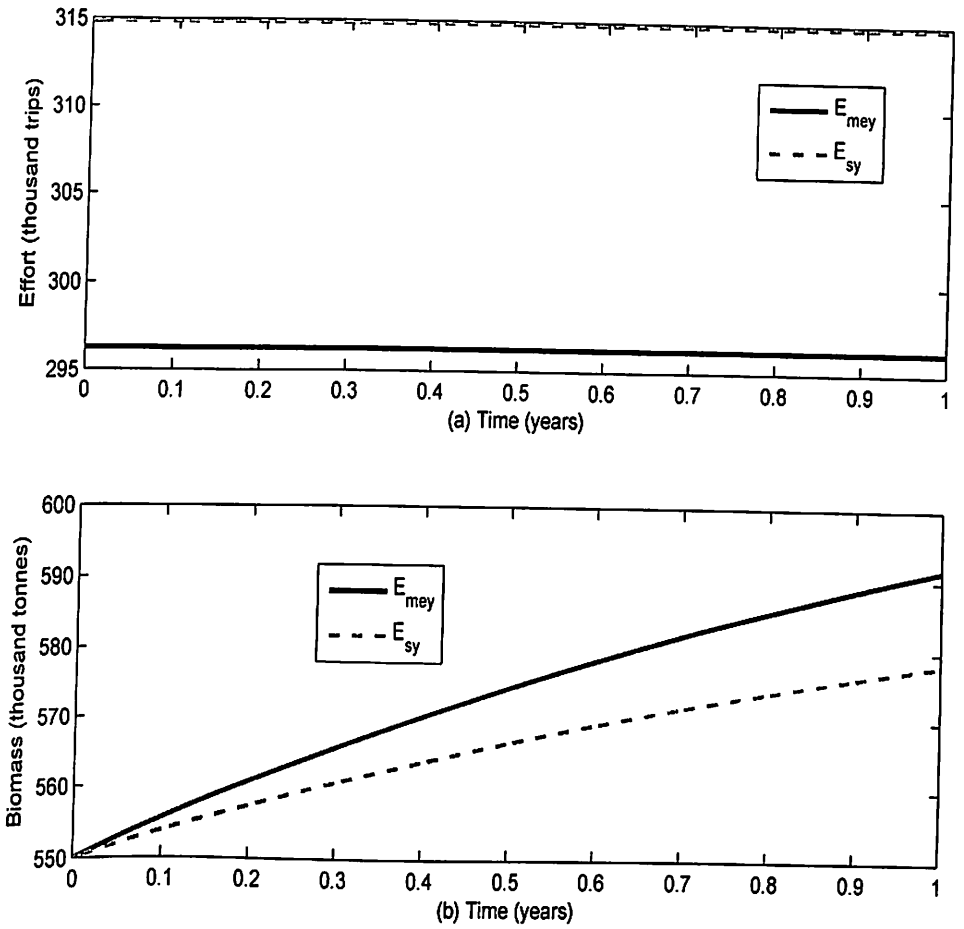

Figure 54: (a) Effort and (b) Biomass Levels for $E_{max} = 296,380$; $315,000$, $x_0 = 550,000$ and $T = 1$

Simulation results for the fishing effort and stock size relating to the case where $x_0 = 550,000$ tonnes, $T = 20$ years, $E_{max} = 296,380$ trips and $E_{max} = 315,000$ trips are presented in Figures 55. In Figure 55 (a), it is observed that when the maximum effort rate E_{max} is set at the MEY and SY levels, the optimal effort rate appears to follow different paths corresponding respectively to the equilibrium MEY and SY levels throughout the twenty-year horizon. Furthermore, the fish biomass levels follow different trajectories. The biomass increases for effort level at MEY to its equilibrium value of 624,000 tonnes, and also increases for effort level at SY to its equilibrium value of 600,000 tonnes (Figure 55 (b)).

Assuming an initial population size of 550,000 tonnes, the total net revenues over the twenty-year horizon corresponding to the effort levels at MEY and SY

are computed as US$806,620,000 and US$809,690,000, respectively.

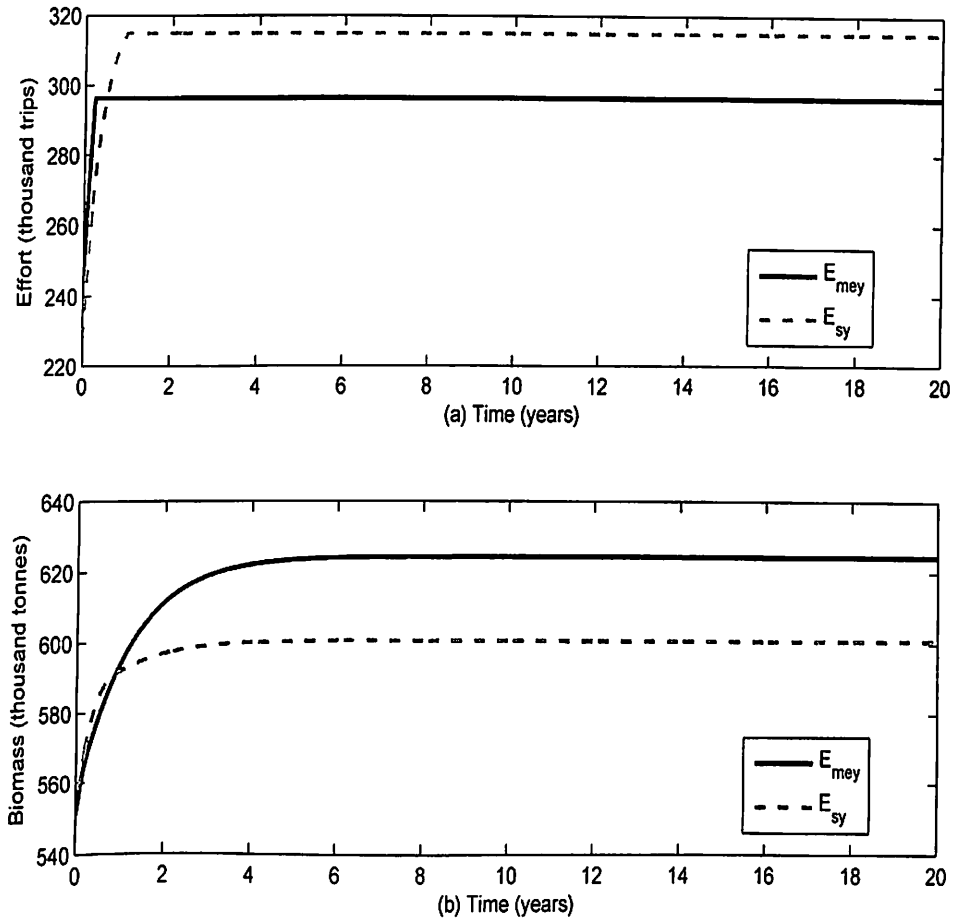

Figure 55: (a) Effort and (b) Biomass Levels for $E_{max} = 296,380$; $315,000$, $x_0 = 550,000$ and $T = 20$

Simulation results for the fishing effort and stock size relating to the case where $x_0 = 750,000$ tonnes, $T = 1$ year, $E_{max} = 200,000$ trips, $\theta = 0$ and $\theta = 0.25$ are presented in Figure 56. In Figure 56 (a), it is observed that when the maximum effort rate E_{max} is set at about half the MSY level, the optimal effort rate appears to follow the same path of a little below 200,000 trips corresponding to both values of θ for the one-year horizon. However, the fish biomass levels follow different trajectories. The biomass decreases for both catchability levels, to a value of around 748,000 tonnes for $\theta = 0$, and a value of about 707,000 tonnes for $\theta = 0.25$ (Figure 56 (b)).

Assuming an initial population size of 750,000 tonnes, the total net revenues over the one-year horizon corresponding to $\theta = 0$ and $\theta = 0.25$ are computed

as US$109,320,000 and US$140,970,000, respectively. In other words, a 25% increment in the catchability results in a revenue increase of 29%, and a decrease in final biomass level of about 5%.

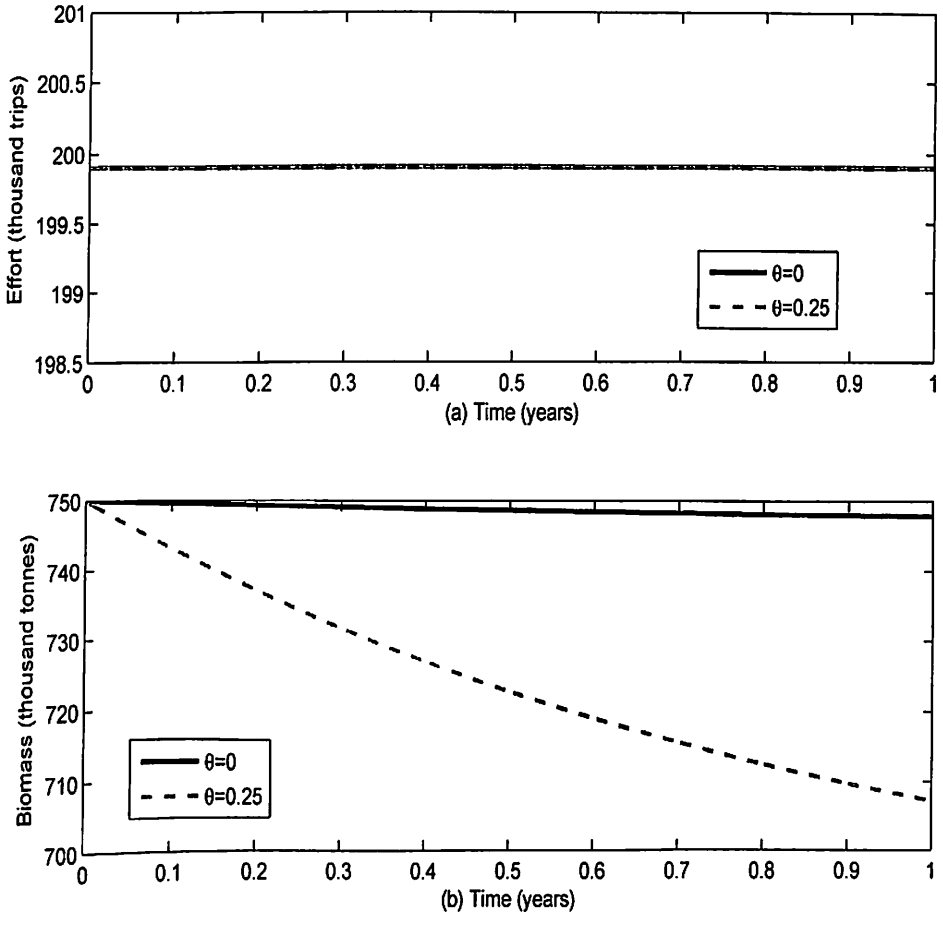

Figure 56: (a) Effort and (b) Biomass Levels for $E_{max} = 200,000$, $\theta = 0$, 0.25 and $T = 1$

Simulation results for the fishing effort and stock size relating to the case where $x_0 = 750,000$ tonnes, $T = 20$ years, $E_{max} = 200,000$ trips, $\theta = 0$ and $\theta = 0.25$ are presented in Figure 57. In Figure 57 (a), it is observed that when the maximum effort rate E_{max} is set at the MSY level, the optimal effort rate appears to follow the same path of around 200,000 trips corresponding to both values of θ throughout the twenty-year horizon. However, the fish biomass levels follow different trajectories. The biomass decreases for both catchability levels to their respective equilibrium levels of around 747,000 tonnes for $\theta = 0$ and around 683,000 tonnes for $\theta = 0.25$ (Figure 57 (b)).

Assuming an initial population size of 750,000 tonnes, the total net revenues over the twenty-year horizon corresponding to $\theta = 0$ and $\theta = 0.25$ are computed as US\$743,540,000 and US\$905,340,000, respectively. In other words, a 25% increment in the catchability results in a revenue increase of about 22%, and a decrease in final biomass level of 9%.

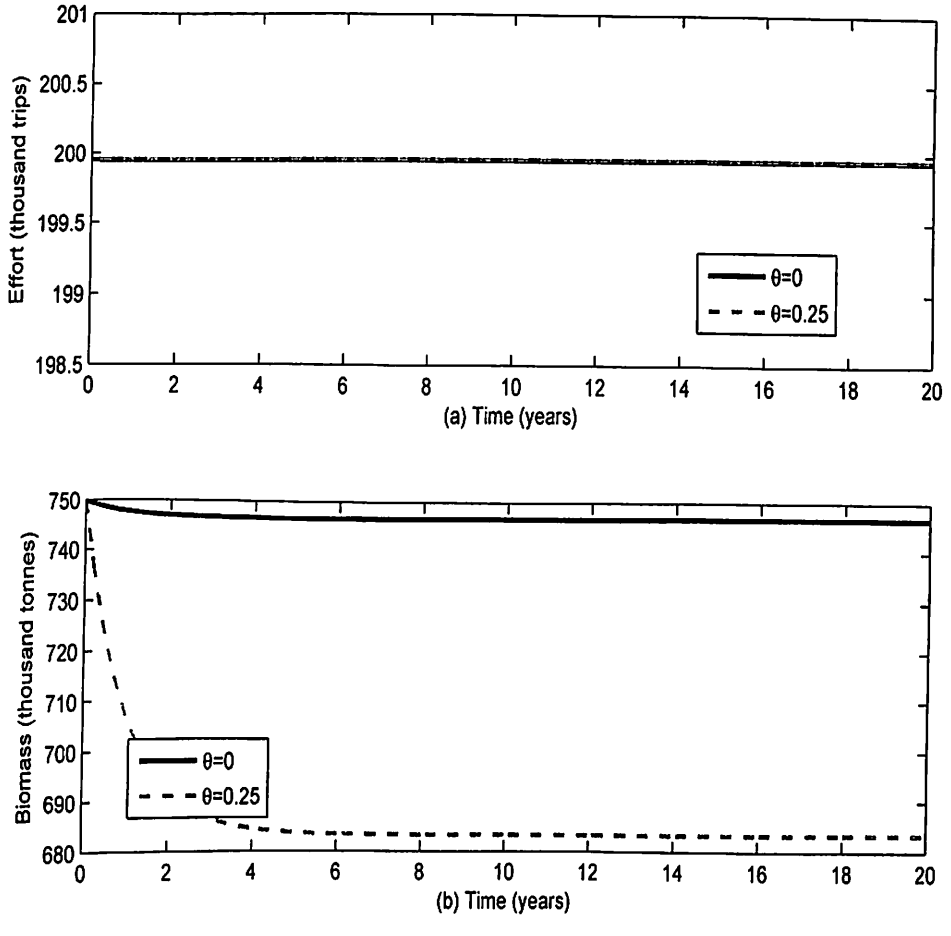

Figure 57: (a) Effort and (b) Biomass Levels for $E_{max} = 200,000$, $\theta = 0$, 0.25 and $T = 20$

Simulation results for the fishing effort and stock size relating to the case where $x_0 = 750,000$ tonnes, $T = 1$ year, $E_{max} = 200,000$ trips, $\theta = 0$ and $\theta = 0.5$ are presented in Figure 58. In Figure 58 (a), it is observed that when the maximum effort rate is set at 200,000 trips the optimal effort rate appears to follow the same path of a little below 200,00 trips corresponding to both values of θ for the one-year horizon. However, the fish biomass levels follow different trajectories. The biomass decreases for both catchability levels, to a value of around 748,000

tonnes for $\theta = 0$, and a value of about 668,000 tonnes for $\theta = 0.5$ (Figure 58 (b)).

Assuming an initial population size of 750,000 tonnes, the total net revenues over the one-year horizon corresponding to $\theta = 0$ and $\theta = 0.5$ are computed as US$109,320,000 and US$170,480,000, respectively. In other words, a 50% increment in the catchability results in a revenue increase of 56%, and a decrease in final biomass level of about 11%.

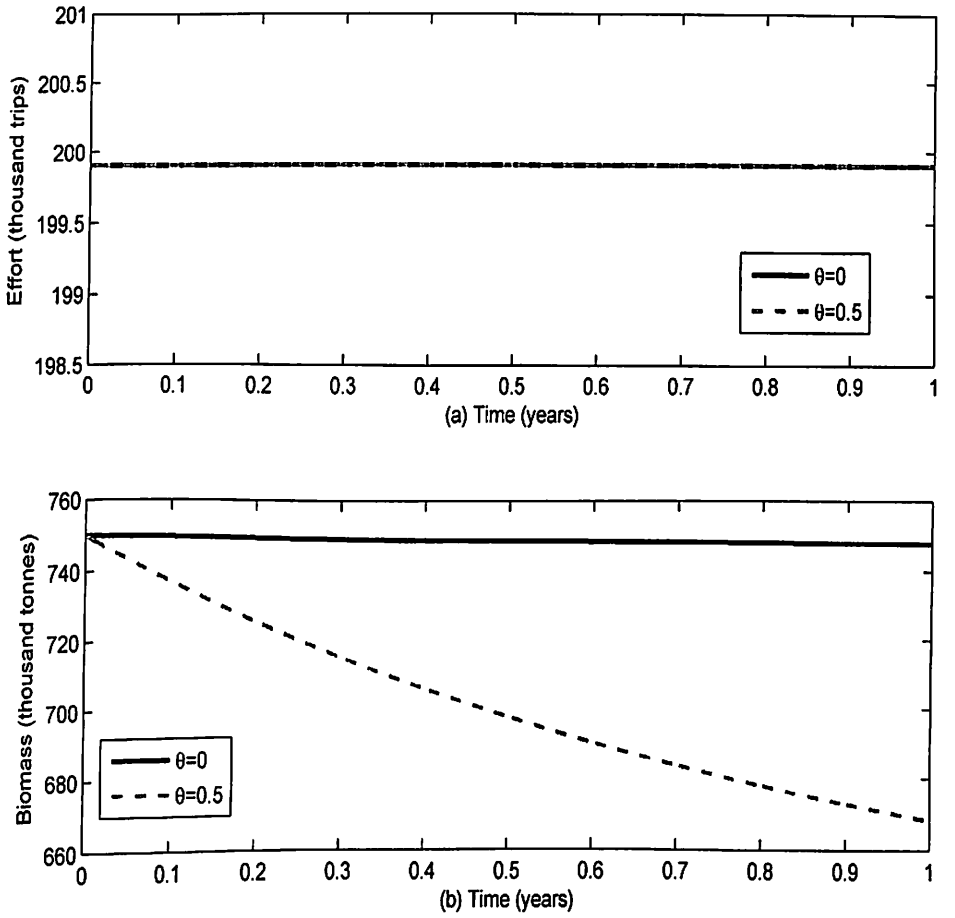

Figure 58: (a) Effort and (b) Biomass Levels for $E_{max} = 200,000$, $\theta = 0$, 0.5 and $T = 1$

Simulation results for the fishing effort and stock size relating to the case where $x_0 = 750,000$ tonnes, $T = 20$ years, $E_{max} = 200,000$ trips, $\theta = 0$ and $\theta = 0.5$ are presented in Figure 59. In Figure 59 (a), it is observed that when the maximum effort rate is 200,000 trips, the optimal effort rate appears to follow the same trajectory of around 200,000 trips for both catchability levels throughout the twenty-year horizon. However, the fish biomass levels follow different

trajectories. The biomass decreases for both catchability levels to their respective equilibrium levels of around 747,000 tonnes for $\theta = 0$, and around 620,000 tonnes for $\theta = 0.5$ (Figure 59 (b)).

Assuming an initial population size of 750,000 tonnes, the total net revenues for the twenty-year horizon corresponding to $\theta = 0$ and $\theta = 0.5$ are computed as US$743,540,000 and US$1,031,000,000, respectively. In other words, a 50% increment in the catchability results in a revenue increase of 39%, and a decrease in final biomass level of 17%.

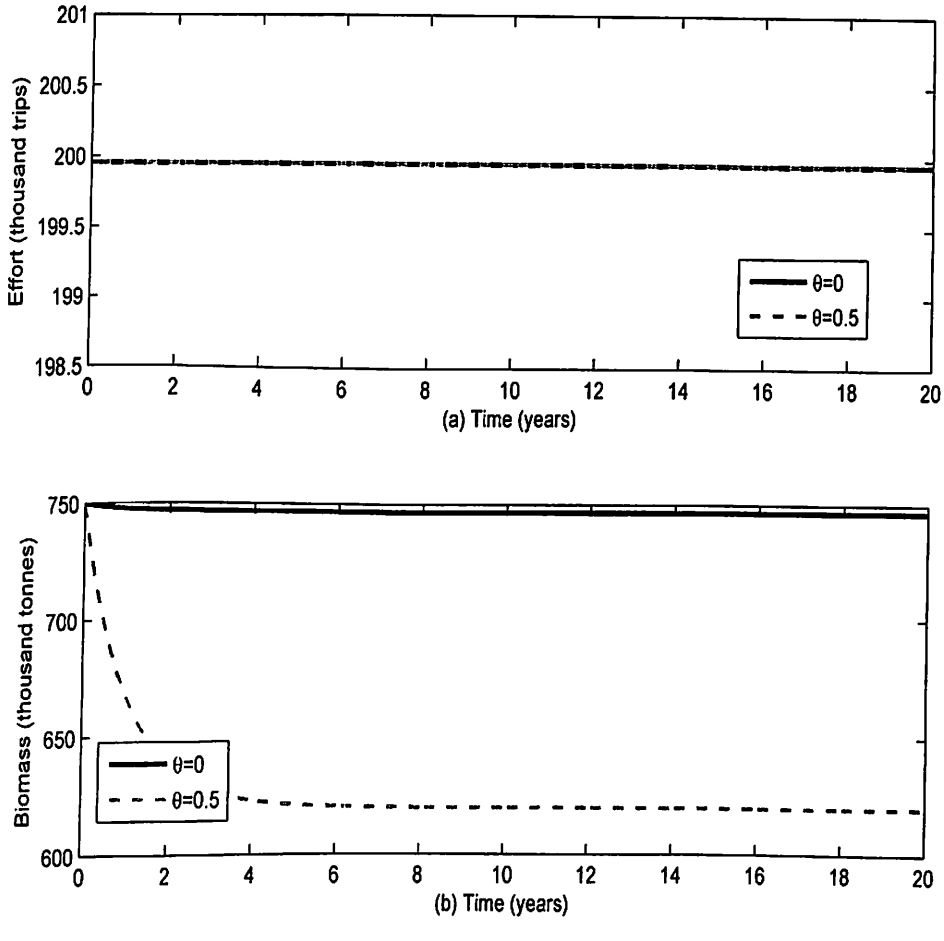

Figure 59: (a) Effort and (b) Biomass Levels for $E_{max} = 200,000$, $\theta = 0$, 0.5 and $T = 20$

Simulation results for the fishing effort and stock size relating to the case where $x_0 = 750,000$ tonnes, $T = 1$ year, $E_{max} = 200,000$ trips, $\theta = 0$ and $\theta = 0.75$ are presented in Figure 60. In Figure 60 (a), it is observed that when the maximum effort rate is set at 200,000 trips, the optimal effort rate appears to follow

the same path of about 200,000 trips corresponding to both values of θ for the one-year horizon. However, the fish biomass levels follow different trajectories. The biomass decreases for both catchability levels, to a value of around 748,000 tonnes for $\theta = 0$, and a value of about 630,000 tonnes for $\theta = 0.75$ (Figure 60 (b)).

Assuming an initial population size of 750,000 tonnes, the total net revenues over the one-year horizon corresponding to $\theta = 0$ and $\theta = 0.75$ are computed as US$109,320,000 and US$197,960,000, respectively. In other words, a 75% increment in the catchability results in a revenue increase of 45%, and a decrease in final biomass level of about 16%.

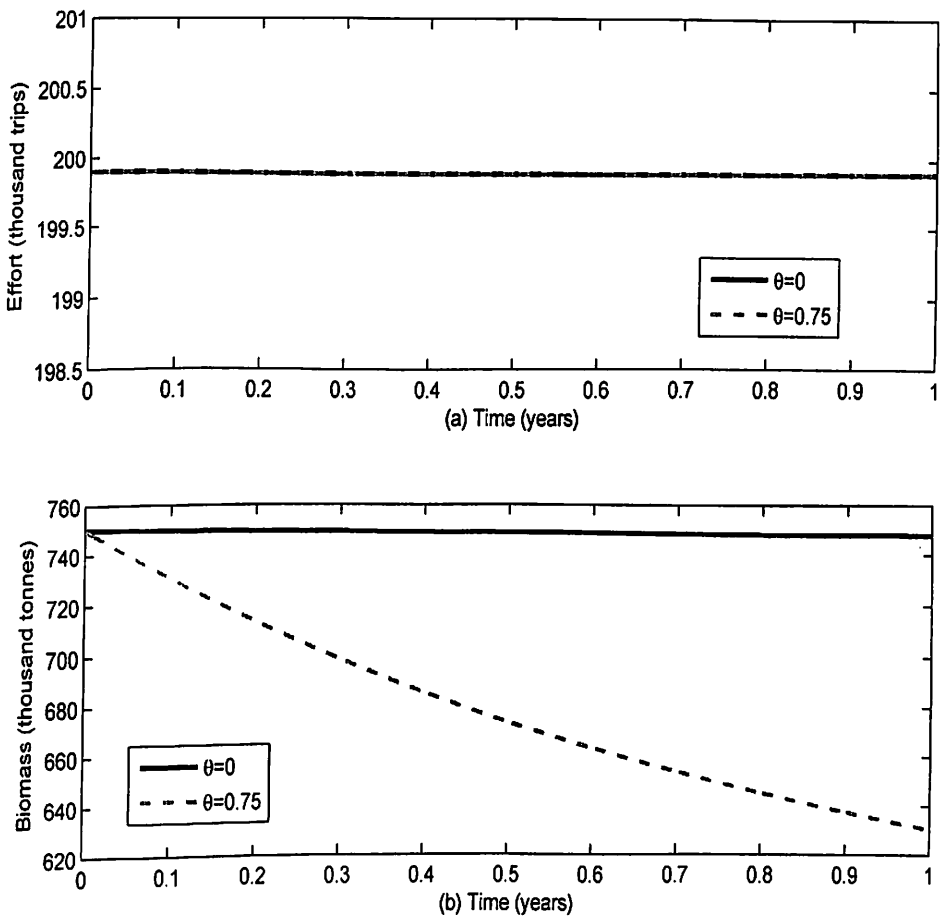

Figure 60: (a) Effort and (b) Biomass Levels for $E_{max} = 200,000$, $\theta = 0$, 0.75 and $T = 1$

Simulation results for the fishing effort and stock size relating to the case where $x_0 = 750,000$ tonnes, $T = 20$ years, $E_{max} = 200,000$ trips, $\theta = 0$ and

$\theta = 0.75$ are presented in Figures 61. In Figure 61 (a), it is observed that when the maximum effort rate E_{max} is set at 200,000 trips, the optimal effort rate appears to follow the same trajectory of almost 200,000 trips for both $\theta = 0$ and $\theta = 0.75$ throughout the twenty-year horizon. However, the fish biomass levels follow different trajectories. The biomass decreases for both catchability levels, to the equilibrium value of 747,000 tonnes for $\theta = 0$, and a value of about 557,000 tonnes for $\theta = 0.75$ (Figure 61 (b)).

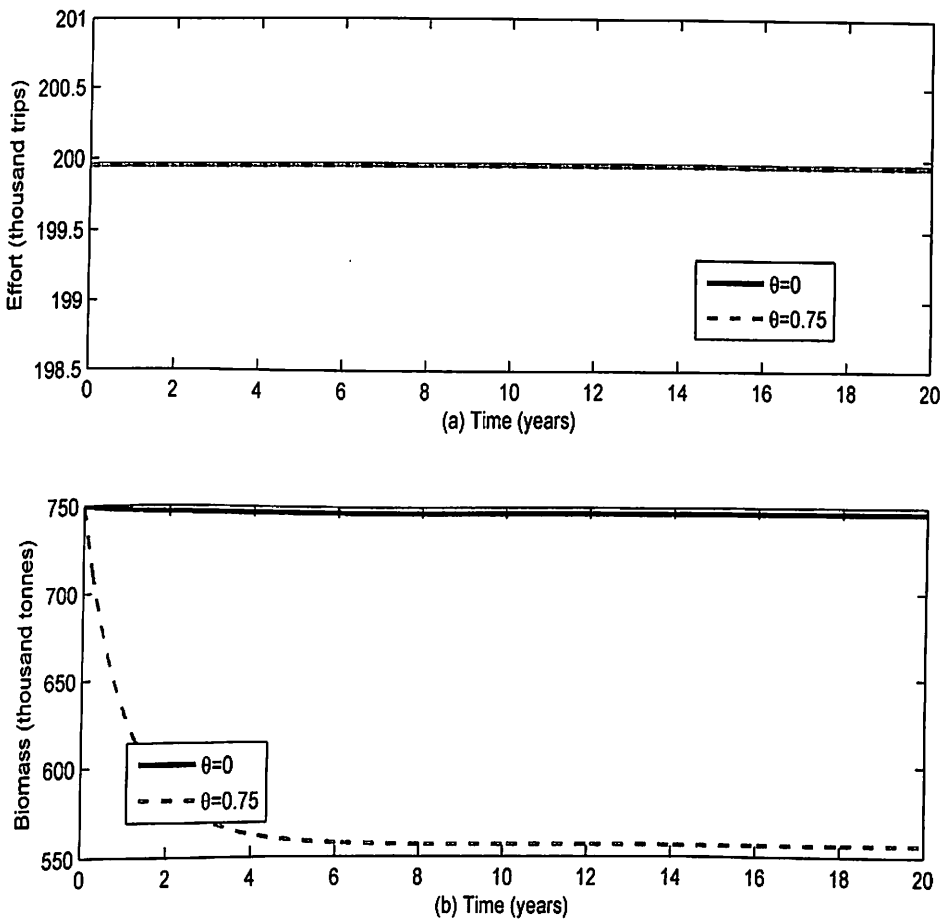

Figure 61: (a) Effort and (b) Biomass Levels for $E_{max} = 200,000$, $\theta = 0$, 0.75 and $T = 20$

Assuming an initial population size of 750,000 tonnes, the total net revenues over the twenty-year horizon corresponding to $\theta = 0$ and $\theta = 0.75$ are computed as US\$743,540,000 and US\$1,121,500,000, respectively. In other words, a 75% increment in the catchability results in a revenue increase of 51%, and a decrease in final biomass level of 25%.

Simulation results for the fishing effort and stock size relating to the case where $x_0 = 750,000$ tonnes, $T = 1$ year, $E_{max} = 200,000$ trips, $\theta = 0$ and $\theta = 1$ are presented in Figure 62. In Figure 62 (a), it is observed that when the maximum effort rate is 200,000 trips, the optimal effort rate appears to follow the same path of about 200,000 trips corresponding to both values of θ for the one-year horizon. However, the fish biomass levels follow different trajectories. The biomass decreases for both catchability levels, to a value of around 748,000 tonnes for $\theta = 0$, and a value of about 594,000 tonnes for $\theta = 1$ (Figure 62 (b)).

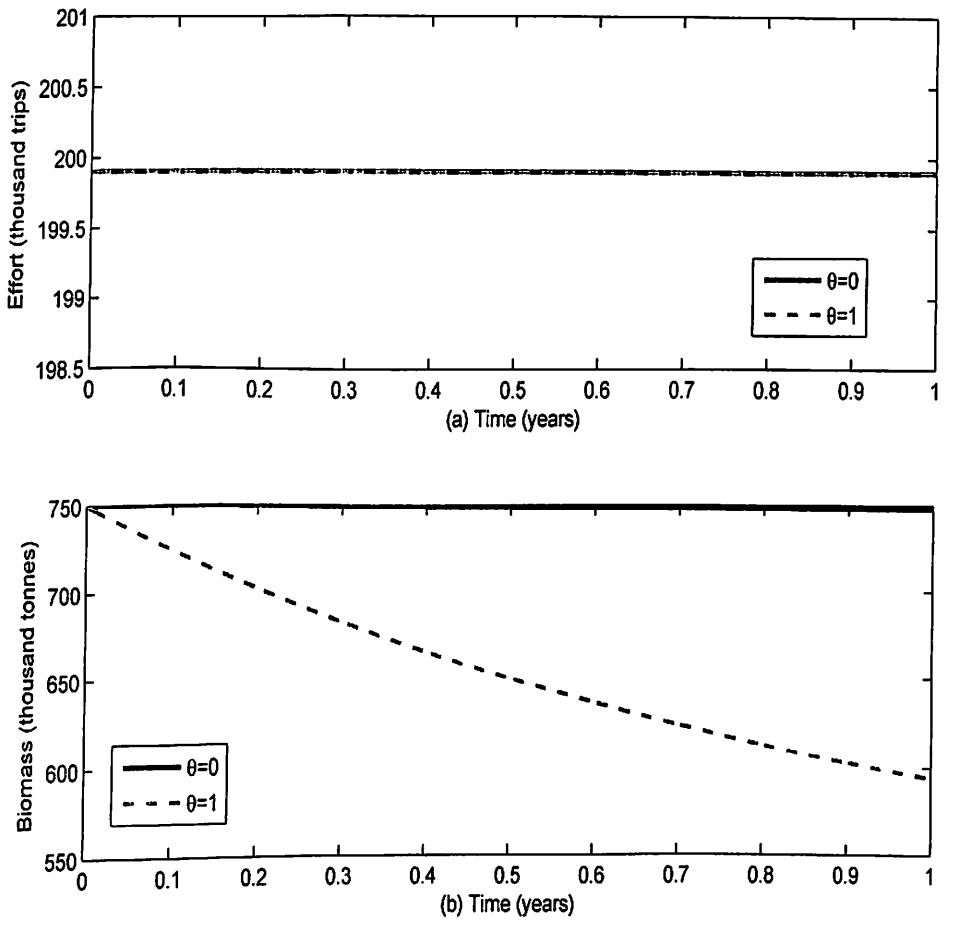

Figure 62: (a) Effort and (b) Biomass Levels for $E_{max} = 200,000$, $\theta = 0$, 1 and $T = 1$

Assuming an initial population size of 750,000 tonnes, the total net revenues over the one-year horizon corresponding to $\theta = 0$ and $\theta = 1$ are computed as US\$109,320,000 and US\$223,500,000, respectively. In other words, a 100% increment in the catchability results in a revenue increase of over 100%, and a

decrease in final biomass level of about 21%.

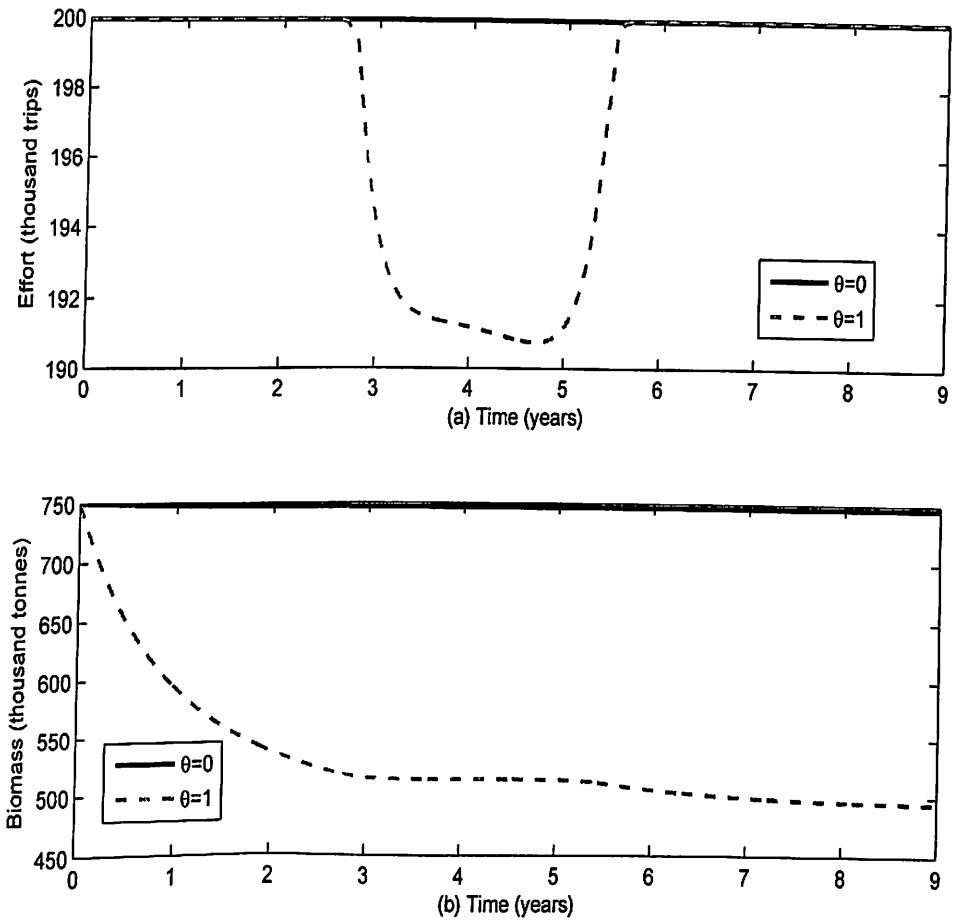

Figure 63: (a) Effort and (b) Biomass Levels for $E_{max} = 200,000$, $\theta = 0$, 1 and $T = 9$

Simulation results for the fishing effort and stock size relating to the case where $x_0 = 750,000$ tonnes, $T = 9$ years, $E_{max} = 200,000$ trips, $\theta = 0$ and $\theta = 1$ are presented in Figure 63. In Figure 63 (a), it is observed that when the maximum effort rate is 200,000, the optimal effort rate appears to follow significantly different trajectories (at least for some period in the interval) for the nine-year horizon. The effort rate corresponding to $\theta = 0$ is almost 200,000 trips; and also about 200,000 trips for $\theta = 1$, except for a brief period where it is almost convex and attaining a minimum value of 190,748 trips. Furthermore, the fish biomass levels follow different trajectories. The biomass decreases for both catchability levels, to the equilibrium value of 747,000 tonnes for $\theta = 0$, and a value of about 495,000 tonnes for $\theta = 1$ (Figure 63 (b)). It is instructive to note that the iterates

failed to converge when the time horizon is beyond nine years.

Assuming an initial population size of 750,000 tonnes, the total net revenues over the nine-year horizon corresponding to $\theta = 0$ and $\theta = 1$ are computed as US$579,770,000 and US$941,440,000, respectively. In other words, a 100% increment in the catchability results in a revenue increase of 62%, and a decrease in final biomass level of 34% (with no equilibrium or sustainable level achieved).

Effects of varying discount rate

Figures 64 and 65 show the plot of the net revenue against the modification on the catchability coefficient, θ for a time horizon of twenty years ($E_{max} = 200,000$ and $x_0 = 750,000$). In Figure 64, it can be seen that when the discount rate, δ is 15% per year, the net revenue curve is concave, starting from a value of US$743,540,000 and increasing to a maximum value of US$1,106,200,000 at $\theta = 0.7$.

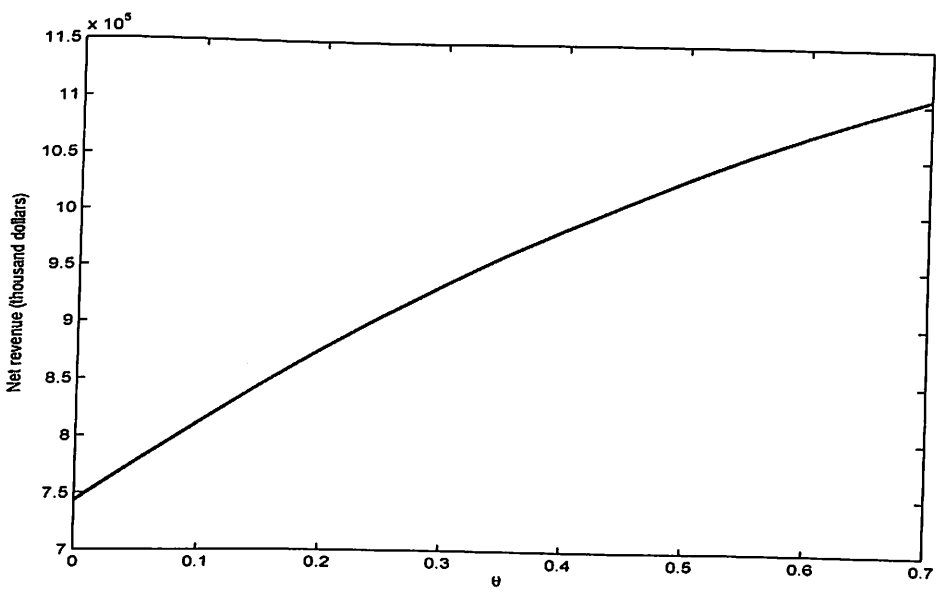

Figure 64: Net Revenue against θ for $\delta = 0.15$ and $T = 20$

Figure 65 depicts the case where δ varies from 0 to 15% per year. It shows that when the discount rate, δ is 0 per year, the net revenue curve is concave, starting from a value of US$2,346,300,000 and increasing to a maximum value of US$3,371,700,000 at $\theta = 0.7$. The curve for $\delta = 0$ is always above the curve

for $\delta = 0.15$ for the given values of θ. Additionally, the maximum revenue for the case where $\delta = 0$ is 67% greater than the case where $\delta = 0.15$.

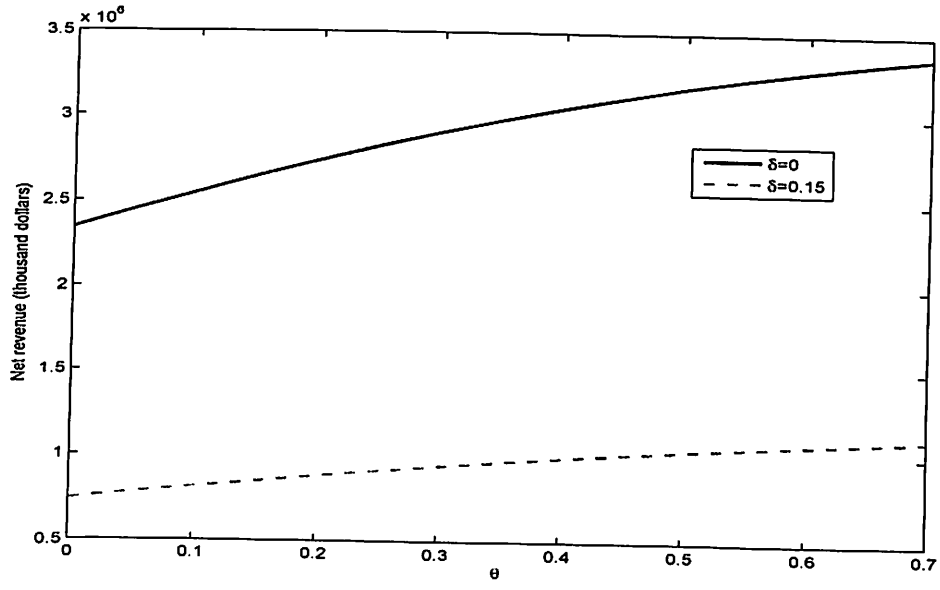

Figure 65: Net Revenue against θ for $\delta = 0$, 0.15 and $T = 20$

Model summary

This section looked into the fishing effort strategies of the sardinella fishery under the modified Gordon-Schaefer model in order to determine the optimal strategy. Dynamics of the biomass were modelled using the Schaefer equation. Bifurcation analysis was performed on this model incorporating the sensitivity analysis of the catchability coefficient. However, the objective functional of the canonical Gordon-Schaefer model was subjected to a modification. Instead of the linear costs in the model, a more realistic cost option—quadratic costs—was considered. The reference points under this modified model—the MEY and OAY—were determined. It was realised that when the coefficient of the quadratic cost term is zero, the modified reference points reduced to the canonical Gordon-Schaefer model reference points.

The existence of an optimal control was proven as well as the characterisation of the optimal control using Pontryagin's maximum principle. Uniqueness of the optimality system is guaranteed due to the Lipschitz property of the system.

Numerical simulations were performed on the modified model in which the quadratic costs are seen as perturbations on the usual linear costs. The model has been found to attain equilibrium status when the fishing effort is set at the MEY and SY levels. However, the model failed to achieve equilibrium status when the fishing effort is at the OAY level, no matter the size of the initial fish population. In fact, at the OAY level, the iterates failed to converge beyond a time horizon of only two years.

The effort strategies at MEY and SY levels were compared at various time-horizon values as well as at different initial biomass levels. It was observed that at equilibrium, the total net revenue for SY was greater than the revenue for MEY. However, the final biomass level for MEY was greater than the biomass level for SY at initial biomass levels of 75% and 55% of the carrying capacity. This result agrees with the theoretical result that MEY is not optimal under dynamic conditions.

Sensitivity analysis was performed on the catchability coefficient to simulate the effects of IUU fishing (especially the use of under-sized mesh gears) on fish stocks. The results show that in the long run, IUU fishing has a disastrous effect on fish biomass without very substantial increase in total net revenue.

At higher levels of increased catchability as a result of the illegal practices, the consequences on the fish stock size are near catastrophic levels: as low as less than half of the carrying capacity in finite time. This may lead to the fishery being formally declared as overfished, since the biomass level is less than the stock size at MSY.

Chapter Summary

This chapter has discussed models with the biological dynamics modelled by the logistic equation and the rate of harvesting being proportional. These models are the canonical Gordon-Schaefer model, the optimal yield model, the Craven model and a model with an isoperimetric constraint.

The canonical model was subjected to bifurcation analysis and the equilibrium points and their stability properties determined. Optmality of the model gave rise to both singular and bang-bang controls. Simulations performed on the dynamic model showed the optimal fishing effort must be set at the OSY level. Furthermore, the current rate of fishing effort was estimated to be above the bifurcation point of the model.

With regard to the optimal yield model, as the name of the model implies, the objective is to determine the optimal yield without taking into account the cost of fishing. Optimality of the model was determined and the optimal control characterised. The results of the simulations indicate that, in general, the optimal rate of fishing effort must be pegged at the MSY level.

The Craven model is a modification of the canonical model in the sense that it includes a diminishing returns factor in the objective functional. Also, the control for the model is the level of harvesting, which is the product of the catchability coefficient and the fishing effort. Bifurcation and optimality of the model were determined. Results from the simulations on the dynamic model show that it is optimal to harvest at a level corresponding to OAY.

A model with an isoperimetric constraint was also discussed. This constraint translates into an annual catch quota called the TAC. Optmality of the model was determined and simulations carried out to ascertain certain properties of the model. It was found that, when the TAC is set at the MSY level, the rate of fishing effort has to significantly reduce to ensure sustainability of the resource.

The last section in the chapter investigated a model with modified catchability and quadratic costs. Bifurcation analysis was carried on the model ascertain the stability properties of the equilibrium points. The existence of an optimal control and uniqueness of the optimality system were proven. Simulations on the model reveal that the increased catchability induced by the IUU fishing has a disastrous effect on the stock size.

CHAPTER FIVE

CONSTANT AND PERIODIC HARVESTING MODELS

Introduction

Ghana's sardinella fishery current crisis is a concern to all stakeholders in the industry. As mentioned earlier, the catches are among the lowest in recent history. Therefore, every effort is needed to help address the present predicament. Hence, the present study.

We turn our attention now to the canonical Gordon-Schaefer model with a constant rate of harvesting. Afterwards, some modifications to this model will be investigated with the aid of bifurcation and numerical analyses to further shed light on the sardinella fishery in Ghana.

The Gordon-Schaefer Model

The constant harvesting version of the dynamic Gordon-Schaefer model can be presented in the following form:

$$\begin{aligned} \max_h Z(h) &= \int_0^\infty e^{-\delta t}(p-c)h\,dt \\ \text{subject to} \quad \frac{dx}{dt} &= rx\left(1-\frac{x}{K}\right)-h \\ x(0) &= x_0 \\ 0 \le h &\le h_{max}, \end{aligned} \tag{5.1}$$

where h_{max} is the maximum allowable harvest rate and p and c are the price and cost per unit harvest, respectively. The model aims to determine the harvest strategy h that results in the largest possible net economic benefit as expressed by the present value integral Z of Model (5.1).

Bifurcation analysis

We shall investigate the stability dynamics of the state equation in order to determine the number of equilibrium points and the associated structural stability of the dynamical system. As mentioned earlier, there are two equilibrium points associated with the state dynamics of the model (5.1) when the harvest rate is less than the bifurcation point. These are:

$$x_1^* = \frac{K}{2}\left(1 - \sqrt{1 - \frac{4h}{rK}}\right) \quad \text{and} \quad x_2^* = \frac{K}{2}\left(1 + \sqrt{1 - \frac{4h}{rK}}\right),$$

and the bifurcation point is given by $h = \frac{rK}{4}$.

Figure 66 presents the solution curves for the case where $h = 200,000$ tonnes per year. It is observed that there are two hyperbolic equilibrium points: $x_1^* = 169,614$ tonnes and $x_2^* = 830,386$ tonnes. For any initial population size or biomass level, $x_0 > 830,386$ tonnes, the population approaches the equilibrium population, 830,386 tonnes in the long run. Similarly, for $169,614 < x_0 < 830,386$ tonnes, the population asymptotically approaches 830,386 tonnes. Also, for $x_0 < 169,614$ tonnes, the population goes into extinction in finite time. Thus the biomass level, 169,614 tonnes is unstable while 830,386 tonnes is stable (making the system structurally stable). Of course, biomass levels starting from the equilibrium levels, 169,614 and 830,386 tonnes remain there indefinitely. Hence, a harvest rate corresponding to $h = 200,000$ tonnes per year induces a long-term biomass level of more than a half the carrying capacity provided $x_0 > 169,614$ tonnes.

Figure 67 presents the solution curves for the case where $h = h_{MSY} = 355,000$ tonnes per year, the saddle-node bifurcation point. It is observed that there is a single nonhyperbolic equilibrium point, $x^* = 500,000$ tonnes. For any initial population size or biomass level, $x_0 > 500,000$ tonnes, the population approaches the equilibrium population, 500,000 tonnes in the long run. However, for $x_0 < 500,000$ tonnes, the population goes into extinction in finite time. Thus the biomass level 500,000 tonnes is semi-stable (making the system structurally

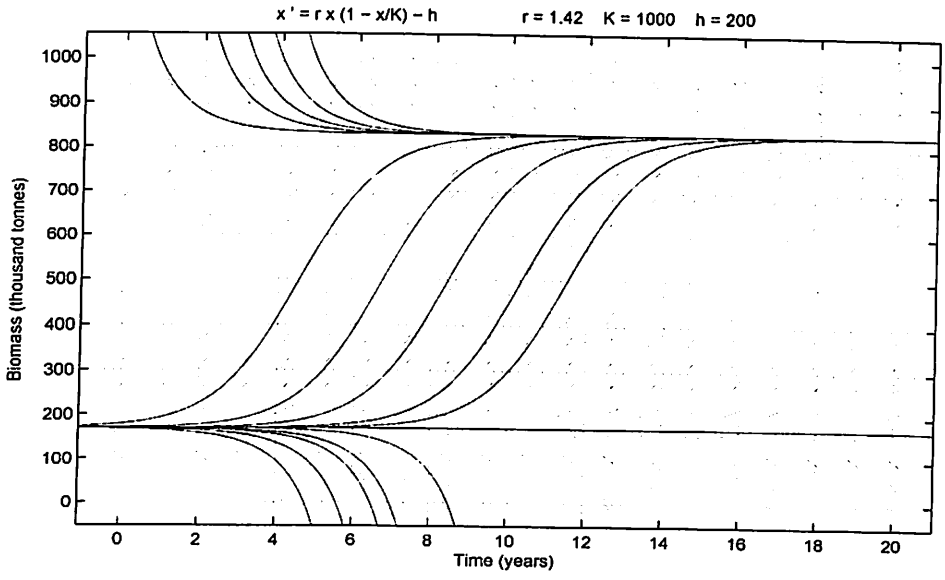

Figure 66: Solution Curves for $h = 200,000$

unstable). Of course, biomass levels starting from the equilibrium level, 500,000 tonnes remain there indefinitely. Hence, a harvest rate corresponding to $h =$ 355,000 tonnes per year induces a long-term biomass level of exactly half the carrying capacity provided $x_0 \geq 500,000$ tonnes.

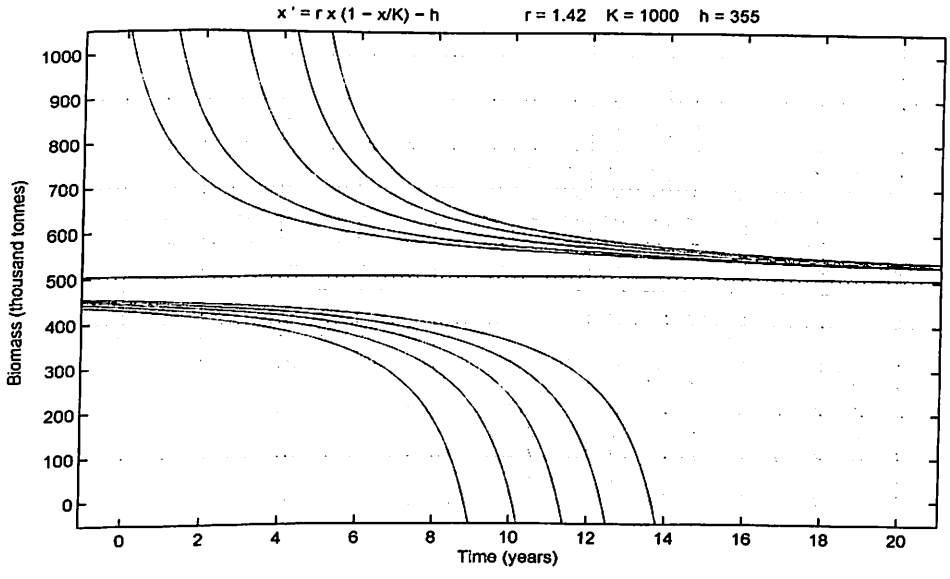

Figure 67: Solution Curves for $h = 355,000$

Figure 68 presents the solution curves for the case where $h = 400,000$ tonnes per year. It is observed that there is no equilibrium point for this rate of harvest. For any initial population size or biomass level, the population goes into extinction

in finite time. Thus, a harvest rate corresponding to $h = 400,000$ tonnes per year, just 13% greater the MSY level, sends the population into extinction in finite time.

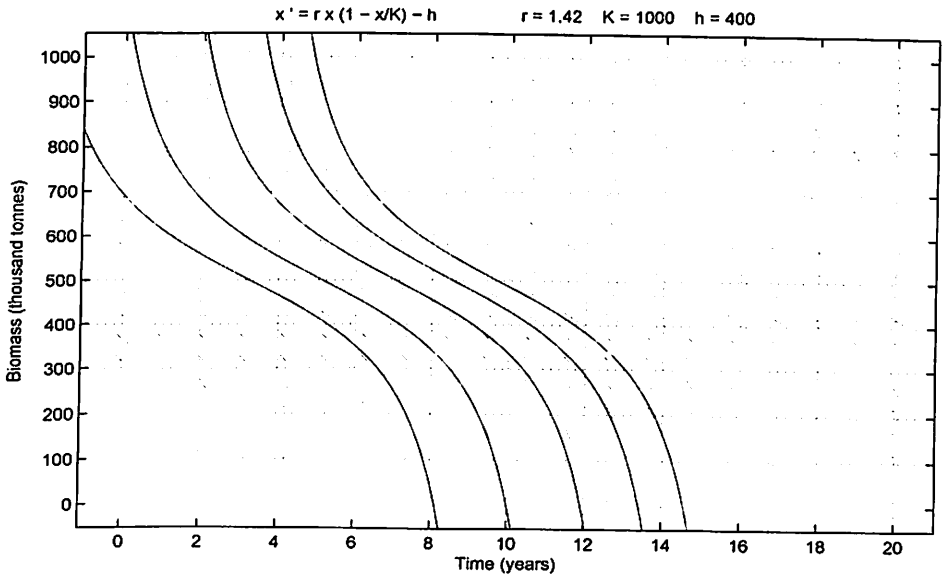

Figure 68: Solution Curves for $h = 400,000$

Optimality of the model

The characterisation of the optimal control is sought for in this section. Also, the model is analysed to determine whether or not the singular path is attainable by the control. The goal is to maximise the discounted present value of future net revenues. Thus, we seek an optimal control h_δ such that

$$Z(h_\delta) = \max\{Z(h) \,|\, h \in U\},$$

where the control set, which is Lebesgue measurable for an infinite time horizon, is defined by

$$U = \{h(t) \,|\, 0 \leq h(t) \leq h_{max},\ t \in [0,\infty)\}.$$

To derive the necessary conditions for the optimal control, Pontryagin's maximum principle (Pontryagin *et al.*, 1962) is employed. The current value Hamiltonian for the optimal control problem (5.1) is

$$H = (p-c)h + \lambda\left[rx\left(1-\frac{x}{K}\right) - h\right]. \tag{5.2}$$

The adjoint variable λ is governed by

$$\begin{aligned}\lambda' &= \delta\lambda - \frac{\partial H}{\partial x} \\ &= \delta\lambda - \lambda\left(r - \frac{2rx}{K}\right).\end{aligned} \tag{5.3}$$

The switching function is defined by

$$\begin{aligned}\psi(t) &= \frac{\partial H}{\partial h} \\ &= (p-c) - \lambda.\end{aligned} \tag{5.4}$$

The characterisation of the optimal control is

$$\begin{cases} h_\delta = 0 & \text{if} \quad \psi(t) < 0, \\ 0 < h_\delta < h_{max} & \text{if} \quad \psi(t) = 0, \\ h_\delta = h_{max} & \text{if} \quad \psi(t) > 0. \end{cases} \tag{5.5}$$

Singularity analysis of the model

This analysis will enable us determine whether the optimal control would be bang-bang or follow a singular path. For a singular control, we assume that there is an interval I for all $t \in I \subset [0,\infty)$ such that

$$\psi(t) = 0. \tag{5.6}$$

Thus, from Equations (5.4) and (5.6),

$$(p-c) - \lambda = 0. \tag{5.7}$$

So, solving for λ we find

$$\lambda = p - c. \tag{5.8}$$

Differentiating Equation (5.8) with respect to t, it follows that

$$\lambda' = 0. \tag{5.9}$$

By plugging the λ expression in Equation (5.8) into the adjoint equation (5.3), we get

$$\lambda' = (p-c)\left(\delta - r + \frac{2rx}{K}\right). \tag{5.10}$$

Setting the expressions in Equations (5.9) and (5.10) equal to each other and simplifying, we obtain the positive optimal biomass level as

$$x_\delta = \frac{K}{2}\left(1 - \frac{\delta}{r}\right), \tag{5.11}$$

provided $\delta < r$.

Substituting the value of x_δ in Equation (5.11) into the optimal harvest,

$$h_\delta = r x_\delta \left(1 - \frac{x_\delta}{K}\right)$$

gives

$$h_\delta = \frac{rK}{4}\left(1 - \frac{\delta^2}{r^2}\right). \tag{5.12}$$

However, from the bifurcation analysis, since $h_\delta < \frac{rK}{4}$ (the bifurcation point), there exists two hyperbolic equilibrium points. Therefore, solving

$$rx\left(1 - \frac{x}{K}\right) - h_\delta = 0$$

for the optimal biomass level x_δ gives

$$x_\delta = \begin{cases} \frac{K}{2}\left(1 - \frac{\delta}{r}\right) & \text{if} \quad x_0 = \frac{K}{2}\left(1 - \frac{\delta}{r}\right), \\ \frac{K}{2}\left(1 + \frac{\delta}{r}\right) & \text{if} \quad x_0 > \frac{K}{2}\left(1 - \frac{\delta}{r}\right). \end{cases} \tag{5.13}$$

Additionally, from the bifurcation analysis, x_δ approaches zero in finite time if $x_0 < \frac{K}{2}\left(1 - \frac{\delta}{r}\right)$.

Hence the optimal harvesting rate is

$$h_\delta = \begin{cases} 0 & \text{if} \quad \lambda > p - c, \\ \frac{rK}{4}\left(1 - \frac{\delta^2}{r^2}\right) & \text{if} \quad \lambda = p - c, \\ h_{max} & \text{if} \quad \lambda < p - c. \end{cases} \tag{5.14}$$

This implies that the optimal control comprises both the extreme controls and the singular control. The extreme controls indicate that the resource should be harvested if and only if the net revenue per unit harvest (or the marginal net revenue of harvest) exceeds the current value shadow price of the resource (or the marginal net revenue of stock).

Numerical simulations

In order to ensure that both the proportional and constant harvesting models have the same net revenue at the MSY level, we compute the cost per unit harvest, c from the cost per unit effort, $c(E)$ as follows:

$$\begin{aligned} c &= \frac{c(E)}{qx_{MSY}} \\ &= \$216.67/\text{tonne}. \end{aligned}$$

Additionally, for a discount rate of 15%, the optimal harvest rate is

$$\begin{aligned} h_\delta &= \frac{rK}{4}\left(1 - \frac{\delta^2}{r^2}\right) \\ &= 351,039 \text{ tonnes/year}; \end{aligned}$$

and the corresponding optimal biomass level is

$$x_\delta = \begin{cases} 447,183 & \text{if} \quad x_0 = 447,183, \\ 552,815, & \text{if} \quad x_0 > 447,183, \end{cases}$$

where $x_\delta = 552,815$ tonnes, is stable while $x_\delta = 447,183$ tonnes is unstable. Furthermore, for $x_0 < 447,183$ tonnes, the fish population goes into extinction in finite time

We present simulations results corresponding to OSY (which is optimal under dynamic conditions). The results for the harvest level and stock size relating to the case where $h_{max} = 351,039$ tonnes per year, $T = 1$ year, $x_0 = 450,000$ tonnes and $x_0 = 600,000$ tonnes are presented in Figure 69. In Figure 69 (a), it is observed that when the maximum harvest rate h_{max} is set at the OSY level, the optimal harvest rate follows the same path of around 350,700 tonnes per year for both initial biomass levels for the one-year horizon. However, the biomass levels appear to differ. The higher initial biomass level ends at about 590,000 tonnes, while the lower initial biomass level appears to show no significant change (Figure 69 (b)).

Assuming an initial population size of 600,000 tonnes, the total net revenue over the one-year horizon corresponding to the given rate of harvesting is com-

puted as US $124,840,000. The same net revenue is realised for an initial population size of 450,000 tonnes, since the optimal harvest is the same for both initial biomass levels.

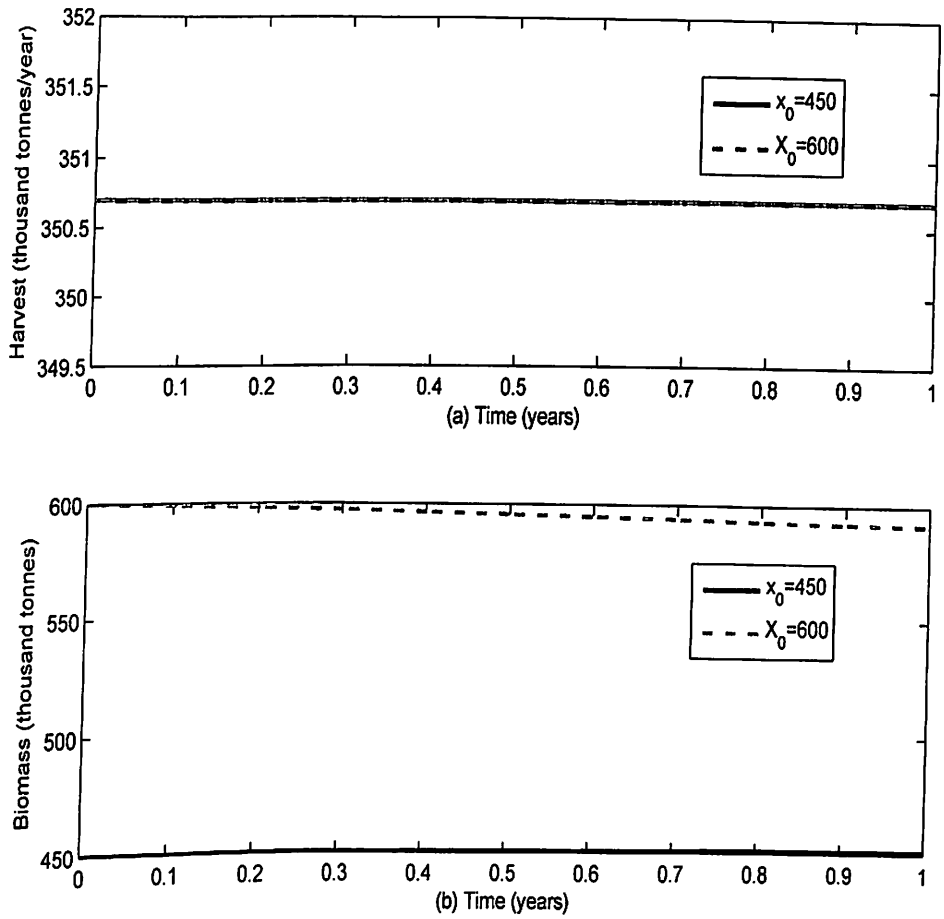

Figure 69: (a) Harvest and (b) Biomass Levels for $h_{max} = 351,039$, $x_0 = 450,000$; 600,000 and $T = 1$

Simulation results for the harvest level and fish stock size relating to the case where $h_{max} = 351,039$ tonnes per year, $T = 100$ years, $x_0 = 450,000$ tonnes and $x_0 = 600,000$ tonnes are presented in Figure 70. In Figure 70 (a), it is observed that when the maximum harvest rate h_{max} is set at the OSY level, the optimal harvest rate follows marginally different paths of around 350,996 tonnes per year and 351,028 tonnes per year for $x_0 = 600,000$ tonnes and $x_0 = 450,000$ tonnes, respectively throughout the hundred-year horizon. However, the biomass levels converge at the stable equilibrium level of around 552,815 tonnes (Figure 70 (b)).

Assuming an initial population size of 600,000 tonnes, the total net revenue

over the hundred-year horizon corresponding to the given rate of harvesting is computed as US \$897,000,000. The net revenue for an initial population size of 450,000 tonnes is marginally higher at US \$897,080,000; about 0.01% greater.

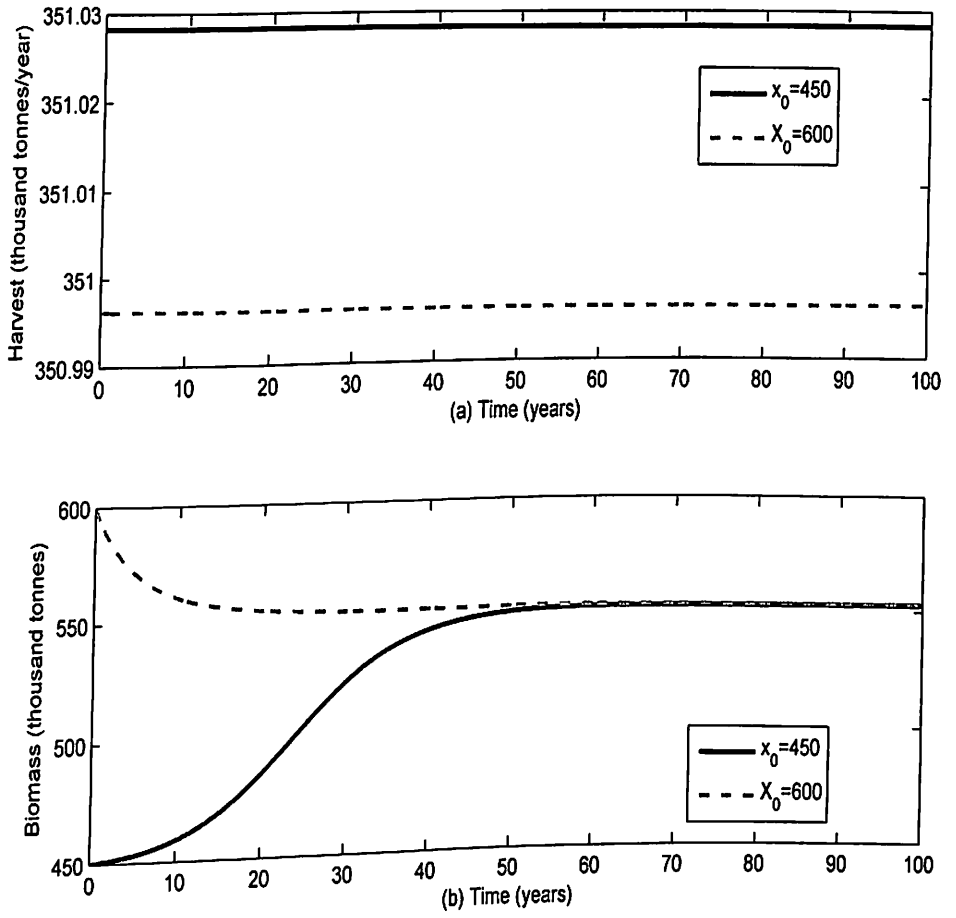

Figure 70: (a) Harvest and (b) Biomass Levels for $h_{max} = 351,039$, $x_0 = 450,000$; 600,000 and $T = 100$

Simulation results for the harvest level and fish stock size relating to the case where $h_{max} = 351,039$ tonnes per year, $x_0 = 400,000$ and $T = 6$ years are presented in Figure 71. In Figure 71 (a), it is observed that when the maximum harvest rate h_{max} is set at the OSY level, the optimal harvest rate follows the maximum path of around 351,039 tonnes per year throughout the six-year horizon. On the other hand, the biomass level monotonically decreases to about 120,000 tonnes (Figure 71 (b)).

Assuming an initial population size of 400,000 tonnes, the total net revenue over the six-year horizon corresponding to the given rate of harvesting is com-

puted as US $532,350,000.

It is worthy of note that, when the initial biomass level is 400,000 tonnes (below the lower equilibrium point of 447,183 tonnes) the population goes into extinction beyond six years. This perfectly agrees with theoretical results.

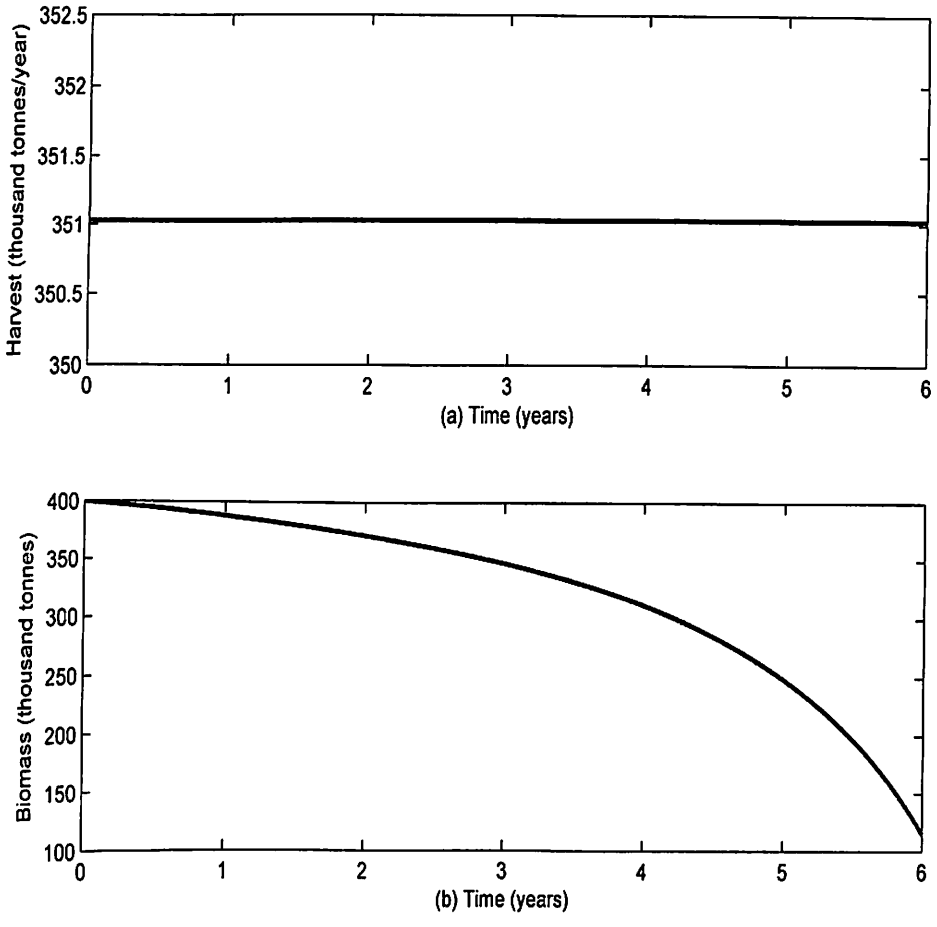

Figure 71: (a) Harvest and (b) Biomass Levels for $h_{max} = 351,039$, $x_0 = 400,000$ and $T = 6$

Simulation results for the harvest level and fish stock size relating to the case where $h_{max} = 400,000$ tonnes per year, $x_0 = 750,000$ and $T = 8$ years are presented in Figure 72. In Figure 72 (a), it is observed that when the maximum harvest rate h_{max} is set beyond the harvest rate at MSY, the optimal harvest rate follows the maximum path of around 400,000 tonnes per year throughout the eight-year horizon. On the other hand, the biomass level decreases to about 180,000 tonnes (Figure 72 (b)).

Assuming an initial population size of 750,000 tonnes, the total net revenue

over the eight-year horizon corresponding to the given rate of harvesting is computed as US $714,290,000.

It is worthy of note that, when the initial biomass level is as high as 75% of the carrying capacity and the harvest rate is set at 400,000 tonnes (just 13% higher than the MSY level) the population goes into extinction beyond eight years. This validates theoretical results.

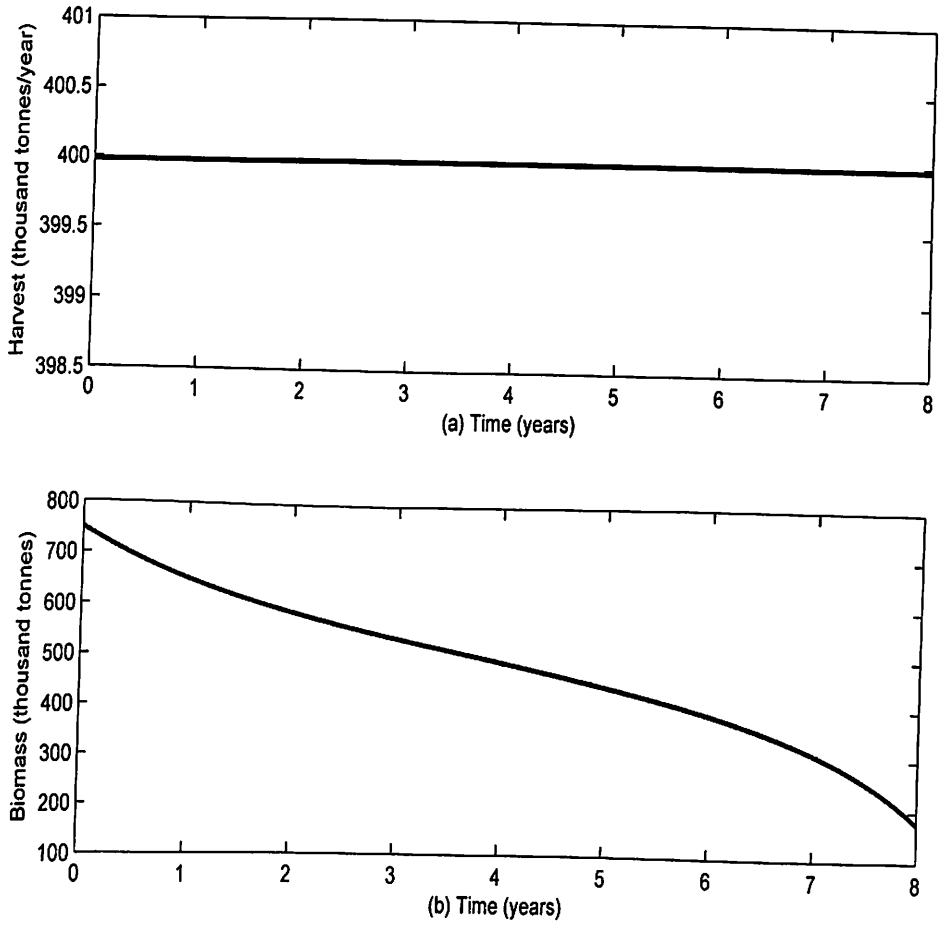

Figure 72: (a) Harvest and (b) Biomass Levels for $h_{max} = 400,000$, $x_0 = 750,000$ and $T = 8$

Model summary

This section looked into the harvesting strategies of the sardinella fishery under the Gordon-Schaefer model with a constant rate of removals in order to determine the optimal strategy. The biomass was subjected to a bifurcation analysis to determine the bifurcation and the equilibrium points as well as the stability properties

of the dynamical system. Unlike in the proportional harvesting model where the harvest rate at the MSY level was 50% of the bifurcation point, in the constant harvesting model the MSY level and the bifurcation point are identical. Thus, any harvest strategy (with zero discounting) that positively deviates from the MSY level could create a catastrophe (see Figure 68).

Numerical simulations were performed on the model to highlight further useful insights. Recall that the optimal yield generated two equilibrium points—the larger one being stable and the smaller one, unstable. These equilibrium points are attained depending on the initial biomass level. It was observed that the model takes a longer time to reach equilibrium compared with the proportional harvesting model; and at equilibrium, the lower initial biomass level had a marginally higher total net revenue than the higher initial biomass level.

It was further observed that for the same harvesting level, a lower initial biomass level requires a higher harvest rate than for a higher initial biomass level.

The Goh Model

We present a model that seeks the optimal harvest strategy in order to attain the maximum harvest (or yield). The model, originally proposed by Goh (1969), is given as

$$\begin{aligned} \max_h Z(h) &= \int_0^\infty h\,dt \\ \text{subject to} \quad \frac{dx}{dt} &= rx\left(1-\frac{x}{K}\right)-h \\ x(0) &= x_0 \\ 0 \le h &\le h_{max}. \end{aligned} \tag{5.15}$$

Optimality of the model

The characterisation of the optimal control is sought for in this section. Therefore, the model will be analysed for the determination of a singular path and/or the boundary solutions. This is to enable us establish the conditions necessary for

optimality by the use of Pontryagin's maximum principle. The Hamiltonian for the optimal control problem (5.15) can be expressed as

$$H = h + \lambda \left[rx\left(1 - \frac{x}{K}\right) - h \right]. \tag{5.16}$$

The adjoint variable λ is governed by

$$\begin{aligned} \lambda' &= -\frac{\partial H}{\partial x} \\ &= -\lambda \left(r - \frac{2rx}{K} \right). \end{aligned} \tag{5.17}$$

The switching function is defined by

$$\begin{aligned} \psi(t) &= \frac{\partial H}{\partial h} \\ &= 1 - \lambda. \end{aligned} \tag{5.18}$$

The characterisation of the optimal control is

$$\begin{cases} h_\delta = 0 & \text{if} \quad \psi(t) < 0, \\ 0 < h_\delta < h_{max} & \text{if} \quad \psi(t) = 0, \\ h_\delta = h_{max}, & \text{if} \quad \psi(t) > 0. \end{cases} \tag{5.19}$$

Singularity analysis of the model

The task is to determine whether the optimal control would be bang-bang or follow a singular path. For a singular control, we assume that there is an interval I for all $t \in I \subset [0, \infty)$ such that

$$\psi(t) = 0. \tag{5.20}$$

Thus, from Equations (5.18) and (5.20),

$$1 - \lambda = 0. \tag{5.21}$$

So, solving for λ we find

$$\lambda = 1. \tag{5.22}$$

Differentiating Equation (5.22) with respect to t, it follows that

$$\lambda' = 0. \tag{5.23}$$

By plugging the λ expression in Equation (5.22) into the adjoint equation (5.17), we get

$$\lambda' = \frac{2rx}{K} - r. \tag{5.24}$$

Setting the expressions in Equations (5.23) and (5.24) equal to each other and simplifying, we obtain the optimal biomass level as

$$x_\delta = \frac{K}{2}. \tag{5.25}$$

The harvest rate corresponding to x_δ is found from the state equation in Model (5.15), after noting that $x' = 0$, since x_δ is a constant. Thus

$$h_\delta = \frac{rK}{4}. \tag{5.26}$$

Hence the optimal rate of harvesting is

$$h_\delta = \begin{cases} 0 & \text{if} \quad \lambda > 1, \\ \dfrac{rK}{4} & \text{if} \quad \lambda = 1, \\ h_{max} & \text{if} \quad \lambda < 1. \end{cases} \tag{5.27}$$

This implies that the optimal control comprises both the extreme controls and the singular control. The marginal yield, λ may be viewed as the additional yield associated with an increase in stock size of one tonne. Thus, the extreme controls indicate that the resource should be harvested if and only if the marginal yield does not exceed one tonne.

In addition, the harvested resource could follow the OSY path (or singular path) if the marginal yield exactly equals a tonne. Thus the OSY parameters are x_δ and h_δ, which are exactly the parameters at the MSY level (since the costs as well as the discount factor are assumed to be zero).

Numerical simulations

Simulation results for the harvest level and stock size relating to the case where $h_{max} = 355,000$ tonnes per year, $T = 1$ year and $x_0 = 550,000$ and $x_0 = 750,000$

tonnes are presented in Figure 73. In Figure 73 (a), it is observed that when the maximum harvest rate h_{max} is set at the OSY level (same as MSY level), the optimal harvest rate follows the same path of around 354,570 tonnes per year for both initial biomass levels for the one-year horizon. However, the biomass levels appear to differ. The higher initial biomass level ends at about 680,000 tonnes, while the lower initial biomass level appears to show only a slight decrease (Figure 73 (b)).

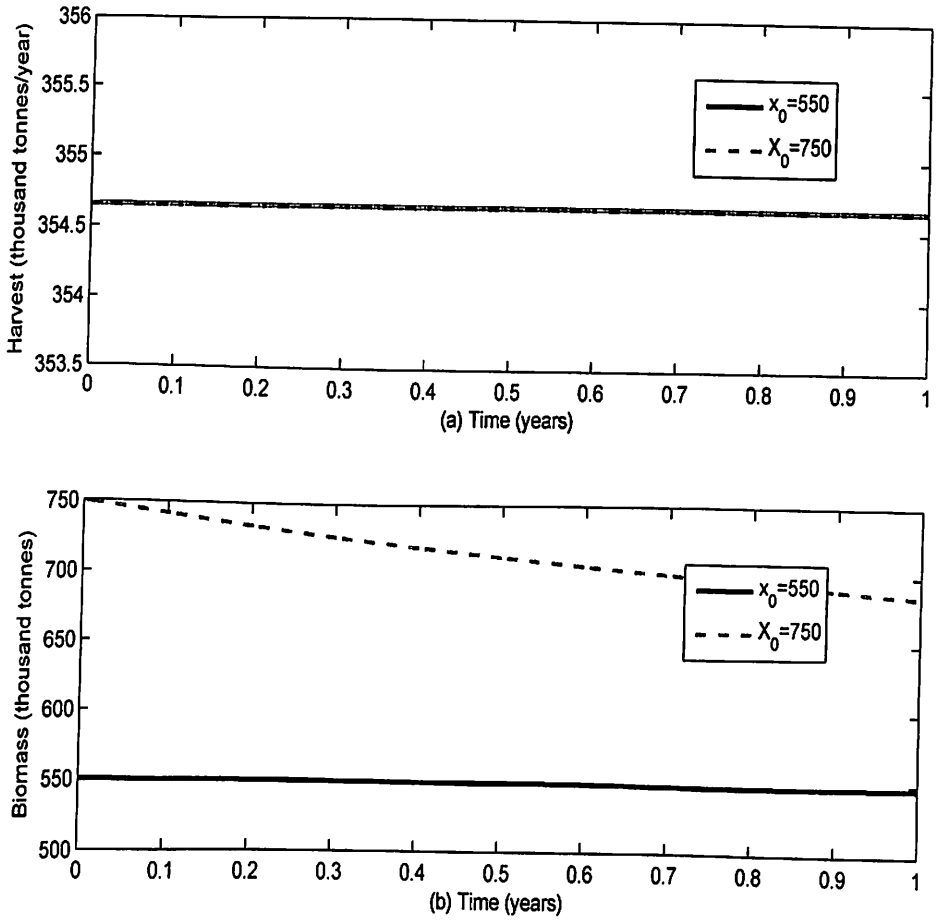

Figure 73: (a) Harvest and (b) Biomass Levels for $h_{max} = 355,000$, $x_0 = 550,000$; 750,000 and $T = 1$

Assuming an initial population size of 750,000 tonnes, the total yield over the one-year horizon corresponding to the given rate of harvesting is computed as 354.653 tonnes. The same total yield is realised for an initial population size of 550.000 tonnes, since the optimal harvest is the same for both initial biomass levels.

Simulation results for the harvest level and stock size relating to the case where $h_{max} = 355,000$ tonnes per year, $T = 500$ years, $x_0 = 550,000$ tonnes and $x_0 = 750,000$ tonnes are presented in Figure 74. In Figure 74 (a), it is observed that when the maximum harvest rate h_{max} is set at the OSY level, the optimal harvest rate follows the equilibrium path of around 355,000 tonnes per year throughout the five hundred-year horizon. Similarly, the biomass levels converge at the semi-stable equilibrium level of around 500,000 tonnes (Figure 74 (b)).

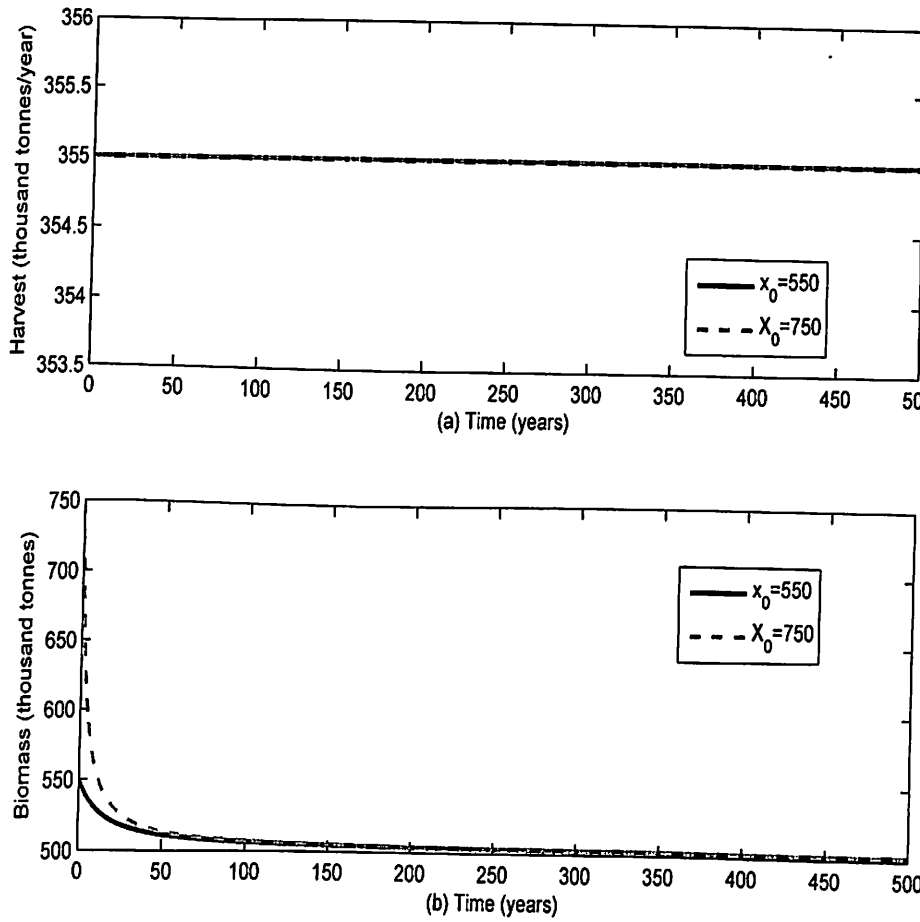

Figure 74: (a) Harvest and (b) Biomass Levels for $h_{max} = 355,000$, $x_0 = 550,000$; $750,000$ and $T = 500$

Assuming an initial population size of 750,000 tonnes, the total net revenue over the five hundred-year horizon corresponding to the given rate of harvesting is computed as 177,500,000 tonnes. The same total yield is realised for an initial population size of 550,000 tonnes, since the optimal harvest is the same for both initial biomass levels.

Simulation results for the harvest level and stock size relating to the case where $h_{max} = 355,000$ tonnes per year, $x_0 = 450,000$ and $T = 12$ years are presented in Figure 75. In Figure 75 (a), it is observed that when the maximum harvest rate h_{max} is set at the OSY level, the optimal harvest rate follows the maximum path of around 355,000 tonnes per year throughout the twelve-year horizon. On the other hand, the biomass level monotonically decreases to about 170,000 tonnes (Figure 75 (b)).

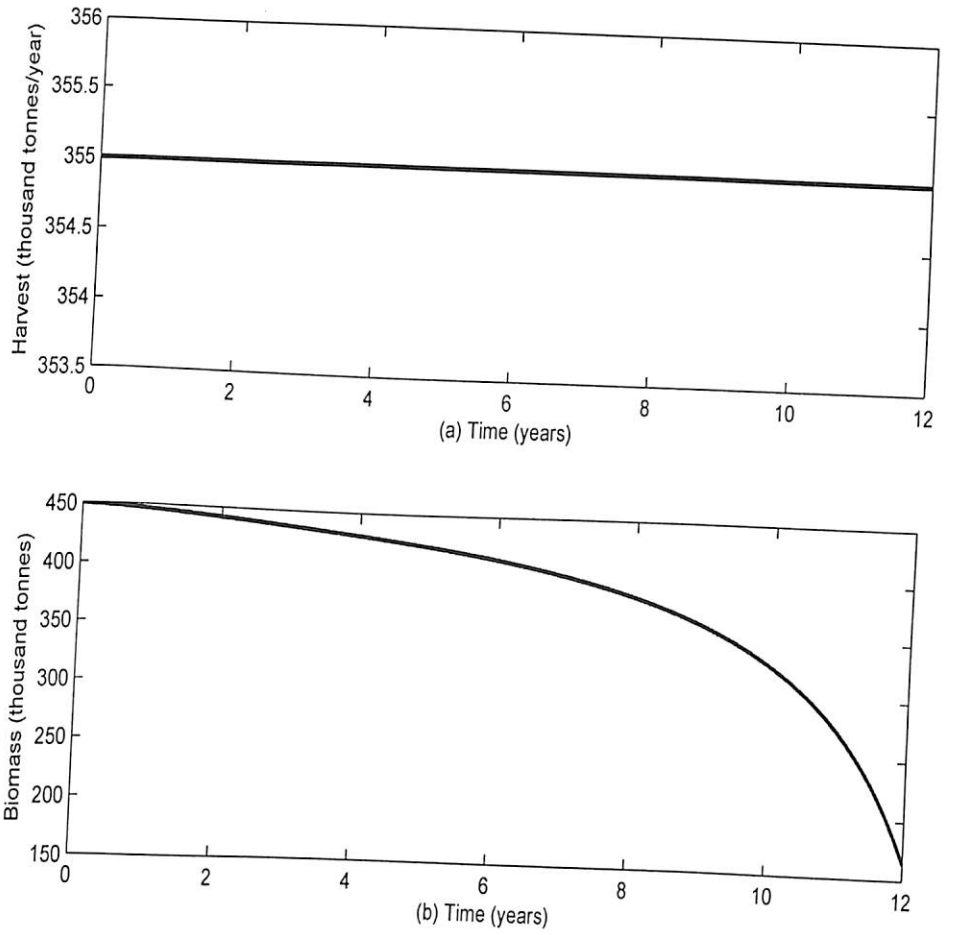

Figure 75: (a) Harvest and (b) Biomass Levels for $h_{max} = 355,000$, $x_0 = 450,000$ and $T = 12$

Assuming an initial population size of 450,000 tonnes, the total yield over the twelve-year horizon corresponding to the given rate of harvesting is computed as 4,259,900 tonnes. It is worthy of note that, when the initial biomass level is 450,000 tonnes (below the single equilibrium point of 500,000 tonnes) the population goes into extinction beyond twelve years. This perfectly agrees with

theoretical results.

Simulation results for the harvest level and stock size relating to the case where $h_{max} = 380,000$ tonnes per year, $x_0 = 750,000$ and $T = 12$ years are presented in Figure 76. In Figure 76 (a), it is observed that when the maximum harvest rate h_{max} is set at a level above the OSY level, the optimal harvest rate follows the maximum path of around 380,000 tonnes per year throughout the twelve-year horizon. On the other hand, the biomass level decreases to about 200,000 tonnes (Figure 76 (b)).

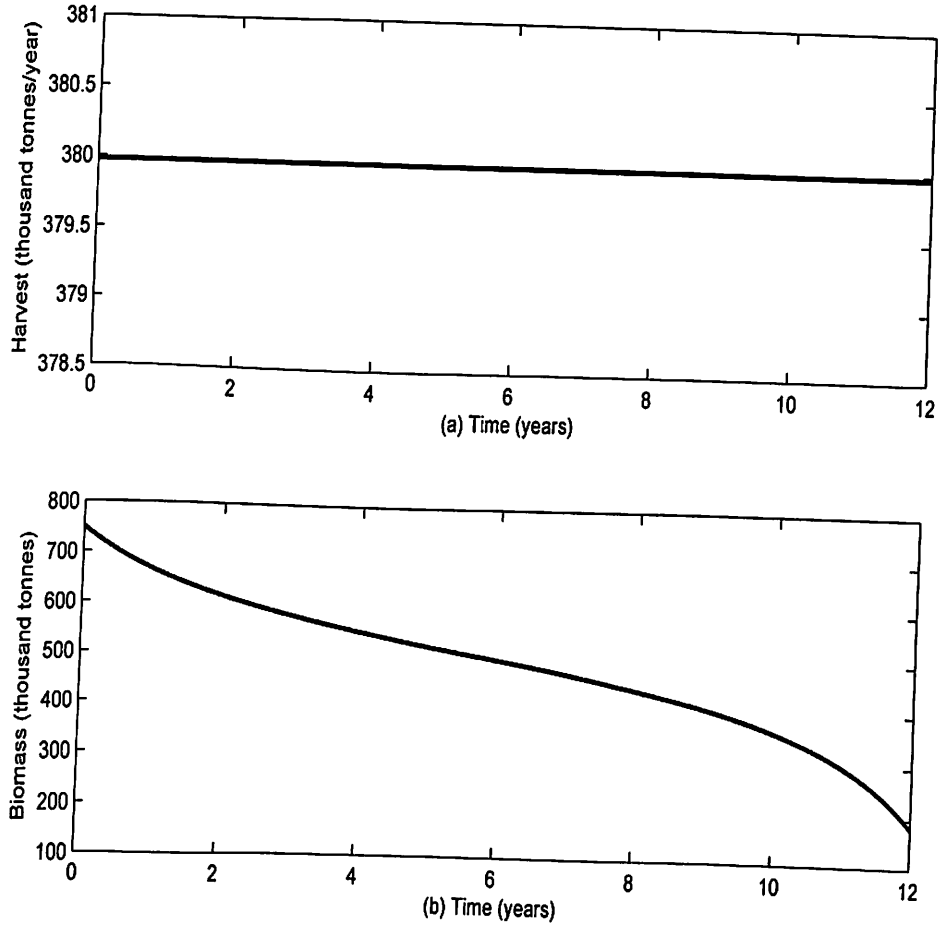

Figure 76: (a) Harvest and (b) Biomass Levels for $h_{max} = 380,000$, $x_0 = 750,000$ and $T = 12$

Assuming an initial population size of 750,000 tonnes, the total yield over the twelve-year horizon corresponding to the given rate of harvesting is computed as 4,559,700 tonnes. It is worthy of note that, when the rate of harvesting is 380,000 tonnes (just 7% above the equilibrium point of 355,000 tonnes) the population

goes into extinction beyond twelve years for an initial biomass level as high as 75% of the carrying capacity. This validates theoretical results.

Model summary

This section looked into the harvesting strategies of the sardinella fishery under the optimal yield model in order to determine the optimal strategy. Characterisation of the optimal rate of fishing gives room for both the bang-bang and singular controls. The boundary controls indicate that the fish stocks should only be exploited if and only if the marginal yield is less than one tonne, and the singular path recommended the harvest rate at the MSY level.

However, in almost all the simulations carried out, the optimal strategy recommended is along the singular path for long-term (or equilibrium) scenario, and along the boundary path for short-term conditions. That is, the optimal harvest rate is mostly at h_{max}, thereby making the constraints on harvest to be binding.

From most of the simulation results, the recommended level of rate of harvesting is at the h_{max} level, with an initial fish stock size of at least 55% of the carrying capacity for sustainability.

A Model with Effective Utilisation Factor

We present a model that seeks the optimal harvest strategy in order to attain the maximum net revenue. To ensure that the fishery is managed in a sustainable way so as to avoid wastage and pollution to the ecosystem, we incorporate an effective utilisation factor (or rate),

$$s(t) = 1 - ae^{-bt}, \quad a, b > 0$$

into the objective functional. The model, originally proposed by Wu, Shen and Liao (2015), is given by

$$\max_h Z(h) = \int_0^T e^{-\delta t}(p-c)h(1-ae^{-bt})\,dt$$
$$\text{subject to} \quad \frac{dx}{dt} = rx\left(1-\frac{x}{K}\right) - h \tag{5.28}$$
$$x(0) = x_0, \qquad x(T) = x_T$$
$$0 \le h \le h_{max}.$$

Let the initial utilisation rate be $s(0) = s_0$ and the achievable effective utilisation rate at the terminal time T be $s(T) = s_T$. Then, the parameters a and b in $s(t)$ can be obtained as follows:

$$a = 1 - s_0,$$
$$b = \frac{1}{T}\ln\frac{1-s_0}{1-s_T}.$$

Additionally, $s(t)$ must satisfy the following assumptions:

1. With the development of technology, the effective utilisation rate $s(t)$ will gradually increase with respect to time t; that is, $s'(t) > 0$.

2. The increase in $s(t)$ will become more difficult after it reaches a certain level in time (diminishing returns); that is, $s''(t) < 0$.

3. The ideal is for the complete or total utilisation of the resource; that is, $\lim_{t\to\infty} s(t) = 1$.

Optimality of the model

The characterisation of the optimal control is sought for in this section. In this vein, the model will be analysed for the determination of a singular path and/or the boundary solutions. This is to enable us establish the conditions necessary for optimality by the use of Pontryagin's maximum principle. The Hamiltonian for the optimal control problem (5.28) can be expressed as

$$H = (p-c)h(1-ae^{-bt}) + \lambda\left[rx\left(1-\frac{x}{K}\right) - h\right]. \tag{5.29}$$

The adjoint variable λ is governed by

$$\begin{aligned}\lambda' &= \delta\lambda - \frac{\partial H}{\partial x} \\ &= \delta\lambda - \lambda\left(r - \frac{2rx}{K}\right).\end{aligned} \tag{5.30}$$

The switching function is defined by

$$\begin{aligned}\psi(t) &= \frac{\partial H}{\partial h} \\ &= (p-c)(1-ae^{-bt}) - \lambda.\end{aligned} \tag{5.31}$$

The characterisation of the optimal control is

$$\begin{cases} h_\delta = 0 & \text{if} \quad \psi(t) < 0, \\ 0 < h_\delta < h_{max} & \text{if} \quad \psi(t) = 0, \\ h_\delta = h_{max} & \text{if} \quad \psi(t) > 0. \end{cases} \tag{5.32}$$

Singularity analysis of the model

This analysis will enable us determine whether the optimal control would be bang-bang or follow a singular path. For a singular control, we assume that there is an interval I for all $t \in I \subset [0,T]$ such that

$$\psi(t) = 0. \tag{5.33}$$

Thus, from Equations (5.31) and (5.33),

$$(p-c)(1-ae^{-bt}) - \lambda = 0. \tag{5.34}$$

So, solving for λ we find

$$\lambda = (p-c)(1-ae^{-bt}). \tag{5.35}$$

Differentiating Equation (5.35) with respect to t, it follows that

$$\lambda' = (p-c)abe^{-bt}. \tag{5.36}$$

By plugging the λ expression in Equation (5.35) into the adjoint equation (5.30), we get

$$\lambda' = (p-c)(1-ae^{-bt})\left(\delta - r + \frac{2rx}{K}\right). \tag{5.37}$$

Setting the expressions in Equations (5.36) and (5.37) equal to each other and simplifying, we obtain

$$x = \frac{K}{2r}\left(r - \delta + \frac{abe^{-bt}}{1 - ae^{-bt}}\right). \tag{5.38}$$

Thus, on the singular interval I we can take the derivative of Equation (5.38) with respect to t. This gives us

$$x' = \frac{K}{2r}\frac{-ab^2e^{-bt}}{\left(1 - ae^{-bt}\right)^2}. \tag{5.39}$$

Comparing Equation (5.39) to the state equation in the model (5.28), we see that they are not equal for all t. So h_δ is nowhere singular and thus it is bang-bang with at most two switching times, occurring where the functions $\lambda(t)$ and $(p - c)(1 - ae^{-bt})$ intersect. Therefore, the inclusion of the utilisation factor effectively rules out the singular path and only the bang-bang approach is feasible. Hence the bang-bang control is

$$h_\delta = \begin{cases} 0 & \text{if} \quad \lambda > (p - c)(1 - ae^{-bt}), \\ h_{max} & \text{if} \quad \lambda < (p - c)(1 - ae^{-bt}). \end{cases} \tag{5.40}$$

Therefore the optimal harvesting regime involves extreme policies only, either harvesting at full capacity or none at all. In other words, the resource should be harvested if and only if the net revenue per unit harvest, taking into consideration the effective utilization rate, exceeds the shadow price of the resource. For further details, see Ibrahim and Benyah (2017).

Numerical simulations

Assuming an effective utilisation rate of between 60 and 62%, the values of the parameters a and b are respectively, 0.4 and 0.05. Also, the discount rate, δ used in the simulations is 10%. Illustration is made of the optimal harvesting strategies corresponding to three values of the maximum rate of harvest h_{max}. These are; 200,000, 250,000, and 300,000 tonnes per year at $x_0 = 500{,}000$ tonnes and $x_T = 650{,}000$ tonnes. Simulation results detailing the relationship between the shadow price and net revenue are also illustrated.

Figure 77 depicts harvesting at the maximum rate of 200,000 tonnes per year, where the shadow price is convex and the revenue, linear. At the start of the harvesting period, the shadow price of fish, US \$175.94 is significantly lower than the net revenue, US \$230.00. This signifies that the revenue due an additional tonne of fish being added to the biomass is less than the expected revenue from harvesting the tonne of fish. So at this instance, it is prudent to harvest at the maximum rate. As time progresses the shadow price experiences a sharp increase in value while the revenue slightly increases until the two intersect at the switching time $t^* = 0.97$ year. Thereafter, the shadow price continues to appreciate in value, ending at US \$240.58. Meanwhile, the revenue has appreciated and ends with a terminal value of US \$237.48. Thus, after little over eleven and a half months (the switching time) it is now less profitable to harvest the fish as the revenue would be lower than the shadow price.

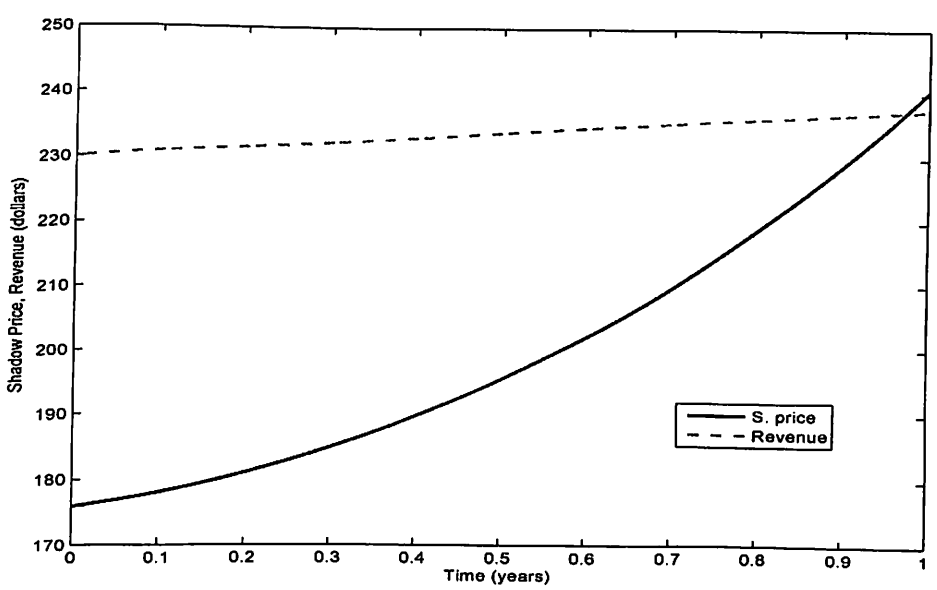

Figure 77: Shadow Price and Net Revenue for $h_{max} = 200,000$ and $T = 1$

Simulation results for the harvesting strategy and biomass level relating to the case where $h_{max} = 200,000$ tonnes per year are presented in Figure 78. In Figure 78 (a), it is observed that the switching time occurs at $t^* = 0.97$ year (see Figure 77) indicating that for the initial eleven and a half months of the year, the maximum rate of harvest should be applied. Thereafter, no harvesting should

occur. This harvest policy allows the fishery resource to be exploited for about eleven and a half months before harvesting stops. A slight change in the growth of fish biomass can be observed once the harvesting is discontinued; see Figure 78 (b). The annual net revenue for this harvest policy is computed and has a value of US $43,321,000.

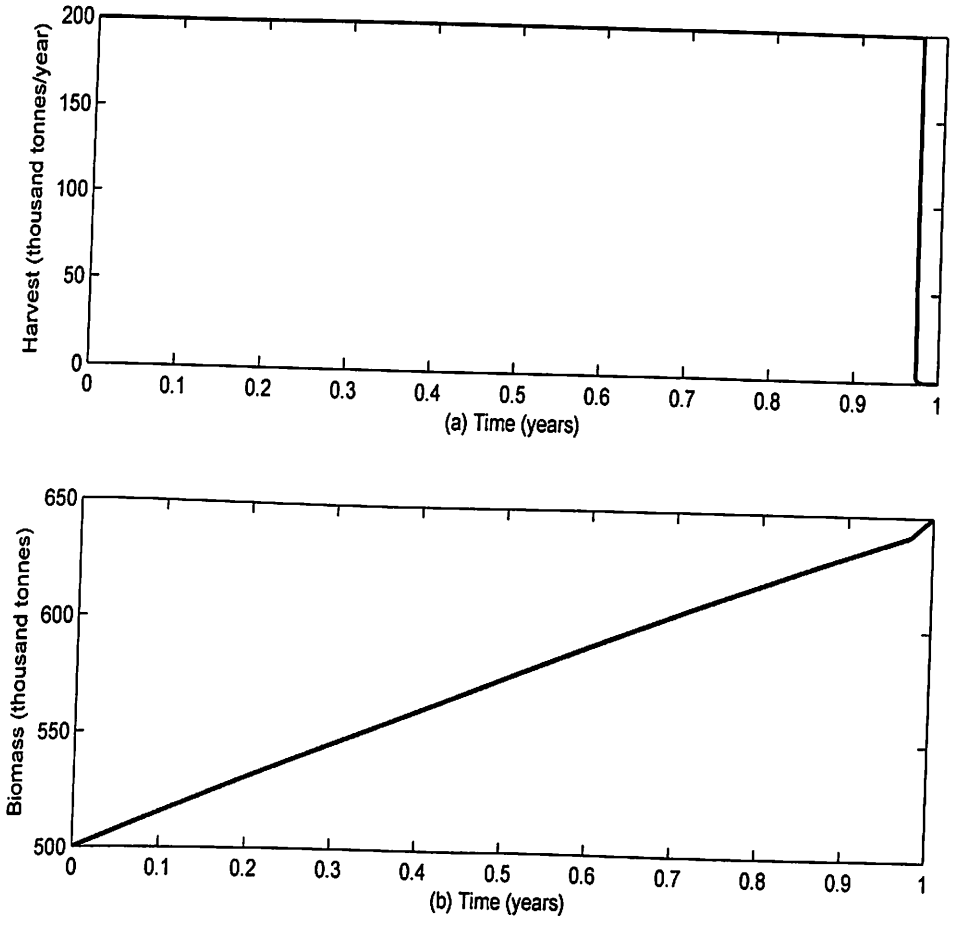

Figure 78: (a) Harvest Strategy and (b) Biomass Level for $h_{max} = 200,000$ and $T = 1$

Figure 79 depicts harvesting at the maximum rate of 250,000 tonnes per year, where the shadow price is convex and the revenue, linear. At the start of the harvesting period, the shadow price of fish, US $198.66 is significantly lower than the net revenue, US $230.00. This signifies that the revenue due an additional tonne of fish being added to the biomass is less than the expected revenue from harvesting the tonne of fish. So at this instance, it is prudent to harvest at the maximum rate. As time progresses the shadow price experiences a sharp increase

in value while the revenue slightly increases until the two intersect at the switching time $t^* = 0.79$ year. Thereafter, the shadow price continues to appreciate in value, ending at US \$257.81. Meanwhile, the revenue has appreciated and ends with a terminal value of US \$237.48. Thus, after about nine and a half months (the switching time) it is now less profitable to harvest the fish as the revenue would be lower than the shadow price.

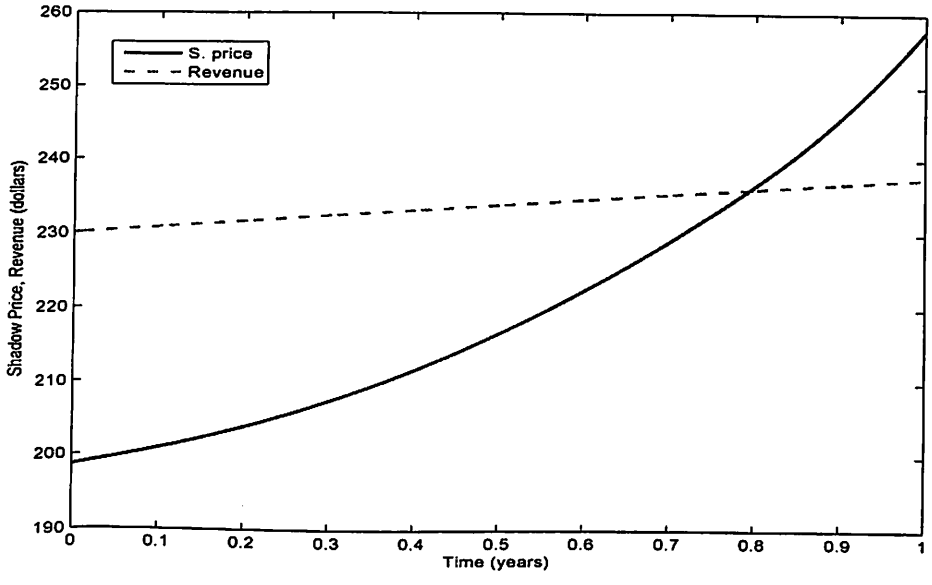

Figure 79: Shadow Price and Net Revenue for $h_{max} = 250,000$ and $T = 1$

Simulation results for the harvesting strategy and biomass level relating to the case where $h_{max} = 250,000$ tonnes per year are presented in Figure 80. In Figure 80 (a), it is observed that the switching time occurs at $t^* = 0.79$ year (see Figure 79) indicating that for the initial nine and a half months of the year, the maximum rate of harvest should be applied. Thereafter, no harvesting should occur. This harvest policy allows the fishery resource to be exploited for about nine and a half months before harvesting stops. A significant change in the growth of fish biomass can be observed once the harvesting is discontinued; see Figure 80 (b). The annual net revenue for this harvest policy is computed and has a value of US \$44,428,000.

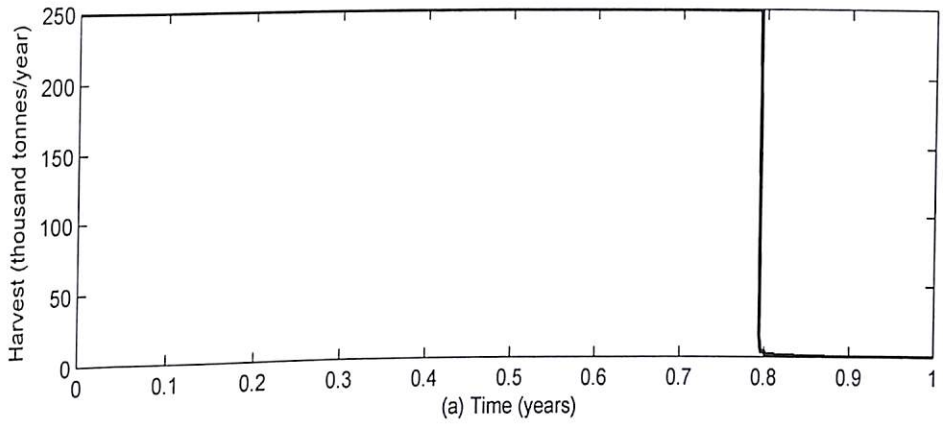

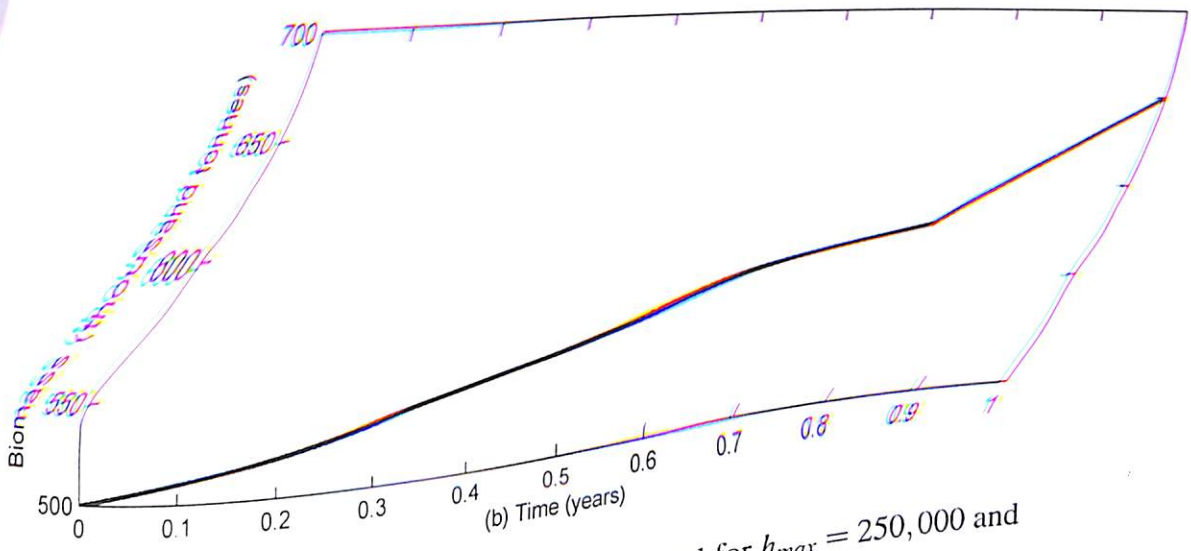

Figure 80: (a) Harvest Strategy and (b) Biomass Level for $h_{max} = 250,000$ and $T = 1$

Figure 81 depicts harvesting at the maximum rate of 300,000 tonnes per year where the shadow price is convex and the revenue, linear. At the start of the harvesting period, the shadow price of fish, US \$212.41 is lower than the net revenue, US \$230.00. This signifies that the revenue due an additional tonne of fish being added to the biomass is less than the expected revenue from harvesting the tonne of fish. So at this instance, it is prudent to harvest at the maximum rate. As time progresses the shadow price experiences a sharp increase in value while the revenue slightly increases until the two intersect at the switching time $t^* = 0.67$ year. Thereafter, the shadow price continues to appreciate in value, ending at US \$265.62. Meanwhile, the revenue has appreciated and ends with a terminal value of US \$237.48. Thus, after about eight months (the switching time) it is now less profitable to harvest the fish as the revenue would be lower than the shadow price.

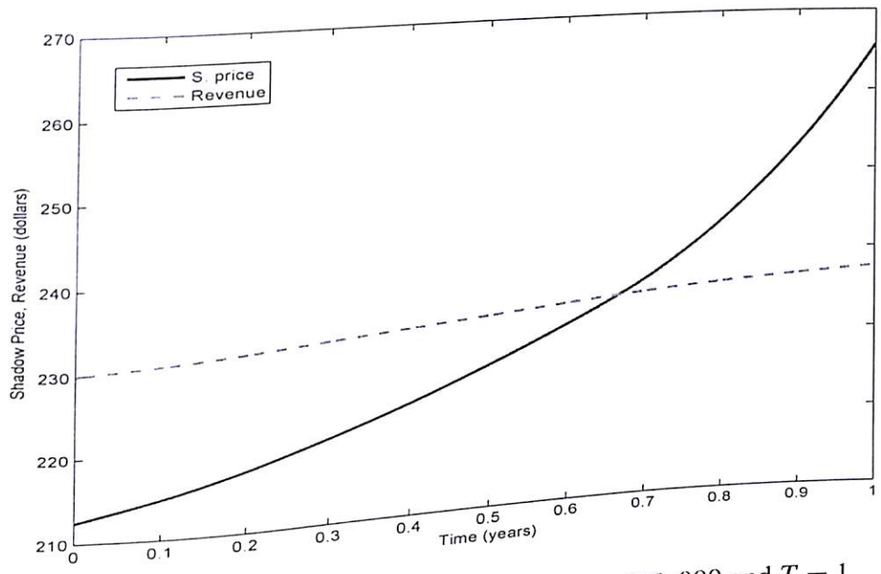

Figure 81: Shadow Price and Net Revenue for $h_{max} = 300,000$ and $T = 1$

Simulation results for the harvesting strategy and biomass level relating to the case where $h_{max} = 300,000$ tonnes per year are presented in Figure 82. In Figure 82 (a), it is observed that the switching time occurs at $t^* = 0.67$ year (see Figure 81) indicating that for the initial eight months of the year, the maximum rate of harvest should be applied. Thereafter, no harvesting should occur. This harvest policy allows the fishery resource to be exploited for about eight months before harvesting stops. A significant change in the growth of fish biomass can be observed once the harvesting is discontinued; see Figure 82 (b). The annual net revenue for this harvest policy is computed and has a value of US $44,974,000.

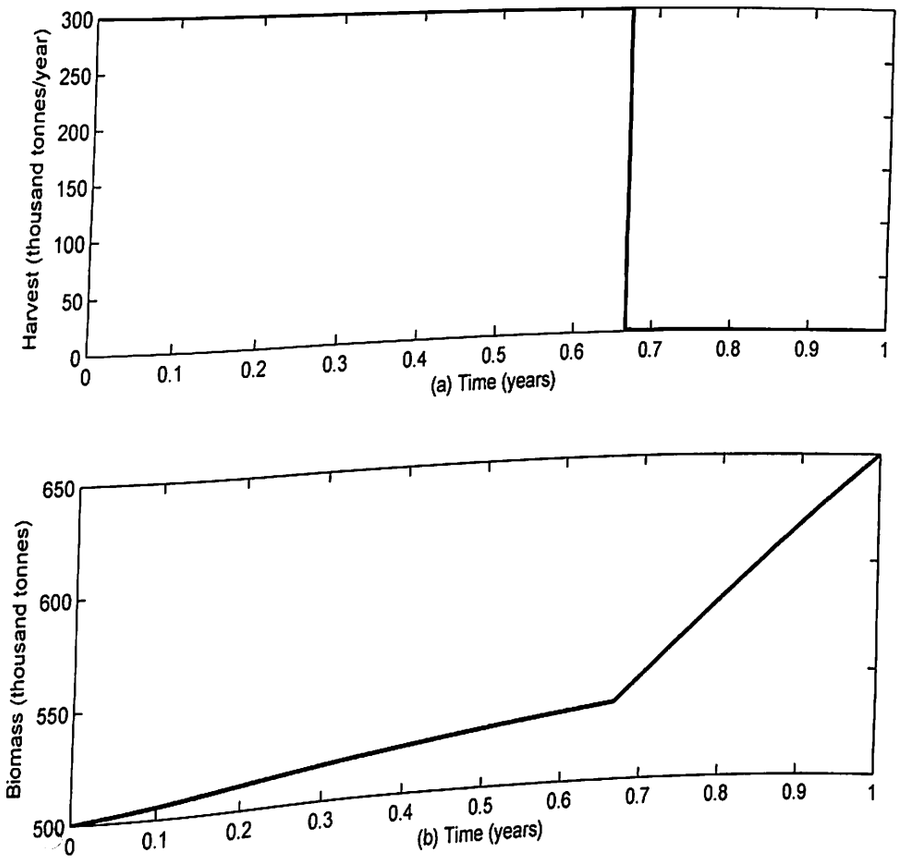

Figure 82: (a) Harvest Strategy and (b) Biomass Level for $h_{max} = 300,000$ and $T = 1$

Model summary

This section considered an optimal control model that incorporated into the objective functional the effective utilisation of the fishery resource. This has become necessary in view of the dwindling catches and the need to effectively utilise these catches. In determining the optimality of the model, characterisation of the optimal control—the rate of harvest—was performed. Also, the model was analysed for singularity and the outcome showed that only the bang-bang approach was applicable.

Afterwards, simulations were carried out for the scenario of the fish stock exploited down to the x_{MSY} level and the need to build up the stock to a level that is 65% of the carrying capacity. Assuming continuing rates of harvest at $h_{max} =$

200,000 tonnes per year, $h_{max} = 250,000$ tonnes per year and $h_{max} = 300,000$ tonnes per year, the results indicate that the case where $h_{max} = 300,000$ tonnes per year provides the greatest revenue. This is also the scenario where the harvest duration is shortest.

Periodic Harvesting Model

As mentioned earlier, the current crisis facing the sardinella fishery in Ghana is of great concern to all stakeholders in the industry. Therefore, every effort is needed to help address the present predicament. Hence, the proposition of the present model.

We take a look at a modified version of the Gordon-Schaefer model with a periodic rate of harvesting. Afterwards, this model will be investigated with the aid of bifurcation and numerical analyses to further shed light on the sardinella fishery in Ghana.

The periodic harvesting version of the dynamic Gordon-Schaefer model can be presented in the following form:

$$\begin{aligned} \max_h Z(h) &= \int_0^\infty e^{-\delta t}(p-c)h\,dt \\ \text{subject to} \quad \frac{dx}{dt} &= rx\left(1-\frac{x}{K}\right) - h(1+a\sin(2\pi t)) \\ x(0) &= x_0 \\ 0 \le h &\le h_{max}, \end{aligned} \tag{5.41}$$

where h_{max} is the maximum allowable harvest, a is the amplitude, p and c are the price and cost per unit harvest, respectively. The model aims to determine the harvest strategy h that results in the largest possible net economic benefit as expressed by the present value integral Z of Model (5.41).

Bifurcation analysis

The periodic harvesting rate, $h(t) = h(1 + a\sin(2\pi t))$ has a mean harvesting rate of h. For example, given $n = 0, 1, 2, \ldots$ and

$$h(t) = 200(1 + 0.25\sin(2\pi t)),$$

then

$$h(t) = \begin{cases} h(0.25 + n) = 250, \\ h(0.75 + n) = 150. \end{cases}$$

Thus, $h(t)$ has a maximum value of 250 and a minimum of 150, with the mean value being $h(0.5n) = 200$ (see Figure 83).

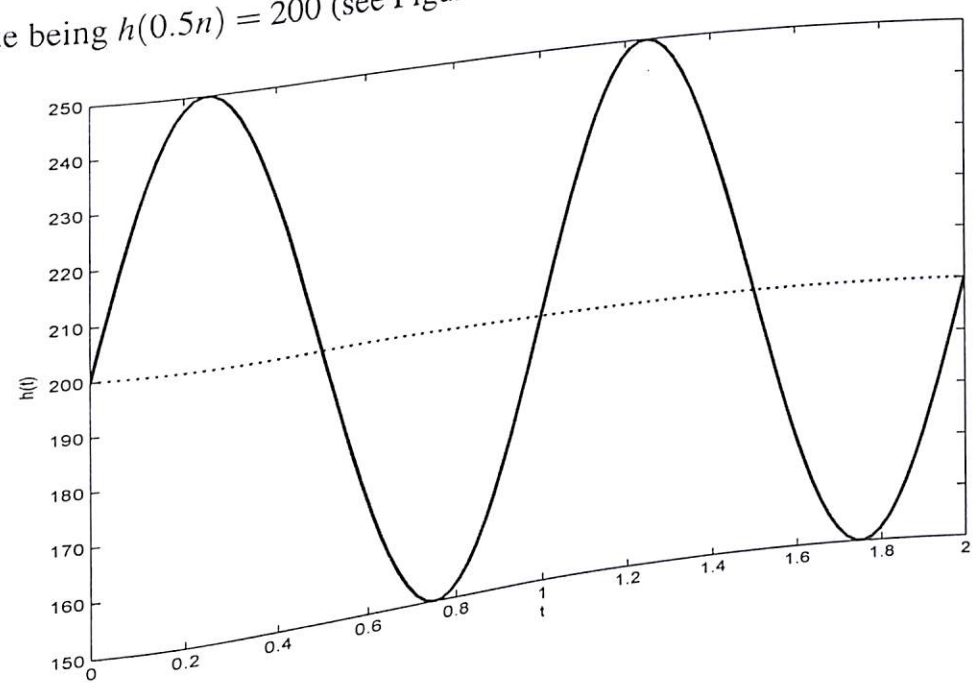

Figure 83: Periodic Rate Harvesting

Furthermore,

$$\lim_{T\to\infty}\int_0^T h\,dt = \lim_{T\to\infty}\int_0^T h(1 + a\sin(2\pi t))\,dt.$$

We shall investigate the stability dynamics of the modified state equation in order to determine the number of equilibrium points and the associated structural stability of the dynamical system.

Invoking Theorem 3.2, there are two equilibrium 'points' associated with the state dynamics of the model (5.41) when the harvest rate is less than the bifurca-

SAM JONAH LIBRARY
UNIVERSITY OF CAPE COAST
CAPE COAST

tion 'point'. These are:

$$x_1^* = \frac{K}{2}\left(1 - \sqrt{1 - \frac{4h}{rK} - \frac{4ha\sin(2\pi t)}{rK}}\right) \quad \text{and}$$

$$x_2^* = \frac{K}{2}\left(1 + \sqrt{1 - \frac{4h}{rK} - \frac{4ha\sin(2\pi t)}{rK}}\right);$$

and the bifurcation point is given by $h = \dfrac{rK}{4(1 + a\sin(2\pi t))}$.

It is worth noting that, when $a = 0$, the equilibrium and bifurcation points reduce to those of the constant rate harvesting model.

Figure 84 presents the periodic cycles for the case where $h = 200{,}000$ tonnes per year. It is observed that there are two periodic solutions of period $P = 1$ oscillating around the mean values: $x_1^* = 169{,}614$ tonnes and $x_2^* = 830{,}386$ tonnes. For any initial population size or biomass level, $x_0 > 830{,}386$ tonnes, the population sinusoidally approaches the mean equilibrium population, 830,386 tonnes in the long run. Similarly, for $169{,}614 < x_0 < 830{,}386$ tonnes, the population asymptotically approaches 830,386 tonnes. Also, for $x_0 < 169{,}614$ tonnes, the population goes into extinction in finite time. Thus the mean biomass level, 169,614 tonnes is unstable while 830,386 tonnes is stable. Of course, biomass levels starting from the mean equilibrium levels, 169,614 and 830,386 tonnes remain there indefinitely. Hence, a harvest rate corresponding to $h = 200{,}000$ tonnes per year induces a long-term biomass level of more than a half the carrying capacity provided $x_0 > 169{,}614$ tonnes.

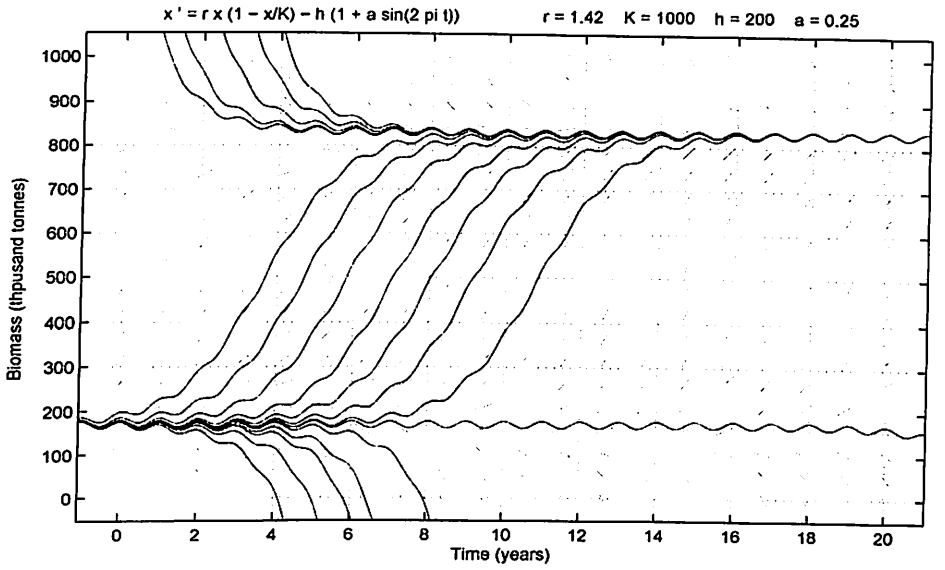

Figure 84: Periodic Cycles for $h = 200,000$

Figure 85 presents the periodic cycles for the case where $h = h_{MSY} = 355,000$ tonnes per year, the bifurcation point. It is observed that there is a single periodic solution, $x^* = 500,000$ tonnes. For any initial population size or biomass level, $x_0 > 500,000$ tonnes, the population approaches the mean equilibrium population, 500,000 tonnes in the long run. However, for $x_0 < 500,000$ tonnes, the population goes into extinction in finite time. Thus the biomass level 500,000 tonnes is semi-stable. Of course, biomass levels starting from the equilibrium level, 500,000 tonnes remain there indefinitely. Hence, a harvest rate corresponding to $h = 355,000$ tonnes per year induces a long-term biomass level of exactly half the carrying capacity provided $x_0 \geq 500,000$ tonnes.

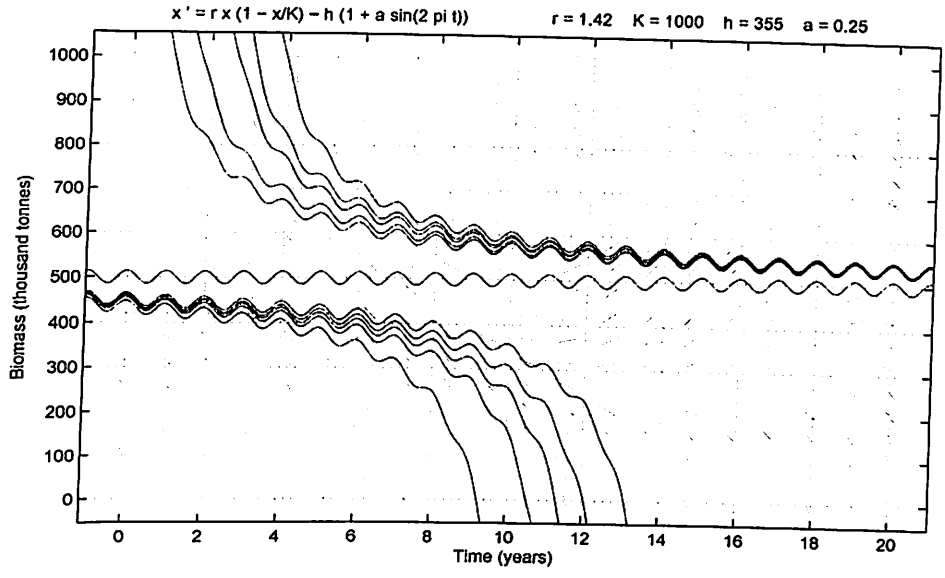

Figure 85: Periodic Cycles for $h = 355,000$

Figure 86 presents the periodic cycles for the case where $h = 400,000$ tonnes per year. It is observed that there is no equilibrium point for this rate of harvest. For any initial population size or biomass level, the population goes into extinction in finite time. Thus, a harvest ratel corresponding to $h = 400,000$ tonnes per year, just 13% greater the MSY level, sends the population into extinction in finite time.

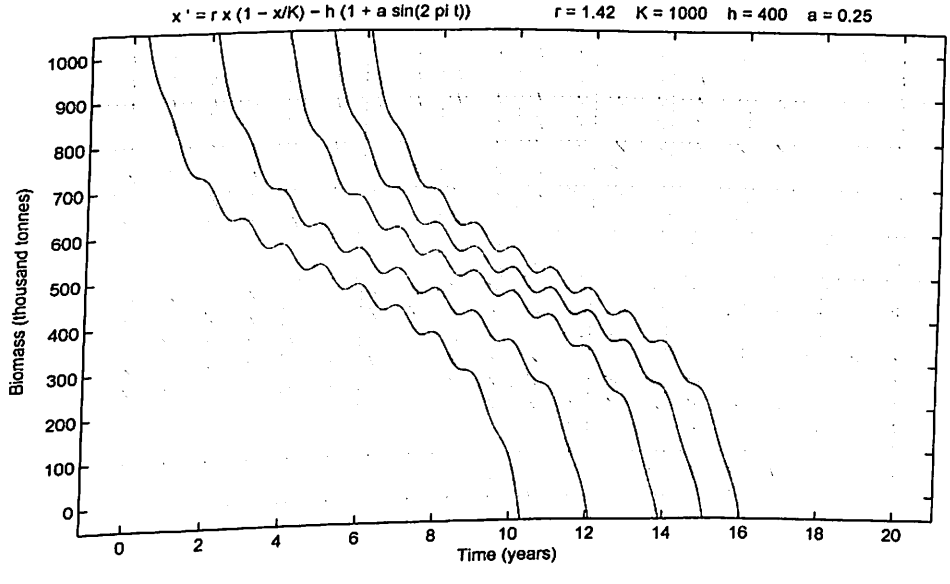

Figure 86: Periodic Cycles for $h = 400,000$

Optimality of the model

The characterisation of the optimal control is sought for in this section. Also, the model is analysed to determine whether or not the singular path is attainable by the control. The goal is to maximise the discounted present value of future net revenues. Thus, we seek an optimal control h_δ such that

$$Z(h_\delta) = \max\{Z(h) \,|\, h \in U\},$$

where the control set, which is Lebesgue measurable for an infinite time horizon, is defined by

$$U = \{h(t) \,|\, 0 \leq h(t) \leq h_{max},\ t \in [0,\infty)\}.$$

To derive the necessary conditions for the optimal control, Pontryagin's maximum principle (Pontryagin *et al.*, 1962) is employed. The current value Hamiltonian for the optimal control problem (5.41) is

$$H = (p-c)h + \lambda\left[rx\left(1-\frac{x}{K}\right) - h(1+a\sin(2\pi t))\right]. \tag{5.42}$$

The adjoint variable λ is governed by

$$\begin{aligned} \lambda' &= \delta\lambda - \frac{\partial H}{\partial x} \\ &= \delta\lambda - \lambda\left(r - \frac{2rx}{K}\right). \end{aligned} \tag{5.43}$$

The switching function is defined by

$$\begin{aligned} \psi(t) &= \frac{\partial H}{\partial h} \\ &= (p-c) - \lambda(1+a\sin(2\pi t)). \end{aligned} \tag{5.44}$$

The characterisation of the optimal control is

$$\begin{cases} h_\delta = 0 & \text{if} \quad \psi(t) < 0, \\ 0 < h_\delta < h_{max} & \text{if} \quad \psi(t) = 0, \\ h_\delta = h_{max} & \text{if} \quad \psi(t) > 0. \end{cases} \tag{5.45}$$

Singularity analysis of the model

This analysis will enable us determine whether the optimal control would be bang-bang or follow a singular path. For a singular control, we assume that there is an interval I for all $t \in I \subset [0,\infty)$ such that

$$\psi(t) = 0. \tag{5.46}$$

Thus, from Equations (5.44) and (5.46),

$$(p-c) - \lambda(1 + a\sin(2\pi t)) = 0. \tag{5.47}$$

So, solving for λ we find

$$\lambda = \frac{p-c}{1+a\sin(2\pi t)}. \tag{5.48}$$

Differentiating Equation (5.48) with respect to t, it follows that

$$\lambda' = -\frac{2\pi a(p-c)\cos(2\pi t)}{(1+a\sin(2\pi t))^2}. \tag{5.49}$$

By plugging the λ expression in Equation (5.48) into the adjoint equation (5.43), we get

$$\lambda' = \frac{p-c}{1+a\sin(2\pi t)}\left(\delta - r + \frac{2rx}{K}\right). \tag{5.50}$$

Setting the expressions in Equations (5.49) and (5.50) equal to each other and simplifying, we obtain the mean optimal biomass level as

$$x_\delta = \frac{K}{2}\frac{ar\sin(2\pi t) - a\delta\sin(2\pi t) - 2\pi a\cos(2\pi t) - \delta + r}{r(1+a\sin(2\pi t))}. \tag{5.51}$$

As in the constant rate harvesting model, if

$$h_\delta < \frac{rK}{4(1+a\sin(2\pi t))},$$

which is the bifurcation level, there exists two periodic solutions. Obviously, the first is Equation (5.51) and the second is given by

$$\hat{x}_\delta = \frac{K}{2}\frac{ar\sin(2\pi t) + a\delta\sin(2\pi t) + 2\pi a\cos(2\pi t) + \delta + r}{r(1+a\sin(2\pi t))}, \tag{5.52}$$

depending on the initial population level. The corresponding harvest level is given by

$$h_\delta = \frac{rK}{4}\frac{\alpha(t)}{\beta(t)}, \tag{5.53}$$

where

$$\begin{aligned}
\alpha(t) &= a^2(r^2-\delta^2)\sin^2(2\pi t) - a^2b^2\cos^2(2\pi t) \\
&\quad + 2a(r^2-\delta^2)\sin(2\pi t) - 2ab\delta(1+a\sin(2\pi t))\cos(2\pi t) + r^2 - \delta^2, \\
\beta(t) &= r^2(1+3a\sin(2\pi t) + 3a^2\sin^2(2\pi t) + a^3\sin^3(2\pi t)).
\end{aligned}$$

Hence the optimal harvesting level is

$$h_\delta = \begin{cases} 0 & \text{if} \quad \lambda > \dfrac{p-c}{1+a\sin(2\pi t)}, \\ \dfrac{rK}{4}\dfrac{\alpha(t)}{\beta(t)} & \text{if} \quad \lambda = \dfrac{p-c}{1+a\sin(2\pi t)}, \\ h_{max} & \text{if} \quad \lambda < \dfrac{p-c}{1+a\sin(2\pi t)}. \end{cases} \tag{5.54}$$

This implies that the optimal control comprises both the extreme controls and the singular control. The extreme controls indicate that the resource should be harvested if and only if the mean net revenue per unit harvest exceeds the current value shadow price of the resource (or the marginal net revenue of stock). It is instructive to note that, if $a = 0$, Equations (5.51) to (5.53) reduce to their respective equations in the constant rate harvesting model.

Numerical simulations

We present simulations results corresponding to OSY. The values employed are those of the constant rate harvesting model, which can be seen as the mean values of the periodic rate harvesting model. The initial simulations are for the case when the amplitude, $a = 0.25$. Later simulations will vary the amplitude. It must be reiterated that, when $a = 0$, we have the constant rate harvesting model. Also, we shall first consider the transient case where T is finite, and then extend it to the equilibrium scenario where $T \to \infty$.

Figure 87 depicts harvesting at a maximum mean rate of 351,039 tonnes per year, $x_0 = 750{,}000$ tonnes, $a = 0.25$ and $T = 1$ year, where the mean net revenue

per unit harvest appears to be sinusoidal and the shadow price is constant. At the start of the harvesting period, the mean net revenue, US \$383.33 is significantly higher than the shadow price, which is zero. This signifies that the revenue due an additional tonne of fish being added to the biomass is much less than the expected revenue from harvesting the fish. So at this instance it is prudent to harvest close to the maximum rate. As time progresses the shadow price is identically zero while the net revenue oscillates from a minimum of US \$306.66 (at $t = 0.25$ year) to a maximum of US \$511.11 (at $t = 0.75$ year) around a mean value of US \$408.89. Obviously, the shadow price is always lower than the net revenue for the one-year horizon. Thus the optimal strategy is bang-bang without switching; that is, fishing at a rate close to the maximum rate throughout the time horizon (see Figure 88).

The shadow price is identically zero as a result of the oscillatory nature of the biomass (see Figure 88). Within a periodic cycle of a year, any increase in marginal net revenue due to an increase in biomass level is cancelled out by a corresponding decrease in marginal net revenue due to a decrease in biomass level.

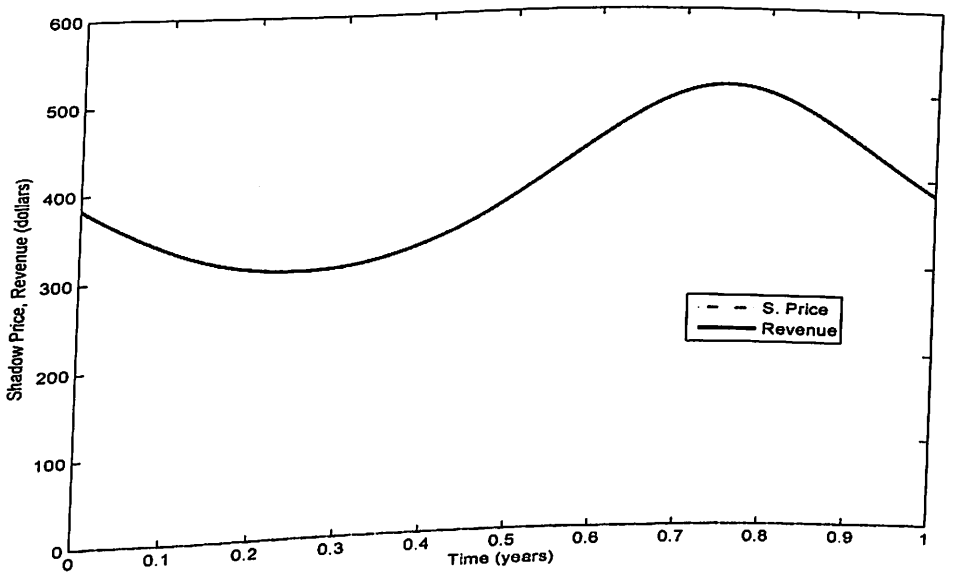

Figure 87: Shadow Price and Net Revenue for $h_{max} = 351,039$, $x_0 = 750,000$, $a = 0.25$ and $T = 1$

Simulation results for the harvest level and stock size relating to the case where $h_{max} = 351,039$ tonnes per year, $a = 0.25$, $T = 1$ year, $x_0 = 500,000$ and $x_0 =$

750,000 tonnes are presented in Figure 88. In Figure 88 (a), it is observed that when the maximum harvest rate h_{max} is set at the OSY level, the optimal harvest rate follows the same path of around 350,700 tonnes per year for both initial biomass levels for the one-year horizon. However, the biomass levels appear to differ. The higher initial biomass level sinusoidally ends at a little below 700,000 tonnes, while the lower initial biomass level ends at a little above 500,000 tonnes (Figure 88 (b)).

Assuming an initial population size of 750,000 tonnes, the total net revenue over the one-year horizon corresponding to the given rate of harvesting is computed as US $124,840,000. The same net revenue is realised for an initial population size of 500,000 tonnes, since the optimal harvest rate is the same for both initial biomass levels.

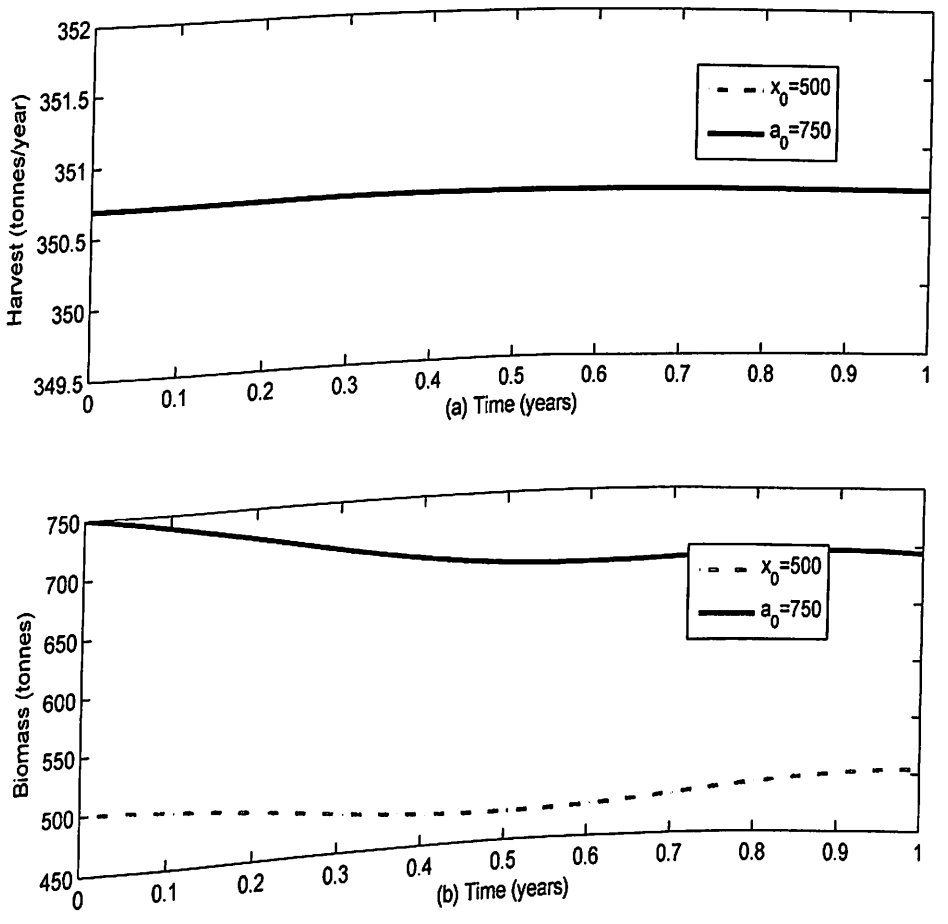

Figure 88: (a) Harvest and (b) Biomass Levels for $h_{max} = 351,039$, $x_0 = 500,000$; 750,000, $a = 0.25$ and $T = 1$

Figure 89 depicts harvesting at a mean maximum rate of 351,039 tonnes per year, $x_0 = 750,000$ tonnes and $T = 50$ years, where the mean net revenue per unit harvest appears to be sinusoidal and the shadow price is constant. At the start of the harvesting period, the mean net revenue, US \$383.33 is significantly higher than the shadow price, which is zero. This signifies that the revenue due an additional tonne of fish being added to the biomass is much less than the expected revenue from harvesting the fish. So at this instance it is prudent to harvest close to the maximum rate. As time progresses the shadow price is identically zero while the net revenue oscillates from a minimum of US \$306.66 (at $t = 0.25$ year) to a maximum of US \$511.11 (at $t = 0.75$ year) around a mean value of US \$408.89. Obviously, the shadow price is always lower than the net revenue throughout the fifty-year horizon. Thus the optimal strategy is bang-bang without switching; that is, fishing at a rate close to the maximum rate throughout the time horizon (see Figure 90). This shows that for a long-term time horizon (or under equilibrium conditions), it is optimal to harvest at a rate close to the maximum level (see Figure 90).

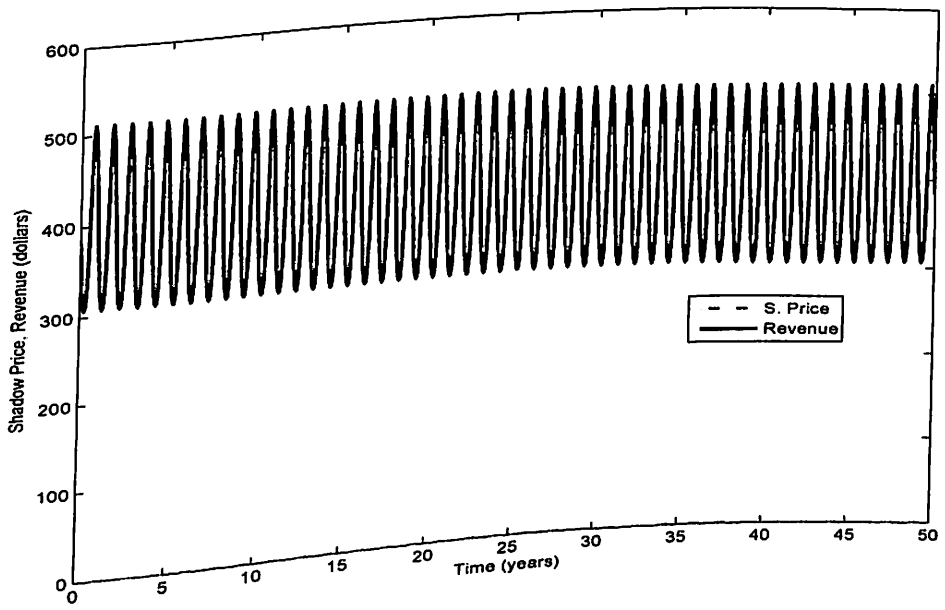

Figure 89: Shadow Price and Net Revenue for $h_{max} = 351,039$, $x_0 = 750,000$, $a = 0.25$ and $T = 50$

Simulation results for the harvest level and stock size relating to the case

where $h_{max} = 351,039$ tonnes per year, $a = 0.25$, $T = 50$ years, $x_0 = 500,000$ and $x_0 = 750,000$ tonnes are presented in Figure 90. In Figure 90 (a), it is observed that when the maximum harvest rate h_{max} is set at the OSY level, the optimal harvest rate follows marginally different paths of around 350,996 tonnes per year and 351,018 tonnes per year for $x_0 = 750,000$ tonnes and $x_0 = 500,000$ tonnes respectively throughout the fifty-year horizon. However, the biomass levels sinusoidally converge around the mean stable equilibrium level of about 553,000 tonnes (Figure 90 (b)).

Assuming an initial population size of 750,000 tonnes, the total net revenue over the fifty-year horizon corresponding to the given rate of harvesting is computed as US \$896,490,000. The net revenue for an initial population size of 500,000 tonnes is marginally higher at US \$896,550,000; about 0.01% greater.

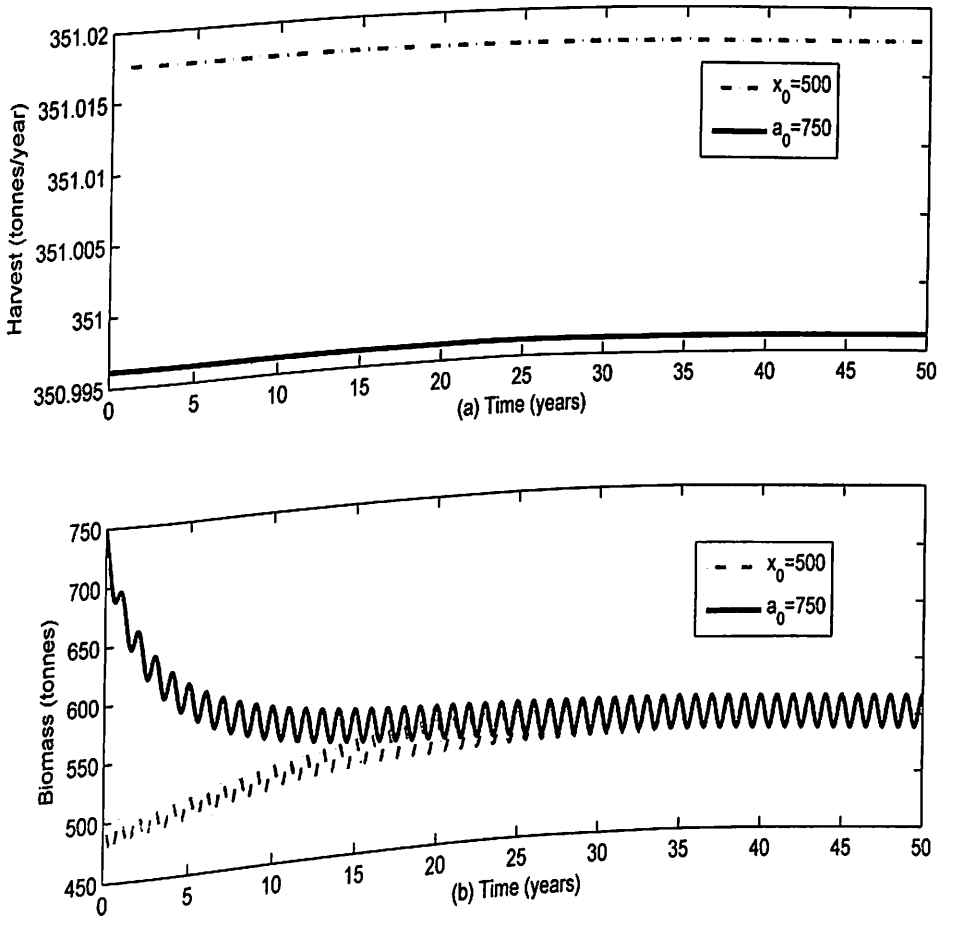

Figure 90: (a) Harvest and (b) Biomass Levels for $h_{max} = 351,039$, $x_0 = 500,000$; 750,000, $a = 0.25$ and $T = 50$

Simulation results for the harvest level and stock size relating to the case where $h_{max} = 351,039$ tonnes per year, $x_0 = 400,000$ tonnes, $a = 0.25$ and $T = 5$ years are presented in Figure 91. In Figure 91 (a), it is observed that when the maximum harvest rate h_{max} is set at the mean OSY level, the optimal harvest rate follows the maximum path of around 351,039 tonnes per year throughout the five-year horizon. On the other hand, the biomass level sinusoidally decreases to around 100,000 tonnes (Figure 91 (b)). For an initial stock size of 400,000 tonnes, the total net revenue over the five-year horizon corresponding to the given rate of harvesting is computed as US \$473,320,000. It is worth noting that, when the initial biomass level is 400,000 tonnes (a little below the lower equilibrium level, and of course the x_{MSY}) the population goes into extinction in just five years. This perfectly agrees with theoretical results.

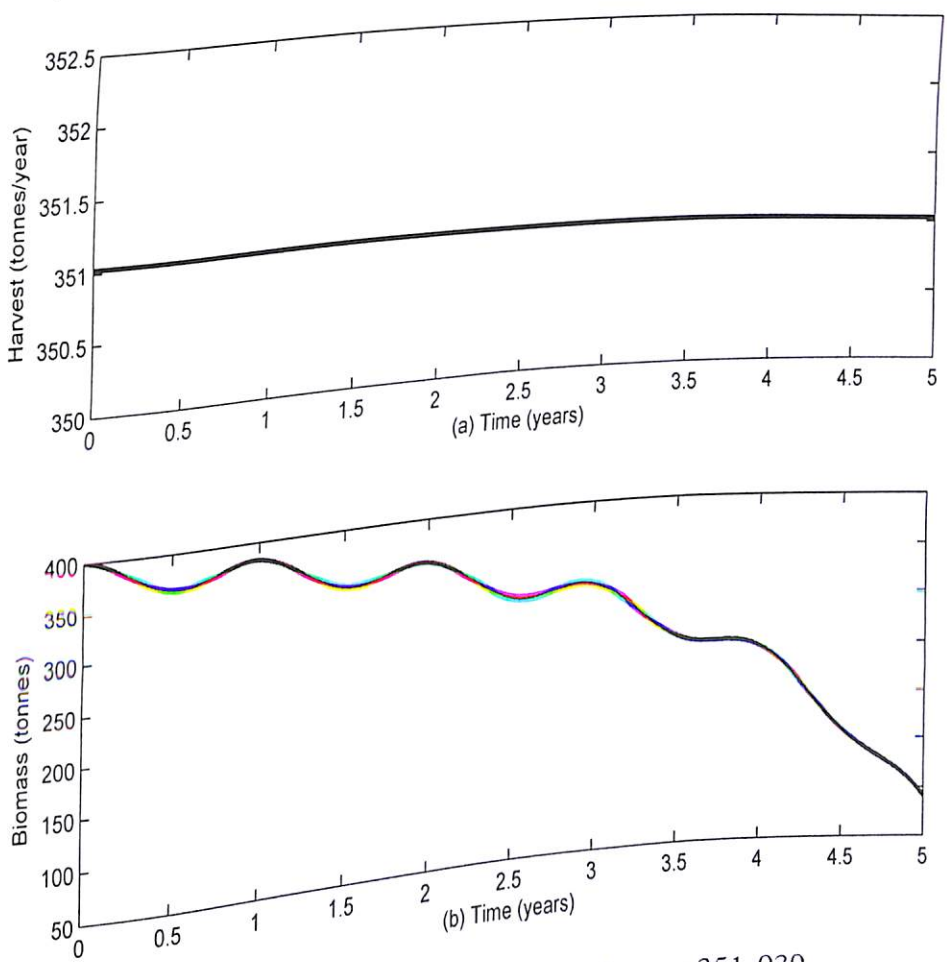

Figure 91: (a) Harvest and (b) Biomass Levels for $h_{max} = 351,039$, $x_0 = 400,000$, $a = 0.25$ and $T = 5$

Simulation results for the harvest level and stock size relating to the case where $h_{max} = 400,000$ tonnes per year, $x_0 = 750,000$, $a = 0.25$ and $T = 8$ years are presented in Figure 92. In Figure 92 (a), it is observed that when the maximum harvest rate h_{max} is set beyond the harvest level at OSY, the optimal harvest rate follows the maximum mean path of around 400,000 tonnes per year throughout the eight-year horizon. On the other hand, the biomass level sinusoidally decreases to about 170,000 tonnes (Figure 92 (b)). For an initial stock size of 750,000 tonnes, the total net revenue over the eight-year horizon corresponding to the given rate of harvesting is computed as US \$714,290,000. It is worth noting that, when the initial biomass level is as high as 75% of the carrying capacity and the harvest rate is set at 400,000 tonnes (just 14% higher than the OSY level) the population goes into extinction beyond eight years. This is in agreement with theoretical results.

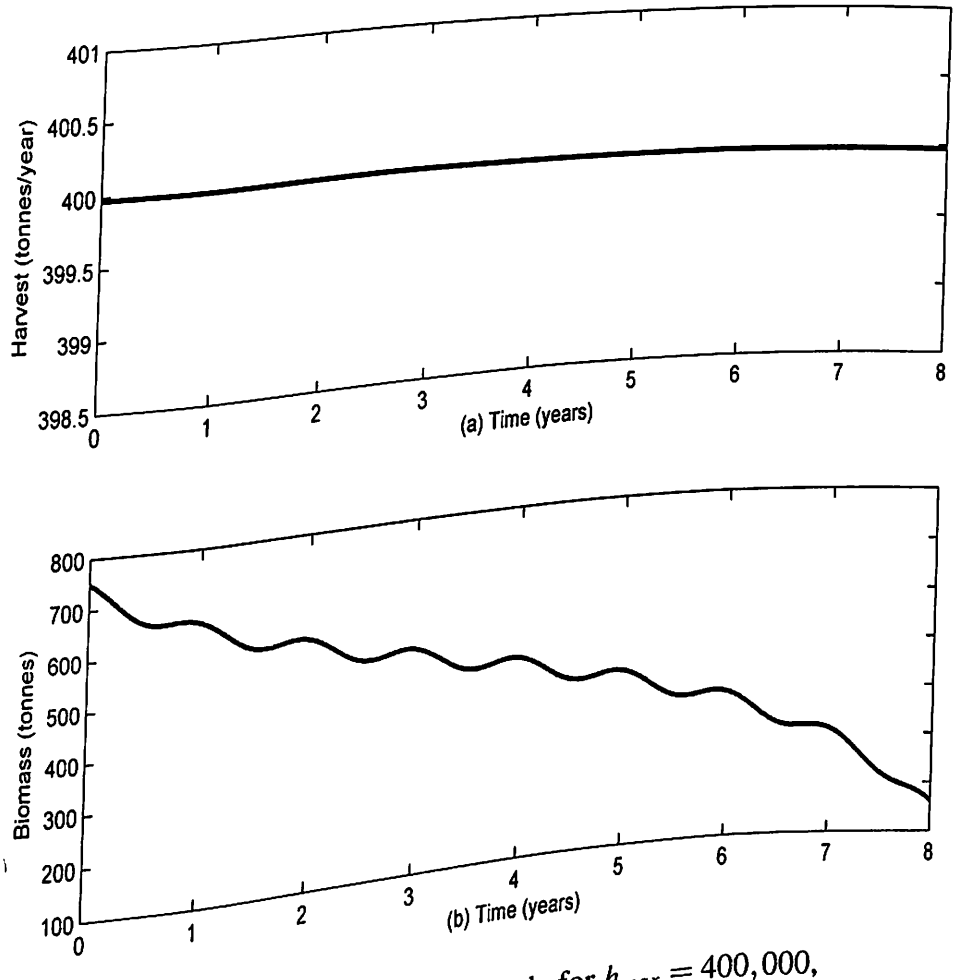

Figure 92: (a) Harvest and (b) Biomass Levels for $h_{max} = 400,000$, $x_0 = 750,000$, $a = 0.25$ and $T = 8$

Simulation results for the harvest level and stock size relating to the case where $h_{max} = 351,039$ tonnes per year, $T = 1$ year, $x_0 = 750,000$ tonnes, $a = 0$ and $a = 0.5$ are presented in Figure 93. In Figure 93 (a), it is observed that when the maximum harvest rate h_{max} is set at the OSY level, the optimal harvest rate follows the same path of around 350,700 tonnes per year for both amplitude values for the one-year horizon. However, the biomass levels appear to differ. The higher amplitude biomass level sinusoidally ends at 700,000 tonnes, while the lower amplitude biomass level ends at about 690,000 tonnes (Figure 93 (b)).

Assuming an initial population size of 750,000 tonnes and an an amplitude of 0.5, the total net revenue over the one-year horizon corresponding to the given rate of harvesting is computed as US $124,840,000. The same net revenue is realised for an amplitude of zero, since the optimal harvest rate is the same for both amplitude levels. It should be stressed that an amplitude of zero effectively reduces the periodic rate harvesting model to the constant rate harvesting model.

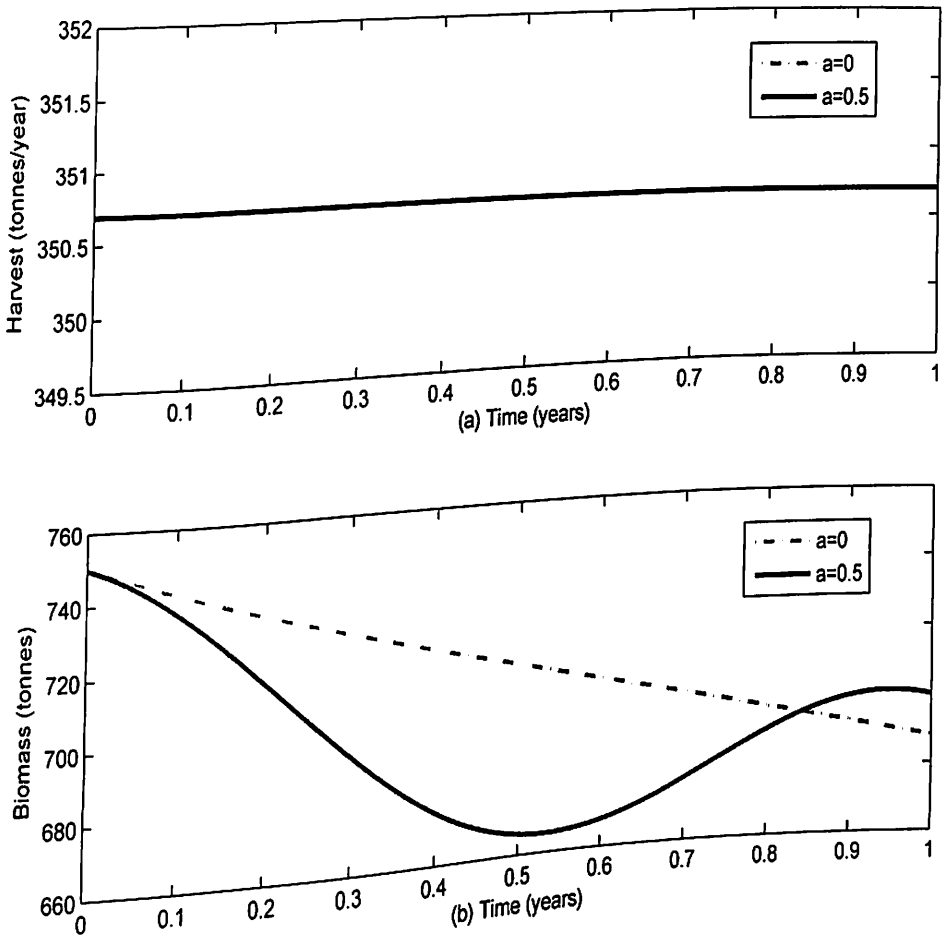

Figure 93: (a) Harvest and (b) Biomass Levels for $h_{max} = 351{,}039$, $a = 0$, 0.5 and $T = 1$

Simulation results for the harvest level and stock size relating to the case where $h_{max} = 351{,}039$ tonnes per year, $T = 50$ years, $x_0 = 750{,}000$ tonnes, $a = 0$ and $a = 0.5$ are presented in Figure 94. In Figure 94 (a), it is observed that when the maximum harvest rate h_{max} is set at the OSY level, the optimal harvest rate follows the same path of around 351,000 tonnes per year for both amplitude values throughout the fifty-year horizon. However, the biomass levels appear to differ. The higher amplitude biomass level sinusoidally ends around the mean stable equilibrium value of 553,000 tonnes, while the lower amplitude biomass level ends at the same equilibrium value (Figure 94 (b)).

Assuming an initial population size of 750,000 tonnes and an amplitude of 0.5, the total net revenue over the fifty-year horizon corresponding to the given rate of harvesting is computed as US \$896,490,000. The same net revenue is

realised for an amplitude of zero, since the optimal harvest rate is the same for both amplitude levels.

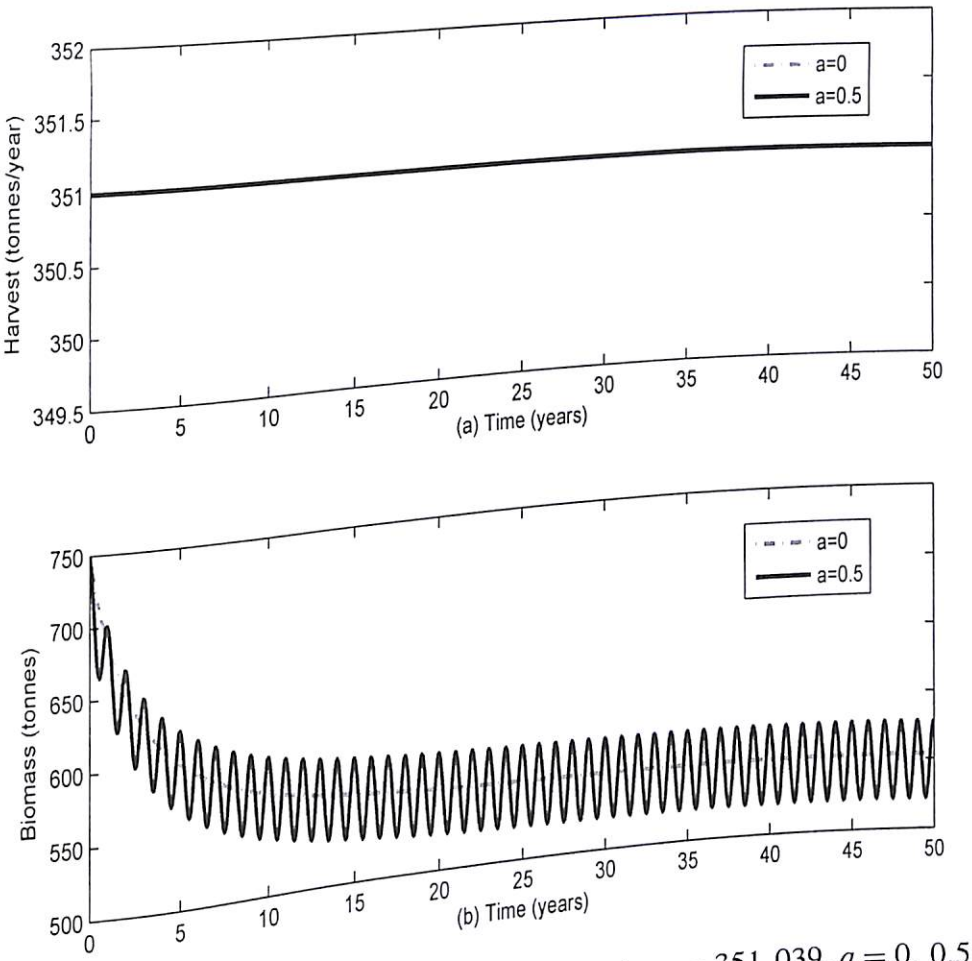

Figure 94: (a) Harvest and (b) Biomass Levels for $h_{max} = 351,039$, $a = 0$, 0.5 and $T = 50$

Simulation results for the harvest level and stock size relating to the case where $h_{max} = 351,039$ tonnes per year, $T = 4$ years, $x_0 = 400,000$ tonnes, $a = 0$ and $a = 0.5$ are presented in Figure 95. In Figure 95 (a), it is observed that when the maximum harvest rate h_{max} is set at the OSY level, the optimal harvest rate follows marginally different paths of around 350,996 tonnes per year and 351,018 tonnes per year for the lower and higher amplitude values, respectively, throughout the four-year horizon. Also, the biomass levels appear to differ. The higher amplitude biomass level sinusoidally ends around the value of 140,000 tonnes, while the lower amplitude biomass level ends at about 310,000 tonnes (Figure 95 (b)).

Assuming an initial population size of 400,000 tonnes and an amplitude of

0.5, the total net revenue over the four-year horizon corresponding to the given rate of harvesting is computed as US \$404,730,000. The net revenue realised for an amplitude of zero is US \$404,710,000, a 0.01% reduction. It is worth noting that, when the initial biomass level is 400,000 tonnes (a little below x_{MSY}) the population goes into extinction in just four years for the fish stock undergoing periodic rate harvesting, while it may take a little longer for the constant rate harvesting (see Figure 71).

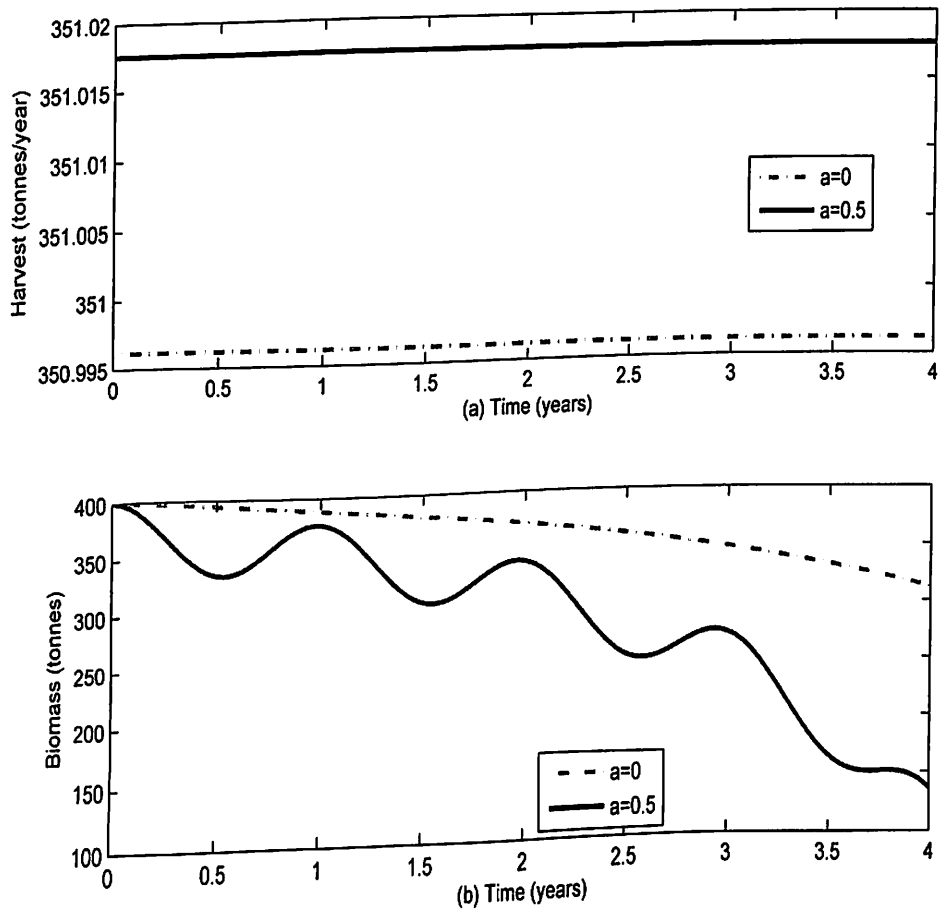

Figure 95: (a) Harvest and (b) Biomass Levels for $h_{max} = 351,039$, $x_0 = 400,000$, $a = 0$, 0.5 and $T = 4$

Simulation results for the harvest level and stock size relating to the case where $h_{max} = 400,000$ tonnes per year, $T = 8$ years, $x_0 = 750,000$ tonnes, $a = 0$ and $a = 0.5$ are presented in Figure 96. In Figure 96 (a), it is observed that when the maximum harvest rate h_{max} is set at value slightly higher than the OSY level, the optimal harvest rate follows the same path of around 400,000 tonnes per year

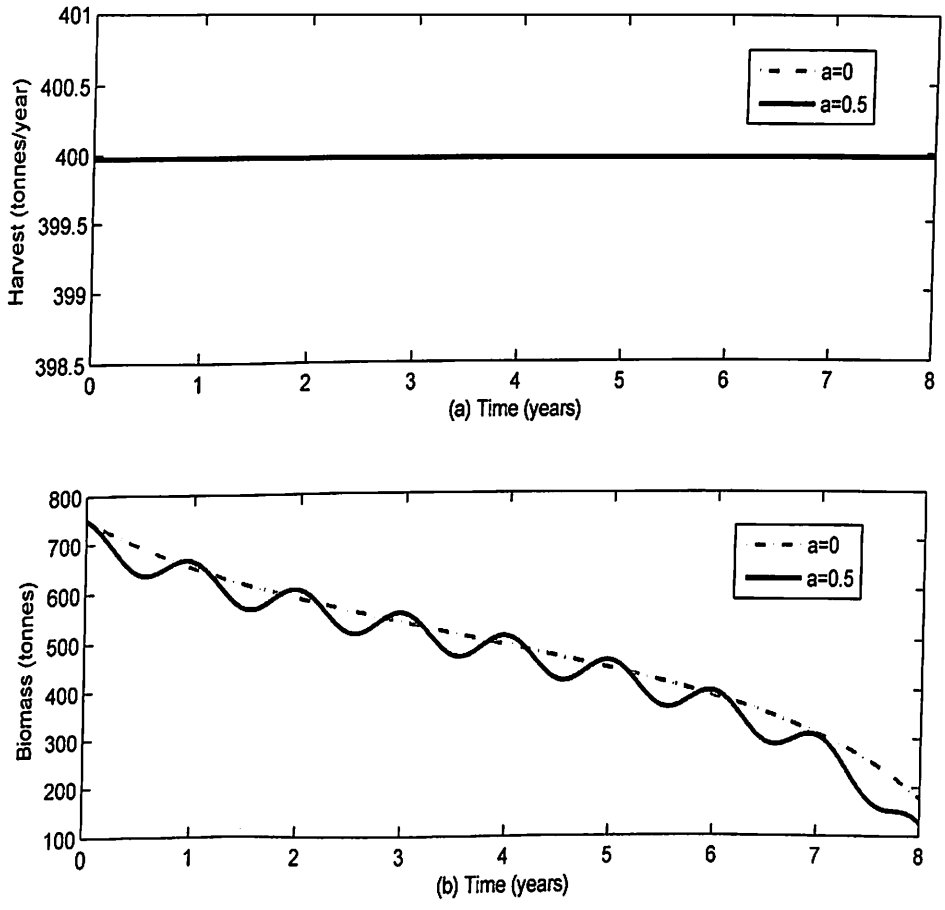

Figure 96: (a) Harvest and (b) Biomass Levels for $h_{max} = 400,000$, $x_0 = 750,000$, $a = 0$, 0.5 and $T = 8$

for both amplitude values throughout the eight-year horizon. Additionally the biomass levels appear to show the periodic rate harvesting scenario almost oscillating around the constant rate harvesting scenario. The higher amplitude biomass level sinusoidally ends at the value of about 140,000 tonnes, while the lower amplitude biomass level ends at about 190,000 tonnes (Figure 96 (b)).

Assuming an initial population size of 400,000 tonnes and an amplitude of 0.5, the total net revenue over the eight-year horizon corresponding to the given rate of harvesting is computed as US \$714,290,000. The same net revenue is realised for an amplitude of zero, since the optimal harvest rate is the same for both amplitudes.

It is worthy of note that, when $x_0 = 750,000$ and the harvest rate is 400,000 tonnes (a little above h_{MSY}), the population goes into extinction in just eight years

for the fish stock undergoing either periodic rate harvesting or constant rate harvesting.

Model summary

This section has looked into the harvesting strategies of the sardinella fishery under the Gordon-Schaefer model with a periodic rate of removals in order to determine the optimal strategy. The biomass was subjected to a bifurcation analysis to determine the bifurcation and the equilibrium points and their stability properties. The non-autonomous periodic rate model may be seen as a perturbation of the autonomous constant rate model, and so the stability properties of the periodic rate model mirror those of the constant rate model.

Numerical simulations were performed on the model to highlight further useful insights. The model was found to attain equilibrium status when the initial biomass level was above the bifurcation point or in between the equilibrium points provided the harvest rates were less than the OSY level. It was also observed that the fish stock faced extinction in finite time when the initial biomass level is relatively low, and also when the harvest rate is above the OSY level.

Simulations were also carried out to compare the relative performance of the periodic rate model and the constant rate model. The observation was that the periodic rate model oscillates around the trajectory of the constant rate model, especially when both models attain equilibrium. It was also observed that the periodic rate model was quicker to send the fish stock into extinction than the constant rate model given the same initial biomass level and harvest rate.

It was further observed that for the same harvesting level, a lower initial biomass level requires a higher harvest rate than for a higher initial biomass level.

Chapter Summary

The chapter has analysed models with the biological dynamics modelled by the logistic equation and the rate of harvesting being constant. These models are the

Gordon-Schaefer model, the Goh model, and a model incorporating an effective utilisation factor.

The canonical model was subjected to bifurcation analysis and the equilibrium points and their stability properties determined. Optmality of the model gave rise to both singular and bang-bang controls. Simulations performed on the dynamic model showed the optimal harvesting rate must be set at the OSY level.

With regard to the Goh model, the objective is to determine the optimal yield without taking into account the cost of fishing. Optimality of the model was determined and the optimal control characterised. The results of the simulations indicate that, in general, the optimal rate of fishing effort must be pegged at the MSY level.

A model with an effective utilisation factor was also investigated. This utilisation factor modifies the objective functional of the canonical model. Optmality of the model was determined and the singular control was ruled out, leaving only the bang-bang control. The results of the simulations indicate that harvest rates at 300,000 tonnes per year provided the greatest revenue and also the shortest duration of harvest compared to rates at 200,000 and 250,000 tonnes per year.

The periodic rate harvesting model was the last to be discussed in the chapter. This model, which is non-autonomous, can be viewed as a perturbation of the autonomous constant rate model. Simulations reveal that harvesting at a periodic rate has a more debilitating effect on the stock size compared to the constant rate harvesting scenario.

CHAPTER SIX

A PREDATOR-PREY MODEL WITH RESERVE AREA

Introduction

There is the need to develop innovative ways to address the current dire situation facing the artisanal fishery in Ghana. Therefore, the adoption and implementation of marine reserves or marine protected areas (MPAs) should be given careful consideration; especially for areas where the fish stocks are known to spawn.

MPAs are defined as spatially well-defined areas where no harvesting takes place, and have become a popular approach to managing marine fisheries (Kar & Matsuda, 2008). The authors further argued that MPAs have provided many general benefits that include serving as a tool for conservation and marine environmental management. Also, it is relatively easy to enforce fishing bans in MPAs, if the necessary will and resources exist: quite simply, any fisherman working in such a reserve is breaking the rules. The more effectively a reserve is functioning, the more carefully these restrictions must be enforced.

According to Kar and Chakraborty (2010), the implementation of marine reserve areas can protect and enhance the stock biomass by protecting the species inside the reserve area and increase fish abundance in adjacent areas. Additionally, the migration rates of the stock biomass between the protected and unprotected areas provide the way to recover the exploited stock and thus enhance the stock biomass.

Furthermore, the protected part of the population serves a 'source' for continuously re-stocking the harvested segment—the 'sink'. Such source-sink dynamics are known to exist in many natural populations (Hanski, 1999; Clark, 2010).

Therefore, a bioeconomic model is developed to assess the possible impact of the marine reserves on sardinella stocks. In the second section, the biological aspect of the model—the state dynamics—is formulated. Stability analysis of

the model is carried out in the third section. This comprises the local and global stability as well as the existence, or lack thereof, of limit cycles. Optimality of the model, which consists of the characterisation of the optimal control as well as the singularity analysis of the model, is discussed in the fourth section. Numerical and graphical illustrations of the model are portrayed in the fifth section while the last section deals with the summary and conclusion.

Model Formulation

The following model, originally proposed by Schaefer (1954) (with $u = 1$), is a Lokta-Volterra type model:

$$\begin{aligned} \frac{dx}{dt} &= rx\left(1 - \frac{x}{K}\right) - uqEx, \\ \frac{dE}{dt} &= uqE(x - a), \end{aligned} \tag{6.1}$$

where $x(t)$ denotes the size of fish population—the prey—and $E(t)$ denotes the fishing effort, and may be considered as the size of the 'population' of fishermen—the predator. Additionally, u $(0 < u < 1)$ is the fraction of fish stock available for harvesting, and a $(0 < a < K)$ is the economically critical level of stock size at which further investment in fishing becomes unprofitable. That is, when the stock size falls below this level, vessels will tend to leave the fishery (Schaefer, 1954). Furthermore, the fraction of the marine reserve is given by $1 - u$.

The main assumption of the model is that the fish population grows logistically in the absence of fishing, while the rate of decrease in the stock size caused by human predation equals $uqEx$. Additionally, the rate of effort exerted by the fishermen declines exponentially when $x < a$, while the rate of effort increases exponentially when $x > a$. Obviously, the rate of change of the effort exerted is zero when $x = a$. It is worthy to note that the fishing effort, $E(t)$ is now a dynamic variable, unlike in the standard Gordon-Schaefer model (see Chapter Four).

Stability Analysis

We shall determine the equilibrium points of the system of equations (6.1) and find the compact, positively invariant region (that is, a region where all the solutions are positive and uniformly bounded). In this region the model is well-posed, both mathematically and in terms of natural resource harvesting (that is, biologically). Furthermore, the local and global stability of the system will be explored as well as the model examined for the existence of periodic orbits (or limit cycles).

Existence of equilibria

The equilibria of the system (6.1) can be obtained by solving $x' = E' = 0$. It is easily checked that there are three equilibrium points:

$$P_0(0,0), \qquad P_1(K,0) \qquad \text{and} \qquad P_2(x^*,E^*),$$

where

$$x^* = a \qquad \text{and} \qquad E^* = \frac{r(K-a)}{uqK}.$$

The following lemma shows that all the solutions of the system (6.1) are positive and uniformly bounded.

Lemma 6.1. *For* $0 < \eta \leq uqa$ *and* $\mu = \frac{K}{4r}(r+\eta)^2$, *the set*

$$\Omega = \left\{(x,E) \in \mathbb{R}_2^+ : 0 \leq x \leq K,\ 0 \leq x+E \leq \frac{\mu}{\eta}\right\}$$

is a region of attraction for all solutions starting in the interior of the positive quadrant.

Proof. : We begin by verifying the first part of the lemma, $0 \leq x \leq K$, using

$$x' = rx\left(1-\frac{x}{K}\right) - uqEx, \quad x(0) = x_0.$$

We apply the comparison theory of differential equations and the theorem on differential inequalities to determine the bounds. Since

$$x' = rx\left(1-\frac{x}{K}\right) - uqEx \leq rx\left(1-\frac{x}{K}\right)$$

for $0 \leq t < \infty$ and $x_0 > 0$, then

$$x' \leq rx\left(1 - \frac{x}{K}\right).$$

Thus,

$$0 \leq x(t) \leq \frac{x_0 K}{x_0 + (K - x_0)e^{-rt}}.$$

Therefore, as $t \to \infty$

$$0 \leq x \leq K.$$

The second part, $0 \leq x + E \leq \frac{\mu}{\eta}$, is verified as follows:

Let $w(t) = x(t) + E(t)$, and $\eta > 0$ be a constant. Then we have

$$\begin{aligned}
\frac{dw}{dt} + \eta w &= \frac{dx}{dt} + \frac{dE}{dt} + \eta x + \eta E \\
&= rx - \frac{rx^2}{K} - uqEa + \eta x + \eta E \\
&= (r+\eta)x - \frac{rx^2}{K} - (uqa - \eta)E \\
&= \frac{K}{4r}(r+\eta)^2 - \frac{r}{K}\left[x - \frac{K}{2r}(r+\eta)\right]^2 - (uqa - \eta)E \\
&\leq \frac{K}{4r}(r+\eta)^2 = \mu, \qquad \eta \leq uqa.
\end{aligned}$$

Invoking Lemma (3.1) on differential inequalities, we have

$$0 \leq w(x(t), E(t)) \leq \frac{\mu}{\eta}(1 - e^{-\eta t}) + w(x(0), E(0))e^{-\eta t};$$

and when $t \to \infty$,

$$0 \leq w \leq \frac{\mu}{\eta}, \quad \text{or} \quad 0 \leq x + E \leq \frac{\mu}{\eta}. \qquad \square$$

Local stability of equilibria

We analyse the local stability of the system (6.1) using the Routh-Hurwitz criteria. The Jacobian matrix for the system is given by

$$J(x, E) = \begin{bmatrix} r\left(1 - \frac{2x}{K}\right) - uqE & -uqx \\ uqE & uq(x - a) \end{bmatrix}.$$

Evaluating the matrix J at $P_0(0,0)$ gives

$$J(0,0) = \begin{bmatrix} r & 0 \\ 0 & -uqa \end{bmatrix}.$$

Since the matrix is diagonal, the associated eigenvalues are $\lambda_1 = r > 0$ and $\lambda_2 = -uqa < 0$. Thus the trivial equilibrium point yields a saddle, which of course is always unstable.

Evaluating the matrix J at $P_1(K,0)$ gives

$$J(K,0) = \begin{bmatrix} -r & uqK \\ 0 & uq(K-a) \end{bmatrix}.$$

Since the matrix is upper triangular, the associated eigenvalues are $\lambda_1 = -r < 0$ and $\lambda_2 = uq(K-a) > 0$. Thus the boundary equilibrium point, $P_1(K,0)$ also produces a saddle.

Evaluating the matrix J at $P_2(x^*,E^*)$ gives

$$J(x^*,E^*) = \begin{bmatrix} -\frac{ar}{K} & -uqa \\ \frac{r(K-a)}{K} & 0 \end{bmatrix}.$$

Thus,

$$\mathrm{Tr}(J(x^*,E^*)) = -\frac{ar}{K} < 0 \qquad \text{and} \qquad \det(J(x^*,E^*)) = \frac{uqar(K-a)}{K} > 0.$$

Hence the equilibrium point is asymptotically stable.

The characteristic polynomial of $J(x^*,E^*)$ is given by

$$\begin{aligned} p(\lambda) &= \left(-\frac{ar}{K} - \lambda\right)(-\lambda) + \frac{uqar(K-a)}{K} \\ &= \lambda^2 - \left(-\frac{ar}{K}\right)\lambda + \frac{uqar(K-a)}{K}. \end{aligned}$$

Given λ_1 and λ_1 are the zeros of $p(\lambda)$, then we have

$$\lambda_1 + \lambda_2 = -\frac{ar}{K} < 0, \qquad \lambda_1 \cdot \lambda_2 = \frac{uqar(K-a)}{K} > 0.$$

Therefore,

$$\lambda_{1,2} \in \{(\lambda_1,\lambda_2) \in \mathbb{R}_2 : \lambda_1 < \lambda_2 < 0\}$$

or

$$\lambda_{1,2} \in \{(\lambda_1, \lambda_2) \in \mathbb{C}_2 : \lambda_{1,2} = a \pm bi,\ a < 0\}.$$

Thus the interior equilibrium point is either a stable node or stable spiral.

The phase-plane portrait relating to the case where $a = 200,000$ tonnes and $u = 0.5$ is presented in Figure 97. It can be observed that the trajectories spiral inwardly to the stable equilibrium point of 200,000 tonnes and 1,262,222 trips, assuming that 50% of the fish stock is available for harvest. Thus, when the critical biomass level is set at a fifth of the carrying capacity and half of the fish stock is open for harvest (50% marine reserve), an effort rate of up to 1,262,222 trips is achievable. This scenario could depict the open access nature of the sardinella fishery in Ghana.

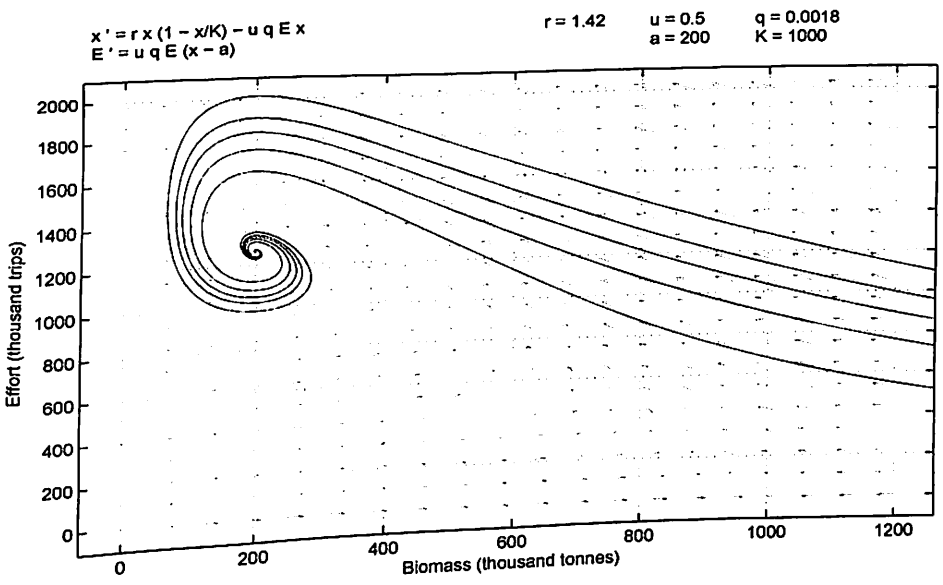

Figure 97: Phase-Plane Portrait for $a = 200,000$ and $u = 0.5$

The phase-plane portrait relating to the case where $a = 500,000$ tonnes and $u = 0.5$ is presented in Figure 98. It can be observed that the trajectories spiral inwardly to the stable equilibrium point of 500,000 tonnes and 788,889 trips, assuming that 50% of the fish stock is available for harvest. Thus, when the critical biomass level is set at half of the carrying capacity and half of the fish stock is open for harvest, an effort rate of up to 788,889 trips (the bifurcation point) is achievable. This scenario depicts a fishery that is being sustainably managed.

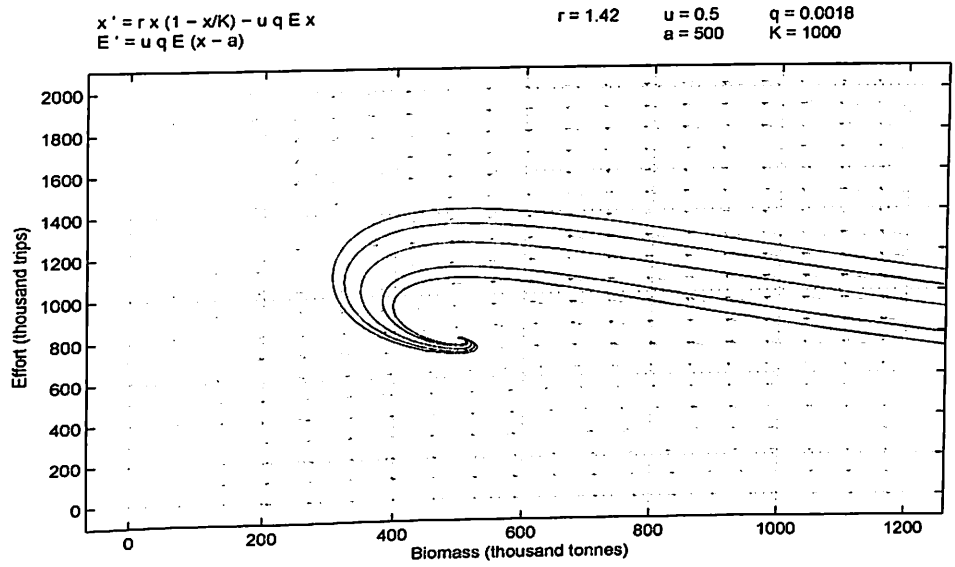

Figure 98: Phase-Plane Portrait for $a = 500,000$ and $u = 0.5$

Global stability

We determine the global stability of the interior equilibrium point through the application of an appropriate Lyapunov function.

Theorem 6.1. *For all solutions starting in the interior of the positive quadrant, the non-trivial equilibrium point $P_2(x^*, E^*)$ is globally asymptotically stable.*

Proof. We shall consider a positive definite function about $P_2(x^*, E^*)$:

$$V = \left(x - x^* - x^* \ln \frac{x}{x^*}\right) + \left(E - E^* - E^* \ln \frac{E}{E^*}\right).$$

Differentiating V with respect to time t along the trajectories of System (6.1) gives

$$V' = \left(1 - \frac{x^*}{x}\right) x' + \left(1 - \frac{E^*}{E}\right) E'.$$

Substituting for x' and E' gives

$$V' = (x - x^*)\left[r\left(1 - \frac{x}{K}\right) - uqE\right] + uq(E - E^*)(x - a).$$

At the interior equilibrium, we have

$$r\left(1 - \frac{x^*}{K}\right) - uqE^* = 0,$$

$$x^* - a = 0.$$

Thus,

$$\begin{aligned} V' &= -(x-x^*)\left[\frac{r}{K}(x-x^*)+uq(E-E^*)\right]+uq(E-E^*)(x-x^*) \\ &= -\frac{r}{K}(x-x^*)^2 < 0. \end{aligned}$$

Hence V' is negative definite and V is radially unbounded. Therefore by Lyapunov's theorem on stability, it implies that the interior equilibrium point $P_2(x^*, E^*)$ is globally asymptotically stable. □

The following theorem indicates that the system (6.1) does not possess any closed trajectories or limit cycles in the interior of the positive quadrant of the $x-E$ plane.

Theorem 6.2. *The system (6.1) does not possess any limit cycles in the interior of the positive quadrant.*

Proof. Let

$$\begin{aligned} \phi(x,E) &= \frac{1}{xE}, \\ f(x,E) &= rx\left(1-\frac{x}{K}\right)-uqEx, \\ g(x,E) &= uqE(x-a). \end{aligned}$$

Obviously, $\phi(x,E) > 0$ in the interior of the positive quadrant. Therefore, we have

$$\begin{aligned} \Delta(x,E) &= \frac{\partial(\phi f)}{dx}+\frac{\partial(\phi g)}{dE} \\ &= \frac{\partial}{dx}\left[\frac{r}{E}\left(1-\frac{x}{K}\right)-uq\right]+\frac{\partial}{dE}\left[\frac{uq}{x}(x-a)\right] \\ &= -\frac{r}{EK} < 0. \end{aligned}$$

Since $\Delta(x,E)$ does not change sign in the positive quadrant, then by the Bendixson-Dulac Theorem, the system has no limit cycles (Dubey *et al.*, 2003). □

Optimality of the Model

As previously stated, only a proportion of the fish stock is subjected to harvesting. Thus the optimal control problem is to maximise the present value of the

net revenue derived from the partial harvests; and can be expressed as

$$\begin{aligned} \max_u Z(u) &= \int_0^\infty e^{-\delta t}(puqx - c)E\,dt \\ \text{subject to} \quad \frac{dx}{dt} &= rx\left(1 - \frac{x}{K}\right) - uqEx \\ \frac{dE}{dt} &= uqE(x-a) \\ x(0) = x_0, \qquad & E(0) = E_0 \\ 0.4 \le u \le u_{max}. & \end{aligned} \tag{6.2}$$

It is assumed that the least proportion of fish stock available for harvesting is 0.4, and the maximum is $u_{max} < 1$ (Kar & Chakraborty, 2010).

The characterisation of the optimal control is determined in this section. Also, the model is analysed to ascertain whether or not the singular path is attainable by the control.

Characterisation of the optimal control

The goal is to maximise the discounted present value of future net revenues. Thus, we seek an optimal control u_δ such that

$$Z(u_\delta) = \max\{Z(u) \,|\, u \in U\},$$

where the control set, which is piecewise continuous for an infinite time horizon, is defined by

$$U = \{u(t) \,|\, 0.4 \le u(t) \le u_{max},\ t \in [0,\infty)\}.$$

To derive the necessary conditions for the optimal control, Pontryagin's maximum principle is employed. The current value Hamiltonian for the optimal control problem (6.2) is

$$H = (puqx - c)E + \lambda_1\left[rx\left(1 - \frac{x}{K}\right) - uqEx\right] + \lambda_2 uqE(x-a). \tag{6.3}$$

The adjoint variables λ_1 and λ_2 are governed by

$$\begin{aligned} \lambda_1' &= \delta\lambda_1 - \frac{\partial H}{\partial x} \\ &= \left(\delta - r + \frac{2rx}{K} + uqE\right)\lambda_1 - uqE\lambda_2 - puqE, \end{aligned} \tag{6.4}$$

and

$$\begin{aligned}\lambda_2' &= \delta\lambda_2 - \frac{\partial H}{\partial E} \\ &= [\delta - uq(x-a)]\lambda_2 + uqx\lambda_1 - puqx + c. \end{aligned} \tag{6.5}$$

The switching function is defined by

$$\frac{\partial H}{\partial u} = pqEx - qEx\lambda_1 + qE(x-a)\lambda_2. \tag{6.6}$$

The characterisation of the optimal control is

$$\begin{cases} u_\delta = 0.4 & \text{if} \quad \frac{\partial H}{\partial u} < 0, \\ 0.4 < u_\delta < u_{max} & \text{if} \quad \frac{\partial H}{\partial u} = 0, \\ u_\delta = u_{max} & \text{if} \quad \frac{\partial H}{\partial u} > 0. \end{cases} \tag{6.7}$$

Singularity analysis of the model

The optimal control problem (6.2) has a linear control. Therefore, there arises the possibility of singular arcs; and the higher order necessary conditions are given by the Generalised Legendre-Clebsch conditions (de Pillis *et al.*, 2007; Krener, 1977).

Given an interval and $n \geq 1$ control variables u_i, $i = 1, 2, \ldots, n$, a singular arc occurs when at least one of the control variables satisfies

$$\frac{\partial H}{\partial u_i} = 0.$$

It can be verified that a singular control u will first make an appearance in an even order time derivative of $\frac{\partial H}{\partial u}$. Additionally, the order of singularity of a control u on this interval is defined as the least integer k such that

$$\frac{\partial}{\partial u}\left[\left(\frac{d}{dt}\right)^{2k}\frac{\partial H}{\partial u}\right] \neq 0.$$

Theorem 6.3 (Generalised Legendre-Clebsch Condition). *Suppose the controls u_i, for $i = 1, 2, \ldots, n$ are singular on an interval. Let A be an $n \times n$ matrix given by*

$$A_{i,j} = (-1)^{k_j}\frac{\partial}{\partial u_i}\left[\left(\frac{d}{dt}\right)^{k_i+k_j}\frac{\partial H}{\partial u_j}\right];$$

where k_i is the order of singularity of the control u_i. Then A must be non-negative definite (or negative semi-definite) for the control to be maximising.

If there is only one singular control u, this reduces to

$$(-1)^k \frac{\partial}{\partial u}\left[\left(\frac{d}{dt}\right)^{2k}\frac{\partial H}{\partial u}\right] \leq 0.$$

(de Pillis *et al.*, 2007)

For a singular control, we assume that there is an interval I for all $t \in I \subset [0,\infty)$ such that

$$\frac{\partial H}{\partial u} = 0.$$

This implies, from Equation (6.6), that

$$\frac{\partial H}{\partial u} = px - x\lambda_1 + (x-a)\lambda_2 = 0.$$

Next, we compute

$$\frac{d}{dt}\left(\frac{\partial H}{\partial u}\right) = 0,$$

and then it will be shown that the control cannot be found in that equation. To solve for the value of the singular control, we will further compute

$$\frac{d^2}{dt^2}\left(\frac{\partial H}{\partial u}\right) = 0.$$

First, after substituting for x', E', λ_1' and λ_2' with

$$\lambda_1 = p + \lambda_2\left(1 - \frac{a}{x}\right),$$

the simplification of $\frac{d}{dt}\left(\frac{\partial H}{\partial u}\right) = 0$ is given by

$$-(2\lambda_2 r + 2pr)x^2 + (K\lambda_2 r - K\delta p + Kpr + a\lambda_2 r + Kc)x - Kac = 0.$$

Clearly, the control does not explicitly appear in the equation, so we proceed to compute the second derivative with respect to time. Therefore, $\frac{d^2}{dt^2}\left(\frac{\partial H}{\partial u}\right) = 0$ can be written in the form

$$\alpha(x,E)u + \beta(x,E) = 0,$$

or

$$u = -\frac{\beta(x,E)}{\alpha(x,E)},$$

where

$$\alpha(x,E) = EKq(4\lambda_2 r + 4pr)x - EKq(K\lambda_2 r - K\delta p + Kpr + a\lambda_2 r + Kc),$$

and

$$\begin{aligned}\beta(x,E) &= r(4\lambda_2 r + 4pr)x^2 + r(-2K\delta\lambda_2 + K\delta p - 5\lambda_2 r - 5Kpr \\ &\quad - a\lambda_2 r - 3Kc)x + r(K^2\delta\lambda_2 - K^2\delta p + K^2\lambda_2 r \\ &\quad + K^2 pr + Ka\delta\lambda_2 + Ka\lambda_2 r + 2K^2 c + Kac).\end{aligned}$$

The Generalised Legendre-Clebsch condition needs to be satisfied for the singular control to be maximising; that is, $\alpha(x,E)$ would have to be non-negative on this interval.

The order of singularity, $k = 1$. To determine the sign of $\alpha(x,E)$, we plot $\alpha(x,E)$ against x and E, after noting that $\lambda_1(t) = 0$ and $\lambda_2(t) = 0$ (as $t \to \infty$). It should be noted that $\alpha(x,E)$ is only negative in a very specific region. In this region, there can be a guarantee that there are no singular maximising arcs, so the control is bang-bang. In other regions, the possibility for singular arcs cannot be ruled out (see Figure 99).

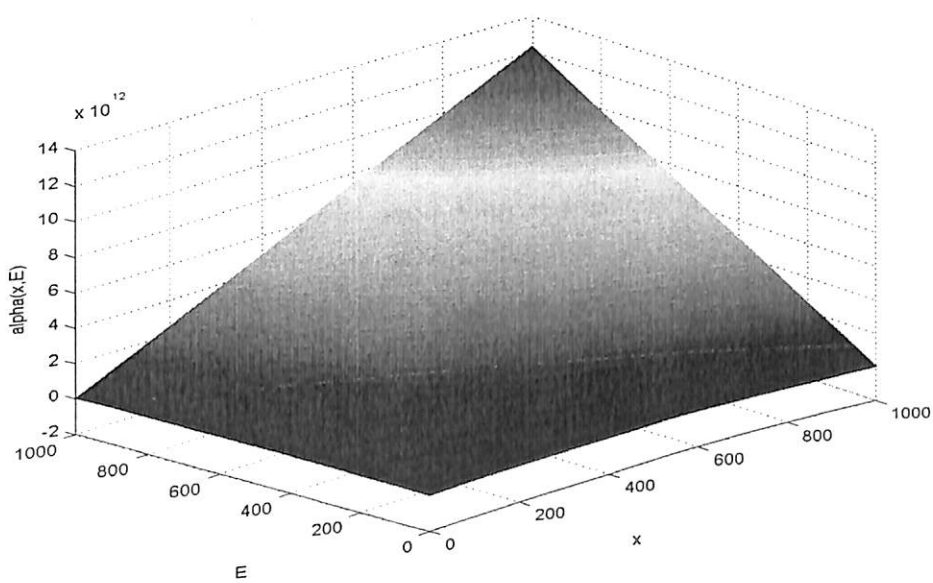

Figure 99: Determination of Sign of $\alpha(x,E)$

Hence, the optimal proportion of biomass available for harvesting is

$$u_\delta = \begin{cases} 0.4 & \text{if} \quad \lambda_1 - \left(1 - \frac{a}{x}\right)\lambda_2 > p, \\ -\frac{\beta(x,E)}{\alpha(x,E)} & \text{if} \quad \lambda_1 - \left(1 - \frac{a}{x}\right)\lambda_2 = p, \\ u_{max} & \text{if} \quad \lambda_1 - \left(1 - \frac{a}{x}\right)\lambda_2 < p. \end{cases} \tag{6.8}$$

The following discussion is on the coefficient of the shadow price of effort λ_2:

$$\left(1 - \frac{a}{x}\right) \geq 0 \quad \text{if} \quad x \geq a,$$

and

$$\left(1 - \frac{a}{x}\right) < 0 \quad \text{if} \quad x < a.$$

Therefore, the boundary controls indicate that when the price of landed fish is greater than the difference (or sometimes, the sum) of the shadow price of fish stock and a fraction of the shadow price of effort, the optimal control must be set at the maximum proportion of biomass available for harvesting; otherwise, the control should be set at the minimum level.

The shadow price of effort (or the marginal net revenue of effort) may be viewed as the change in net revenue as a result of one additional fishing trip.

It is instructive to note that, while λ_1 is non-negative, λ_2 assumes all real values (that is, both non-negative and negative values).

The existence of the optimality system is easily verified. That is, the boundedness of the solutions of the state system has already been established (see Lemma 6.1). Also, the state system and the objective functional are both linear in the control u. Therefore, by standard arguments, an optimal control as well as the optimal states exist (Fleming & Rishel, 1995; Joshi *et al.*, 2015).

Numerical Simulations

We shall subject the model to numerical simulations and the results will be illustrated graphically. First, a number of simulations are performed with the maximum proportion of biomass available for harvesting set at 50%, while varying the

initial stock level. Subsequently, the maximum proportion of biomass available for harvesting will be set at 90%. Initially, we shall consider the transient case

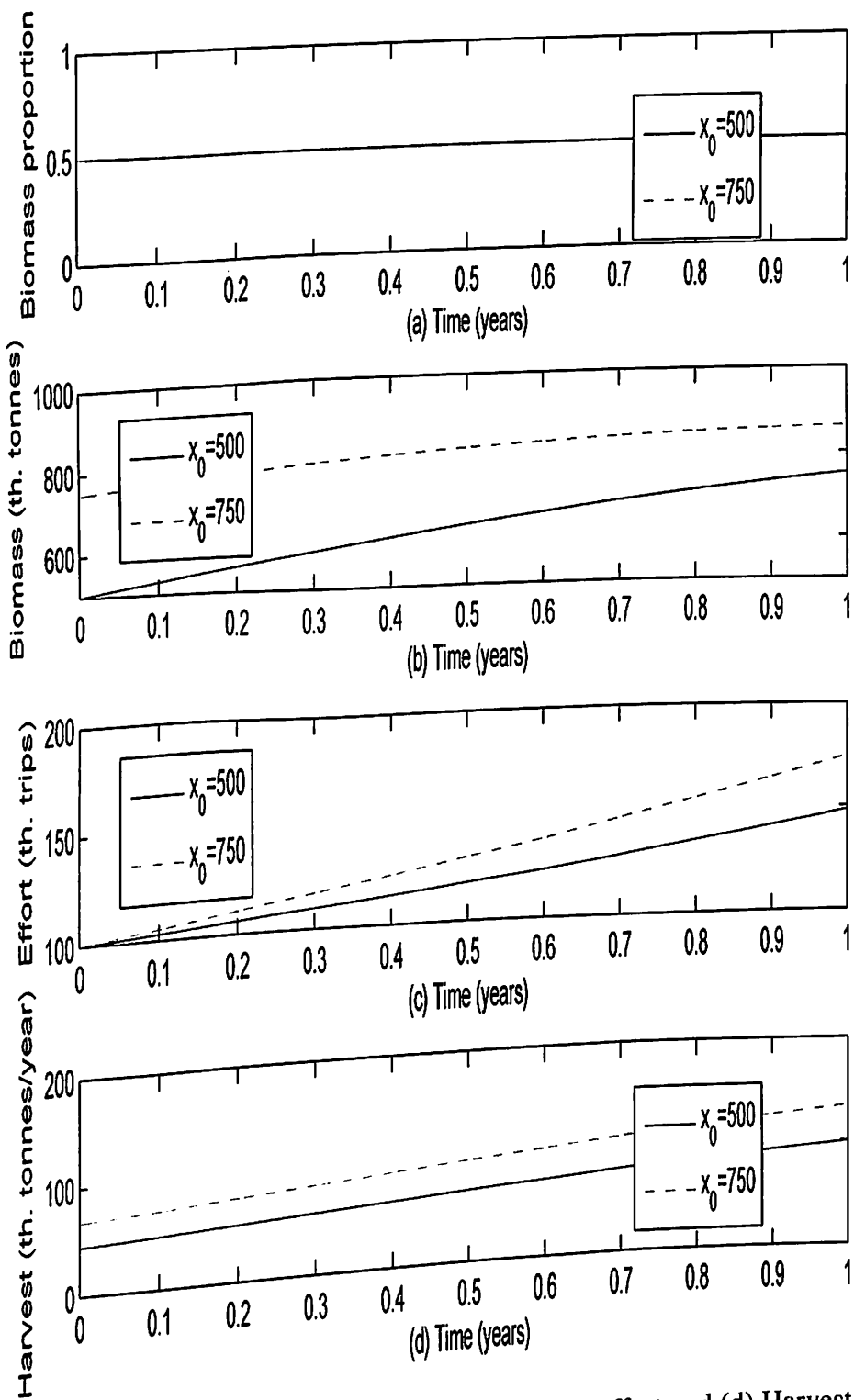

Figure 100: (a) Biomass Proportion, (b) Biomass, (c) Effort and (d) Harvest Levels for $a = 200.000$, $u_{max} = 0.5$ and $T = 1$

where T is finite, and then extend it to the equilibrium scenario where $T \to \infty$.

Simulation results for the biomass proportion, biomass, effort and harvest levels relating to the case where $a = 200,000$ tonnes, $u_{max} = 0.5$, $T = 1$ year, $E_0 = 100,000$ trips, $x_0 = 500,000$ tonnes and $x_0 = 750,000$ tonnes are presented in Figure 100. In Figure 100 (a), it is observed that when the maximum proportion of biomass available for harvesting, u_{max} is set at 50%, the optimal biomass proportion appears to follow a path of around 0.5 for both initial biomass levels for the one-year horizon. Furthermore, the fish biomass increases to a value of around 750,000 tonnes for the initial lower biomass level and around 860,000 tonnes for the initial higher biomass level (Figure 100 (b)). The Effort plot (Figure 100 (c)) also shows an increase for both initial biomass levels; to a value close to 150,000 trips and 175,000 trips for the initial lower and higher biomass levels, respectively. Figure 100 (d) shows that the harvest rate increases to about 100,000 tonnes per year for the initial lower biomass level, and to about 140,000 tonnes per year for the initial higher biomass level.

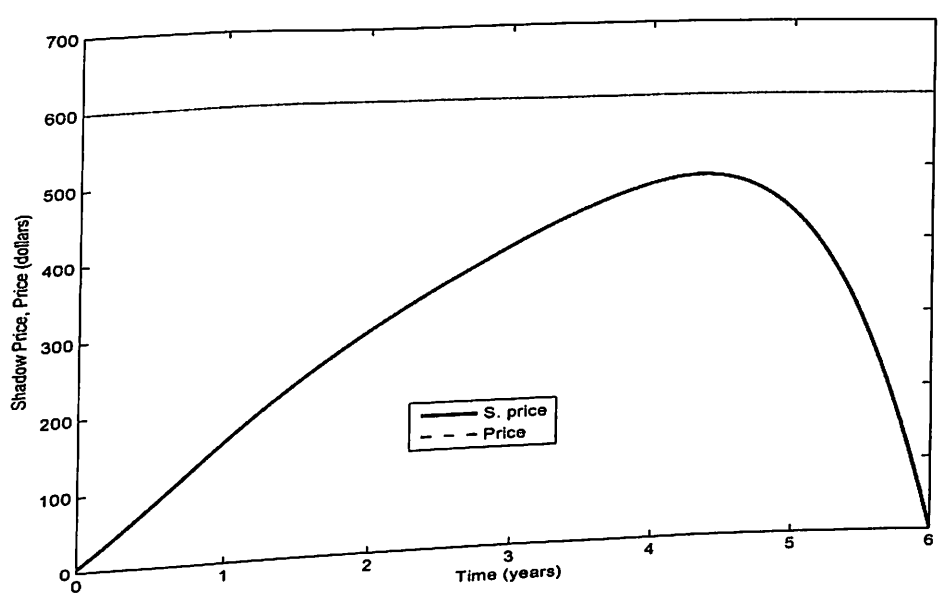

Figure 101: Shadow Price and Price for $a = 200,000$, $u_{max} = 0.5$ and $T = 6$

Assuming an initial population size of 750,000 tonnes, the total net revenue over the one-year horizon corresponding to the given proportion of biomass available is computed as US$30,499,000. A net revenue of US$16,909,000 is realised

for an initial population size of 500,000 tonnes; about 45% lower.

Figure 101 depicts setting the maximum biomass proportion available, $u_{max} = 0.5$ and the critical biomass level at 200,000 tonnes with an initial biomass level of 750,000 tonnes. The combined shadow price appears concave-like and the price, linear. At the start of the harvesting period, the shadow price, US \$4.70 is significantly lower than the price, US \$600.00. This signifies that the revenue due to the combined effect of the shadow prices of stock and effort is less than the expected price from harvesting a tonne of fish, so at this instance, it is beneficial to harvest at the maximum available biomass proportion. As time progresses the shadow price increases in value until it reaches its maximum at US \$490.80 (with $t = 4.5$ years), while the price remains constant. Thereafter, the shadow price declines in value before finally going to zero at the final horizon. Thus the shadow price is always lower the price for the entire duration, signifying that it is optimal to harvest.

Simulation results for the biomass proportion, biomass, effort and harvest levels relating to the case where $a = 200,000$ tonnes, $u_{max} = 0.5$, $T = 6$ years, $E_0 = 100,000$ trips, $x_0 = 500,000$ tonnes and $x_0 = 750,000$ tonnes are presented in Figure 102. In Figure 102 (a), it is observed that when the maximum propor- tion of biomass available for harvesting, u_{max} is set at 50%, the optimal biomass proportion appears to follow a path of around 0.5 for both initial biomass lev- els throughout the six-year horizon. Furthermore, the fish biomass increases to a value of around 400,000 tonnes for the initial lower biomass level and around 350,000 tonnes for the initial higher biomass level (Figure 102 (b)). The Effort plot (Figure 102 (c)) also shows an increase for both initial biomass levels; to a value close to 1,324,000 trips and about 1,400,000 trips for the initial lower and higher biomass levels, respectively. Figure 102 (d) shows that the harvest rate in- creases to about 470,000 tonnes per year for the initial lower biomass level, and to about 435,000 tonnes per year for the initial higher biomass level. It should be noted that it is only at the last year of the horizon that the harvest rate of the initial lower biomass level is marginally higher.

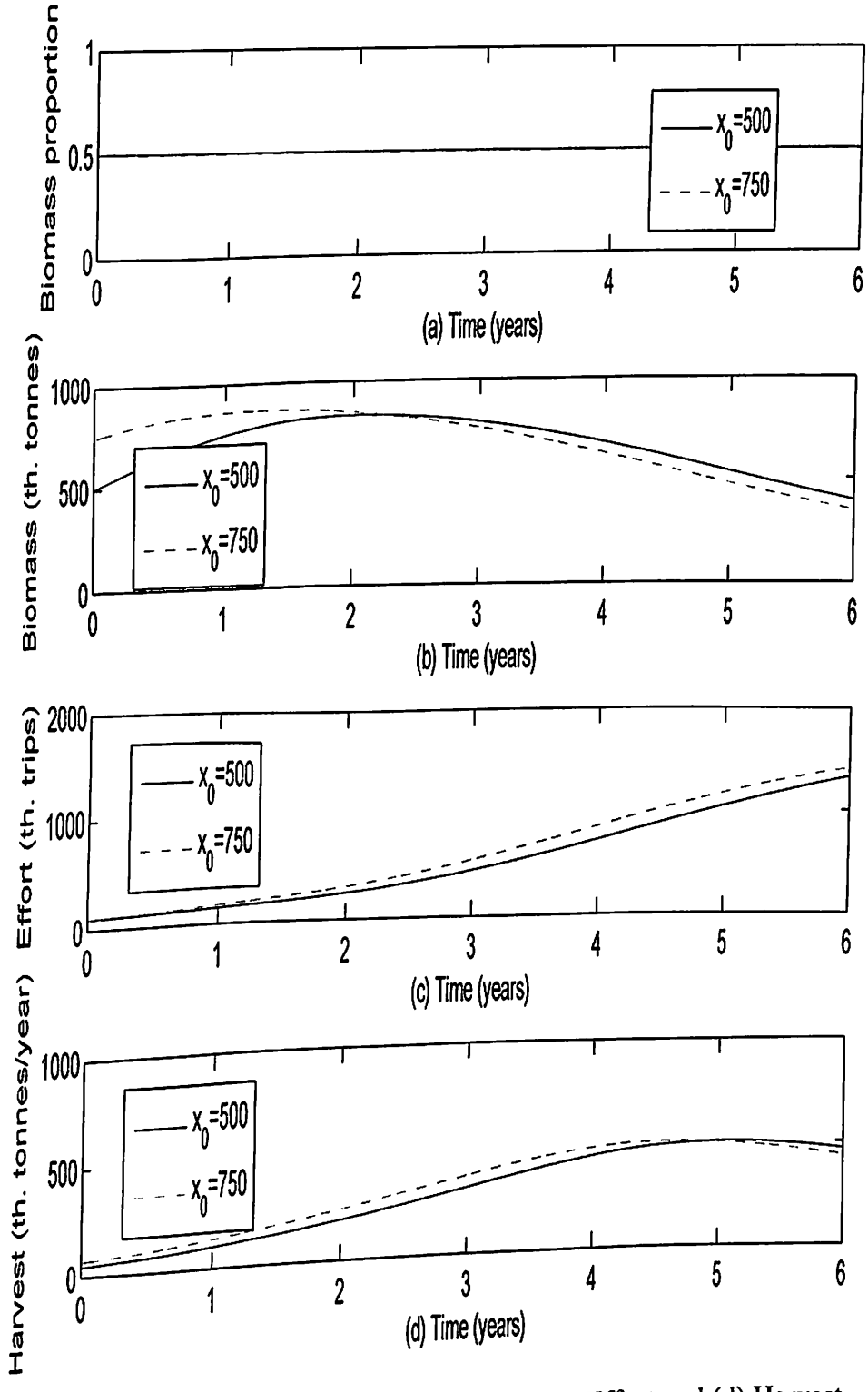

Figure 102: (a) Biomass Proportion, (b) Biomass, (c) Effort and (d) Harvest Levels for $a = 200.000$, $u_{max} = 0.5$ and $T = 6$

Thus, the total harvest over the entire horizon of the initial higher biomass level is higher.

Assuming an initial population size of 750,000 tonnes, the total net revenue over the six-year horizon corresponding to the given proportion of biomass available is computed as US$290,010,000. A net revenue of US$268,320,000 is realised for an initial population size of 500,000 tonnes; about 7% lower. It is worth noting that beyond six years the iterates do not converge.

Simulation results for the biomass proportion, biomass, effort and harvest levels relating to the case where $a = 500,000$ tonnes, $u_{max} = 0.5$, $T = 1$ year, $E_0 = 100,000$ trips, $x_0 = 500,000$ tonnes and $x_0 = 750,000$ tonnes are presented in Figure 103. In Figure 103 (a), it is observed that when the maximum proportion of biomass available for harvesting, u_{max} is set at 50%, the optimal biomass proportion appears to follow a path of around 0.5 for both initial biomass levels for the one-year horizon. Furthermore, the fish biomass increases to a value of around 758,000 tonnes for the initial lower biomass level and around 870,000 tonnes for the initial higher biomass level (Figure 103 (b)). The Effort plot (Figure 103 (c)) also shows an increase for both initial biomass levels; to a value close to 113,000 trips and 134,000 trips for the initial lower and higher biomass levels, respectively. Figure 103 (d) shows that the harvest rate increases to about 77,000 tonnes per year for the initial lower biomass level, and to about 105,000 tonnes per year for the initial higher biomass level.

Assuming an initial population size of 750,000 tonnes, the total net revenue over the one-year horizon corresponding to the given proportion of biomass available is computed as US$26,560,000. A net revenue of US$14,581,000 is realised for an initial population size of 500,000 tonnes; about 45% lower.

Figure 104 depicts setting the maximum biomass proportion available, $u_{max} =$ 0.5 and the critical biomass level at 500,000 tonnes with an initial biomass level of 750,000 tonnes. The combined shadow price appears concave-like and the price, linear. At the start of the harvesting period, the shadow price, US $ -189.77 is significantly lower than the price, US $600.00. This signifies that the revenue due to the combined effect of the shadow prices of stock and effort is less than the expected price from harvesting a tonne of fish, so at this instance, it is beneficial

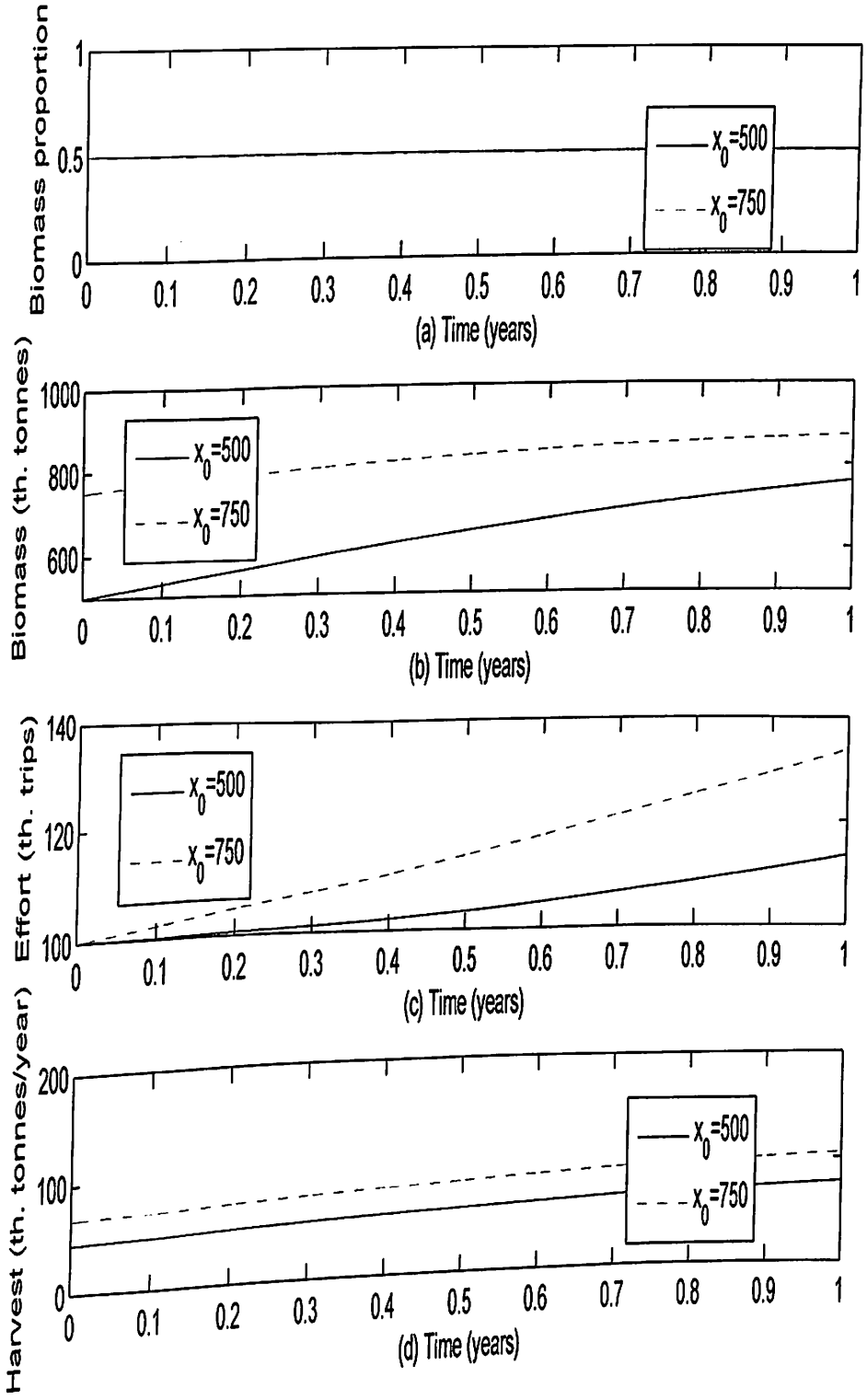

Figure 103: (a) Biomass Proportion, (b) Biomass, (c) Effort and (d) Harvest Levels for $a = 500,000$, $u_{max} = 0.5$ and $T = 1$

to harvest at the maximum available biomass proportion. As time progresses the shadow price fluctuates in value while the price remains constant; with the two

never intersecting. The shadow price continues to fluctuate in value, reaching its peak at $t = 17.5$ years with a value of US \$396.03. Thereafter, it declines in value, going to zero at the time horizon. Thus the shadow price is always lower than the price for the entire horizon, signifying that it is beneficial to harvest at the maximum proportion of biomass available.

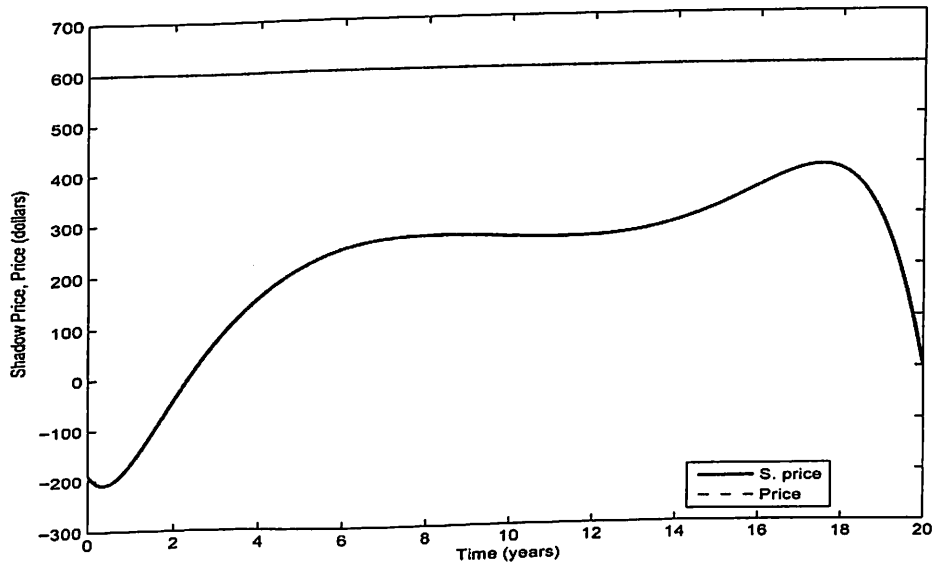

Figure 104: Shadow Price and Price for $a = 500,000$, $u_{max} = 0.5$ and $T = 20$

Simulation results for the biomass proportion, biomass, effort and harvest levels relating to the case where $a = 500,000$ tonnes, $u_{max} = 0.5$, $T = 20$ years, $E_0 = 100,000$ trips, $x_0 = 500,000$ tonnes and $x_0 = 750,000$ tonnes are presented in Figure 105.

In Figure 105 (a), it is observed that when the maximum proportion of biomass available for harvesting, u_{max} is set at 50%, the optimal biomass proportion appears to follow the same maximum path of 0.5 for both initial biomass levels throughout the twenty-year horizon. Furthermore, the fish biomass attains the steady state value of around 500,000 tonnes for both initial biomass levels (Figure 105 (b)). The Effort plot (Figure 105 (c)) also shows an increase for both initial biomass levels; settling at a value of around 788,000 trips, which is very close to the steady state value. Figure 105 (d) shows that the harvest rate increases to about 355,000 tonnes per year for both initial biomass levels.

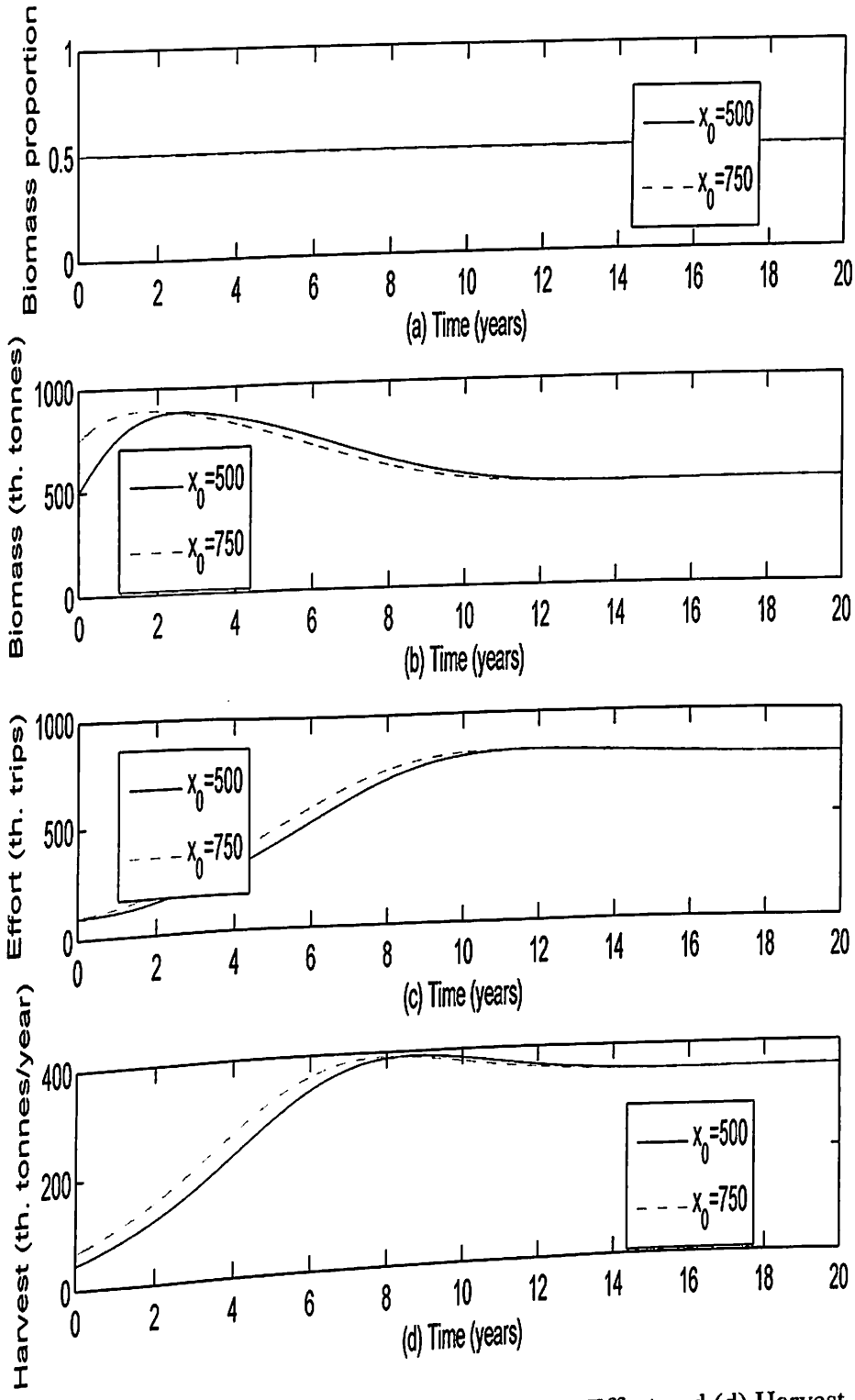

Figure 105: (a) Biomass Proportion, (b) Biomass, (c) Effort and (d) Harvest Levels for $a = 500,000$, $u_{max} = 0.5$ and $T = 20$

Assuming an initial population size of 750,000 tonnes, the total net revenue over the twenty-year horizon corresponding to the given proportion of biomass

available is US$426,240,000. A net revenue of US$389,720,000 is realised for an initial population size of 500,000 tonnes; about 9% lower.

Simulation results for the biomass proportion, biomass, effort and harvest levels relating to the case where $a = 200,000$ tonnes, $u_{max} = 0.9$, $T = 1$ year, $E_0 = 100,000$ trips, $x_0 = 500,000$ tonnes and $x_0 = 750,000$ tonnes are presented in Figure 106. In Figure 106 (a), it is observed that when the maximum proportion of biomass available for harvesting, u_{max} is set at 90%, the optimal biomass proportion appears to follow the maximum path of 0.9 for both initial biomass levels for the one-year horizon. Furthermore, the fish biomass increases to a value of around 692,000 tonnes for the initial lower biomass level and around 780,000 tonnes for the initial higher biomass level (Figure 106 (b)). The Effort plot (Figure 106 (c)) also shows an increase for both initial biomass levels; to a value close to 195,000 trips and 257,000 trips for the initial lower and higher biomass levels, respectively. Figure 106 (d) shows that the harvest rate increases to about 219,000 tonnes per year for the initial lower biomass level, and to about 325,000 tonnes per year for the initial higher biomass level.

Assuming an initial population size of 750,000 tonnes, the total net revenue over the one-year horizon corresponding to the given proportion of biomass available is computed as US$86,495,000. A net revenue of US$52,139,000 is realised for an initial population size of 500,000 tonnes; about 45% lower.

Simulation results for the biomass proportion, biomass, effort and harvest levels relating to the case where $a = 200,000$ tonnes, $u_{max} = 0.9$, $T = 3$ years, $E_0 = 100,000$ trips, $x_0 = 500,000$ tonnes and $x_0 = 750,000$ tonnes are presented in Figure 107. In Figure 107 (a), it is observed that when the maximum proportion of biomass available for harvesting, u_{max} is set at 90%, the optimal biomass proportion appears to follow a path of around 0.9 for both initial biomass levels throughout the three-year horizon. Furthermore, the fish biomass increases to a value of around 456,000 tonnes for the initial lower biomass level and around 364,000 tonnes for the initial higher biomass level (Figure 107 (b)). The Effort plot (Figure 107 (c)) also shows an increase for both initial biomass levels; to

a value close to 783,000 trips and about 929,000 trips for the initial lower and higher biomass levels, respectively. Figure 107 (d) shows that the harvest rate increases to about 578,000 tonnes per year for the initial lower biomass level, and to about 548,000 tonnes per year for the initial higher biomass level.

Assuming an initial population size of 750,000 tonnes, the total net revenue over the three-year horizon corresponding to the given proportion of biomass available is US$384,870,000. A net revenue of US$309,210,000 is realised for an initial population size of 500,000 tonnes; about 20% lower. It is instructive to note that the iterates failed to converge beyond four years for the initial lower biomass level and beyond five years for the initial higher biomass level.

Simulation results for the biomass proportion, biomass, effort and harvest levels relating to the case where $a = 500,000$ tonnes, $u_{max} = 0.9$, $T = 1$ year, $E_0 = 100,000$ trips, $x_0 = 500,000$ tonnes and $x_0 = 750,000$ tonnes are presented in Figure 108. In Figure 108 (a), it is observed that when the maximum proportion of biomass available for harvesting, u_{max} is set at 90%, the optimal biomass proportion appears to follow the maximum path of 0.9 for both initial biomass levels for the one-year horizon. Furthermore, the fish biomass increases to a value of around 720,000 tonnes for the initial lower biomass level and around 816,000 tonnes for the initial higher biomass level (Figure 108 (b)). The Effort plot (Figure 108 (c)) also shows an increase for both initial biomass levels; to a value close to 122,000 trips and 161,000 trips for the initial lower and higher biomass levels, respectively. Figure 108 (d) shows that the harvest rate increases to about 142,000 tonnes per year for the initial lower biomass level, and to about 213,000 tonnes per year for the initial higher biomass level.

Assuming an initial population size of 750,000 tonnes, the total net revenue over the one-year horizon corresponding to the given proportion of biomass available is computed as US$68,009,000. A net revenue of US$40,666,000 is realised for an initial population size of 500,000 tonnes; about 45% lower.

Simulation results for the biomass proportion, biomass, effort and harvest levels relating to the case where $a = 500,000$ tonnes, $u_{max} = 0.9$, $T = 20$ years,

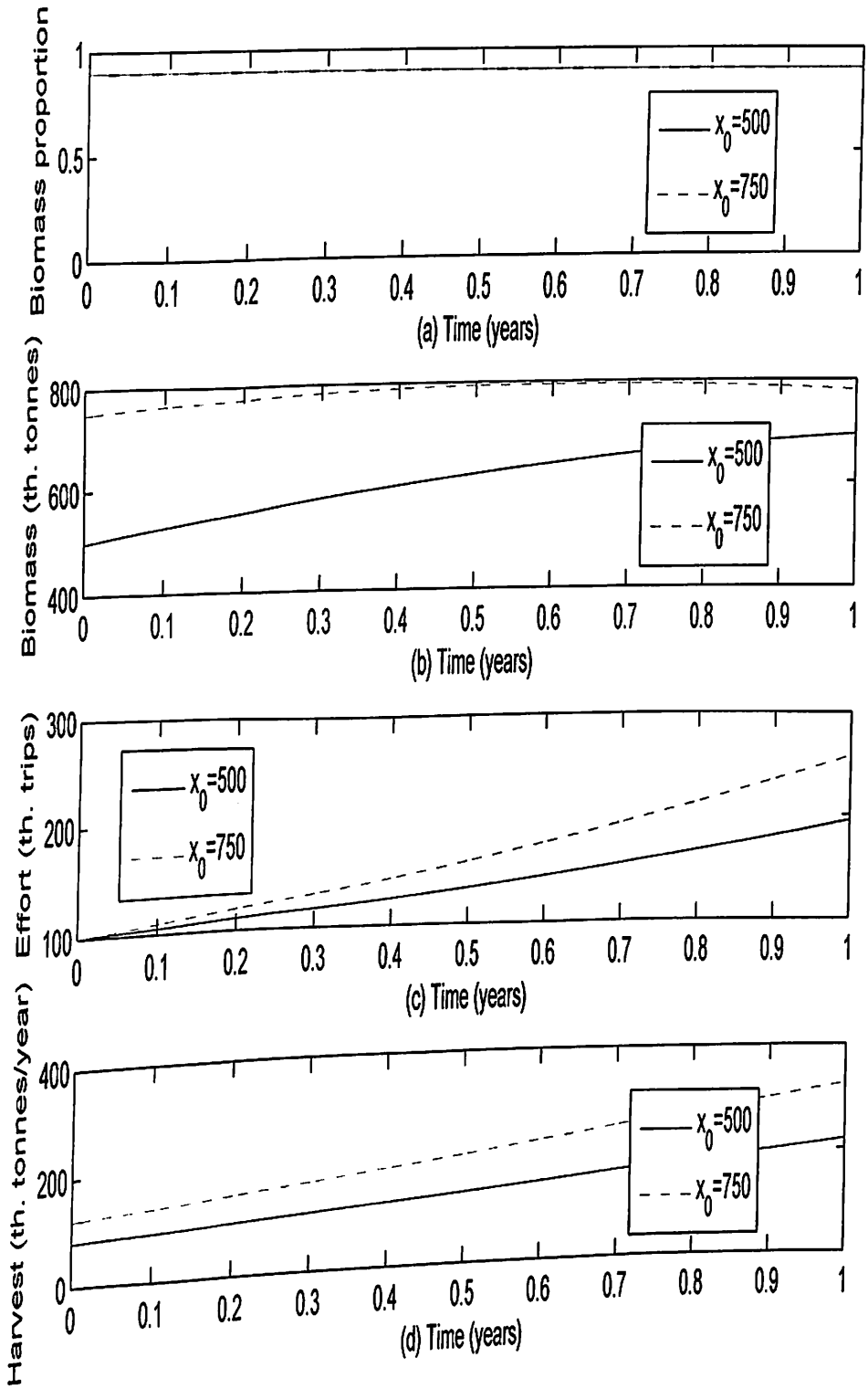

Figure 106: (a0 Biomass Proportion, (b) Biomass, (c) Effort and (d) Harvest Levels for $a = 200,000$, $u_{max} = 0.9$ and $T = 1$

$E_0 = 100,000$ trips, $x_0 = 500,000$ tonnes and $x_0 = 750,000$ tonnes are presented in Figure 109. In Figure 109 (a), it is observed that when the maximum proportion

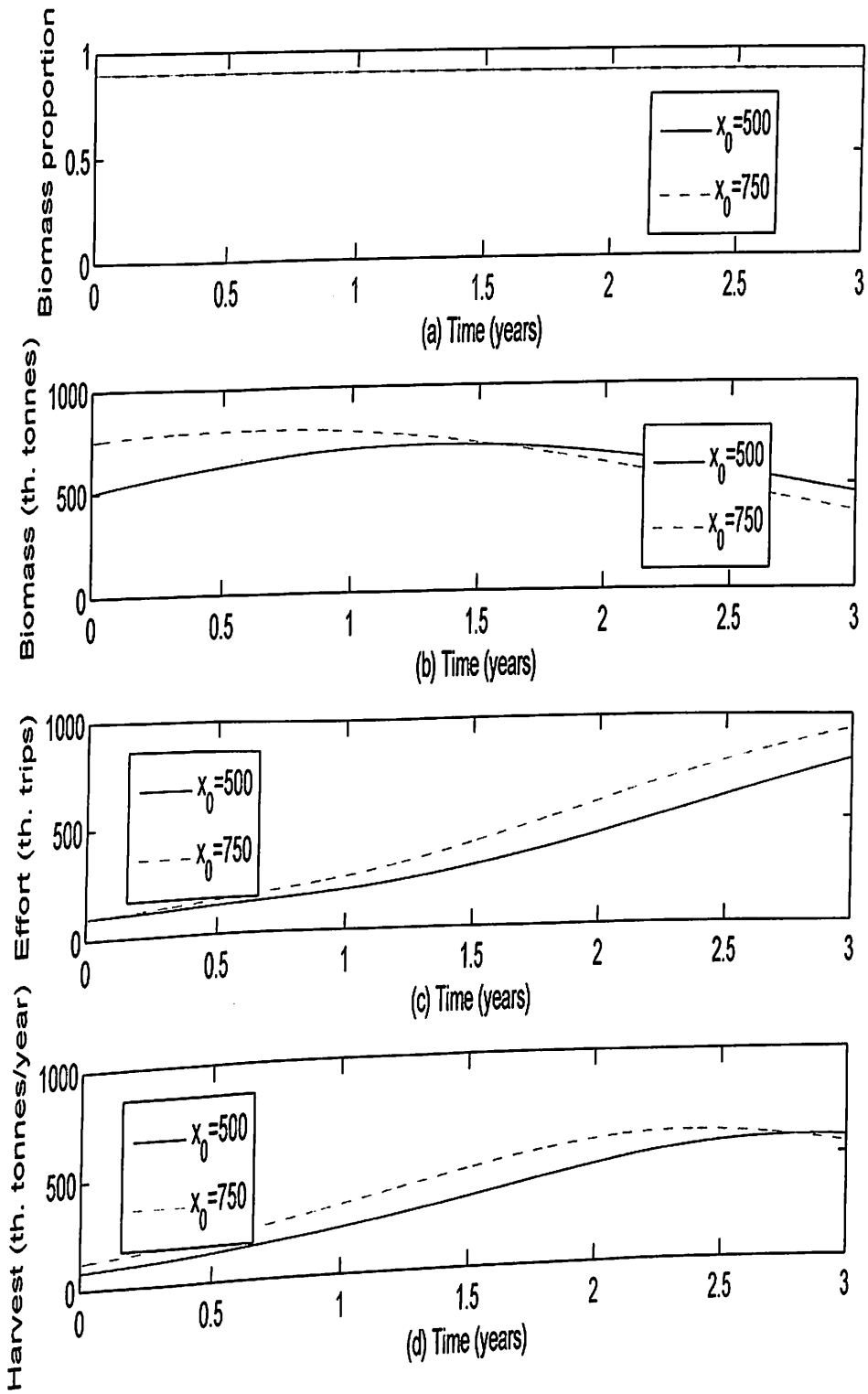

Figure 107: (a) Biomass Proportion, (b) Biomass, (c) Effort and (d) Harvest Levels for $a = 200,000$, $u_{max} = 0.9$ and $T = 3$

of biomass available for harvesting, u_{max} is set at 90%, the optimal biomass proportion appears to follow the same maximum path of 0.9 for both initial biomass

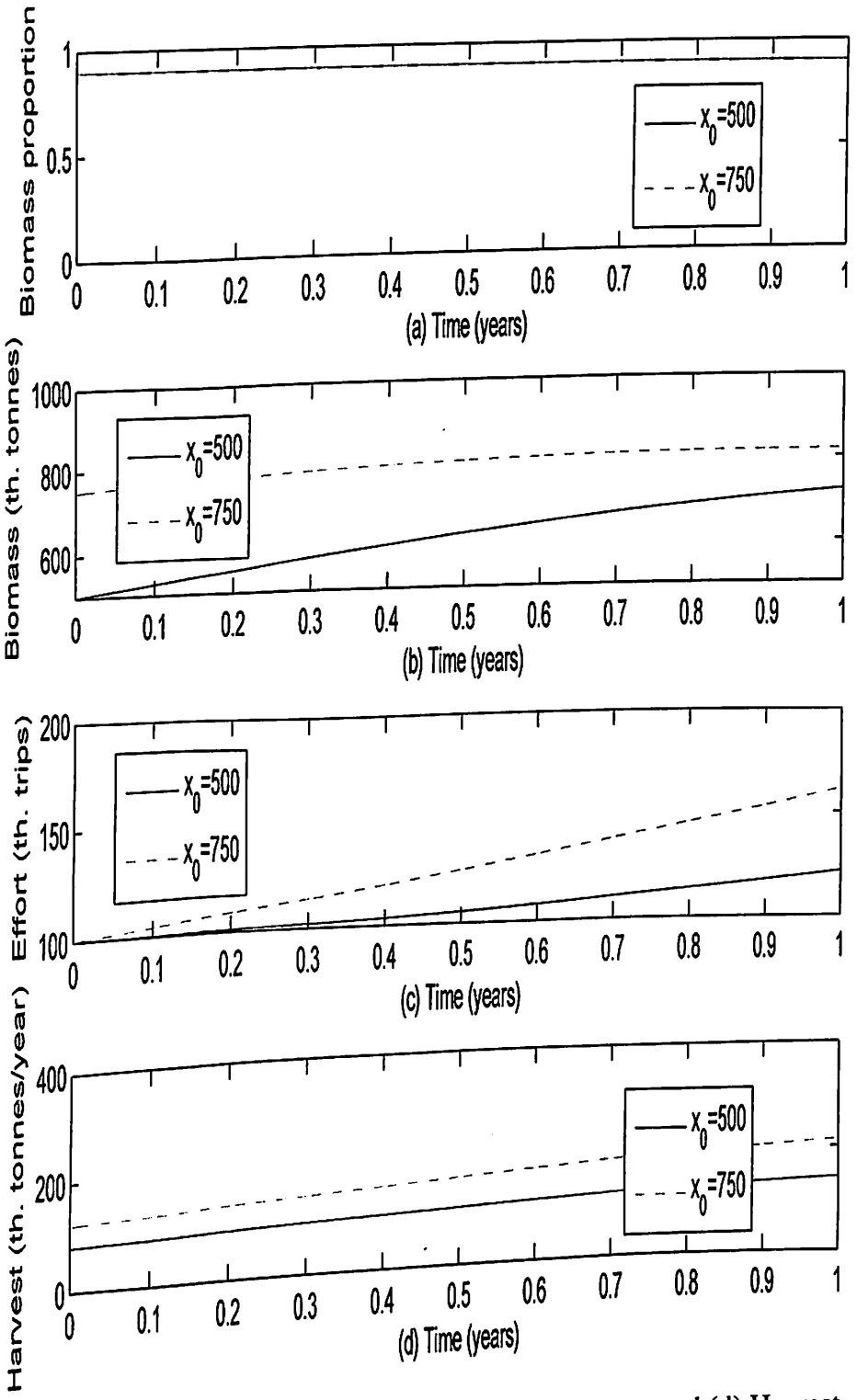

Figure 108: (a) Biomass Proportion, (b) Biomass, (c) Effort and (d) Harvest Levels for $a = 500,000$, $u_{max} = 0.9$ and $T = 1$

levels throughout the twenty-year horizon. Furthermore, the fish biomass attains the steady state value of around 500,000 tonnes for both initial biomass levels

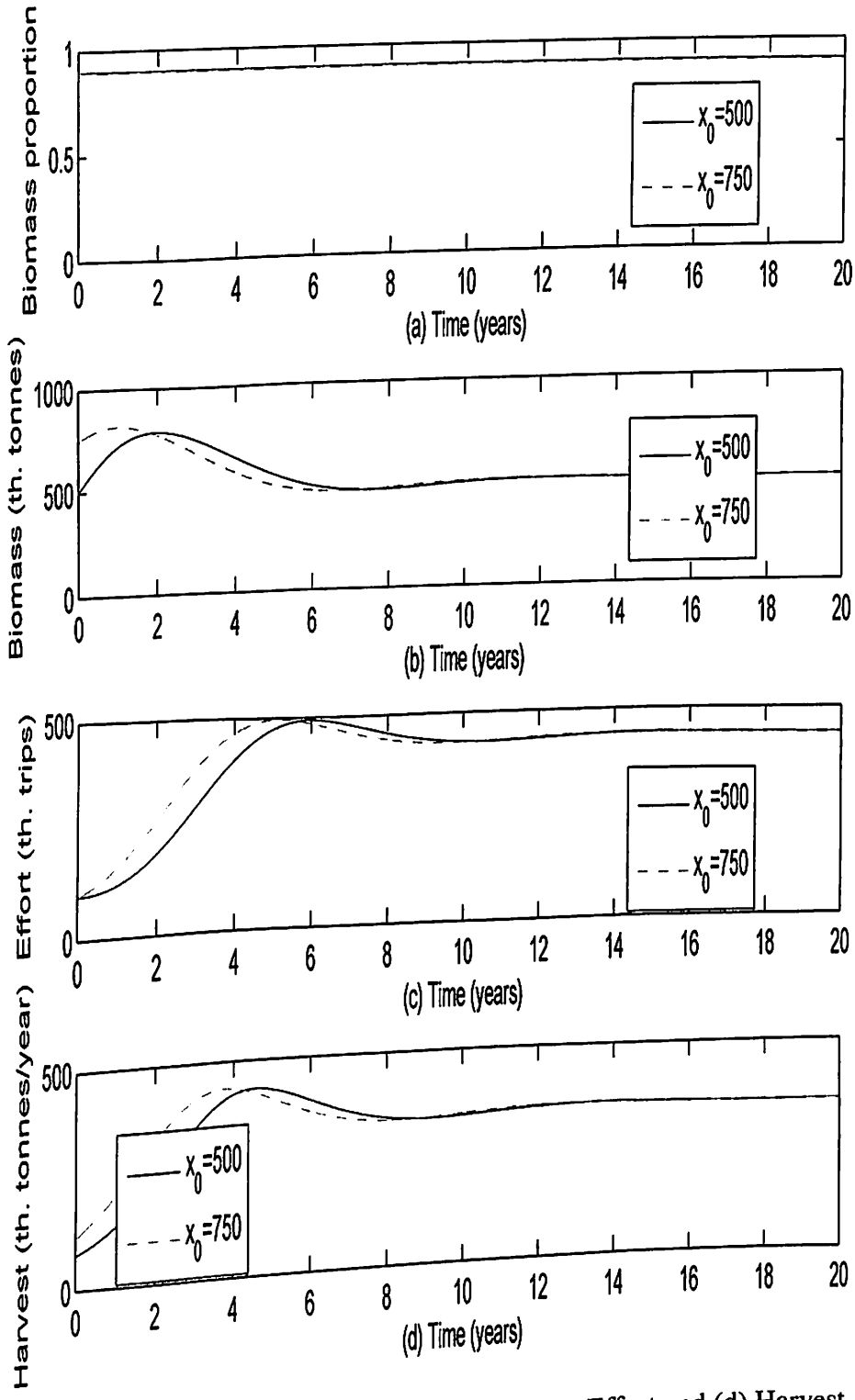

Figure 109: (a) Biomass Proportion, (b) Biomass, (c) Effort and (d) Harvest Levels for $a = 500,000$, $u_{max} = 0.9$ and $T = 20$

(Figure 109 (b)). The Effort plot (Figure 109 (c)) also shows an increase for both initial biomass levels; settling at a value of around 438,000 trips. Figure 109 (d)

shows that the harvest rate increases to about 355,000 tonnes per year for both initial biomass levels.

Assuming an initial population size of 750,000 tonnes, the total net revenue over the twenty-year horizon corresponding to the given proportion of biomass available is US$818,320,000. A net revenue of US$749,300,000 is realised for an initial population size of 500,000 tonnes; about 8% lower.

Chapter Summary

This chapter has taken a look at the fishing strategies of the sardinella fishery under a predator-prey model with a marine reserve in order to determine the optimal strategy.

The stated dynamics were modelled using a modified version of the predator-prey model originally proposed by Schaefer (1954). The model was subjected to stability analysis, by first finding the equilibrium points and then determining the characteristics of the local and global stability. It was found that the model is locally as well as globally asymptotically stable for the interior equilibrium point. Furthermore, by the Dulac-Bendixson criterion, the model does not possess limit cycles.

The optimal control was characterised and the singularity, or lack thereof, of the model determined using the Generalised Legendre-Clebsch condition. It was shown that the singular path could not be ruled out.

Numerical simulations were performed on the model by varying the initial biomass level while keeping the critical biomass level and proportion of biomass available for harvesting fixed. The model was found to attain equilibrium status when the critical biomass level was set at the x_{MSY} level. However, the model failed to achieve equilibrium status when the critical biomass level was set at a fifth of the carrying capacity and the proportion of biomass available for harvesting at 90%, no matter the size of the initial fish population. This may be likened to the OAY scenario. In fact, the iterates failed to converge beyond a time horizon of

only three years.

When the critical biomass level is set at 200,000 tonnes, the initial net revenues accruing to the fishermen is higher than the situation where the critical biomass level is set at 500,000 tonnes. However, the economic rent due the fishermen soon starts to dissipate as time progresses; and also the iterates fail to converge beyond certain time horizons (if $a = 200$ and the proportion of biomass available for harvesting is set at 0.5 and at 0.9).

It is interesting to note that a singular control for u was not encountered in all the simulations carried out for the model. This may be due to the fact that the parameters employed in the model are such that the region of the singular arcs was not optimal.

CHAPTER SEVEN

SUMMARY, CONCLUSIONS AND RECOMMENDATIONS

Overview

The concluding chapter presents the summary and conclusions drawn from the study on the application of optimal control in determining the optimal harvesting effort for the sardinella fishery. At the end of the chapter, recommendations are provided for relevant stakeholders and suggestions for future research are outlined.

Summary

The primary focus of the study was to apply optimal control techniques to determine the sustainable harvesting strategies of Ghana's sardinella fishery. In this regard, various standard models in fishery were reviewed as well as original models proposed to achieve the set objectives.

One of the preeminent models in fishery research is the Gordon-Schaefer bioeconomic model. Thus all the models considered in this study revolve around this canonical model. The model was initially analysed using three different rates of harvest—constant, proportional and periodic. Each of these models was subjected to bifurcation analysis to observe the behaviour of the equilibrium points and their associated stability. Thereafter, the static equilibrium reference points—MEY, MSY and OAY—were determined and discussed. Furthermore, the dynamic equilibrium reference point—OSY—was established. Numerical simulations were performed on each model to highlight the important characteristics associated with it.

The Goh model, which has as its state dynamics the Schaefer model with constant rate harvesting and the objective of determining the optimal yield, was also reviewed and discussed. This model is not bioeconomic, as the objective

functional is not total net revenue but total yield. A variant of this model which considered the proportional rate harvesting scenario was reviewed as well. The dynamic behaviour of these models were studied by performing numerical simulations on them.

A model taking into account the effective utilisation of a renewable resource was also reviewed and discussed. This is especially important as the current catches of the sardinella fishery in Ghana are very low, and therefore there is the need for proper and effective utilisation of this resource.

The Craven model, which considered the effect of unusually high catches on price of landed fish, was studied. This model has a quadratic control, as opposed to the standard Gordon-Schaefer model that employs a linear control. Additionally, the control in this model is the level of harvesting, not the rate of fishing effort as in the standard model. The model was subjected to bifurcation analysis, static reference points determined, optimal level of harvesting established and numerical simulations performed.

The standard Gordon-Schaefer model is one dimensional. An original two dimensional model centred on this model was proposed and discussed. This two dimensional model includes an isoperimetric constant (or integral constraint). The integral constraint takes care of the annual quota set by the fishery managers—TAC. One of the ways to deal with problems involving this type of constraint is to introduce a new variable to supplant the constraint. This model also employs a quadratic constraint as well as being of finite horizon. The optimal rate of fishing effort was determined and numerical simulations performed.

The main thrust of the study was to account for the current low yields of the sardinella fishery in Ghana and the role played by the artisanal fishermen. In particular, certain unorthodox fishing practices exhibited by the fishermen were analysed and discussed. Catchability is an important parameter in the standard Gordon-Schaefer model. However, this parameter is assumed constant in the model. Sensitivity analyses were conducted on the catchability coefficient to simulate the effects of unapproved fishing gears on the fish stock. The model also

employed a quadratic objective functional. Static reference points for the model were determined and analysed. The existence of the optimal control as well its uniqueness was established. Numerical simulations were performed to shed more light on the impact of the enhanced catchability on the optimal rate of fishing effort, and ultimately, on the long-term sustainability of the sardinella fishery.

An original two dimensional model incorporating a marine reserve was proposed to help address the precarious nature of the sardinella fishery currently pertaining in Ghana. The model's state dynamics employ a predator-prey model with the objective functional being the total net revenue derived from the portion of biomass made available for harvesting. The model also features a critical biomass level for the fish stock. Local as well as global stability of the model was determined and discussed. The optimality of the model was analysed with the help of the Generalised Legendre-Clebsch condition to determine the existence of the singular path. Numerical simulations were carried out to give meaning to, and illustrate, the theoretical results.

Therefore, the main findings of the research are as follows:

1. The optimal rate of fishing effort for the dynamic model is $E_{OSY} = 351,328$ trips annually at 15% discount rate with the initial biomass level set at least 554,654 tonnes.

2. Regarding the static model, the effort rate of $E_{MEY} = 323,225$ trips annually is only optimal when the discount rate is considered to be zero while $E_{OAY} = 646,450$ trips annually is optimal when the discount rate is considered to be infinity. Furthermore, $E_{MSY} = 394,444$ trips annually is considered optimal when both the cost of fishing and the discount rate are assumed to be zero.

3. The current level of harvesting effort for the fishery has been estimated at 1,219,200 trips annually, which is well beyond the bifurcation point of the model (788,889 trips).

4. At higher levels of increased catchability as a result of the IUU fishing practices, the consequences on the size of the fish stocks are near catastrophic levels—as low as 15% of the carrying capacity in finite time.

5. The periodic rate model was quicker to send the fish stock into extinction than the constant rate model given the same initial biomass level and harvest rate.

6. When the TAC is set at $h_{MSY} = 355,000$ tonnes per year, the rate of fishing effort must not exceed 277,000 trips per year.

7. The Predator-Prey model with reserve area indicated that the critical biomass level must be set at $x_{MSY} = 500,000$ tonnes to enable the model attain equilibrium status.

Conclusions

The bifurcation analyses of the standard Gordon-Schaefer model with proportional rate harvesting revealed that the model possesses two hyperbolic equilibrium points when the rate of fishing effort is less than the bifurcation point. The higher equilibrium point is stable while the lower one is unstable. At the transcritical bifurcation point, there exists a single nonhyperbolic equilibrium point, which is semi-stable. Fishing at effort rates greater than the bifurcation point produces one non-negative hyperbolic equilibrium point, which is stable.

The rate of fishing effort at the static reference points were all below the bifurcation point; therefore, for any initial biomass level above the lower equilibrium point, the fish biomass approaches their respective steady state levels in the long run. Further analysis of the reference points showed that fishing at the MSY level provided the maximum yield while fishing at the MEY level provided the maximum revenue, which confirms theoretical results. Additionally, at the OAY level, most effort is expended and yet produces the lowest yield as well as having the most adverse effect on fish stocks. Simulations results from the dynamic

model showed that the rate of fishing effort must be set at the OSY with the initial biomass level at least at the corresponding OSY level to ensure sustainability of the resource.

It must be reiterated that when the objective is to maximise the total discounted present value of future net revenues, OSY is optimal (MEY is only optimal when the discount rate is zero). However, when the objective is to maximise the total yield (both the discount rate and the cost are assumed to be zero), MSY is optimal.

The autonomous constant rate harvesting model is structurally stable, especially when the effort rate is below the bifurcation point. Therefore the non-autonomous periodic rate harvesting model can be seen as the periodic perturbation of the former model. The key observation was that the periodic rate model was comparatively quicker to send the fish stock into extinction than the constant rate model given the same initial biomass level and harvest rate.

The rate of fishing effort at the MSY level of the proportional rate model is 50% of the value of the bifurcation point, unlike in the constant rate harvesting model where the rate of harvest at the MSY level coincides with the value of the bifurcation. Therefore, any harvesting strategy that positively deviates from the bifurcation point for the constant rate model could lead to disastrous consequences. Thus a harvesting strategy based on the proportional rate model is potentially less catastrophic as compared with the constant rate model.

Regarding the optimal yield models, the extreme controls indicate that the resource should be harvested (by exerting an effort rate up to the available maximum) if and only if the marginal yield does not exceed one tonne. In addition, the harvested resource could follow the OSY path (or singular path) if the marginal yield exactly equals a tonne. It was however observed that the constant rate harvesting model took a longer time to reach equilibrium, 500 years, compared with the proportional rate model, 20 years, for the equivalent set of parameter values.

For the model incorporating the effective utilisation rate, the optimal control only admitted extreme policies—either harvesting at full capacity or none at all. The observation was that the greater the harvest rate, the shorter the duration of

harvest. Obviously, larger harvest rates yielded the greater net revenues.

The model that set quota for annual harvest revealed that the resource should be harvested if and only if the marginal net revenue of harvest as a result of applying the maximum effort exceeds the difference of the shadow price of fish stock and the shadow price of the TAC. Thus the model provides that, any additional catch beyond the TAC will result in revenue loss to the fishermen, as the cost of fishing will exceed the revenue generated from the activity.

The assumption of constant catchability in the Gordon-Schaefer model does not reflect reality. Therefore the model developed by incorporating a modification to the catchability to account for the measures (sometimes, illegal) adopted by fishermen to enhance catches showed that, in extreme circumstances the increased catchability has disastrous effect on fish stocks. One of the key findings was that, at higher levels of increased catchability as a result of the illegal practices, the fish stocks are severely depleted—as low as 15% of the carrying capacity in finite time. Meanwhile, the increase in net revenue is very minimal; and in some cases, actually results in a revenue decrease.

In a dynamic effort, predator-prey model with reserve area and critical biomass level, the optimal fishing strategy indicate that, when the price of landed fish is greater than the sum (or difference) of the shadow price of fish stock and a fraction of the shadow price of effort, the optimal control must be set at the maximum proportion of biomass available for harvesting; otherwise, the control should be set at the minimum level. This represents the boundary controls; and by the Generalised Legendre-Clebsch condition, the singular control could not be ruled out, even though in almost all the simulations, this was not encountered.

The model also yielded an interior equilibrium point which was found to be locally as well as globally stable. In fact, this equilibrium point was a spiral. Furthermore, the existence of limit cycles or periodic orbitals was expressly ruled out by Dulac-Bendixson criterion.

Recommendations

The models employed in this study to achieve the stated objectives include both autonomous and non-autonomous models, one- and two-dimensional models, models with linear and non-linear controls, models with finite and infinite time horizons, models with one endpoint and both endpoints fixed and models with bounded controls.

Additionally, the models were analysed using both qualitative and quantitative methods. These included bifurcation analyses and numerical simulations. Pontryagin's maximum principle was the main tool in establishing the necessary conditions, while the sufficiency conditions were discussed using a result from Fleming and Rishel (1995). Furthermore, the models were subjected to different types of harvesting strategies in order to determine the optimal strategy for the sardinella fishery.

The artisanal marine fishery in Ghana is essentially open access, and as Koranteng (1998) observed, there does not appear to be any sustained management strategy for fisheries. Given the current state of the artisanal fishery in general and the sardinella fishery in particular, the fishery managers must put in place certain measures if the sustainability of the fishery is to be ensured. From the analyses and findings of the study, the following are recommended towards the management of the resource. The Fisheries Commission, under the aegis of MOFAD, has the mandate to regulate and manage the utilisation of fisheries resources and coordinate policies in relation to them (MOFAD, 2016).

1. The open access nature of the fishery inevitably leads to overcapacity of fishing effort. The conservative estimate of 1,219,200 trips in a given year far exceeds the bifurcation point of 788,889 fishing days. Therefore, to ensure sustainability of the resource, a cap (at the level of $E_{OSY} = 351,328$ trips) must be placed on fishing effort in the artisanal sector by the Fisheries Commission.

2. The Fisheries Commission must seriously consider the idea of imposing closed fishing seasons of up to six months in a year to cut down on fishing effort, as this option is easier to implement than the direct approach of reducing the number of canoes.

3. An annual quota of catches—TAC—set around the MSY level must be introduced by the Fisheries Commission. This has the effect of drastically reducing the fishing effort to well below the bifurcation point in a given season.

4. Implementation of MPAs coupled with size of fish stock set at the MSY level should be considered by the Fisheries Commission. This will go a long way towards ensuring sustainability of the sardinella fishery.

5. Artisanal fishers sometimes resort to the use of under-sized mesh gear among other IUU fishing practices. The Fisheries Commission should strictly enforce the regulations on mesh size and other illegal methods, and culprits given stiffer punishment to serve as a deterrent to would-be offenders.

6. The Fisheries Commission can ensure the full benefit of the resource—both for fishers and posterity—by jettisoning the open access model in favour of some sort of management. The introduction of licences delineating which species and the period to fish will ultimately lead to the protection of the stocks from overexploitation.

Future research

The study presented a comprehensive study of the optimal harvesting strategies for the sardinella fishery. However, not all areas of optimal control as it applies to the sustainable harvesting of renewable resources could be covered. For future research, the following areas would be of interest: models incorporating delay equations and the Allee effect. Also considered would be the stochastic, Gompertz

and linear-quadratic regulator models. Of additional interest would be the skewed-logistic model and the logistic model incorporating minimum viable population (MVP), as well as the application of Green's theorem to the determination of the optimality of a model.

REFERENCES

Akpalu, W. (2002). *Compliance to mesh size regulations in artisanal marine fishery in Ghana*. Paper presented at the Beijer Research Seminar, Durban, South Africa. Retrieved from https://www.oceandocs.org/bitstream/handle/1834/878/ Akpalu34.pdf

Akpalu, W., & Vondolia, G. K. (2011). *Bioeconomic model of spatial fishery management in developing countries* (Working Papers in Economics, No. 490). Gothenburg, Sweden: University of Gothenburg.

Akyempon, S., Bannerman, B., Amador, K., & Nkrumah, B. (2013). *Ghana canoe frame survey*. (Information Report No. 35). Accra: Fisheries Survey Division, MOFAD.

Allen, L. J. S. (2006). *An introduction to mathematical biology*. Upper Saddle River: Prentice-Hall.

Bailey, M., Quaatey, S., Armah, A. K., Jacquet, J., Khan, A., Alder, J., & Sumaila, U. R. (2011). Meeting socioeconomic objectives in Ghana's sardinella fishery. In D. M. Nanang, & T. K. Nunifu (Eds.). *Natural resources in Ghana: Management, policy and economics* (pp. 293-308). Hauppauge: Nova Science Publishers.

Bannerman, P., & Quartey, S. (2006). *Report on the observations of commercial light fishing operation in Ghana*. Accra: MFRD.

Benardete, D. M., Noonburg, V. W., & Pollina, B. (2008). Qualitative tools for studying periodic solutions and bifurcations as applied to the periodically harvested logistic equation. *The Mathematical Association of America, 115*, 202-219.

Bonocoeur, J., Alban, F., Guyader, O., & Thebaud, O. (2002). Fish, fishers, seals and tourists: Economic consequences of creating a marine reserve in a multi-species, multi-activity context. *Natural Resource Modeling, 25(4)*, 1-25.

Brinson, A. A., Die, D. J., Bannerman, P. O., & Diatta, Y. (2009). Socioeconomic performance of West African fleets that target Atlantic billfish. *Fish-*

eries Research, *99*, 55-62.

Caddy, J. F. (1996). Regime shifts and paradigm changes: Is there a place for equilibrium thinking? *Fisheries Research*, *25*, 219-230.

Caddy, J. F. (1999). Fisheries management in the twenty-first century: Will new paradigms apply? *Reviews in Biology and Fisheries*, *9*, 1-43.

Chiang, A. C. (1992). *Elements of dynamic optimization*. Singapore: McGraw-Hill.

Clark, C. W. (1973). The economics of overexploitation. *Science*, *181*, 630-634.

Clark, C. W. (2010). *Mathematical bioeconomics: The mathematics of conservation* (3rd ed.). Hoboken: Wiley.

Clark, C. W., & Munro, G. R. (1975). The economics of fishing and modern capital theory: A simplified approach. *Journal of Environmental Economics and Management*, *2*, 92-106.

Clark, D. N. (Ed.). (2000). *Dictionary of analysis, calculus, and differential equations*. New York: CRC Press.

Craven, B. D. (1995). *Control and optimization*. New York: CRC Press.

Daci, A., & Spaho, A. (2013). *Bifurcation in a dynamical system: Harvest models*. Paper presented at the International Conference on Research and Engineering: Challenges Toward the Future, Albania. Retrieved from konferenca.unishk.edu.al/icrae2013/icraecd2013/doc/411.pdf

Daly, H. E., & Cobb, J. B. (1989). *For the common good: Redirecting the economy toward community, environment and a sustainable future*. Boston: Beacon.

Defeo, O., & Caddy, J. F. (2001). Evaluating a dynamic approach to yield-mortality models. *ICES Journal of Marine Science*, *58*, 1253-1260.

de Pillis, L. G., Gu, W., Fister, K. R., Head, T,. Maples, K., Neal, T., Murugan, A., & Yoshida, K. (2007). Chemotherapy for tumors: An analysis of the dynamics and a study of quadratic and linear controls. *Mathematical Biosciences*, *209*(1), 292-315.

Doyi, B. A. (1984). *Catalogue of small-scale fishing gear of Ghana*. (CECAF/

ECAF Series 84/31). Rome: The FAO.

Dubey, B., Chandra, P., & Sinha, P. (2003). A model for fishery resource with reserve area. *Nonlinear Analysis: Real World Applications*, *4*(4), 625-637.

Dubey, A., & Patra, A. (2013a). A mathematical model for optimal management and utilization of a renewable resource by population. *Journal of Mathematics* (Article ID 613706), 1-9.

Dubey, A., & Patra, A. (2013b). Optimal management of a renewable resource utilized by a population with taxation as a control variable. *Nonlinear Analysis: Modelling and Control*, *18*(1), 37-52.

Edwards, C. H., & Penney, D. E. (2004). *Differential equations and boundary value problems* (3rd ed.). Upper Saddle River: Pearson Education.

Elmqvist, T., Folke, C., Nystrom, M., Peterson, G., Bengtsson, J., Walker, B., & Norberg. J. (2003). Response diversity, ecosystem change and resilience. *Frontiers in Ecology and the Environment*, *1*(9), 488-494.

Fan, M., & Wang, K. (1998). Optimal harvesting policy for single population with periodic coefficients. *Mathematical Biosciences*, *152*, 165-177.

FAO (2016). *The state of world fisheries and aquaculture: Contributing to food security and nutrition for all*. Rome: The FAO.

FASDP (2016). *Republic of Ghana fisheries and aquaculture sector development plan, 2011 - 2016*. Retrieved from rhody.crc.uri.edu/wp-content/uploads/sites/10/2018/04/Ghana-Fisheries-and-Aquaculture-Sector-Development-Plan-2011-2016.pdf

Fister, K. R., & Panetta, J. C. (2000). Optimal control applied to cell-cycle-specific cancer chemotherapy. *SIAM Journal of Applied Mathematics*, 60(3), 1059-1072.

Fleming, W. H., & Rishel, R. W. (1975). *Deterministic and stochastic optimal control*. New York: Springer-Verlag.

Freedman, H. I. (1984). Persistence in models of three interacting predator-prey populations. *Mathematical Biosciences*, *68*, 213-231.

Goh, B. S. (1969). Optimal control of a fish resource. *Malayan Scientist*, *5*, 65-

70.

Gordon, H. S. (1954). The economic theory of a common property resource. *Journal of Political Economy, 62*, 124-42.

GSS (2014). *Gross domestic product 2014*. Accra: The GSS.

Habib, A., Ullah, M. H., & Duy, N. N. (2014). Bioeconomics of commercial marine fisheries of Bay of Bengal: Status and direction. *Economics Research International* (Article ID 538074), 1-10.

Hanski, I. (1999). *Metapopulation ecology*. Oxford: Oxford University Press.

Hanson, F. B., & Ryan, D. (1998). Optimal harvesting with both population and price dynamics. *Mathematical Biosciences, 148*, 129-146.

Hardin, C. (1968). The tragedy of the commons. *Science, 162*, 1243-1247.

Hasanbulli, M., Rogovchenko, S. P., & Rogovchenko, Y. U. (2013). Dynamics of a single species harvesting in a fluctuating environment under periodic yield harvesting. *Journal of Applied Mathematics* (Article ID: 167671), 1-12.

Hilborn, R., Micheli, F., & De Leo, G. (2006). Integrating marine protected areas with catch regulation. *Canadian Journal of Fisheries and Aquatic Sciences, 63*, 642-649.

Hilborn, R., & Walters, C. J. (Eds.). (1992). *Quantitative fisheries stock assessment: Choice, dynamics and uncertainty*. New York: Springer.

Holland, D. S., & Brazee, R. J. (1996). Marine reserves for fisheries management. *Marine Resource Economics, 11*, 157-171.

Holt, C. C., Modigliani, F., Muth, J., & Simon, H. (1960). *Planning production inventories and workforce*. New Jersey: Prentice-Hall.

Ibrahim, M., & Benyah, F. (2017). An application of optimal control to the effective utilization of a renewable resource. *Afrika Statistika, 12*(2), 1315-1333.

Idels, L. V., & Wang, M. (2008). Harvesting fisheries management strategies with modified effort function. *International Journal of Modelling, Identification and Control, 3*(1), 83-87.

Joshi, H. R., Lenhart, S., Hota, S., & Agusto, F. (2015). Optimal control of a SIR model with changing behaviour through an education campaign. *Electronic*

Journal of Differential Equations, 50, 1-14.

Kamien, M. I., & Schwarz, N. L. (1991). *Dynamic optimization: The calculus of variations and optimal control in economics and management*. New York: Elsevier Science Publishing Co.

Kaplan, J. D., & Smith, M. D. (2000). *Optimal fisheries management in the presence of an endangered predator and harvestable prey*. IIFET 2000 Proceedings. Retrieved from www.shanamcdermott.com/uploads/4/1/6/9/4169556/kaplan_smith.pdf

Kar, T. K., & Chakraborty, K. (2009). Bioeconomic analysis of Maryland's Chesapeake Bay oyster fishery with reference to the optimal utilization and management of the resource. *International Journal of Engineering, Science and Technology, 1*(1), 172-189.

Kar, T. K., & Chakraborty, K. (2010). Effort dynamics in a predator-prey model with harvesting. *International Journal of Information and Systems Sciences, 6*(3), 318-332.

Kar, T. K., & Matsuda H. (2008). A bioeconomic model of a single-species fishery with marine reserve. *Journal of Environmental Management, 86*, 171-180.

Kar, T. K., & Misra S. (2010). A resource based stage-structured fishery model with selective harvesting of mature species. *Applications and Applied Mathematics: An International Journal, 5*(1), 42-58.

Keesom, N., Macrae, T., Uhlig, A., & Wang, R. (2010). *Fishing for answers: Investigating sustainable harvesting rate models*. TARNADO Environmental Group. Retrieved from educ.jmu.edu/ strawbem/math_201/final_reports/Keesom_Macrae_Uhlig_Wang

King, A. C., Billingham, J., & Otto, S. R. (2003). *Differential equations: Linear, nonlinear, ordinary, partial*. Cambridge: Cambridge University Press.

Kirk, D. E. (1998). *Optimal control theory: An introduction*. Englewood Cliffs: Prentice-Hall.

Klein, M. W. (2001). *Mathematical methods for economics* (2nd ed.). Boston: Pearson Education.

Koenig, E. F. (1984). Controlling stock externalities in common property fisheries subject to uncertainty. *Journal of Environmental Economics and Management 11*, 124-138.

Koranteng, K. A. (1991). *Some aspects of the sardinella fishery in Ghana.* Retrieved from fishcomghana.com/wp-content/uploads/2017/03/Some-aspects-of-the-sardinella-fishery-in-Ghana.pdf

Koranteng, K. A. (1994) *The Ghanaian fishery for sardinellas.* Paper presented at Workshop on Dynamics and Uses of Sardinella Resources from Upwelling off Ghana and Cote d'Ivoire (DUSRU), Accra, Ghana. Retrieved from fishcomghana.com/wp-content/uploads/2017/03/The-Ghanaian-Fishery-for-Sardinellas.pdf

Koranteng K. A. (1996). The marine artisanal fishery in Ghana: Recent developments and implications for resource evaluation. In R. M. Meyer, C. Zhang, M. L. Windsor, B. J. McCay, L. J. Hushak, & R. M. Muth (Eds.). *Proceedings of the World Fisheries Congress, Theme 2 on Fisheries Resource Utilisation and Policy* (pp. 498-509). New Delhi, India: Oxford & IBH Publishing Co.

Koranteng, K. A. (1998). *The impacts of environmental forcing on the dynamics of demersal fishery resources of Ghana.* Unpublished doctoral dissertation. Department of Biological Sciences, University of Warwick.

Krener, A. J. (1977). The high order maximal principle and its application to singular extremals. *SIAM Journal on Control and Optimization, 15*(2), 256-293.

Kuang, Y., Fagan, W., & Loladze, I. (2003). Biodiversity, habitat area, resource growth rate and interference competition. *Bulletin of Mathematical Biology, 65*, 497-518.

Laham, M. F., Krishnarajah, I. S., & Shariff, J. M. (2012). Fish harvesting management strategies using logistic growth model. *Sains Malaysiana, 41*(2), 171-177.

Lauck, T., Clark, C. W., Mangel, M., & Munro, G. R. (1998). Implementing the precautionary principles in fisheries management through marine reserves.

Ecological Applications, *8*(1), 72-78.

Lawson, R. M., & Kwei, E. A. (1974). *African entrepreneurship and economic growth: A case study of the fishing industry of Ghana*. Accra: Ghana Universities Press.

Lenhart, S., & Workman, J. (2007). *Optimal control applied to biological models*. Boca Raton, FL: Chapman & Hall/CRC.

Lewis, T. R. (1981). Exploitation of a renewable resource under uncertainty. *Canadian Journal of Economics*, *14*, 422-439.

Lewis, T. R. (1982). *Stochastic modeling of ocean fisheries resource management*. Seattle, WA: University of Washington Press.

Lleonart, J., & Merino, G. (2010). Immediate maximum economic yield; a realistic fisheries economic reference point. *ICES Journal of Marine Science*, *67*, 577-588.

Lukes, D. L. (1982). *Differential equations: Classical to controlled*. New York: Academic Press.

Mackinson, S., Sumaila, U. R., & Pitcher, T. J. (1997). Bioeconomics and catchability: Fish and fishers behaviour during stock collapse. *Fisheries Research*, *31*, 11-17.

Manetsch, T. J., & Park, G. L. (1982). *System analysis and simulation with applications to economic and social systems*. Michigan, MI: University of Michigan.

Mansal, F., Nguyen-Huu, T., Auger, P., & Balde, M. (2014). A mathematical model of a fishery with variable market price: Sustainable fishery/over-exploitation. *Acta Biotheor*, *62*, 305-323.

MFRD (2007). *Marine fisheries bulletin for 2006*. Tema, Ghana: The MFRD.

Minta, S. O. (2003). *An assessment of the vulnerability of Ghana's coastal artisanal fishery to climate change*. Unpublished master's dissertation. Department of Aquatic Biosciences, University of Tromso.

MOFAD (2016). *2015 annual report*. Accra: The MOFAD.

Mullon, C., Freon, P., & Curry, P. (2005). The dynamics of collapse in world

fisheries. *Fish and Fisheries*, *6*(2), 111-120.

Murray, J. D. (2003). *Mathematical biology II: Spatial models and biomedical applications* (3rd ed.). New York: Springer.

Myers, R. A., & Worm, B. (2003). Rapid worldwide depletion of large predatory fish communities. *Nature*, *423*, 280-283.

Nansen, F. (2001). *Report of the FAO working group on the assessment of small pelagic fish off Northwest Africa* (FAO Fisheries Reports R657). Rome: The FAO/Nansen Programme.

Neubert, M. G. (2003). Marine reserves and optimal harvesting. *Ecology Letters*, *6* (9), 843-849.

Nunoo, F. K. E., Asiedu, B., Amador, K., Belhabib, D., & Pauly, D. (2014). *Reconstruction of marine fisheries catches for Ghana, 1950 - 2010* (Working Paper No. 2014 - 13). Canada: The University of British Columbia.

Nunoo, F. K. E., Asiedu, B., Olauson, J., & Intsiful, G. (2015). Achieving sustainable fisheries management: A critical look at traditional fisheries management in the marine artisanal fisheries of Ghana, West Africa. *JENRM*, *2*(1), 15-23.

Okosun, K. O., Makinde, O. D., & Takaidza, I. (2013). Impact of optimal control on the treatment of HIV/AIDS and screening of unaware infectives. *Applied Mathematical Modelling*, *37*, 3802-3820.

Palm, W. J. (1975). Fishery regulation via optimal control theory. *Fishery Bulletin*, *73*(4), 830-837.

Patra, A. (2013). *Dynamics of biological species: Some mathematical models.* Unpublished doctoral dissertation. Department of Mathematics, Birla Institute of Technology and Science

Pauly, D. (1994). *On the sex of fish and the gender of scientists: A collection of essays in fisheries science*. Chapman & Hall Fish and Fisheries Series 14.

Pauly, D., Christensen, V., Dalsgaard, J., Froese, R., & Torres, F. (1998). Fishing down marine food webs. *Science*, *279*, 860-863.

Pauly, D., Silvetre, G., & Smith, I. R. (1989). On development, fisheries and

dynamite: A brief review of tropical fisheries management. *Natural Resource Modeling*, *3*(3), 307-329.

Pikitch, E. K., Santora, C., Babcock, E. A., Bakun, A., Bonfil, R., Conover, D. O., Dayton, P., Doukakis, P., Fluharty, D., Heneman, B., Houde, E. D., Link, J., Livingston, P. A., Mangel, M., McAllister, M. K., Pope, J., & Sainsbury, K. J. (1998). Ecosystem-based fishery management. *Science*, *305*, 346-347.

Polacheck, T. (1990). Year-round closed areas as a management tool. *Natural Resource Modeling*, *4*, 327-354.

Pontryagin, L. S., Boltyanskii, V. G., Gamkrelize, R. V., & Mishchenko, E. F. (1962). *The mathematical theory of optimal control*. New York: Wiley.

Powers, J. E., & Monk, M. H. (1988). Current and future use of indicators for ecosystem based fisheries management. *Marine Policy*, *34*, 723-727.

Rodwell, L., Barbier, E., Roberts, C., & McClanahan, T. (2002). A model of tropical marine reserve-fishery linkages. *Natural Resource Modeling*, *15*(4), 453-486.

Royden, H. L. (1988). *Real analysis* (3rd ed.). New York: Macmillan Publishing.

Sanchirico, J. N., & Wilen, J. E. (1999). Bioeconomics of spatial exploitation in a patchy environment. *Journal of the Environmental Economics and Management*, *37*, 129-150.

Sanchirico, J. N., & Wilen, J. E. (2001). A bioeconomic model of marine reserve creation. *Journal of Environmental Economics and Management*, *42*, 257-276.

Sanchirico, J. N., & Wilen, J. E. (2005). Optimal spatial management of renewable resources: Matching policy scope to ecosystem scale. *Journal of Environmental Economics and Management*, *50*, 23-46.

Sancho, N. G. F., & Mitchell, C. (1975). Economic optimization in controlled fisheries. *Mathematical Biosciences*, *27*, 1-7.

Sancho, N. G. F., & Mitchell, C. (1977). Optimal effort of Canada's offshore ground fisheries—An application of economic optimization techniques. *Mathematical Biosciences*, *34*, 157-166.

Schaefer, M. B. (1954). Some aspects of the dynamics of population importance to the management of commercial marine fisheries. *Bulletin of the Inter-American Tropical Tuna Commission, 1*(2), 25-56.

Scott, A. D. (1955). The fishery: The objectives of sole ownership. *Journal of Political Economy, 63*, 116-124.

Seijo, J. C., Defeo, O., & Salas, S. (1998). *Fisheries bioeconomics: Theory, modelling and management* (FAO Fisheries Technical Paper 368). Rome: The FAO.

Stavins, R. (2012). *Fundamentals of Environmental Economics and Policy*. Retrieved from https://scholar.harvard.edu/stavins/classes

Sterner, T. (2007). Unobserved diversity, depletion and irreversibility—The importance of subpopulations for management of cod stocks. *Ecological Economics, 61*, 566-574.

Suri, R. (2008). Optimal harvesting strategies for fisheries: A differential equations approach. Unpublished doctoral dissertation. Institute of Information and Mathematical Sciences, Massey University.

Teschl, T. (2012). *Ordinary differential equations and dynamical systems*. Providence: American Mathematical Society.

Udumyan, N., Ami, D., & Cartigny, P. (2010). Integrating habitat concerns into Gordon-Schaefer Model < halshs-00520328 >. Retrieved from https://halshs.archives-ouvertes.fr/halshs-00520328/halshs-00520328

USAID/Ghana SFMP (2015). *Ghana's small pelagic fishery in crisis: National and regional food security at risk*. Narragansett, RI: University of Rhode Island.

Weber, T. (2009). *Optimal control theory with applications in economics*. Moscow: MAKS Press.

Woodward, C. (2000). *Oceans end*. New York: Basic Books.

Worm, B., Barbier, E. B., Beaumont, N., Duffy, J. E., Folke, C., Halpern, B. S., Jackson, J. B. C., Lotze, H. K., Micheli, F., Palumbi, S. R., Sala, E., Selkoe, K. A., Stachowicz, J. J., & Watson, R. (2006). Impacts of biodiversity loss on

ocean ecosystem services. *Science*, *314*, 787-790.

Wu, R., Shen, Z., & Liao, F. (2017). Optimal control of renewable resources based on effective utilization rate. *Abstract and Applied Analysis* (Article ID 369493), 1-7.

Zhang, X., Shuai, Z., & Wang (2003). Optimal impulsive harvesting policy for single population. *Nonlinear Analysis: Real World Applications*, *4*, 639-651.

APPENDIX

A CALCULUS OF VARIATIONS APPROACH FOR DETERMINING OPTIMAL STOCK SIZE

$$\max_E Z(E) = \int_0^\infty e^{-\delta t}\left(p - \frac{c}{qx}\right) qEx\,dt$$

$$\text{subject to} \quad \frac{dx}{dt} = rx\left(1 - \frac{x}{K}\right) - qEx$$

$$x(0) = x_0\,.$$

Applying calculus of variations, we have the following:

$$\max_x Z(x) = \int_0^\infty e^{-\delta t}\left(p - \frac{c}{qx}\right)\left[rx\left(1 - \frac{x}{K}\right) - x'\right] dt\,.$$

To solve for the optimal sustainable population size x_δ, we employ Euler's equation

$$\frac{\partial f}{\partial x} = \frac{d}{dt}\left(\frac{\partial f}{\partial x'}\right)$$

to obtain the following

$$e^{-\delta t}\left\{\left(p - \frac{c}{qx}\right) r\left(1 - \frac{2x}{K}\right) + \frac{c}{qx^2}\left[rx\left(1 - \frac{x}{K}\right) - x'\right]\right\} = \frac{d}{dt}\left[-e^{-\delta t}\left(p - \frac{c}{qx}\right)\right].$$

This implies

$$e^{-\delta t}\left\{\left((p - \frac{c}{qx}\right) r\left(1 - \frac{2x}{K}\right) + \frac{c}{qx^2} rx\left(1 - \frac{x}{K}\right)\right\} = \delta e^{-\delta t}\left(p - \frac{c}{qx}\right);$$

$x' = 0$, since x_δ is a constant.

Simplifying, we have the following

$$r\left(1 - \frac{2x}{K}\right) + \frac{\frac{c}{qx} r\left(1 - \frac{x}{K}\right)}{p - \frac{c}{qx}} = \delta\,.$$

Therefore, solving for the positive optimal population size, we have

$$x_\delta = \frac{K}{4}\left[\left(1 + \frac{c}{pqK} - \frac{\delta}{r}\right) + \sqrt{\left(1 + \frac{c}{pqK} - \frac{\delta}{r}\right)^2 + \frac{8\delta c}{pqrK}}\right].$$

SAM JONAH LIBRARY
UNIVERSITY OF CAPE COAST
CAPE COAST